THERMODYNAMIC STATES OF ADSORBED HYDROGEN AT NOBLE-METAL ELECTROCATALYSTS IN ABSENCE/PRESENCE OF CHEMISORBED SULFUR

by

Alireza Zolfaghari-Hesari

A thesis presented to the Département de chimie
in fulfillment of the requirements for
the degree of Philosophiae Doctor (Ph.D.)

FACULTÉ DES SCIENCES
UNIVERSITÉ DE SHERBROOKE

Sherbrooke, Canada, January 1998

Le 2 avril 1998, le jury suivant a accepté cette thèse, dans sa version finale.

MEMBRES	SIGNATURES
M. Brian E. Conway University of Ottawa	_____
M. Gregory Jerkiewicz Département de chimie	_____
M. Andrzej Lasia Département de chimie	_____
M. André Bandrauk Département de chimie	_____

to my dearest parents

SUMMARY

The experimental and theoretical research on the hydrogen under-potential deposition (UPD) on Rh and Pt electrodes has led to determination of the Gibbs free energy (ΔG_{ads}), the standard entropy (ΔS°_{ads}) and the standard enthalpy (ΔH°_{ads}) of adsorption based on a general adsorption isotherm rederived in the course of this work. The research has resulted in development of theoretical methodology allowing to evaluate, for the first time, the bond energy between the metal substrate, M, and the under-potential deposited H (H_{UPD}), $E_{M-H_{UPD}}$ (here M = Pt or Rh). The impact of the specifically adsorbed anions on ΔG_{ads}, ΔS°_{ads} and ΔH°_{ads} has also been studied. Cyclic-voltammetry measurements have been conducted on Pt(poly), Rh(poly), Pt(111) and Pt(100) electrodes in three different concentrations of aqueous H_2SO_4 (0.05, 0.1 and 0.5 M) in the 273 - 353 K temperature range.

Theoretical treatment of the experimental data based on the general electrochemical adsorption isotherm has allowed elucidation of ΔG_{ads} as a function of the temperature, T, and the H surface coverage, $\theta_{H_{UPD}}$. Temperature dependence of ΔG_{ads} for a constant surface coverage of the under-potential deposited H (H_{UPD}) results in determination of ΔS°_{ads} and, subsequently, ΔH°_{ads}. Knowledge of ΔH°_{ads} is essential in following determination of the bond energy between M and H_{UPD}, $E_{M-H_{UPD}}$, which is found to depend on $\theta_{H_{UPD}}$. The experimentally evaluated value of $E_{M-H_{UPD}}$ is close to that of the bond energy between M and the chemisorbed H (H_{chem}), $E_{M-H_{chem}}$. Proximity of the magnitude of $E_{M-H_{UPD}}$ to that of $E_{M-H_{chem}}$ (here M = Pt or Rh) points to the similar binding mechanism of H under the conditions involving presence of the electrified solid/liquid interface. Closeness of $E_{M-H_{UPD}}$ to $E_{M-H_{chem}}$ might also point to the same adsorption site of the two distinct H surface species, thus indicating that H_{UPD} alike H_{chem} is strongly embedded in the surface lattice of the Rh and Pt substrates.

Temperature-dependent research on the UPD H and anion adsorption on Pt(111) and Pt(100) in 0.5 M aqueous H_2SO_4 solution by cyclic-voltammetry, cv, conducted for the first time ever, indicates that the overall adsorption/desorption charge density is affected by temperature variation. In the case of Pt(100), the H_{UPD} coverage is affected only slightly by T increase

whereas that of the anion decreases by 1/3 when T is raised from 293 to 328 K. This behavior may be assigned to lateral repulsive interactions between the anionic species. Similar measurements have been completed on a Pt(111) electrode. An analysis of the CV profiles for Pt(111) shows that the UPD H and anion adsorption regions shift towards less-positive potentials when T is raised. Integration of the CV's for Pt(111) discloses that the overall adsorption-desorption charge density is only slightly affected by temperature, T, variation and that it decreases by 25 $\mu C\,cm^{-2}$ when T is raised from 275 to 338 K. Introductory deconvolution of the CV into two components assigned to the UPD H and the anion adsorption indicates that the charge density associated with the UPD H decreases by 20 $\mu C\,cm^{-2}$ whereas that of the anion adsorption decreases by only 5 $\mu C\,cm^{-2}$. Because the H_{UPD} and anion adsorption regions on Pt(111) in 0.05 M aq. H_2SO_4 are separated, one may determine $\Delta G_{ads}(H_{UPD})$, $\Delta S^{\circ}_{ads}(H_{UPD})$, $\Delta H^{\circ}_{ads}(H_{UPD})$ and the $Pt(111)-H_{UPD}$ surface bond energy, $E_{Pt(111)-H_{UPD}}$. An analysis of the $\Delta G_{ads}(H_{UPD})$ versus $\theta_{H_{UPD}}$ plots reveal that the UPD H follows the Frumkin isotherm and the energy of lateral repulsions, ω, and the respective dimensionless parameter g are coverage independent. The value of $E_{Pt(111)-H_{UPD}}$ is close to the surface bond energy between the chemisorbed H, H_{chem}, and Pt(111), $E_{Pt(111)-H_{chem}}$.

The influence of submonolayers of chemisorbed sulfur, S_{chem}, on the UPD H on Pt(poly) and Pt(111) electrodes was studied. The objectives of this part of research work have been: (a) examination of changes in enthalpy of electroadsorption of H brought about by a submonolayer of S_{chem} of a well-defined coverage, (b) study of the lateral interaction energy between H adatoms. The research has demonstrated that a monolayer of S_{chem} on Pt can be formed by its immersion in aqueous Na_2S solution. The S_{chem} can be gradually removed through oxidative desorption and its coverage can be controlled with the precision of some 1-2% of a mono layer. Theoretical treatment of the experimental results indicates that a submonolayer of S_{chem} having the nominal coverage of 0.10 increases the Gibbs free energy, the entropy and the enthalpy of adsorption for H_{UPD}. The bond energy between Pt and H_{UPD} decreases in presence of S_{chem} and the effect is brought about by local electron withdrawing effects that propagate through the underlying metal which acts as a mediator.

SOMMAIRE

La recherche expérimentale et théorique sur la déposition sous-nernstienne (DSN, *angl.* UPD) de l'hydrogène sur les électrodes de Rh et de Pt a mené à la détermination de l'énergie libre de Gibbs (ΔG_{ads}), de l'entropie standard (ΔS°_{ads}) et de l'enthalpie standard (ΔH°_{ads}) d'adsorption, basée sur un isotherme général d'adsorption rédérivé au cours de ce travail. Cette recherche a eu pour résultat un développement de la méthodologie théorique, ayant permis pour la première fois l'évaluation de l'énergie de liaison entre le substrat métallique, M, et H_{UPD}, $E_{M-H_{UPD}}$ (ici M = Pt ou Rh). Le rôle des anions spécifiquement adsorbés sur ΔG_{ads}, ΔS°_{ads} et ΔH°_{ads} a également été étudié. Des mesures de voltampérométrie cyclique ont été conduites sur des électrodes Pt(poly), Rh(poly), Pt(111) et Pt(100) dans des solutions aqueuses de H_2SO_4 et $HClO_4$ à trois concentrations différentes (0,01; 0,1 et 0,5 M) et dans un domaine de température de 273 à 353 K.

Le traitement théorique des données expérimentales, basé sur l'isotherme général d'adsorption électrochimique, a permis l'élucidation de ΔG_{ads} en fonction de la température, T, et du recouvrement de la surface par H, $\theta_{H_{UPD}}$. La dépendance de ΔG_{ads} de la température pour une valeur de $\theta_{H_{UPD}}$ constant a pour résultat la détermination de ΔS°_{ads} et, par la suite, de ΔH°_{ads}. La connaissance de ΔH°_{ads} est essentielle pour la détermination ultérieure de l'énergie de liaison entre M et H_{UPD}, $E_{M-H_{UPD}}$, dépendante de $\theta_{H_{UPD}}$. La valeur de $E_{M-H_{UPD}}$ évaluée est proche de celle de l'énergie de liaison entre M et H chimisorbé, (H_{chem}), $E_{M-H_{chem}}$. La similitude des valeurs de $E_{M-H_{UPD}}$ et de $E_{M-H_{chem}}$ (ici M = Pt ou Rh) indique un mécanisme de liaison de H similaire dans les deux cas, et ceci dans des conditions impliquant la présence d'une interface liquide/solide électrifiée. La proximité de $E_{M-H_{UPD}}$ et $E_{M-H_{chem}}$ pourrait également signifier un même site d'adsorption pour les deux espèces de surface distinctes (H_{UPD}, H_{chem}), indiquant ainsi leur lien fort dans le réseau de surface de Rh et Pt.

L'étude de l'influence de la température sur l'UPD de H et l'adsorption des anions sur Pt(100) dans la solution aqueuse de H_2SO_4 (0,5 M) par voltampérométrie cyclique, VC, effectuée pour la première fois, démontre que la densité de charge d'adsorption/désorption totale est fortement affectée par la variation de température. Dans le cas de Pt(100), le recouvrement

de H_{UPD} ne dépend que légèrement de l'augmentation de T, alors que celui de l'anion diminue de 1/3 lorsque T varie de 293 à 328 K. Ce comportement peut être assigné aux intéractions latérales répulsives entre les espèces anioniques. Des mesures semblables ont été effectuées sur l'électrode Pt(111). L'analyse des courbes VC pour Pt(111) montre un déplacement des domaines d'adsorption de H_{UPD} et des anions vers les potentiels moins positifs avec l'augmentation de la température. L'intégration des courbes VC dans le cas de Pt(111) révèle que la densité de charge d'adsorption-désorption totale est faiblement influencée par la variation de temperature et qu'elle diminue de 25 $\mu C\,cm^{-2}$ lorsque T augmente de 275 à 338 K. Une première déconvolution des courbes VC en deux composantes assignées à l'adsorption de H_{UPD} et à celle des anions indique que la densité de charge de H_{UPD} diminue de 20 $\mu C\,cm^{-2}$ tandis que celle d'adsorption des anions diminue seulement de 5 $\mu C\,cm^{-2}$ en élevant la température de 273 á 338 K. Grâce au fait que les domaines d'adsorption de H_{UPD} et des anions sur Pt(111) dans 0,05 M H_2SO_4 aqueuse soient séparés, le $\Delta G_{ads}(H_{UPD})$, $\Delta S^{\circ}_{ads}(H_{UPD})$, $\Delta H^{\circ}_{ads}(H_{UPD})$ ainsi que l'énergie de liaison de surface du lien $Pt(111)-H_{UPD}$, $E_{Pt(111)-H_{UPD}}$, peuvent être déterminés. Une analyse des courbes $\Delta G_{ads}(H_{UPD})$ en fonction de $\theta_{H_{UPD}}$ révèle que H_{UPD} obéit à l'isotherme de Frumkin et que l'énergie des répulsions latérales, ω, ainsi que le paramètre sans dimension, g, ne dépendent pas du recouvrement. La valeur de $E_{Pt(111)-H_{UPD}}$ est proche à l'énergie de liaison de surface entre H chimisorbé, H_{chem}, et Pt(111), $E_{Pt(111)-H_{chem}}$.

L'influence des sous-monocouches du soufre chimisorbé, S_{chem}, sur l'UPD de H sur les électrodes Pt(poly) et Pt(111) a également été étudiée. Les objectifs de cette partie de la recherche ont été les suivants: (a) étude des changements de l'enthalpie d'électroadsorption de H causés par une sous-monocouche de S_{chem} ; (b) étude de l'énergie d'intéraction latérale entre les adatomes de H. Selon les résultats, une monocouche de S_{chem} sur Pt est formée par son immersion dans une solution aqueuse de Na_2S. Le S_{chem} est graduellement éliminé par une désorption oxydante et son recouvrement peut être contrôlé avec une précision de 1-2% de monocouche. Un traitement théorique des résultats expérimentaux démontre qu'une sous-monocouche de S_{chem} au recouvrement nominal de 0,10 fait augmenter l'énergie libre, l'entropie et l'enthalpie d'adsorption de H_{UPD}. L'énergie de liaison entre Pt et H_{UPD} décroit en présence de S_{chem}, l'effet étant dû aux effets de retrait des électrons locaux qui se propagent à travers le substrat métallique qui joue un rôle de médiateur.

ACKNOWLEDGMENTS

I would like to express my sincere gratitude to Prof. Gregory Jerkiewicz, my research supervisor, for his guidance, advice and support throughout the course of this research and for his help and stimulation in studying the simplest and the most complex experimental and theoretical problems. To me, Prof. Jerkiewicz is not only an outstanding scientist with remarkable potential for scientific research but also an underestanding and supportive friend. I thank him from my heart for his friendly guidance and support during my Ph.D. studies while being far away from my family home I wish to express my special thanks to Prof. Gregory Jerkiewicz.

I wish to thank Prof. Andrzej Wieckowski and his group at the University of Illinois at Urbana-Champaign for their help in performing certain experiments which constitute a part of this research. I wish to express my gratitude to Prof. Brian E. Conway, FRSC, and Prof. Andrzej Lasia for their professional advices and truly stimulating scientific discussions.

I would like to acknowledge collaboration with Francis Villiard, Martine Chayer and Sonia Blais during their term projects. In particular, I thank Sonia Blais and Milan Petkovic, my laboratory colleagues, for their friendship and help. I wish to thank the Professors of the Chemistry Department, in particular Prof. Jean Lessard, the Support Staff members and all my departmental colleagues for their help throughout my studies.

I would like to gratefully acknowledge the Ministry of Culture and Higher Education (MCHE) of Iran for a graduate fellowship (April 1993-April 1997).

I wish to express my gratitude to the following organization for their fellowships and awards: The Electrochemical Society Inc., a US Department of Energy Summer Fellowship (Summer 1997); Université de Sherbrooke for la Bourse de la Famille Roger-Beaudoin (Autumn 1997); American Electroplaters and Surface Finishers Society for AESFE Student Award (Summer 1995) and Université de Sherbrooke for Bourse d'Exemption Des Droits d'Inscription Pour Étudiantes et Étudiants Étrangers (Summer 1994). Also, I would like to acknowledge the financial support towards the research from the NSERC of Canada and le FCAR du Québec.

Above all, I am greatly indebted and thankful to my parents for their love, great encouragement, support and understanding throughout the course of this work. Even with the Atlantic Ocean between us, they have been with me since the very beginning of the studies.

Once again, let me express to all of you my sincere gratitude in the three languages that I speak:

Merci beacoup!

با تشکر فراوان

Thank you very much!

TABLE OF CONTENTS

LIST OF TABLES

CHAPTER 3

LIST OF FIGURES

CHAPTER 1

1.2 Figures from G. Jerkiewicz and A. Zolfaghari, J. Phys. Chem., 100, 8454 (1996).

CHAPTER 2

2.1 Figures from A. Zolfaghari, M. Chayer and G. Jerkiewicz, J. Electrochem. Soc., 144, 3034 (1997).

INTRODUCTION

i. General Outlook

The motivation to investigate the hydrogen-electrode surface interaction phenomena, the hydrogen evolution reaction (HER), hydrogen adsorption on metallic surfaces and H absorption into host metals/alloys, originates from various sources. The domain of heterogeneous catalysis, hydrogen storage and energy conversion, material science, metallurgy, corrosion, electro-hydrogenation of organic compound are of significance in current technology and hydrogen adsorption has practical implication in these areas (1-24).

Water electrolysis and hydrogen oxidation are two important processes of heterogeneous catalysis and they constitute a main area research and technology development. Hydrogen is converted electrochemicaly to electricity in fuel cells with high efficiency. The process is not a subject to the limitations of the Carnot Cycle, as it is in the case of fossil fuel and nuclear in thermal power plants. In this context, knowledge of the thermodynamic and electronic state of hydrogen on the surface of the electrocatalysts is of primary importance to hydrogen-based fuel cells and the water electrolysis. It is the interaction with the substrate which determines the efficiency of hydrogen oxidation and hydrogen ion reduction. The reasons why a particular metal is the best catalyst for a given reaction are not fully resolved, while the role of specific adsorption sites and the possibility of selective poisoning (25-27) are another interesting problem. Clearly, further research is required and many insights will come from investigations using single-crystals electrodes, It is apparent that the catalytic activity of single crystal Pt electrodes towards hydrogen adsorption (28-30) is quite different. Above all, many aspects of H adsorption or oxidation on polycrystalline Pt still need to be understood.

Hydrogen can dissolve in significant amounts in certain metals or metallic alloys, forming a hydride. The process can be accomplished either under electrochemical or gas-phase conditions. In electrochemical systems, the metal/metallic alloy to be hydrided is placed in aqueous electrolyte and it is cathodically polarized. AB_2-type and AB_5-type intermetallic alloys are frequently used as hosts of the absorbed H and they are commonly utilized as anodes in primary and secondary batteries (15-19). These batteries are of growing importance in portable electronic devices such as portable computers, cellular phones, pagers, etc. Thus,

with regard to the research on modern energy-storage devices, the research on metal-hydride electrodes is clearly of great technological importance. Consequently, progress in the metal-hydride science and technology depends on the comprehension of the basic steps involved in H adsorption on the metal surface as well as H interfacial transfer into the metal bulk.

In corrosion science, knowledge of fundamental steps involved in H entry into the host metal is of vital significance in protecting metal structures from undergoing H embrittlement, a costly and often disastrous process. Undesirable entry of H into host metallic alloys limits its application as a fuel in space and aviation technology as well as a fuel in internal combustion engines; the H-induced material disintegration is highly enhanced by high operating pressures and temperatures. Entry of hydrogen isotopes into metallic alloys is of primary concern in fusion technology where H, D and T are either reactants or products of nuclear events; diffusion of T through the metal shielding to the liquid Li cooling system leads to serious and irreversible environmental problems (1-3, 5).

In general, whenever hydrogen plays any role in electrode processes, the hydrogen adsorption behavior is very frequently discussed as a basic property of the electrode. The knowledge of strength and nature of the electroadsorptive hydrogen bond on the surface of metals as well as in appraisal of the adsorption site of H on metallic surfaces is of great importance in hydrogen-surface electrode processes research. Assessment of the energy of the metal-hydrogen bond which is essential in evaluation of strength, nature and the adsorption site of H on metallic surfaces can be possible by thermodynamic studies. Whereas the energy of the surface-hydrogen bond formed under gas-phase conditions is well documented (6) for various transition metals, such data have not been reported for the surface bond between the underpotentially deposited H and the metal substrate. To study thermodynamic of electrode process, electrochemical methods or electrochemical methods coupled with surface analysis techniques are used as an experimental methodology whereas the theoretical treatment is based on an electrochemical isotherm and adsorption thermodynamics.

ii. Thermodynamics of Electroadsorption, Electrochemical Adsorption Isotherms

An electrochemical adsorption isotherm is a relationship between the coverage of substance *i* adsorbed on the electrode, θ_i, the activity of the adsorbate in the bulk solution, a_i^b , and the

electrical state of the system, E or q^M , at a given temperature, T. The electrochemical adsorption affects electrode processes by (a) determining the local reactant concentrations at the electrode (b) determining indirectly the kinetics of electrochemical reactions proceeding at the surface, e.g. with regard to reaction order.

When adsorbed intermediates are involved in consecutive electrochemical reactions, a more direct and specific influence on the electrode kinetics may arise. So far, it has been supposed that the adsorbed species from gas phase form a mono-molecular layer immediately adjacent to the solid surface. Since the electrolyte is at least a two-component system, this is a problem in mixed adsorption. However, in the adsorption of many strongly adsorbed species from dilute solution it is reasonable approximation to treat the solvent as a continuum (31).

Where there is an equilibrium between the bulk and electroadsorbed species *i* at the polarized electrode, the corresponding electrochemical potentials are equal

$$\underset{(1-\theta_A)}{M} + \underset{a_{A^{z\pm}}}{A^{z\pm}} \pm ze \rightleftharpoons \underset{\theta_A}{M-A_{ads}} \qquad [1]$$

$$\overline{\mu}_i^A = \overline{\mu}_i^b \qquad [2]$$

where the subscripts *A* and *b* refer to electroadsorbed species *i* and species *i* in the bulk, respectively and also

$$\overline{\mu}_i^\alpha = \mu_i^\alpha + z_i F\phi \qquad [3]$$

where the μ_i^α is the chemical potential for species *i* with charge z_i in phase α and ϕ is the interfacial potential difference. Thus

$$\overline{\mu}_i^{0,A} + RT \ln a_i^A = \overline{\mu}_i^{0,b} + RT \ln a_i^b \qquad [4]$$

Where $\overline{\mu}_i^0$ terms are the standard electrochemical potentials. The standard electrochemical free energy of adsorption, $\Delta \overline{G}_i^0$,which is a function of the electrode potential, is defined as

$$\Delta \overline{G}^0 = \overline{\mu}_i^{0,A} - \overline{\mu}_i^{0,b} \qquad [5]$$

Thus

$$a_i^A = a_i^b \exp\left(\frac{-\Delta \overline{G}_i^0}{RT}\right) \qquad [6]$$

or

$$a_i^A = \beta_i \, a_i^b \qquad [7]$$

where

$$\beta_i = \exp\left(\frac{-\Delta \overline{G}_i^0}{RT}\right) \qquad [8]$$

Equation [7] is a general form of the adsorption isotherm, with a_i^A a function of a_i^b and β_i. The problem is now to obtain an expression for a_i^A in terms of the surface coverage, θ_i. To formulate particular adsorption isotherms, it is useful to think of the interactions of the adsorbed particles in the mono-layer as being divided into two categories: particle-metal interactions and particle-particle interactions. It is reasonable to suppose that the particle-metal interactions are the ones most directly affected by the electrical state of the system. If, at constant temperature, the electrical state is held constant, changes in the amount of adsorption produced by changing the bulk activity of the adsorbing material ought to be determined by the nature of particle-particle interactions. The latter should be determined by essentially the same factors as govern ordinary, that is, non electrochemical adsorption, for example, adsorption of gases on solid or liquid surfaces (32). Thus, different specific isotherms result from different assumption or models for the relationship between a_i^b and θ_i. Several isotherms have been proposed in references 31-37 and the results for number of well known isotherms are presented here.

Electrochemical Langmuir Isotherm

The basic isotherm for the adsorption of ions or molecular species on electrodes is that of Langmuir. The electrochemical adsorption isotherm is based on the following assumptions:
(a) the Gibbs energy of adsorption of adsorbate species is potential dependent,
(b) the coverage of the adsorbate, in going from a bare substrate surface to one with full monolayer coverage, is potential dependent in a well-defined manner, determined by (a) above,
(c) there are no lateral interactions between the adsorbed species on the electrode surface (38-41).

The electrochemical Langmuir isotherm may be written for an electrochemical process as that in equation [1] as:

$$\frac{\theta_i}{1-\theta_i} = K_i a_i^b \exp\left(\frac{-z_i EF}{RT}\right) \qquad [9]$$

where E is the difference of electrode potential at any θ_i from the standard potential (31) corresponding to $\theta_i = 0.5$; K_1 is the chemical equilibrium constant of the surface reaction as that in equation [1] and is related to standard Gibbs energy, ΔG_i°, and F and R are physico-chemical constants. Langmuir adsorption conditions are defined by independence of K_1 on coverage, θ_i.

Electrochemical Temkin Isotherm

Temkin assumed that varying Gibbs free energy of adsorption can arise on account of heterogeneity of the surface so that the surface is regarded as made up of a distribution of patches. Based on his treatment of adsorption on experimental evidence, the relation between enthalpy of adsorption, ΔH_{ads}, and coverage, θ_i, is approximately linear at intermediate values of θ_i (i.e. $0.2 < \theta_i < 0.8$). The Standard Gibbs free energy is assumed to decrease with θ_i according to the relation (31,42):

$$\Delta G_{i,\theta}^\circ = \Delta G_{i,\theta=0}^\circ + r\theta_i \qquad [10]$$

Where r is a parameter associated with intrinsic heterogeneity of the surface. The Temkin adsorption isotherm can be derived formally for an electrochemical process such as equation [1] under equilibrium conditions in the form:

$$\frac{\theta_i}{1-\theta_i} = K_1 a_i^b \exp\left(\frac{-z_i EF}{RT}\right) \exp\left(-\frac{r\theta_i}{RT}\right) \qquad [11]$$

At intermediate values of coverage and for sufficiently large r, i.e. when the term $\frac{\theta_i}{1-\theta_i} \approx 1$, its variation with θ_i is small compared with that of $\exp(-r\theta_i/RT)$ term; then

$$\exp\left(\frac{r\theta_i}{RT}\right) = K_1 a_i^b \exp\left(\frac{-z_i EF}{RT}\right) \qquad [12]$$

which upon rearrangement gives

$$\theta_i = \frac{-z_i EF}{r} + \frac{RT}{r} \ln\left(K_1 a_i^b\right) \qquad [13]$$

Which is a form of Temkin's isotherm although his derivation was based on treatment of heterogeneous having distribution of K_1 values. Hence, for constant values of K_1 and a_i^b, the coverage tends to increase linearly with increasing potential difference, E, and increases logarithmically with increasing K_1 and a_i^b at constant potential difference, E.

Electrochemical Frumkin Isotherm

A modification which allows for longer rang interaction between polar species adsorbed at electrode, was proposed by Frumkin who added a new term to the Langmuir equation of state and obtained (35,43):

$$\frac{\theta_i}{1-\theta_i} = K_1 a_i^b \exp\left(\frac{-z_i EF}{RT}\right) \exp\left(\frac{-2g'\Gamma_1\theta_i}{RT}\right) \qquad [14]$$

The parameter g expresses the way in which the adsorption energy of *i* changes with increased coverage and Γ_1 is the surface concentration of *i* at saturation. If g' is positive, the interactions between two species *i* on the surface are repulsive and if g' is negative, the interactions are attractive. If $g' \rightarrow 0$, the Frumkin isotherm approaches the Langmuir isotherm. This isotherm can also be written in the form:

$$\frac{\theta_i}{1-\theta_i} = K_1 a_i^b \exp\left(\frac{-z_i EF}{RT}\right) \exp(-g\theta_i) \qquad [15]$$

where $g = 2g'\Gamma_1 / RT$. It follows from equation [15] that analysis of isotherms as a deviation from a Langmuir isotherm should lead to a linear variation of the standard Gibbs free energy of adsorption with coverage provided according to the relation:

$$\Delta G^\circ_{i,\theta} = \Delta G^\circ_{i,\theta=0} + RTg\theta_i \qquad [16]$$

that the Frumkin isotherm can be applied and g can be associated with lateral interaction between adsorbed species.

iii. Underpotential Deposition (UPD) and Overpotential Deposition (UPD) of Hydrogen at Noble-Metal Electrodes

In electrochemical surface science, two kinds of electroadsorbed H species are known: the underpotential deposited H, H_{UPD}, and the over-potential deposited H, H_{OPD}. An important and unique aspect of H electroadsorption on Pt, Pd, Rh and Ir electrode surfaces is the phenomenon of the underpotential deposition of H (UPD H), a process which takes place *above* the potential required for the onset of the cathodic H_2 evolution, thus above the H^+ / H_2 equilibrium potential, E_{eq}. The over-potential deposition of H, OPD H, takes place at negative potentials with respect to the E_{eq} because H_{OPD} is an intermediate of the HER. Thus H_{OPD} exists on all metal electrode surfaces at negative potentials (7,24,44-54). Both these surface species, namely H_{UPD} and H_{OPD}, are known to absorb into Pd but absorption of H_{UPD} is quantitative whereas absorption of H_{OPD} is not (55). In the case of metals which do not reveal the underpotential deposition of hydrogen, it is obviously H_{OPD} which becomes

absorbed in the lattice of the host metal. The UPD H from an acidic solution may be represented by the following surface reaction:

$$\underset{(1-\theta_{H_{UPD}})}{M} + \underset{a_{H_3O^+}}{H_3O^+} + e \rightarrow \underset{(\theta_{H_{UPD}})}{M-H_{UPD}} + H_2O \qquad [17]$$

where M represents the metal substrate on which the UPD H takes place, $a_{H_3O^+}$ is the activity of H_3O^+ species from which the underpotential deposited H (H_{UPD}) originates, $\theta_{H_{UPD}}$ is the H_{UPD} surface coverage. Charging-curve or cyclic-voltammetry (CV) measurements (4, 7-10, 31) show that up to a *monolayer* of underpotentially deposited H (H_{UPD}) is formed on these metal surfaces prior to the onset of the cathodic H_2 evolution.

Spectroscopic evidence reveals that H_{OPD} adsorbed on Pt and Rh electrodes interacts with water molecules forming a bond whereas H_{UPD} appears to be unavailable for binding H_2O molecules in the double-layer region (56-59). This observation indicates that H_{OPD} is bonded less strongly to the metal substrate than H_{UPD} (7,24,47,51). Experimental data (60-62) also reveal that on Pt electrodes, H_{UPD} co-exist with H_{OPD} in the negative potential region, thus the two species must occupy distinct surface adsorption sites in order to sustain their physico-chemical identity. Subsequently, if H_{UPD} and H_{OPD} occupy different adsorption sites, then their Gibbs free energies of adsorption, enthalpies of adsorption and bond energies should be discrete.

iv. Thermodynamics of Underpotential Deposition (UPD) of Hydrogen

The underpotential deposition (UPD) of hydrogen and certain metals of the *p* and *d* blocks of the periodic table on noble-metal electrodes has been a subject of intense studies in electrochemical surface science (4,8-12,20-25,46-48). In general, knowledge of the Gibbs free energies of adsorption for the electroadsorbed H_{UPD} and H_{OPD}, $\Delta G^\circ_{ads}(H_{UPD})$ and $\Delta G^\circ_{ads}(H_{OPD})$, respectively, leads to determination of the chemical potential gradient associated with the interfacial H transfer from the adsorbed to the absorbed state, thus it leads to elucidation of the thermodynamic driving force of the process (53,54). The latter is of vital

importance to the recently developing metal-hydride science because it defines the nature and strength of the M – H bond on the metal surface prior to the H interfacial transfer into the metal bulk. Studies on the enthalpies of adsorption of H_{UPD} and H_{OPD}, $\Delta H^{\circ}_{ads}(H_{UPD})$ and $\Delta H^{\circ}_{ads}(H_{OPD})$, respectively, and the bond energies between Pt and H_{UPD} or between Pt and H_{OPD}, $E_{Pt-H_{UPD}}$ and $E_{Pt-H_{OPD}}$, respectively, are of importance to electrochemical surface science because they allow assessment, on the thermodynamic basis, of the adsorption sites of the H_{UPD} and H_{OPD} surface species (56-62).

Despite significant amount of thermodynamic data (1,2,6) on the H chemisorbed from the gas phase (H_{chem}), thus Gibbs free energy of hydrogen adsorption, $\Delta G^{\circ}_{ads}(H_{chem})$, enthalpy of hydrogen adsorption, $\Delta H^{\circ}_{ads}(H_{chem})$, entropy of hydrogen adsorption, $\Delta S^{\circ}_{ads}(H_{chem})$ and metal-hydrogen bond energy, $E_{M-H_{chem}}$, there is a limited amount on data on thermodynamics of the UPD H. Thermodynamic measurements of H adsorption at (polycrystalline) Pt and other noble metals electrodes were first made at various temperatures by Breiter et al. (8,9,20-22) using the potentiodynamic sweep method. According to Breiter's approach, isotherms for hydrogen adsorption are plotted coverage versus logarithm of hydrogen pressure, P_{H_2}, for different temperature. The hydrogen pressure needed in the plotting of isotherms is calculated on the assumption of electrode equilibrium, and consequently P_{H_2} is given directly by the Nernst equation. The heat of adsorption, ΔH_i, at constant coverage can be computed from plot of $\ln P_{H_2}$ against the reciprocal of the absolute temperature by application of the following equation:

$$\left(\frac{d \ln P}{dT}\right)_{\theta} = -\frac{\Delta H_i}{RT^2} \qquad [18]$$

At that time, his values were calculated for H_2 and little emphasis was placed on significance of entropy of adsorbed H in relation to the coverage of the chemisorption of H which are found at Pt in very clean and dilute electrolyte solution. This work is an extension to the important, early research of Breiter et al. on Pt-group metals. In chapter 1 a new theoretical approach which allows determination of $\Delta G^{\circ}_{ads}(H_{UPD})$ versus $\left(T, \theta_{H_{UPD}}\right)$, in the form of 3D plots, and evaluation of $\Delta S^{\circ}_{ads}(H_{UPD})$ and $\Delta H^{\circ}_{ads}(H_{UPD})$ as a function of $\theta_{H_{UPD}}$ are demonstrated. In chapter 1 and chapter 2, new data are reported on $\Delta G^{\circ}_{ads}(H_{UPD})$,

$\Delta S^{\circ}_{ads}(H_{UPD})$ and $\Delta H^{\circ}_{ads}(H_{UPD})$ for Rh, Pt polycrystalline electrodes with respect to the concentration of the supporting electrolyte, thus the surface concentration of the specifically adsorbed anions. In chapter 3, the same methodology is applied in order to determine the thermodynamic state functions for Hydrogen adsorption on Pt single crystal electrode. For the first time, the $Pt-H_{UPD}$ surface bond energy, $E_{Pt-H_{UPD}}$ are determined.

v. Underpotential Deposition (UPD) of Hydrogen on Pt Single Crystals

The study of influence of crystallographic orientation for Pt electrode surfaces upon electrochemical reactivity is both technologically and fundamentally important (63-66). By studying single crystal Pt surfaces of controlled and known structure, it is hoped that the effects of site geometry upon the electrocatalytic properties of the electrode surface may be elucidated. The first study of electrosorption of hydrogen on three low index Pt single crystal surface was reported in 1966 by Will (67). These experiments were subsequently repeated by Angerstein-Kozlowska et al. (68). In these works the crystal surfaces were characterized by ultra high vacuum (UHV) techniques located in laboratories other than those in which electrochemical experiments were performed. During the transfer of the crystal from the UHV instrument to the electrochemical cell, the surfaces were exposed to contamination by the impurities present in ambient atmosphere. For that reason, the surfaces were cleaned during the electrochemical experiment by repetitive oxidation and reduction cycles, subsequently it was proven that this procedure damaged the crystallographic structure of the surface. Therefore, the results of these early experiments have mainly a historical significance today. Important progress was made in seventies when apparatus allowing for a fast transfer of crystal from a UHV chamber to an electrochemical cell, without exposure to the ambient atmosphere, were developed in the laboratories of Hubbard (69,70), Ross (71) and Yeager (72,73). These systems allowed for the determination of structure and purity of the single crystal surface by Low Energy Electron Diffraction (LEED) and Auger Electron Spectroscopy just a few minutes before or after an electrochemical experiment. In the following years, transfer systems were further developed (74,75), as described in a number of review articles (76,77). A new stimulus to the development of the single crystal electrochemistry was given by Clavilier et al. (78,79) at the beginning of eighties, when he developed a quenching technique. The method involved heating the Pt crystal in an hydrogen flame to approximately 1100 °C, quenching rapidly in ultra pure water under hydrogen-argon

atmosphere, then transferring to an electrochemical cell with the surface protected by surrounding film of water. The results obtained on the quenched electrodes were extremely reproducible (80,81). Clavilier results were reproduced in other laboratories (82-87). Later, after improvements of experimental procedures and in the cleanness of UHV equipment, results similar to those obtained on the quenched electrodes were reproduced in UHV/electrochemistry systems as well (88-90).

vi. Hydrogen Underpotential Deposition (UPD) on Pt Polycrystalline Pt and Single crystalline Pt in Presence of Chemisorbed Sulfur

It is known that certain elements or compounds adsorbed on the metal surface and referred to as *site blocking elements*, SBE, possess the ability of enhancing or decreasing the H transfer from the *adsorbed* to the *absorbed* state (53,60-62,91-95). The SBE's chemisorbed on the metal surface reveal a *dual action* and behave either as *surface poisons* or as *surface promoters* depending on their physico-chemical nature (53). The surface promoters can effectively enhance the rate of H interfacial transfer and increase the amount of H absorbed in the host metal, thus increasing its capacity. The latter is of vital importance to high energy-density M-H batteries which are an alternative to the Ni-Cd ones. On the other hand surface poisons which suppress the H interfacial transfer are excellent inhibitors of H embrittlement of metal structures. Experimental evidence indicates that chemical species such as CO, urea, thiourea, compounds of As, Se, S and P as well as heterocycles are known to affect the adsorption of H in the region corresponding to the underpotential deposition of H, UPD H, and the kinetics of the HER (53,95-100). Their action was a subject of thorough theoretical research and numerical simulations based on the lateral interactions between the electroadsorbed H and the coadsorbed SBE's (53). SBE's affect catalytic properties of the electrified solid/liquid interface through the following action: (i) they can block surface adsorption sites; (ii) they affect energetics of the reaction at the double-layer; (iii) they change the work function of the substrate; (iv) they influence the charge transfer at the electrode/solution interface; and (v) they affect adsorption behavior of the reaction products and intermediates. Sulfur, S, is of vital interest to electrochemical surface science, metal hydride science and technology, and corrosion science because it is a model SBE. The species undergoes strong chemisorption and sustains its chemical identity on the metal electrode

surface. Cathodic polarization does not lead to its desorption through formation of a reduced derivative and it can be desorbed only through oxidation at high positive potentials (101,102). The results on S chemisorption and its influence on the UPD H on Pt polycrystalline electrodes (in chapter 2.2) and Pt single crystal (in chapter 3.4) electrodes are presented. A relation between the S surface coverage, θ_S, and the coverage by H_{UPD}, $\theta_{H_{UPD}}$ is determined. Temperature dependence experimental studies followed by comprehensive theoretical treatment result in determination of ΔG°_{ads}, ΔS°_{ads} and ΔH°_{ads} in absence and presence of S. The changes of the $Pt(poly)-H_{UPD}$ and $Pt(111)-H_{UPD}$ bond energies brought by the S submonolayer are evaluated.

vii. Experimental Methods for Studies of Hydrogen Adsorption on Metal Electrode Surface in Presence/Absence of Chemisorbed Sulfur

Cyclic-Voltammetry

Electrochemical techniques provide a very sensitive method for study of surface processes down to 2% of monolayer coverage of H_{UPD}. One of the most useful techniques for study of electrode surface processes is linear potential sweep method or cyclic-voltammetry as it is called when applied in a repetitive manner with successive cathodic-and anodic-going changes of potential. The application of cyclic-voltammetry technique of Sevcik (103) to the study of surface processes at Pt by Will and Knorr (4) and employed in many papers by Breiter, Knorr and co-workers showed clearly, for first time, the existence of more that one state of H adsorption.

In cyclic-voltammetry, the potential, E, of the working electrode is changed linearly with time, t, at constant sweep-rate, s ($V\ s^{-1}$), according to the equation

$$E = E_i + s\,t \qquad [19]$$

or

$$\frac{dE}{dt} = s \qquad [20]$$

where E_i is some initial potential that may or may not be held constant for some period of time. The method may employ either a single sweep (half-cycle) between the initial potential, E_i, and the final potential, E_f, or it may be programmed to give a repetitive response of the electrode by varying the potential between E_i and E_f, forward and backward, in a continuous manner.

The information obtained from this technique includes the behavior and characteristics of the electrochemical process involved, indication of any complicating side-reactions such as "pre-electrochemical" or "post-electrochemical" chemical reactions (such as place-exchange in oxide film formation), and general kinetic behavior such as slowness of charge-transfer steps or the development of limiting current due to "pre-electrochemical" chemical steps such as molecular dissociation, chemisorption, isomerization or ionization. The standard electrical circuitry required for this technique was shown in many references (31,104-105).

The cyclic-voltammetry technique is very useful in electrochemical studies due to its high resolution and sensitivity. It is able to: (a) determine surface coverage down to 5% of a mono layer (θ= 0.05); (b) resolve states which differ only by 10 mV i.e. ca. 965 J of Gibbs energy; and (c) characterize time effects down to the 10 μs level. The current response to the applied potential, E, i.e. the current recorded, may be represented as the first derivative of charge with respect to time:

$$i = \frac{dq}{dt} = \frac{dq}{dE} \cdot \frac{dE}{dt} \qquad [21]$$

Since $\frac{dq}{dE} = C$ (capacitance) and $\frac{dE}{dt} = s$ (sweep rate), The current response may be represented by the following formula:

$$i = C \cdot s \qquad [22]$$

It is possible to calculate the total charge passed between two potential limits E_1 and E_2, by rearranging the equation [20] to

$$dq = i\,dt \qquad [23]$$

Integration between the two potential limits allows us determine the charge, q, according to the equations

$$q = \int_{E_1}^{E_2} dq = q(E_2) - q(E_1) \qquad [24]$$

$$q = \int_{E_1}^{E_2} i\,dt = \int_{E_1}^{E_2} \frac{i}{s}\,dE = \int_{E_1}^{E_2} C\,dE \qquad [25]$$

where C can be a function of potential, C=F(E).

For surface processes, small coverage may be determined using the formula

$$dq = q_1\,d\theta \qquad [26]$$

where q_1 is the charge required to form one monolayer of the adsorbed species.

Sweep-rate Dependence of Current: Diffusion Control

The electrode reaction rate (expressed as a current-density) is normally either under activation control (i.e. the reaction kinetics are determined by the rate of formation of activated complexes) or diffusion control. For an electrochemical reaction having sufficiently large rate constant, and/or at sufficient low reagent concentration, the process may be diffusion-controlled, with a concentration gradient developed normal to the electrode surface where the reagent is consumed. This process may be either reversible or irreversible. The activities of oxidized, [Ox], and reduced, [Red], species at the electrode surface are related to potential by the Nernst equation:

$$E = E^\circ + (RT/zF)\ln\frac{[Ox]}{[Red]} \qquad [27]$$

where E° is the standard reversible potential.
Various researchers (103,106-110) have solved the Fick equations for cyclic-voltammetry where the kinetics are under diffusion control. For such conditions, the peak current, i_p, varies linearly with the square root of the sweep rate, $s^{1/2}$, both for reversible and irreversible process, according to the equations:

$$i_p = (2.69 \times 10^5)\, z^{3/2}\, D^{1/2}\, c\, A\, s^{1/2} \qquad \text{(reversible)} \qquad [28]$$

$$i_p = (2.69 \times 10^5)\, z(z_\alpha \alpha)^{1/2}\, D^{1/2}\, c\, A\, s^{1/2} \qquad \text{(irreversible)} \qquad [29]$$

where is the electrode area (cm^2), D is the diffusion coefficient ($cm^2\ s^{-1}$), c is the concentration (mol cm^{-3}), s is the sweep rate ($V\ s^{-1}$), z is the number of electrons transferred, z_α is the number of electrons involved in the rate determining step and α is the transfer coefficient in the irreversible case.

Under diffusion-controlled conditions, the following quantitative characteristics of the i vs E are to be noted:

(a) The difference between anodic and cathodic peak potential at 298 K is:

$$\Delta E = E_{p,c} - E_{p,a} = 2 \times (0.028 / z) \qquad [30]$$

(b) The difference between anodic and half-wave potential, $E_{1/2}$, at 298 K is:

$$E_p - E_{1/2} = -1.1 \times (RT / zF) \qquad [31]$$

Peak potential and Peak Current for surface Process Control

In the case of surface reactions, no mass transfer processes are involved in the kinetics so the current response behavior to a potential sweep is simpler than for the diffusion-control case. A simple one electron surface reaction (z = 1), not influenced by diffusion, may be represented by the reaction [1]. Based on the Langmuir isotherm, the current can be written as:

$$i = q_1\left[k_1 c_A(1-\theta_A)\exp\left(-\alpha F(E-E^{o'})/RT\right) - k_{-1}\theta_A \exp\left((1-\alpha)F(E-E^{o'})/RT\right)\right] \qquad [32]$$

where q_1 is the charge required to form a monolayer of species A, k_1 and k_{-1} are the standard rate constants at the reversible potential, $E^{o'}$ is the formal potential, corresponding to the peak potential of the process, c_A is the concentration of species A in the solution and α is the transfer coefficient. For reversible process, the exponential components of the above equation are comparable and large while an irreversible process the first component is much greater than the second one ($k_1 >> k_{-1}$), or vice versa.

Srinivasan and Gileadi (111) have derived equations which relate current to potential as a function of sweep-rate for a simple Langmuir-type surface process of the equation [32]. For a reversible adsorption process, the peak current and potential are given by the equations:

$$i_p = (q_1 zF/4RT)s \qquad [33]$$

$$E_p = (RT/zF)\ln k_1 \qquad [34]$$

For an irreversible process, i.e. $k_1 >> k_{-1}$,

$$i_p = (q_1 \alpha z_\alpha F/2.718RT)s \qquad [35]$$

$$E_p = (RT/z_\alpha \alpha F)\ln\left[(RT/\alpha z_\alpha F)(k_1/s)\right] \qquad [36]$$

Characterization of Single crystals: The von Laue X-ray Back Reflection Technique

The von Laue method is the oldest of the X-ray diffraction methods (1912). A collimated beam of continuos spectrum falls upon a fixed single crystal. For set of planes (hkl), the spacing d(hkl) and the Bragg angle θ(hkl) are fixed. A reflected beam will be produced if the correct wavelength which satisfies the Bragg Law is contained in the continuous spectrum:

$$n\lambda = 2d(hkl)\sin\alpha; \qquad n = 1, 2, 3 \qquad [36]$$

where α is the incident angle. The different reflected beams have different wavelengths and hence a Laue pattern is "colored" (112-115).

The back reflection Laue pattern is much used today for the orientation of single crystals, particularly for the orientation of single cubic crystals. The interpretation of the back-reflection Laue pattern is greatly facilitated by the use of the Greninger chart (116). Since the interpretation of back-reflection Laue patterns is complex operation and consists of many steps, it will not be discussed further here, specially since the interpretation procedure is well explained in the literature devoted to X-ray diffraction (112-115). However, it is worthwhile mentioning that to interpret a cubic pattern, one looks for the three most important spots on pattern. These will be the low-index reflections (100), (110) or (111), and they will be characterized by the fact that they are quite sharp, that there is an appreciable open space around them, and that they arise at the intersections of several main zone lines.

Surface Analysis Techniques: Low Energy Electron Diffraction (LEED), Auger Electron Spectroscopy (AES) and Core Electron Energy loss spectroscopy (CEELS)

The two most common support surface analysis techniques to an investigation by other methods for studies on well-characterized surfaces are Low Energy Electron Diffraction (LEED) and Auger Electron Spectroscopy (AES). LEED provides a simple and convenient characterization of the surface long range order while AES provides some indication of chemical composition and, in particular, characterizes the cleanness of a surface. Moreover, both can be installed using the same piece of instrumentation. The wide use of standard characterization probes such as LEED and AES has greatly improved our ability to compare studies of any particular adsorption system by different techniques performed in different laboratories. A glance at a LEED diffraction pattern shows the basic periodicity of ordered component of the surface structure. AES has been widely used to determine surface and subsurface composition.

In LEED, low energies of about 10 to 500 eV are used which ensure that the diffraction is caused only by atoms on and close to the surface. A typical LEED pattern is obtained by photographing the fluorescent screen through the viewing port. This pattern reveals the two-dimensional structure of the surface. The pattern is sharp if the surface is well-ordered for

distances long compared with the wavelength of the incident electrons. In practice, sharp patterns are obtained for surfaces ordered to depths of about 20 nm and more. Diffuse patterns indicate either a poorly ordered surface or the presence of impurities (117).

In AES, when an atom is ionized the production of a core hole, either by an incident photon, or by an incident electron of sufficient energy, the ion eventually loses some of its potential energy by filling this core hole with an electron from a shallower level together with the emission of energy. This energy may either appear as a photon, or as kinetic energy given to another shallowly bound electron. These competing processes are dominated by the photon emission only when the initial core hole is deeper than about 10 keV. From conservation of energy, the energy of secondary electron must equal the energy gained when the core hole is filled minus the initial energy of the electron before it is ejected, plus some corrections due to incomplete relaxations and so called final state effects. Indeed, this is the physical process used in a conventional laboratory X-ray generator. The alternative radiationless emission of the energy as electron kinetic energy is Auger effect, named after its discoverer, Pierre Auger. Auger electron emission is an efficient means of filling core holes of low binding energy, thus giving rise to relatively low kinetic energy Auger electron of short mean-free path. their detection outside the solid therefore provides a surface sensitive probe of chemical composition. While the initial core hole may be created by either incident photons or incident electrons, the relative ease of producing sufficiently energetic ($\approx 1.5-5$ keV) electron beams of high intensity (1-100 μA) means that AES is invariably performed with incident electron beams. Most AES studies simply use the Auger spectrum as a fingerprint of the chemical composition and are not concerned with a detailed understanding of basic processes. Nowadays, the collections of fingerprint spectra for essentially all elements exist for the purposes of species identification (118). To suppress the large secondary electron background, the Auger spectrum now being shown in a differentiated form with respect to the energy and this way a simple peak is turned into a positive and negative excursion. Studies of difference in energy between a photoelectron peak and its associated Auger electron have the distinct advantage of showing up "chemical shift" effects without the need to make accurate absolute energy measurements. It is usual to label the Auger transition using the X-ray level notations, for example, a transition involving a 1s level and 2p levels (which may have the same energy) would be labeled as a $KL_{2,3}L_{2,3}$ transition (119).

The chemical states of adsorbed species on the substrate can be identified by a Core Electron Energy loss spectroscopy (CEELS) (120-122). In CEELS, the primary electrons from electron gun undergo inelastic scattering with the energy loss ΔE preceded, or followed by elastic back scattering towards the electron energy analyzer (123). The observed electron energy loss intensity is therefore due to a small angle electron inelastic scattering under dipole scattering condition. By varying the primary electron energy, in the range of a few hundred eV above the electron core level ionization energy, this technique is surface sensitive (120-125). The loss energies is often measured relative to the electron elastic peak. The primary energy must be high enough to be able to ionize the core levels of interest with enough efficiency, and in addition the ionization thresholds will often be several hundreds eV from the elastic peak. Thus primary energies of 2-4 KeV are typical but the kinetic energy range recorded would not usually be continuos up to the elastic peak since it would be only the structure in the region of the threshold itself that would be of interest. When a primary electron of sufficient energy interacts with an electron in a core level, the resultant excitation can be either to an unoccupied continuum state, in with case complete ionization occurs, or to localized or partly localized final states if available in the atom. Since the primary electron need not give up all its energy in the interaction (unlike a photon) and since after interaction in the solid the erstwhile primary and the secondary become indistinguishable, the loss feature observed in the spectrum should appear as a step at the ionization threshold, with a tail of secondaries at all energies from the threshold down to zero. However, because of much greater cross-section near threshold than further away, loss features appear more usually peaks, followed by a tail.

CHAPTER 1

EXAMINATION OF THERMODYNAMICS OF THE UNDERPOTENTIAL DEPOSITION AND IT'S FURTHER DEVELOPMENT

The fundamentals of hydrogen physisorption and chemisorption from the gas phase, and the adsorption sites of the physisorbed H (H_{phys}) and the chemisorbed H (H_{chem}) are fairly well understood. Also, chemical and physical properties of various metal hydrides are well characterized and documented (1-3). However, electrochemical surface-science aspects involved in cathodic H adsorption and absorption still require further research and careful elucidation. The chapter 1 develops the concepts that are needed for the examination of thermodynamics of the underpotential deposition. The objectives of the paper in section 1.1 are as follows: (i) discussing the basic steps involved in the cathodic H adsorption on the metal electrode surface; (ii) comparing the cathodic H adsorption and subsequent absorption, with the gas-phase stages of H chemisorption and entry into the host metal; (iii) defining the underpotential deposited H (H_{UPD}) and the over-potential deposited H (H_{OPD}) and explaining their role in the HER and H absorption; (iv) discussing thermodynamic methodology used in determination of $\Delta G^{\circ}_{ads}(H_{UPD})$, $\Delta S^{\circ}_{ads}(H_{UPD})$ and $\Delta H^{\circ}_{ads}(H_{UPD})$ for H_{UPD}, and compares the value of $\Delta H^{\circ}_{ads}(H_{UPD})$ with $\Delta H^{\circ}_{ads}(H_{chem})$ for Rh; (v) demonstrating a new theoretical formalism for determination of the $M-H_{UPD}$ bond energy ($E_{M-H_{UPD}}$) ; (vi) defining the chemical potentials of H_{chem}, H_{UPD}, H_{OPD} and subsurface H, H_{ss}; (vii) formulating the chemical-potential gradient of H associated with its interfacial transfer across the liquid/solid or gas/solid interfaces in terms of the surface H coverage, θ_H, and the lattice occupancy fraction X_H. The paper in section 1.1 (*G. Jerkiewicz and A. Zolfaghari, J. Electrochem. Soc., 144, 3034 (1997)*) is a result of my essential contribution in experimental and theoretical parts. The contribution of Dr. G. Jerkiewicz was in theoretical and writing constituent.

The section 1.2 deals with a thermodynamic approach to investigate the underpotential deposition of hydrogen (UPD H) on Rh electrodes in three different concentrations of aqueous solutions of H_2SO_4 as an example system for UPD H on metal electrodes, using cyclic voltammetry (CV) over a wide temperature range for providing exprimental data. In the course of this section a theoretical treatment of the experimental data based on an electrochemical adsorption isotherm provides the following the information for the

underpotential deposition of hydrogen (UPD H) on Rh electrodes: (i) the Gibbs free energy of adsorption, $\Delta G^{\circ}_{ads}(H_{UPD})$, as a function of temperature and the H surface coverage; (ii) the standard entropy of adsorption based on temperature dependence of $\Delta G^{\circ}_{ads}(H_{UPD})$ for a constant surface coverage of the underpotential deposited H (H_{UPD}), $\Delta S^{\circ}_{ads}(H_{UPD})$; (iii) the standard enthalpy of adsorption, $\Delta H^{\circ}_{ads}(H_{UPD})$; (iv) the UPD H is an enthalpy-driven process which can be concluded from an analysis of the values of $\Delta H^{\circ}_{ads}(H_{UPD})$ and $\Delta S^{\circ}_{ads}(H_{UPD})$; (v) the bond energy between Rh and H_{UPD}, $E_{Rh-H_{UPD}}$, from knowledge of $\Delta H^{\circ}_{ads}(H_{UPD})$ which depends on the H_{UPD} surface coverage ($\theta_{H_{UPD}}$); (vi) comparing $E_{Rh-H_{UPD}}$ with $E_{Rh-H_{chem}}$ which may point to a similar binding mechanism of H and the same adsorption site of H_{UPD} and H_{chem} under the conditions involving presence of the electrified solid/liquid interface and the gas phase. The paper in section 1.2 (*G. Jerkiewicz and A. Zolfaghari, J. Phys. Chem., 100, 8454 (1996)*) is a result of my essential contribution in experimental, theoretical and writing parts. The contribution of Dr. G. Jerkiewicz was in theoretical and writing constituent.

The section 1.3 stablishes a theoretical methodology which allows determination of the state functions (ΔG°_{ads}, ΔS°_{ads}, ΔH°_{ads}) of the underpotential deposition on metal electrodes. The theoretical treatment is based on a general electrochemical isotherm and adsorption thermodynamics whereas the experimental methodology involves application of cyclic-voltammetry over a wide temperature range, or chronocoulometry. The paper in section 1.3 presents new general approach which permits elucidation of the bond energy between the substrate, S, and underpotential deposited species (hydrogen, $E_{S-H_{UPD}}$, metal or semiconductor, $E_{S-M_{UPD}}$). Understanding of $E_{S-H_{UPD}}$ is essential in assessment of the strength of the $S-H_{UPD}$ bond and the adsorption site of H_{UPD}. Knowledge of $E_{S-M_{UPD}}$ is of importance in: (i) evaluation of the strength of the cohesive forces acting between S and M_{UPD} that are responsible for the adhesion of the adsorbate to the substrate; and (ii) comparison of the $S-M_{UPD}$ bond with that observed for the 3-D bulk deposit of M. The UPD H on Rh and Pt electrodes from aqueous H_2SO_4 solution is discussed as an example of application of this methodology. The paper in section 1.3 (*A. Zolfaghari and G. Jerkiewicz in Solid/Liquid Electrochemical Interface., Eds. G. Jerkiewicz, M. P. Soriaga, K. Uosaki and A. Wieckowski, ACS Symposium Series, ACS, Washington D.C., No. 656, Chapter 4, 45 (1997)*) is a result of my essential contribution in experimental, theoretical and writing parts. The contribution of Dr. G. Jerkiewicz was in theoretical and writing constituent.

1.1 COMPARISON OF HYDROGEN ELECTRO-ADSORPTION FROM THE ELECTROLYTE WITH HYDROGEN ADSORPTION FROM THE GAS PHASE

G. Jerkiewicz and A. Zolfaghari, J. Electrochem. Soc., 143, 1240 (1996)

ABSTRACT

The paper focuses on fundamental aspects associated with H adsorption at the solid/liquid and solid/gas interfaces, and compares H electroadsorption from the electrolyte with dissociative H chemisorption from the gas phase. At the solid/liquid interface, two distinguishable electroadsorbed H species are observed, the underpotential deposited H (H_{UPD}) and the over-potential deposited H (H_{OPD}) and their role in the HER and H absorption is discussed. At the solid/gas interface, there is only one distinguishable H species, chemisorbed H (H_{chem}), which can undergo interfacial transfer into the metal. Three distinct mechanisms of H electroabsorption into the metal electrode are discussed in relation to the adsorption sites of H_{UPD} and H_{OPD}. The paper discusses thermodynamic methodology used in determination of $\Delta G^{\circ}_{ads}(H_{UPD})$, $\Delta S^{\circ}_{ads}(H_{UPD})$ and $\Delta H^{\circ}_{ads}(H_{UPD})$ for H_{UPD}, and compares the value of $\Delta H^{\circ}_{ads}(H_{UPD})$ with $\Delta H^{\circ}_{ads}(H_{chem})$. The authors demonstrate new theoretical formalism which is applied to determination of the $M-H_{UPD}$ bond energy ($E_{M-H_{UPD}}$). New data demonstrate that H_{UPD} and H_{chem} are bonded to Rh with the same energy; this points to the same binding mechanism and the same adsorption sites of H_{UPD} and H_{chem}. The chemical potentials of H_{chem}, H_{UPD}, H_{OPD} and subsurface H, H_{ss}, are defined and the chemical-potential gradient of H associated with its interfacial transfer across the liquid/solid or gas/solid interfaces is formulated in terms of the surface H coverage, θ_H, and the lattice occupancy fraction X_H.

INTRODUCTION

Studies of the hydrogen evolution reaction (HER), hydrogen adsorption on metallic surfaces and H absorption into host metals/alloys are of great relevance to electrochemistry, surface science, gas-phase physics, and materials and corrosion sciences (1-14). Comprehension of the basics of H adsorption on the metal surface, followed by its interfacial transfer into the metal bulk, is also of great importance in recently developing metal-hydride science and technology. For instance, AB -type and AB_5 -type intermetallic alloys (15-19) are becoming more common as anodes in primary and secondary batteries. Understanding of hydrogen on the surface of electrocatalysts is of primary importance to hydrogen-based fuel cells since it is the interaction with the substrate which determines the efficiency of hydrogen oxidation. In corrosion science, knowledge of fundamental steps involved in H entry into the host metal is of vital significance in protecting metal structures from undergoing H embrittlement, a costly and often disastrous process. Undesirable entry of H into host metallic

alloys limits its application as a fuel in space and aviation technology as well as a fuel in internal combustion engines; the H-induced material disintegration is highly enhanced by high operating pressures and temperatures. Entry of hydrogen isotopes into metallic alloys is of primary concern in fusion technology where H, D and T are either reactants or products of nuclear events; diffusion of T through the metal shielding to the liquid Li cooling system leads to serious and irreversible environmental problems (1-3, 5).

The fundamentals of hydrogen physisorption and chemisorption from the gas phase, and the adsorption sites of the physisorbed H (H_{phys}) and the chemisorbed H (H_{chem}) are fairly well understood. Also, chemical and physical properties of various metal hydrides are well characterized and documented (1-3). However, electrochemical surface-science aspects involved in cathodic H adsorption and absorption still require further research and careful elucidation. It is the objective of this paper to discuss the basic steps involved in the cathodic H adsorption on the metal electrode surface, and subsequent absorption where applicable, and compare them with the gas-phase stages of H chemisorption and entry into the host metal. The underpotential deposited H (H_{UPD}) and the over-potential deposited H (H_{OPD}) are defined, and their role in the HER and H absorption is discussed. The authors present experimental and theoretical methodology used in determination of the Gibbs free energy, entropy and enthalpy of adsorption of H_{UPD}, $\Delta G^{\circ}_{ads}(H_{UPD})$, $\Delta S^{\circ}_{ads}(H_{UPD})$ and $\Delta H^{\circ}_{ads}(H_{UPD})$, respectively. They demonstrate new theoretical methodology which is used in evaluation the energy of the bond between the metal substrate and H_{UPD}. They also derive a formula which explains the origin of the UPD H. Finally, the chemical potential of the adsorbed, subsurface and absorbed H species are discussed, as well as the chemical potential gradient associated with the interfacial H transfer from the surface of the metal electrode into its bulk in terms of the surface H coverage (θ_H) and the three-dimensional lattice occupancy fraction (X_H).

ELECTROCHEMICAL vs. GAS-PHASE H ADSORPTION PATHWAY

Electroadsorption

The difference between H adsorption from the electrolyte and from the gas-phase is of major importance in understanding of the elementary steps involved in the processes of hydrogen adsorption on metallic surfaces. In principle, hydrogen electroadsorption (also referred to as electrosorption) can be accomplished from either acidic or basic aqueous solutions or from non-aqueous solutions which are capable of dissolving H-containing acids, thus sources of proton. In aqueous acidic solution, the proton, H^+, cannot exist by itself and

it combines easily with a non-bonding electron pair of a water molecule forming a chemical bond and leading to H_3O^+; this bond formation is associated with an enthalpy change of -754 kJ mol^{-1}. The H_3O^+ is further hydrated to the time-average state $H_9O_4^+$ (it can also be presented as $H^+ \cdot 4H_2O$) with an additional stabilization energy of -356 kJ mol^{-1} due to ion-solvent dipole interactions and long-range order polarization of the solvent (20). Owing to transport phenomena within the electrolyte, brought about by the externally applied electrostatic field, the $H^+ \cdot 4H_2O$ ion encounters the region close to the electrode surface where the H^+ discharge takes place with formation of the *adsorbed* H species (4, 7-10, 21, 22) according to the following equation:

$$H^+ + e^- + M \rightarrow M-H_{ads} \qquad [1]$$

where M represents a surface atom of the metal substrate. In reaction [1] the hydrating H_2O molecules are omitted for simplification. During this process, the hydration shell surrounding H^+ is dismantled and the adsorbed H is formed (20, 22). The adsorbed species is bound to the metal surface with its characteristic $M-H$ bond energy, E_{M-H} (see ref. 23). Such an adsorbed species can undergo subsequent reactions, as follows (21, 22):

$$H^+ + e^- + M-H_{ads} \rightarrow M + H_2^{\uparrow} \qquad [2]$$

$$2M-H_{ads} \rightarrow 2M + H_2^{\uparrow} \qquad [3]$$

$$M-H_{ads} \rightarrow M-H_{abs} \qquad [4]$$

Equations [2] and [3], which follow step [1], are *alternative* pathways of the HER. In the case of metals capable of *absorbing* H, process [4] occurs simultaneously (in a coupled manner) with the HER and competes with it (22). Reaction [4] describes the interfacial H transfer from the *adsorbed* to the *absorbed* state; it is followed by H *diffusion* in the metal bulk (22). The 3-dimensional H diffusion in the host's bulk is often the rate determining step in hydrogen absorption and it limits the charging/discharging kinetics. It should be stressed that another H state, the *subsurface* H, H_{ss}, has been suggested to exist (24-28) on Pt, Pd and Ni surfaces. The existence of H_{ss} on Pt and Ni single-crystal surfaces has been a subject of intense research and it is not proven unambiguously. However, it is evident that in the case of

metals capable of absorbing H such as Pd, the subsurface H represents a H species residing beneath the topmost surface layer of the metal.

Physisorption

In the case of H adsorption from the gas-phase, the adsorption pathway is different and often depends on the very nature of the metallic surface and the temperature at which the process takes place. At very low temperatures (from 5 to 20 K), the H_2 molecule approaches the surface and weak interaction forces of the van der Waals nature set in - this is the *physisorption* of the H_2 molecule (equation 5) and the respective physisorptive binding energy of the H_2 molecule, $E_{phys}(H_2)$, is between 3.5 and 15 kJ mol^{-1}, the process being exothermic (see ref. 6).

$$M + H_2 \rightarrow M - H_{2,\,phys} \qquad [5]$$

It should be emphasized that H physisorption does not involve dissociation of the H – H bond which remains intact.

Chemisorption

A completely different interaction pattern is observed at higher temperatures at which the H_2 molecule is dissociated into atoms prior to interaction with the surface (6). The dissociation energy of some 435 kJ mol^{-1} has to be spent. Afterwards, the *1s* orbitals of the H atoms form chemical bonds with the metallic surface. The depth of the potential energy well of this bond is between 500 and 600 kJ mol^{-1} of H_2 molecules. These steps can be represented by the following scheme:

$$H_2 \rightarrow 2\,H^* \qquad [6]$$

$$2\,H^* + 2\,M \rightarrow 2\,M - H_{chem} \qquad [7]$$

where H^* describes the energetically rich, atomic H prior to adsorption. The process of H chemisorption is known (6) to proceed by two distinctive pathways: (a) *activated*, or (b) *non-activated*. In the non-activated pathway, H_2 undergoes spontaneous dissociation with a release of the *enthalpy of adsorption*, ΔH°_{ads}, and it leads to the chemisorbed H. In the

activated pathway, H_2 has to pass over an *activation barrier* with the respective activation energy, E^*, before the dissociation occurs. Generally, the energy balance of the chemisorption is calculated according to the following equation:

$$E_{M-H_{chem}} = \frac{1}{2} D_{H_2} - \Delta H^\circ_{ads}(H_{chem}) \qquad [8]$$

where D_{H_2} is the dissociation energy of the H_2 molecule and $\Delta H^\circ_{ads}(H_{chem})$ is the enthalpy of H chemisorption (negative value) and $\Delta H^\circ_{ads}(H_{chem}) = - q^\circ_{ads}$, where q°_{ads} is the heat of adsorption; the above formula refers to one mole of chemisorbed H species. The values of the $M - H_{chem}$ bond energy, $E_{M-H_{chem}}$, for various transition metals is almost independent of the nature of the metal substrate or its surface geometry and fall into the range $250 - 270$ kJ mol^{-1} (6).

RELATION BETWEEN UPD H AND OPD H

UPD H and OPD H as Two Distinct Electroadsorbed Species

An important and unique aspect of H electroadsorption on Pt, Pd, Rh and Ir electrode surfaces is the phenomenon of the underpotential deposition of H (UPD H), a process which takes place *above* the potential required for the onset of the cathodic H_2 evolution, thus above the H^+ / H_2 reversible potential, E°_{HER} *. Charging-curve or cyclic-voltammetry (CV) measurements (4, 6-10, 21) show that up to a *monolayer* of underpotentially deposited H (H_{UPD}) is formed on these metal surfaces prior to the onset of the cathodic H_2 evolution. At potentials *below* E°_{HER} **, the over-potential deposition of H (OPD H) takes place on all metallic surfaces and the over-potentially deposited H (H_{OPD}) acts as an intermediate in the HER; the surface coverage by H_{OPD} can be determined experimentally based on potential-decay measurements (7). Interestingly, H_{UPD} and H_{OPD} can coexist on Pt, Pd, Rh and Ir electrodes at potentials below E_{HER}. Both the UPD H and OPD H may be represented by reaction [1] but the two surface species are distinct; their Gibbs free energies of adsorption (ΔG°_{ads}) are different, negative for H_{UPD}, $\Delta G^\circ_{ads}(H_{UPD}) < 0$, and positive for H_{OPD}, $\Delta G^\circ_{ads}(H_{OPD}) > 0$, and the species occupy distinguishable surface adsorption sites, as it will be

---

* The UPD H is a process which takes place above the H^+ / H_2 equilibrium potential, E_{eq}.

** The OPD H is a process which takes place below the H^+ / H_2 equilibrium potential, E_{eq}.

discussed below (29, 30). Thus, the notation H_{ads} is not specific enough and one should use the two explicit symbols, H_{UPD} and H_{OPD}, to distinguish between the two electroadsorbed H species. The UPD H can occur when the following thermodynamic condition is fulfilled: $1/2\,D_{H_2} - \Delta H^{\circ}_{ads}(H_{UPD}) \rangle 0$; the origin of this inequality is discussed in the section on *Thermodynamics of H Electroadsorption*.

The common perception that H_{UPD} and H_{OPD} are two distinct surface species occupying two different surface adsorption sites has been proven by Marcus and Protopopoff (29, 30) who have demonstrated that the UPD H can be completely blocked on Pt electrodes by co-adsorbed S adatoms, yet the HER can still take place. Their experimental and theoretical data on the UPD H and the HER at Pt electrodes covered with a submonolayer of S_{ads} demonstrate unambiguously that H_{UPD} is not an intermediate in the HER at Pt electrodes.

Another significant aspect of H electroadsorption on metal electrodes is the surface coverage that can be accomplished by H_{UPD} and H_{OPD}. In the case of Rh and Pt electrodes, the surface coverage by H_{UPD} is potential dependent and a full monolayer of H_{UPD} is formed prior to the onset of the HER (Fig. 1). Upon stopping the potential cycling, the current drops to the current of double-layer charging* indicating that no adsorption/desorption processes take place; when one restarts the potential cycling, the CV profile follows the profile as during continuous cycling. Contemporary *in-situ* AC impedance and potential-decay measurements (7, 21) on Pt, Pd, Pd-Pt, Ni and Ni-based alloys show that the surface coverage by the H_{OPD}, involved in the cathodic H_2 generation, rarely exceeds the surface coverage of some 30 % ($\theta_{H_{OPD}} \leq 0.30$). Only in the case of Pt electrodes (31), the coverage by H_{OPD} approaches the limiting value of unity at very high negative overpotentials ($\theta_{H_{OPD}} \rightarrow 1$). This experimental evidence and the previously discussed results allows a clear distinction to be made between the H_{UPD} and H_{OPD}. Thus, an obvious questions arises, what are the true surface adsorption sites of these two distinguishable electroadsorbed H species?

Adsorption Sites of the UPD H and OPD H

In recent years, important electrochemistry-FTIR measurements (29-33) have been conducted on the UPD H and the HER taking place at Pt, Rh, Pd and Ir having the (111), (100) or polycrystalline surface orientations. The experiments have been aimed at determination of the true adsorption sites of H_{UPD} and H_{OPD}. The results may be summarized

* Upon stopping the potential cycling, the current drops to zero.

as follows: (i) H_{UPD} forms a covalent bond with the metal substrate and it is multicoordinated; (ii) H_{UPD} occupies the three-fold hollow site on the fcc(111) surface and the four-fold one on the fcc(100) face; (iii) H_{OPD}, which is an intermediate in the HER, forms a weaker bond with the substrate than H_{UPD}; (iv) H_{OPD} interacts with H_2O molecules in the double-layer region; (v) H_{OPD} is singly coordinated, thus it occupies the on-top site. In the case of Pt(poly), two H_{UPD} adsorption peaks are observed; the one at 0.30 V, RHE, has been assigned to the so-called *strongly-bonded* H whereas the peak at 0.15 V, RHE, to the *weakly-bonded* H. It should be added that the discussion on the adsorption sites of these two surface species is still going on and, at present, it is premature to conclude whether the strongly-bonded H corresponds to H being screened in the metal surface (sandwiched between the first two surface layers of the substrate), thus corresponding to the *subsurface* H, H_{ss}.

The above discussed electrochemical and FTIR experimental evidence (29-33) leads to assignment of the actual adsorption sites of H_{UPD} and H_{OPD} which are visualized in Fig. 2 showing the fcc(111) surface with H_{UPD} occupying the *three-fold hollow site* and H_{OPD} the *on-top site*.

There are two kinds of three-fold hollow surface sites on the fcc(111) face which may be occupied by H: (i) the *tetrahedral* site; and (ii) the *octahedral* site. The distinction between the octahedral site and the tetrahedral one is difficult to make since there is very little data to support the viewpoint that the octahedral adsorption site is energetically favored over the tetrahedral one. The only proof that the octahedral site is energetically more stable than the tetrahedral one are the *embedded atom method* (EAM) theoretical calculations (6) which indicate that the H adatom is bonded more strongly in the octahedral arrangement than in the tetrahedral surface geometry.

THERMODYNAMICS OF H ELECTROADSORPTION

Assessment of the energy of the metal-hydrogen bond is essential in evaluation of the *strength* and *nature* of the chemisorptive or electroadsorptive $M-H$ bond as well as in appraisal of the *adsorption site* of H on metallic surfaces. Whereas the energy of the surface $M-H_{chem}$ bond formed under gas-phase conditions, $E_{M-H_{chem}}$ (equation [8]), is well documented (6) for various transition metals, such data have not been reported for the surface bond between the underpotentially deposited H and the metal substrate, M, $E_{M-H_{UPD}}$. The current authors have just determined $E_{M-H_{UPD}}$ for Rh electrodes; the experimental procedure and experimental results are described in detail elsewhere (23) and only the theoretical

approach will be briefly presented in the present paper. It is based on the following electrochemical adsorption isotherm (34-40):

$$\frac{\theta_{H_{UPD}}}{1-\theta_{H_{UPD}}} = a_{H^+} \exp\left(-\frac{E\,F}{R\,T}\right)\exp\left(-\frac{\Delta G^{\circ}_{ads}(H_{UPD})}{R\,T}\right) \qquad [9]$$

where $\theta_{H_{UPD}}$ is the surface coverage by H_{UPD}, a_{H^+} is the activity of H^+ in the bulk of the electrolyte, E is the potential measured vs. the standard hydrogen electrode, SHE (41), $\Delta G^{\circ}_{ads}(H_{UPD})$ is the standard Gibbs free energy of electro-adsorption (UPD H) and it is a function of the H_{UPD} surface coverage, $\theta_{H_{UPD}}$, and temperature, $\Delta G^{\circ}_{ads}(H_{UPD}) = f(T, \theta_{H_{UPD}})$. By application of the Nernst relation, one may rearrange equation [9] to the following formula:

$$\frac{\theta_{H_{UPD}}}{1-\theta_{H_{UPD}}} = P_{H_2}^{1/2} \exp\left(-\frac{(E_2 - E_1)\,F}{R\,T}\right)\exp\left(-\frac{\Delta G^{\circ}_{ads}(H_{UPD})}{R\,T}\right) \qquad [9a]$$

where $E_2 - E_1$ is the experimentally measured potential difference versus the reversible hydrogen electrode (RHE) immersed in the same solution (detailed description of the derivation of these formulae is provided in ref. 23). Both equations may be applied to determination of $\Delta G^{\circ}_{ads}(H_{UPD})$ but the former requires precise knowledge of the activity of H^+ whereas the latter requires pressure data which are more accessible. Thus, based on experimental pairs of values of the H_2 gas pressure in the reference electrode compartment, potential and temperature at which the H_{UPD} surface coverage is the same, $\theta_{H_{UPD}} = \text{const}$, as those presented in Fig. 1, one may determine numerically $\Delta G^{\circ}_{ads}(H_{UPD})$. Fig. 3 shown a 3D plots showing the relation between $\Delta G^{\circ}_{ads}(H_{UPD})$ versus $(\theta_{H_{UPD}}, T)$; $\Delta G^{\circ}_{ads}(H_{UPD})$ assumes values between −8 and −18 kJ mol^{-1}. An analysis of the $\Delta G^{\circ}_{ads}(H_{UPD})$ versus $(\theta_{H_{UPD}}, T)$ relation (Fig. 3) reveals that for a given constant H_{UPD} surface coverage, $\theta_{H_{UPD}} = \text{const}$, the relations $\Delta G^{\circ}_{ads}(H_{UPD})$ versus T are linear, thus allowing determination of the entropy of adsorption from their slope, $\Delta S^{\circ}_{ads}(H_{UPD}) = -\left(\partial\,\Delta G^{\circ}_{ads}(H_{UPD})/\partial\,T\right)_{\theta_{H_{UPD}}=\text{const}}$. Such determined values of $\Delta S^{\circ}_{ads}(H_{UPD})$ fall between −90 for the lowest H_{UPD} surface coverage and −15 J mol^{-1} K^{-1} for the highest (see ref. 23 for details).

The enthalpy of the underpotential deposition of H on Rh electrodes, $\Delta H^{\circ}_{ads}(H_{UPD})$, is readily determined based on the above determined values of $\Delta G^{\circ}_{ads}(H_{UPD})$ and $\Delta S^{\circ}_{ads}(H_{UPD})$, and the well-known formula $\Delta G^{\circ} = \Delta H^{\circ} - T\,\Delta S^{\circ}$. Fig. 4 shows the relation between $\Delta H^{\circ}_{ads}(H_{UPD})$ and $\theta_{H_{UPD}}$ for the UPD H on Rh from 0.1 M H_2SO_4 solution; the dependence demonstrates that $\Delta H^{\circ}_{ads}(H_{UPD})$ accepts negative values between –41 and –20 kJ mol^{-1}.

Another approach (23) that may be applied to determination of $\Delta H^{\circ}_{ads}(H_{UPD})$ involves combination of equation [9] with the Gibbs-Helmholtz relation which leads to the following formula:

$$\frac{\partial(E/T)}{\partial(1/T)} = -\left(\frac{\Delta H^{\circ}_{ads}(H_{UPD})}{F}\right)_{\theta_{H_{UPD}} = const} \qquad [10]$$

where $\Delta H^{\circ}_{ads}(H_{UPD})$ is the enthalpy of the UPD H. Thus, by determining experimentally pairs of values of E and T at which the H_{UPD} surface coverage is constant, $\theta_{H_{UPD}}$ = const, and by plotting E / T vs. 1 / T, one obtains linear relations and from their slope one may evaluate $\Delta H^{\circ}_{ads}(H_{UPD})$. Experimental determination of the pairs of values E and T for various constant H_{UPD} surface coverages is feasible using CV adsorption/desorption profiles as those presented in Fig. 1. Until now, such data have never been determined for H_{OPD} but it seems reasonable to assume that the methodology developed by Conway et al. (7, 21, 31) and based on the potential relaxation can be applied to the H_{OPD} species.

Fig. 3 and Fig. 4 show experimentally determined values of $\Delta G^{\circ}_{ads}(H_{UPD})$ and $\Delta H^{\circ}_{ads}(H_{UPD})$, respectively, for the UPD H on Rh(poly) from 0.1 M aqueous H_2SO_4 solution; the values of $\Delta G^{\circ}_{ads}(H_{UPD})$ and $\Delta H^{\circ}_{ads}(H_{UPD})$ are consistently negative throughout the whole H_{UPD} surface coverage, $\theta_{H_{UPD}}$, and they increase from more negative to less negative ones with increasing H_{UPD} surface coverage pointing to the *repulsive nature* of the lateral interactions between the H_{UPD} adatoms. A visual representation of the modulation of the adsorption energy brought about by lateral interactions between co-adsorbed H adatoms is shown in Fig. 5 (6, 42).

The energy of the bond between H_{UPD} and the metal substrate, M, may be determined based upon the two single-electrode processes and the respective Born-Haber thermodynamic cycles shown below:

working electrode (WE): $H^+ + e + M \rightarrow M - H_{UPD}$ [11]

reference electrode (RE): $1/2\,H_2 \rightarrow H^+ + e$ [12]

For the working-electrode process:

$$\begin{array}{ccccccc} H^+_{(gas)} & + & e_{(gas)} & + & M & \xleftarrow{I_H} & H_{(gas)} + M \\ \downarrow \Delta H^\circ_{solv} & & \uparrow \Phi + EF & & & & \uparrow E_{M-H} \\ H^+ & + & e_{M(E\neq 0)} & + & M & \xrightarrow{\Delta H^\circ_{WE}} & M - H_{UPD} \end{array} \quad [13]$$

and for the reference-electrode process:

$$\begin{array}{ccccc} H_{(gas)} & \xrightarrow{I_H} & H^+ & + & e_{(gas)} \\ \uparrow \frac{1}{2} D_{H_2} & & \uparrow \Delta H^\circ_{solv} & & \uparrow \Phi \\ 1/2\,H_2 & \xrightarrow{\Delta H^\circ_{RE}} & H^+ & + & e_{M(E=0)} \end{array} \quad [14]$$

where ΔH°_{solv} is the standard enthalpy of solvation of H^+, I_H is the ionization potential of H, Φ is the metal work function and it varies linearly with the applied potential, thus $\Phi_{(E\neq 0)} = \Phi_{(E=0)} + FE$, D_{H_2} is the dissociation energy of the hydrogen molecule, ΔH°_{WE} is the enthalpy of the single-electrode process at the working electrode and ΔH°_{RE} is the enthalpy of the single-electrode process at the reference electrode (21). Summation of the two single-electrode processes leads to the following overall reaction:

$$1/2\,H_2 + M \xrightarrow{\Delta H^\circ_{ads}(H_{UPD})} M - H_{UPD} \quad [15]$$

Subsequently, upon adding the respective Born-Haber cycles and bearing in mind that there is a Volta potential difference between the metal and the solution so that the H^+ and the electron extracted from the two solid electrodes are at different electrostatic potentials and

this difference compensates exactly the work function variation shown in scheme [13] at the working electrode, thus EF, one obtains the following relation for the $M-H_{UPD}$ bond energy:

$$E_{M-H_{UPD}} = \frac{1}{2}D_{H_2} - \Delta H^{\circ}_{ads}(H_{UPD}) \qquad [16]$$

Fig. 6 shows the experimentally determined values of the $Rh-H_{UPD}$ bond energy, $E_{Rh-H_{UPD}}$, vs. the H_{UPD} surface coverage, $\theta_{H_{UPD}}$, for H adsorbed from 0.1M aqueous H_2SO_4 solution based on the data demonstrated in Fig. 4. It should be added that through relation [16], $E_{Rh-H_{UPD}}$ follows the changes of $\Delta H^{\circ}_{ads}(H_{UPD})$ versus $\theta_{H_{UPD}}$. The experimental data indicate that the bond energy is within a narrow range between 240 and 260 kJ mol^{-1} and that it varies only slightly with $\theta_{H_{UPD}}$.

It is of interest to compare such determined a value of $E_{Rh-H_{UPD}}$ with that for H adsorbed chemisorptively from the gas phase, $E_{Rh-H_{chem}}$. The heat of chemisorption of H on the Rh(111) and Rh(110) surfaces has been found to be 78 kJ mol^{-1} and 77 kJ mol^{-1} (6), respectively, and $E_{Rh-H_{chem}}$, as calculated according to relation [8], equals 257 kJ mol^{-1}. It is important to emphasize that $E_{Rh-H_{chem}}$ is the same for both single-crystal surfaces indicating that it does not depend on the surface structure of the substrate. It has been reported that the $M-H_{chem}$ bond energy for various transition metals are almost the same and fall in the $250-270$ kJ mol^{-1} range. This observation has led to the conclusion that H_{chem} is strongly embedded in the surface lattice of the metal substrate and as such does not depend on the nature of the transition metal or its surface geometry (6).

Proximity of the value of $E_{Rh-H_{UPD}}$ to that of $E_{Rh-H_{chem}}$ leads to the following conclusions: (i) the natures of the $Rh-H_{UPD}$ and $Rh-H_{chem}$ bonds are alike; (ii) the same binding mechanism sets in under the electrolyte and the gas phase conditions; (iii) the electrified double layer, thus presence of the electrolyte and the applied potential, has no impact on the strength of the $M-H$ bond indicating that H_{UPD} and H_{chem} are equivalent surface species; (iv) equivalence of H_{UPD} and H_{chem} points to the same adsorption sites of the two surface species indicating that H_{UPD} is strongly embedded in the surface lattice of the metal substrate.

Relation Between Overpotential and Hydrogen Pressure

It is of importance to discuss the meaning of the relation between the overpotential, η, and the equivalent H_2 gas pressure as expressed by the Nernst equation:

$$\frac{P_{H_2}}{P^{\circ}_{H_2}} = a_{H^+} \exp\left(-\frac{2\,\eta\,F}{R\,T}\right) \qquad [17]$$

where $P^{\circ}_{H_2}$ is the equilibrium H_2 gas pressure (at $\eta = 0$) and P_{H_2} the equivalent H_2 gas pressure at the overpotential η. It should be stressed that the Nernst equation applies to an equilibrium condition. An equivalent equilibrium relationship for the dissociative H_2 absorption from the gas phase is known as Sievert's Law (5, 11, 12, 22). The Nernst equation represents an equivalent H_2 pressure external to the metal and *not* so-called hydrogen pressure inside the metal lattice. It could be used to describe the pressure of H_2 in a closed pressure cell where the evolved H_2 is allowed to build up until a new reversible, equal to the initial overpotential, has become established.

Mechanism of H Electroabsorption

The relation between H_{UPD}, H_{OPD} and *ab*sorbed H, H_{abs}, and the sites they occupy on the metal surface or in its bulk is an intriguing one and as such not clarified satisfactorily yet. Hydrogen can undergo electroabsorption into metals or metallic alloys such as Fe, Ti, $LaNi_5$, NiZr which do not reveal the UPD H phenomenon (1-5, 15-19, 29, 30, 43, 44), thus it seems evident that it is H_{OPD} which undergoes interfacial transfer from the *ad*sorbed to the *ab*sorbed state. On the other hand, H can become absorbed into Pd, a metal which is covered with a monolayer of H_{UPD} prior to the onset of the HER (45, 46). Also, in the case of Pd, the three H species, H_{UPD}, H_{OPD} and H_{abs}, can *coexist* in the negative potential range. Thus despite extensive experimental evidence, the atomistic mechanism of H electroabsorption into Pd is not well understood and it is not clear whether it is H_{OPD} or H_{UPD} which enters the Pd lattice becoming H_{abs}.

In order to deduce which surface species, namely H_{UPD} or H_{OPD}, undergoes entry into Pd, we have performed a series of cyclic-voltammetry (CV) measurements on a Pd(poly) electrode in 0.5 M aq H_2SO_4 solution at 298 K; we do not discuss the experimental details of the CV measurements since they are trivial and are discussed in detail elsewhere (47-49). The

results shown in Fig. 7 demonstrate that upon decrease of the lower potential limit from 0.40 V to 0.16 V, RHE, a new process, which commences at 0.30 V, RHE, takes place and it reveals CV characteristics significantly different from those associated with the UPD H on Pd (46); we assign these features to H *ab*sorption. It should be emphasized that this CV behavior cannot be simply associated with the UPD H or the HER for the following reasons: (i) the cathodic/anodic charges are over three times greater than the charge required to form a monolayer of H_{UPD} on Pd (46); (ii) the CV diagrams do not reveal the representative fine structure of the UPD H on thin Pd films (46); (iii) the CV profiles cannot be associated with the HER since the process takes place at negative potentials and the observed features are in the $0.10-0.30$ V, RHE, potential range. However, the cyclic-voltammetry H absorption/desorption profiles show that the process occurs in the potential region characteristic of the UPD H on Pt, Rh and Pd electrode surfaces (47, 49). This observation leads to the conclusion that it is H_{UPD} which undergoes entry into Pd. It is worthwhile adding that the electroabsorption and electrodesorption CV profiles (Fig. 7) reveal a hysteresis, thus demonstrating that the H absorption and the H desorption occur in different potential ranges. A hysteresis effect is also observed for H absorption/desorption under gas-phase conditions that is difficult to explain on the thermodynamic basis (1, 2, 5).

It should be added that the interfacial H transfer from the adsorbed to the absorbed state may be strongly affected by presence of small amounts (submonolayer or monolayer surface coverage) of surface impurities (50-52). In fact, the dissociative hydrogen adsorption on atomically clean Pd surfaces, prepared under UHV conditions, is known to be non-activated whereas under "laboratory" conditions, where Pd surfaces are often covered with a layer of C or other impurities, the process becomes activated (50-52). It is of interest to compare the gas-phase and electrochemical experimental conditions. In the case of the electrochemical environment, Pd electrodes are cycles into the region of surface oxidation and one may clearly distinguish whether the Pd electrode surface is contaminated or not by comparing the oxide formation and oxide reduction profiles. In absence of surface impurities, the oxide formation charge equals the oxide reduction one. When impurities are detected on the surface, they may be easily "removed" by repetitive cycling into the oxide formation region (say up to 1.5 V, RHE) since surface oxidation and oxidative impurity desorption occur in the same potential range. Thus, repetitive potential cycling into the oxide formation region leads cleans Pd electrodes which reveal surface cleanliness similar to that of surfaces prepared by ion sputtering under UHV conditions.

The mechanism of hydrogen electroabsorption is drastically different in the case of metals or metallic alloys which do not reveal the UPD H phenomenon. Van Rijswick has demonstrated (44) that in the case of $LaNi_5$, $LaNi_4Cu$ and $LaNi_4Cr$, the H absorption current overlaps that of the HER whereas the H desorption one takes place between 0.10 and 0.40 V, RHE. These experimental data clearly show that it is H_{OPD} which undergoes entry into these intermetallics.

The above presented arguments on experimental results on H absorption into intermetallics and Pd call for deliberation on the possible mechanistic pathways of H absorption. Here, we discuss three mechanisms of H electroabsorption into fcc-type metals through the (111) surface; they are visualized in Fig. 8:

(**a**) H_{UPD} occupying a three-fold, octahedral surface site undergoes interfacial transfer to a subsurface site, H_{ss}, and subsequent transfer to an interstice below the second surface monolayer becoming absorbed H, H_{abs};
(**b**) in this mechanism, H_{UPD} does not undergo entry into the host metal; it is H_{OPD} occupying an on-top surface site which moves to a three-fold, tetrahedral surface site (since the octahedral sites are occupied by H_{UPD}) and subsequent interfacial transfer to a subsurface site, H_{ss}, followed by transfer to an interstice below the second surface monolayer becoming absorbed H, H_{abs};
(**c**) H_{OPD} occupying an on-top surface undergoes direct interfacial transfer to a subsurface site, H_{ss}, followed by transfer to an interstice below the second surface monolayer becoming absorbed H, H_{abs}; this mechanism does not involve H adsorbed in an octahedral or a tetrahedral site as an intermediate of the process.

The mechanism (a) and (b) apply to Pd-type metals/alloys which reveal the UPD H phenomenon whereas the mechanism (c) describes a pathway of H absorption into metals/alloys which do not demonstrate the UPD H phenomenon. In the case of the mechanism (a), H_{UPD} "used up" in the process would be regenerated by subsequent underpotential deposition of H; this pathway would lead to a steady-state condition between H_{UPD}, H_{ss} and H_{abs} as well as a steady-state coverage by H_{UPD}. In the case of the mechanism (b), H_{UPD} in a tetrahedral site acts as an intermediate of the process. According to this mechanism, the total surface coverage by underpotentially deposited H (whether in the octahedral or the tetrahedral site) would be greater than unity (more than one H adatom per

surface metal atom) giving rise to strong H – H repulsive interactions (6, 23). Under this mechanism, a steady-state condition would be established between H_{OPD}, H_{UPD} in a tetrahedral site, H_{ss} and H_{abs}. Finally, the mechanism (c) would involve a steady-state condition between H_{OPD}, H_{ss} and H_{abs}.

Here, we have presented three possible mechanistic pathways of H electroabsorption and based upon the existing and above presented data, it seems apparent that the mechanism (a) can be satisfactorily applied to clean Pd electrodes. However, no experimental evidence has been provided so far in favor of the pathway (b) or (c) for H entry into metals which do not reveal the UPD H phenomenon.

It is of interest to compare the mechanistic pathways of H absorption into the host metal from the gas phase with H electroabsorption from the electrolyte. In the gas-phase mechanism, the adsorbed H is formed in the process of initial chemisorption, H_{chem}, and in the case of the fcc(111) face, H_{chem} occupies the three-fold surface site (6). The chemisorbed H undergoes interfacial transfer from the adsorbed state to an interstice just beneath the top-most surface layer becoming subsurface H, H_{ss}. This surface species subsequently hops to another interstice below the second surface monolayer of the host metal becoming absorbed H, H_{abs}; this process is followed by 3D H diffusion in the metal bulk. In the case of electroadsorption, there is no dissociation of the H_2 molecule, electron transfer from the metal to the solvated H^+ must, however, occur with a simultaneous breakage of the hydration shell. On the contrary, the gas-phase adsorption pathway proceeds through the dissociation of the H_2 molecule before the M – H bond is formed. It ought to be stressed that both of these distinct mechanisms lead to the adsorbed H. However, the electrochemical pathways lead to two discrete electroadsorbed H species, namely H_{UPD} and H_{OPD}, each one having its own distinct chemical potential as well as its own absorption pathway.

THERMODYNAMICS OF HYDROGEN INTERFACIAL TRANSFER

Thermodynamics of (electro)adsorbed, subsurface and absorbed H's are very important in order to evaluate the possibility of H entry into metals and becoming 3D *ab*sorbed H, H_{abs}. In order to establish whether (electro)adsorbed H can undergo absorption into the host metals/alloys, the *chemical potential gradient of H*, $\Delta\mu_H$, associated with its interfacial transfer across the gas/solid or liquid/solid interface, has to be determined. This requires knowledge of the chemical potential of H in the (electro)adsorbed and absorbed states. The

chemical potential of *ab*sorbed H has been defined by Wagner (53) and it is expressed by the following formula:

$$\mu_{H_{abs}} = \mu^{\circ}_{H_{abs}} + RT \ln \frac{X_{H_{abs}}}{1 - X_{H_{abs}}} \qquad [18]$$

where $\mu^{\circ}_{H_{abs}}$ is the standard chemical potential of *ab*sorbed H and $X_{H_{abs}}$ is the three-dimensional lattice occupancy fraction. The chemical potential of the underpotentially deposited H has been related to the H_{UPD} surface coverage, $\theta_{H_{UPD}}$, in a manner similar to that presented by Wagner (22, 53, 54):

$$\mu_{H_{UPD}} = \mu^{\circ}_{H_{UPD}} + RT \ln \frac{\theta_{H_{UPD}}}{1 - \theta_{H_{UPD}}} \qquad [19]$$

where $\mu^{\circ}_{H_{UPD}}$ is the standard chemical potential of H_{UPD}. By analogy, the chemical potential of the over-potentially deposited H is defined according to the following formula:

$$\mu_{H_{OPD}} = \mu^{\circ}_{H_{OPD}} + RT \ln \frac{\theta_{H_{OPD}}}{1 - \theta_{H_{OPD}}} \qquad [20]$$

where $\mu^{\circ}_{H_{OPD}}$ is the standard chemical potential of H_{OPD} and $\theta_{H_{OPD}}$ is the surface coverage by H_{OPD}. The principle difference between H_{UPD} and H_{OPD} is that the chemical potential of the underpotentially deposited H is negative (see refs. 23, 29, 30 and Fig. 3), $\mu^{\circ}_{H_{UPD}} < 0$, whereas that of the over-potentially deposited H is positive, $\mu^{\circ}_{H_{OPD}} > 0$.

Finally, the chemical potential of the *subsurface* H, H_{ss}, has been defined in a manner similar to that for the electroadsorbed H:

$$\mu_{H_{ss}} = \mu^{\circ}_{H_{ss}} + RT \ln \frac{\theta_{H_{ss}}}{1 - \theta_{H_{ss}}} \qquad [21]$$

where $\mu^{\circ}_{H_{ss}}$ is the standard chemical potential of the subsurface H, $\theta_{H_{ss}}$ is the subsurface lattice occupancy fraction analogous to the H surface coverage, θ_H (55). It should be emphasized that the standard states of all these three types of sorbed H species, namely adsorbed H,

subsurface H and absorbed H, refer to X_H, θ_H and $\theta_{H_{ss}}$ equal 0.5 since under this condition the logarithmic component of equations [18] through [21] equal zero (22, 53, 56, 57).

We are able to define the necessary thermodynamic requirement in order for H to undergo absorption into the host metal either through the gas-phase or the electrochemical pathway. In the case of H absorption from the gas phase through the chemisorptive pathway, the interfacial transfer from the chemisorbed to the absorbed state is spontaneous when:

$$\Delta\mu_H = \mu_{H_{abs}} - \mu_{H_{chem}} < 0 \qquad [22]$$

thus, if the following condition is fulfilled:

$$\mu^{\circ}_{H_{abs}} + RT \ln \frac{X_{H_{abs}}}{1 - X_{H_{abs}}} - \mu^{\circ}_{H_{chem}} - RT \ln \frac{\theta_{H_{chem}}}{1 - \theta_{H_{chem}}} < 0 \qquad [23]$$

where $\mu^{\circ}_{H_{chem}}$ is the standard chemical potential of the chemisorbed H and $\theta_{H_{chem}}$ is the surface coverage by H_{chem}. Similarly, H electroabsorption occurs through the mechanism (a) involving H_{UPD} if the following condition is fulfilled:

$$\Delta\mu_H = \mu_{H_{abs}} - \mu_{H_{UPD}} < 0 \qquad [24]$$

and consequently:

$$\mu^{\circ}_{H_{abs}} + RT \ln \frac{X_{H_{abs}}}{1 - X_{H_{abs}}} - \mu^{\circ}_{H_{UPD}} - RT \ln \frac{\theta_{H_{UPD}}}{1 - \theta_{H_{UPD}}} < 0 \qquad [25]$$

If H electroabsorption takes place through the mechanism (b) or (c) involving H_{OPD}, then the thermodynamic condition for H absorption is expressed by relations [26] and [27]:

$$\Delta\mu_H = \mu_{H_{abs}} - \mu_{H_{OPD}} < 0 \qquad [26]$$

and consequently:

$$\mu^{\circ}_{H_{abs}} + RT \ln \frac{X_{H_{abs}}}{1 - X_{H_{abs}}} - \mu^{\circ}_{H_{UPD}} - RT \ln \frac{\theta_{H_{OPD}}}{1 - \theta_{H_{OPD}}} < 0 \qquad [27]$$

According to the above presented formulae, H can undergo interfacial transfer from the *ad*sorbed to the *ab*sorbed state when the corresponding *chemical potential gradient*, $\Delta\mu_H$, associated with the process is *negative*. Thus, assessment of the possibility of H interfacial transfer requires knowledge of standard chemical potentials of H in the chemisorbed and electroadsorbed states, $\mu_{H_{chem}}$, $\mu_{H_{UPD}}$ and $\mu_{H_{OPD}}$.

Finally, we suggest a thermodynamic condition for H transfer from the (electro)adsorbed to the subsurface state, a process which is fast and whose energy barrier is small (6, 24-28). It can occur if the following condition is met:

$$\Delta\mu_H = \mu_{H_{ss}} - \mu_{H_{ads}} < 0 \qquad [28]$$

where $\mu_{H_{ads}}$ is the chemical potential of the (electro)adsorbed H and it refers to the chemisorbed, underpotentially deposited or over-potentially deposited H, depending on the process pathway.

ACKNOWLEDGMENTS

Acknowledgment is made to the NSERC of Canada and le FCAR du Québec for support of this research project. A. Zolfaghari gratefully acknowledges a graduate fellowship from the MHE of Iran and a summer graduate scholarship from l'Université de Sherbrooke.

REFERENCES

1. G. Alefeld and J. Volkl, Eds., "Hydrogen in Metals", Parts I and II, Springer-Verlag, New York (1978).

2. L. Schlapbach, Ed., "Hydrogen in Intermetalic Compounds" Part I, Springer-Verlag, New York (1988); Part II, Springer-Verlag, New York (1992).

3. K.M. Mackay, "Hydrogen Compounds of the Metallic Elements", E.&F.N. Spon, London (1966).

4. F.G. Will and C.A. Knorr, Z. Electrochem., 64 (1960) 258; 270.

5. P.K. Subramanyan, Ch.8 in "Comprehensive Treatise of Electrochemistry", Vol. 4, Eds. J.O'M. Bockris, B.E. Conway, E. Yeager and R.E. White, Plenum Press, New York (1981).

6. K. Christman, Surface Sci. Rep., 9 (1988), 1.

7. B.E. Conway, Sci. Prog., Oxf. 71 (1987) 479; see also M. Elam and B. E. Conway, J. Appl. Electrochem., 17 (1987) 1002; J. Electrochem. Soc., 135 (1988) 1678.

8. W. Böld and M. W. Breiter, Z. Elektrochem., 64 (1960) 897.

9. M. W. Breiter and B. Kennel, Z. Elektrochem., 64 (1960) 1180.

10. A. N. Frumkin, in "Advances of Electrochemistry and Electrochemical Engineering", P. Delahey, P. Ed., Vol. 3, Interscience Publishers, New York (1963).

11. M. Enyo, in "Modern Aspects of Electrochemistry", B. E. Conway and J. O'M. Bockris, Eds., Vol. 11, Plenum Press, New York (1975).

12. M. Enyo, in "Comprehensive Treatise of Electrochemistry", B. E. Conway and J. O'M. Bockris, Eds., Vol. 7, Plenum Press, New York, (1983).

13. E. Fromm, Z. Phys. Chem. Neue Folge, Bd., 147 (1986) 61.

14. F.D. Manchester and D. Khatamian, Materials Science Forum, 31 (1988) 261.

15. J. J. G. Willems, Ph.D. Thesis, Eindhoven (1984).

16. S. R. Ovshinsky, M. A. Fetcenko and J. Ross, Science, 260 (1993) 176.

17. S. R. Ovshinsky, K. Sapru, B. Reichman and A. Reger, US Patents No. 4,623,597; see also S. R. Ovshinsky and M. A. Fetcenko, US Patent No. 5,096,667; No. 5,104,617; No. 5,135,589; No. 5,238,756; No. 5,277,999.

18. M. Ciureanu, D. Moroz, R. Ducharme, D. H. Ryan, J. Ström-Olsen and M. Trudeau, Zeit. Phys. Chem. Bd., 183 (1994) 365; Q. M. Yang, M. Ciureanu, D. H. Ryan and J. Ström-Olsen, J. Electrochem. Soc., 141, (1994) 2108; 141, (1994) 2113; 141, (1994) 2430.

19. S. R. Ovshinsky, M. A. Fetcenko, S. Venkatesan and B. Chao, in "Electrochemistry and Materials Science of Cathodic Hydrogen Absorption and Adsorption", Eds. B. E. Conway and G. Jerkiewicz, The Electrochemical Society (1995).

20. B.E. Conway, "Ionic Hydration in Chemistry and Biophysics", Elsevier, New York (1981) [and refs. therein].

21. B.E. Conway, "Theory and Principles of Electrode Processes", Ronald Press, London (1965).

22. B. E. Conway and G. Jerkiewicz, J. Electroanal. Chem., 357 (1993) 47; see also B. E. Conway and G. Jerkiewicz, Zeit. Phys. Chem. Bd., 183 (1994) 281.

23. G. Jerkiewicz, and A. Zolfaghari, J. Phys. Chem. (submitted).

24. W. Eberhardt, F. Greuter and E. W. Plummer, Phys. rev. Lettters, 46 (1981) 1085.

25. C.T. Chan and S.G. Louie, Solid State Comm., 48 (1983) 417.

26. T.E. Felter, S.M. Foiles, M.S. Daw and R.H. Stulen, Surface Sci., 171 (1986) L379.

27. J.-W. He, D. A. Harrington, K. Griffiths and P. R. Norton, Surface Sci., 198 (1988) 413.

28. E. Kristen, G. Parschau, W. Stocker and K. H. Rieder, Surface Sci. Letters, 231 (1990) L183.

29. P. Marcus and E. Protopopoff, Surface Sci., 161 (1985) 533; Surface Sci. Letters, 169 (1986) L237; J. Vac. Sci. Technol., A5 (1986) 944.

30. E. Protopopoff and P. Marcus, J. Electrochem. Soc., 135 (1988) 3073; J. Chim. Phys. 88 (1991) 1423; C. R. Acad. Sci. Paris, t. 308, Série II (1989) 1685.

31. B.E. Conway and L. Bai, J. Chem. Soc., Faraday Trans. I, 81 (1985) 1841; see also L. Bai, J. Electroanal. Chem., 355 (1993) 37.

32. A. Bewick and J.W. Russell, J. Electroanal. Chem., 132 (1982) 329; 142 (1982) 337.

33. R.J. Nichols and A. Bewick, J. Electroanal. Chem., 243 (1988) 445; see also R. J. Nichols in "Adsorption of Molecules at Metal Electrodes", Eds. J. Lipkowski and P. N. Ross, Ch. 7, VCH, New York (1992).

34. I. Langmuir, J. Am. Chem. Soc., 40 (1918) 1361.

35. R. H. Fowler and F. A. Guggenheim, "Statistical Thermodynamics", Cambridge University Press, London (1939).

36. B. E. Conway, H. Angerstein-Kozlowska, and H. P. Dhar, Electrochim. Acta, 19 (1974) 455.

37. B. E. Conway and H. Angerstein-Kozlowska, Acc. Chem. Res. 14 (1981) 49.

38. B. E. Conway, H. Angerstein-Kozlowska and F. C. Ho, J. Vac. Sci. Technol., 14 (1977) 351.

39. A. N. Frumkin, Ch. 5 in "Advances of Electrochemistry and Electrochemical Engineering", Ed. P. Delahey, Vol. 3, Interscience Publishers, New York (1963).

40. E. Gileadi, "Electrode Kinetics", VCH, New York (1993).

41. S. G. Bratsch, J. Phys. Chem. Ref. Data, Vol. 18, No. 1 (1989).

42. P. Marcus and J. Oudar, Ch. 3 in "Hydrogen Degradation of Ferrous Metals", Eds. R. A. Oriani, J. P. Hirth and M. Smialowski, Noyes Publications, Park Ridge, NJ (1985).

43. L. Schlapbach, A. Zuettel and F. Meli, in "Electrochemistry and Materials Science of Cathodic Hydrogen Absorption and Adsorption", Eds. B. E. Conway and G. Jerkiewicz, The Electrochemical Society (1995).

44. M. H. J. Van Rijswick, in "Hydrides for Energy Storage", Eds. A. F. Andersen and A. J. Maeland, p. 261, Pergamon Press, Oxford (1978).

45. J. Horkans, J. Electroanal. Chem., 209 (1986) 371; see also J. McBreen, J. Electroanal. Chem., 287 (1990) 279.

46. M. Baldauf and D. M. Kolb, Electrochim. Acta, 38 (1993) 2145.

47. H. Angerstein-Kozlowska, B. E. Conway and W. B. A. Sharp, J. Electroanal. Chem., 43 (1973) 9.

48. H. Angerstein-Kozlowska, Ch. 9 in "Comprehensive Treatise of Electrochemistry", Eds. E. Yeager, J. O'M. Bockris, B. E. Conway and S. Sarangapani, Vol. 9, Plenum Press, New York (1984).

49. G. Jerkiewicz and J. J. Borodzinski, Langmuir, 9 (1993) 2202.

50. I. Lundström, M. Armgarth and L.-G. Petersson, CRC Critical Reviews in Solide State and Materials Sciences, 15 (1989) 201.

51. B. C. Kay, C. H. F. Peden and D. W. Goodman, Phys. Rev. B, 34 (1986) 817.

52. C. H. F. Peden, B. C. Kay and D. W. Goodman, Surface Sci., 175 (1986) 215.

53. C. Wagner, Z. Phys. Chem., 193 (1944) 386; 407.

54. B. Love, K. Seto and J. Lipkowski, Rev. Chem. Intermediates, 8 (1987) 87.

55. G. Jerkiewicz and A. Zolfaghari, in "Electrochemistry and Materials Science of Cathodic Hydrogen Absorption and Adsorption", Eds. B. E. Conway and G. Jerkiewicz, The Electrochemical Society (1995).

56. L. Onsager and R. M. Fuoss, J. Phys. Chem., 26 (1932) 2689.

57. J. R. Lacher, Proc. R. Soc. London, Ser. A, 161 (1937) 525.

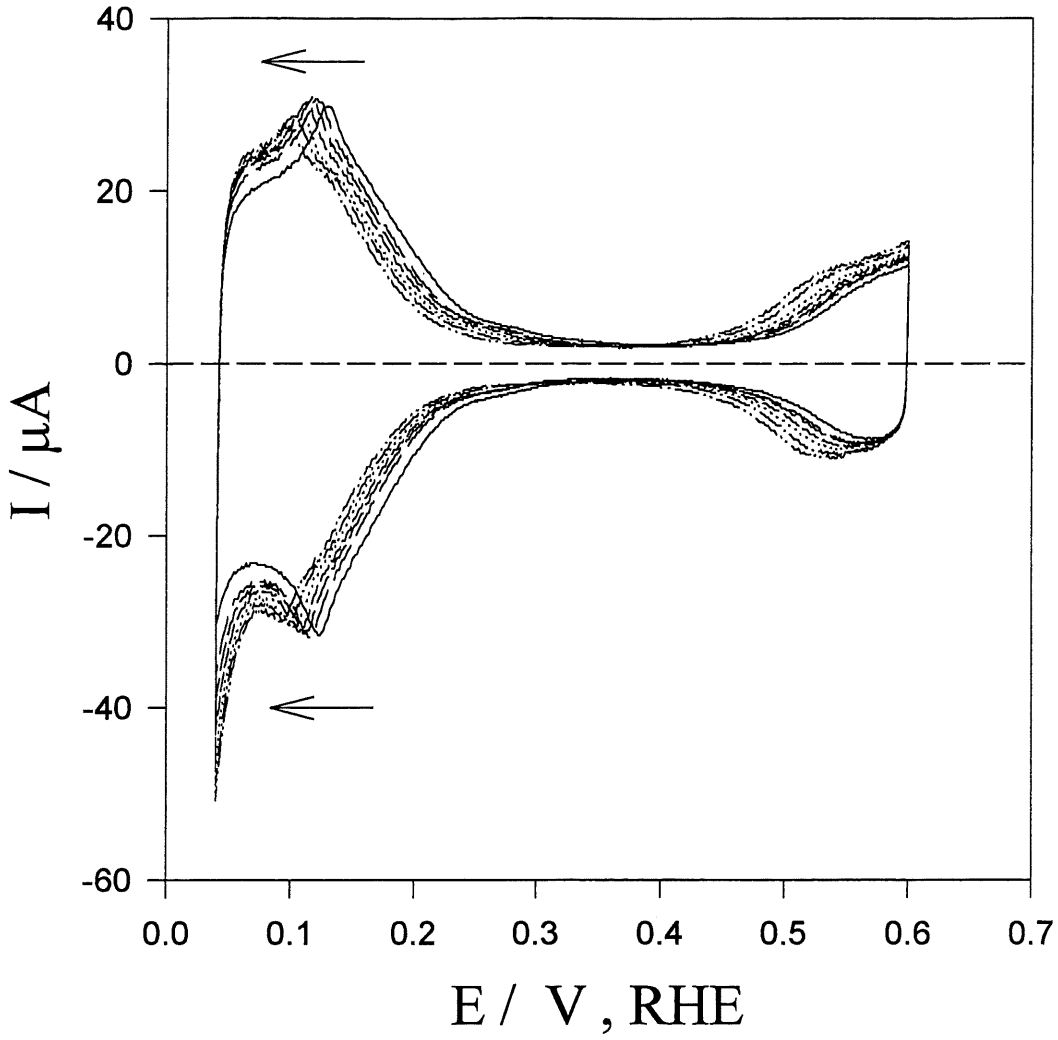

Figure 1. Series of the cyclic-voltammetry (CV) profiles for the under-potential deposition of H (UPD H) on a Rh(poly) electrode in 0.1 M aqueous solution of H_2SO_4 for a temperature range between 298 and 353 K, with an interval of 10 K, and recorded at the sweep rate $s = 20\ mV\ s^{-1}$, the electrode surface area $A_r = 0.70 \pm 0.01\ cm^2$. The arrows indicate the shift of the adsorption and desorption peaks upon the temperature increase.

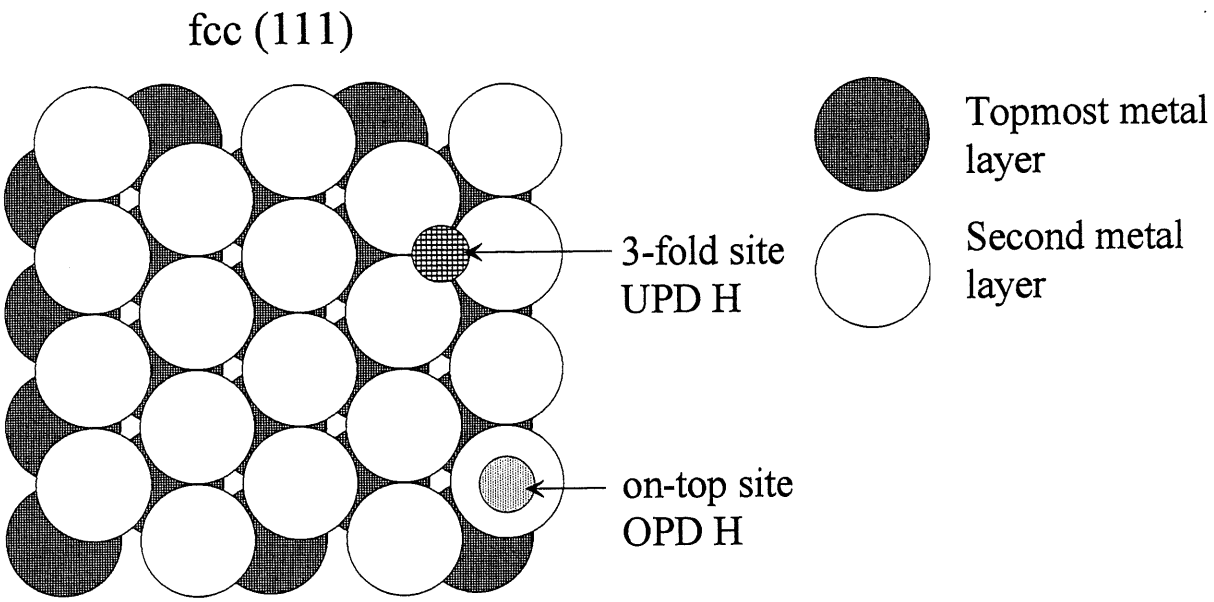

Figure 2. Adsorption sites of H_{UPD} and H_{OPD} on the fcc(111) surface; H_{UPD} occupies the three-fold hollow site on fcc(111) and whereas H_{OPD} resides on top of the surface metal atom.

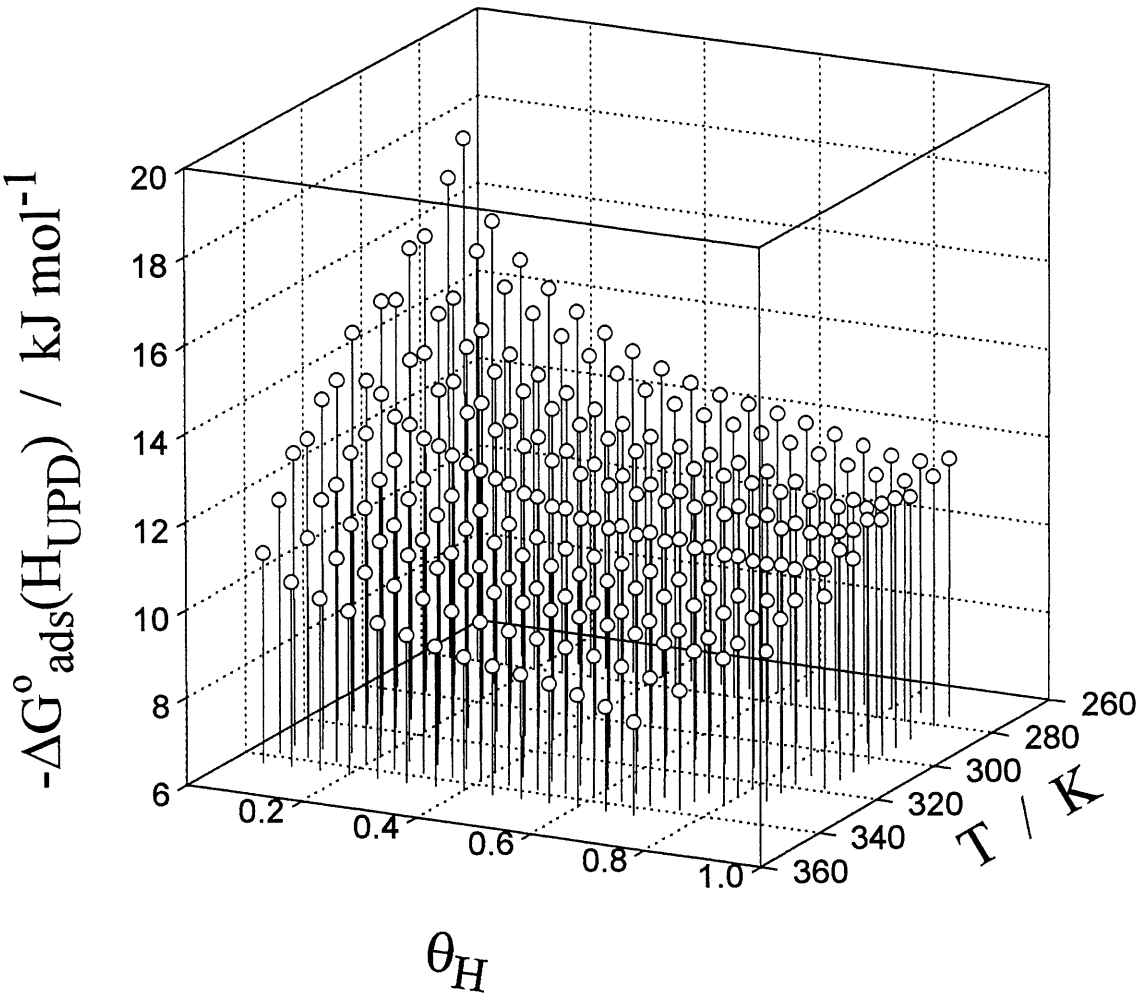

Figure 3. 3D plots showing $\Delta G^{\circ}_{ads}(H_{UPD})$, versus $\theta_{H_{UPD}}$ and T, $\Delta G^{\circ}_{ads}(H_{UPD}) = f(\theta_{H_{UPD}}, T)$, for the under-potential deposition of H on Rh electrodes from 0.1 M aqueous H_2SO_4 solution. $\Delta G^{\circ}_{ads}(H_{UPD})$ assumes values between −18 and −8 kJ mol^{-1} depending on $\theta_{H_{UPD}}$ and T; $\Delta G^{\circ}_{ads}(H_{UPD})$ reaches the most negative values at the lowest temperature and the smallest surface coverage, $\theta_{H_{UPD}}$. Augmentation of $\Delta G^{\circ}_{ads}(H_{UPD})$ with increasing $\theta_{H_{UPD}}$ for T = const points to the repulsive nature of lateral interactions between H_{UPD} adatoms.

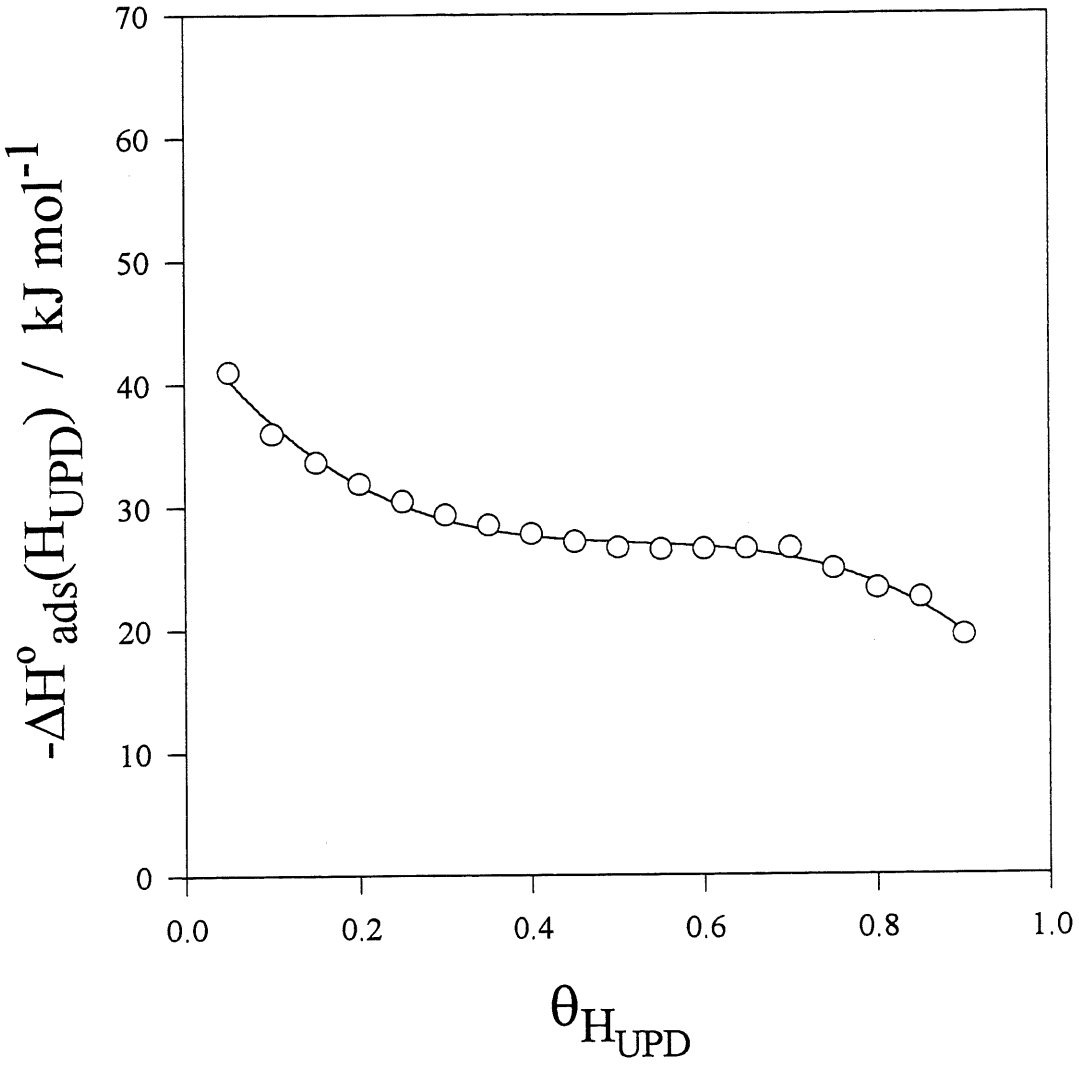

Figure 4. Experimentally determined values of $\Delta H^{\circ}_{ads}(H_{UPD})$ for the UPD H on Rh(poly) from 0.1 M aqueous H_2SO_4 solution; $\Delta H^{\circ}_{ads}(H_{UPD})$ has values between –20 and –41 kJ mol^{-1}.

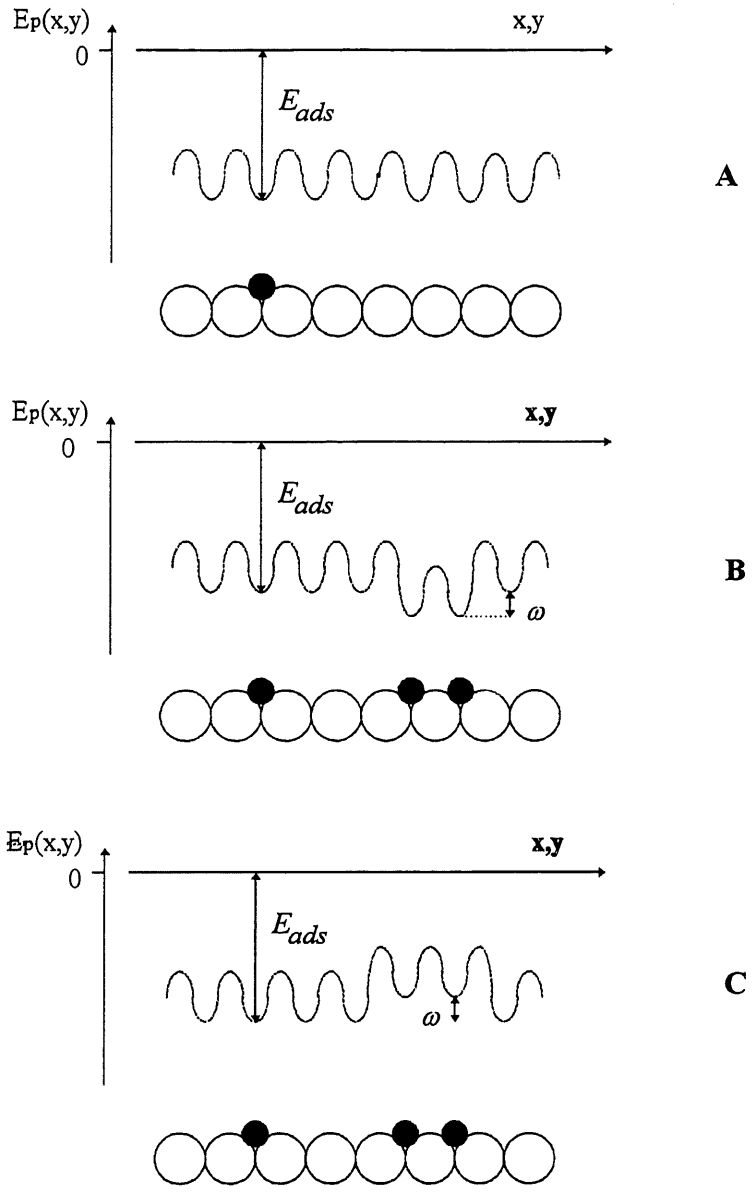

Figure 5. Variation of the potential energy, E_P, of the adsorbed H vs. the surface coordinates (x, y). **(A)** Surface with a single H adatom having the energy of adsorption E_{ads}; in the case of absence of lateral interactions every additional H adatom possesses the same E_{ads}. **(B)** In the case of *attractive* lateral interactions between H adatoms occupying neighbor adsorption sites, the energy of adsorption decreases by the energy of lateral attractions, ω. **(C)** In the case of *repulsive* lateral interactions between H adatoms occupying neighbor adsorption sites, the energy of adsorption increases by the energy of lateral attractions, ω.

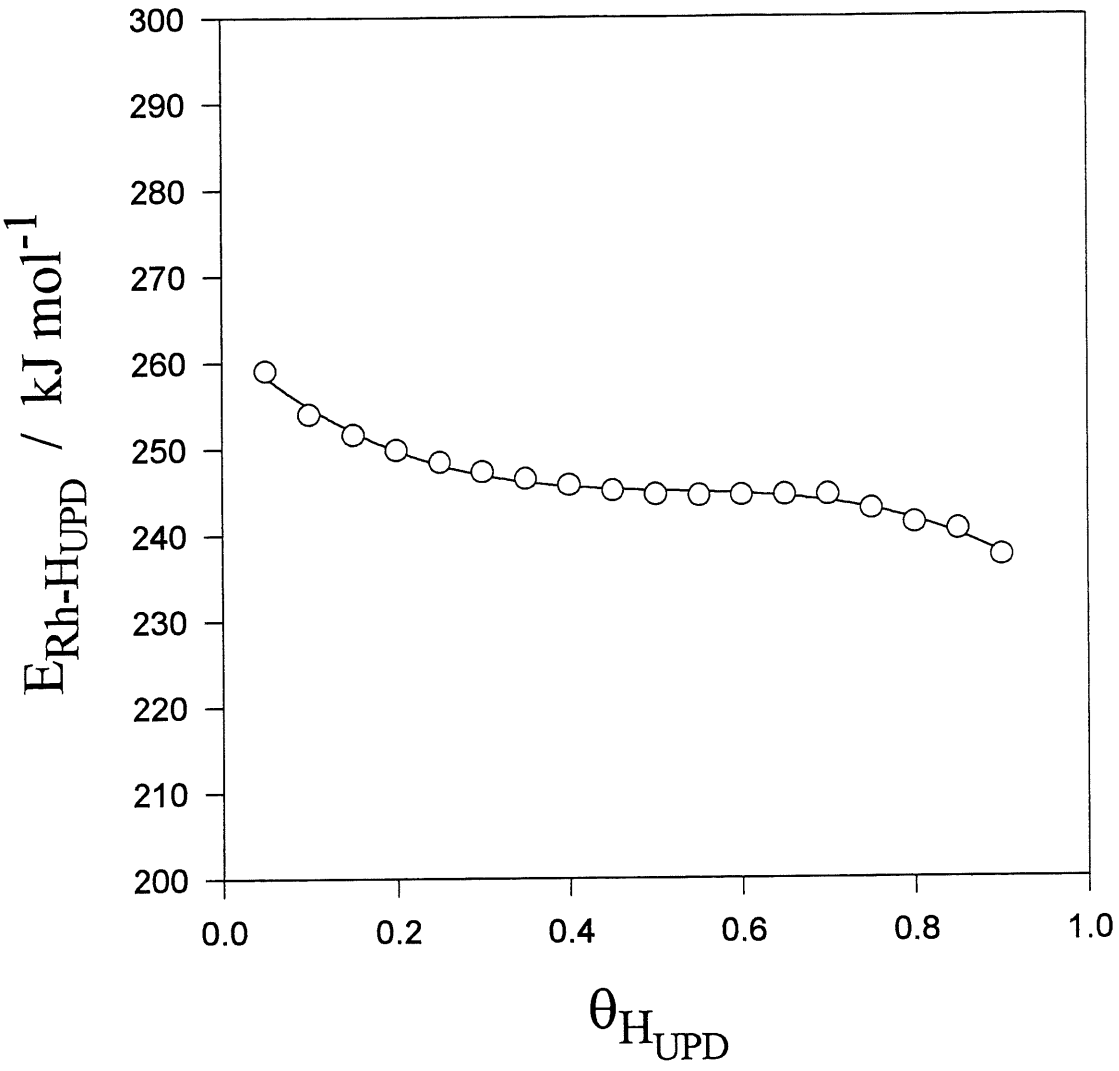

Figure 6. Experimentally determined values of the Rh – H_{UPD} bond energy, $E_{Rh\text{-}H_{UPD}}$, vs. the H_{UPD} surface coverage, $\theta_{H_{UPD}}$, for the UPD H from 0.1 M aqueous H_2SO_4 solution; the data indicate that the bond energy is within the 240 and 260 kJ mol^{-1} range and that it does not depend on $\theta_{H_{UPD}}$.

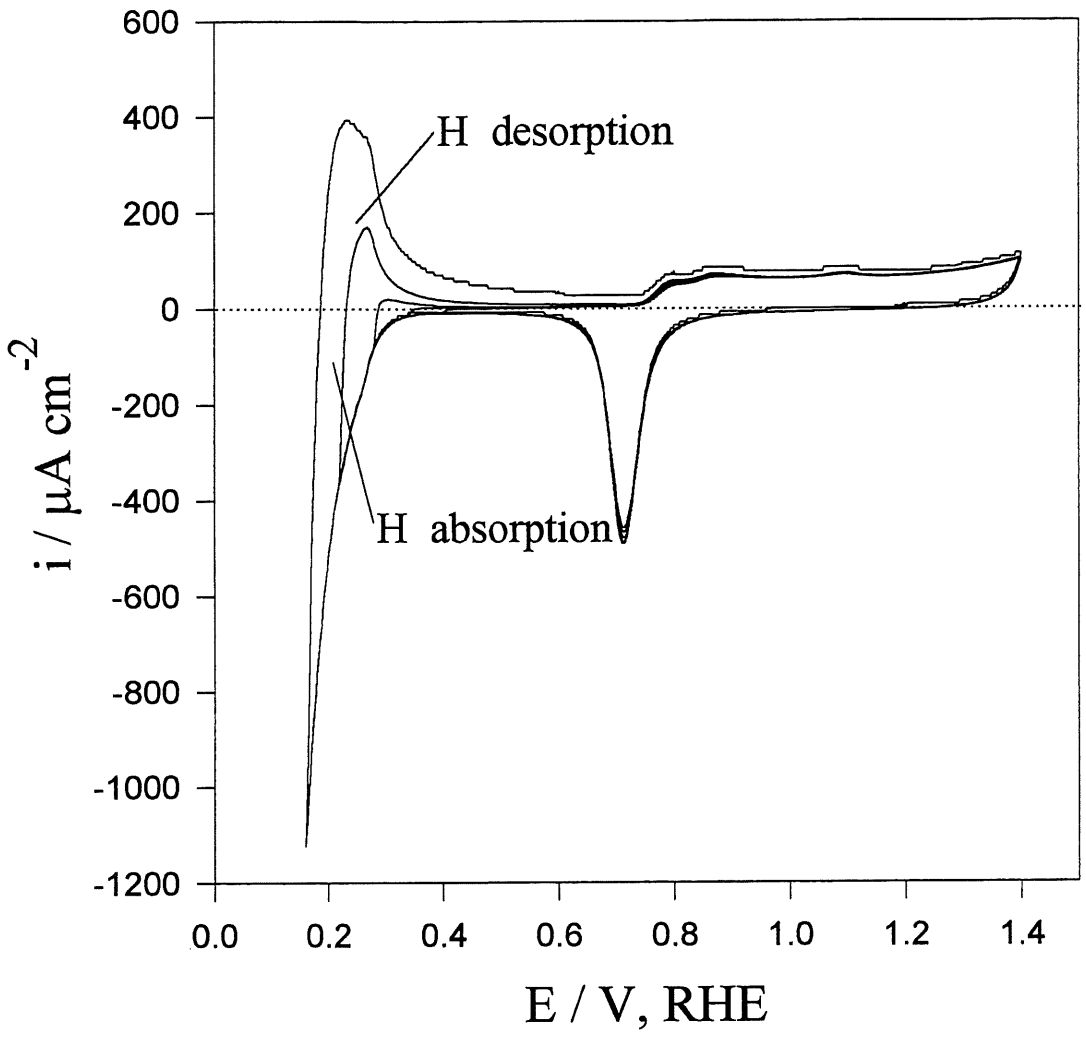

Figure 7. A series of cyclic-voltammograms for a Pd(poly) electrode in 0.5 M aq H_2SO_4 solution at 298 K; the upper potential limit is fixed at 1.40 V, RHE, whereas the lower one is decreased gradually from 0.40 V, to 0.16 V, RHE. They demonstrate that upon decrease of the lower potential limit from 0.40 V, to 0.16 V, RHE, H absorption into Pd can be observed with the process commencing at ca. 0.30 V, RHE. The CV profiles do not reveal the fine features of H_{UPD} on very thin Pd films (46).

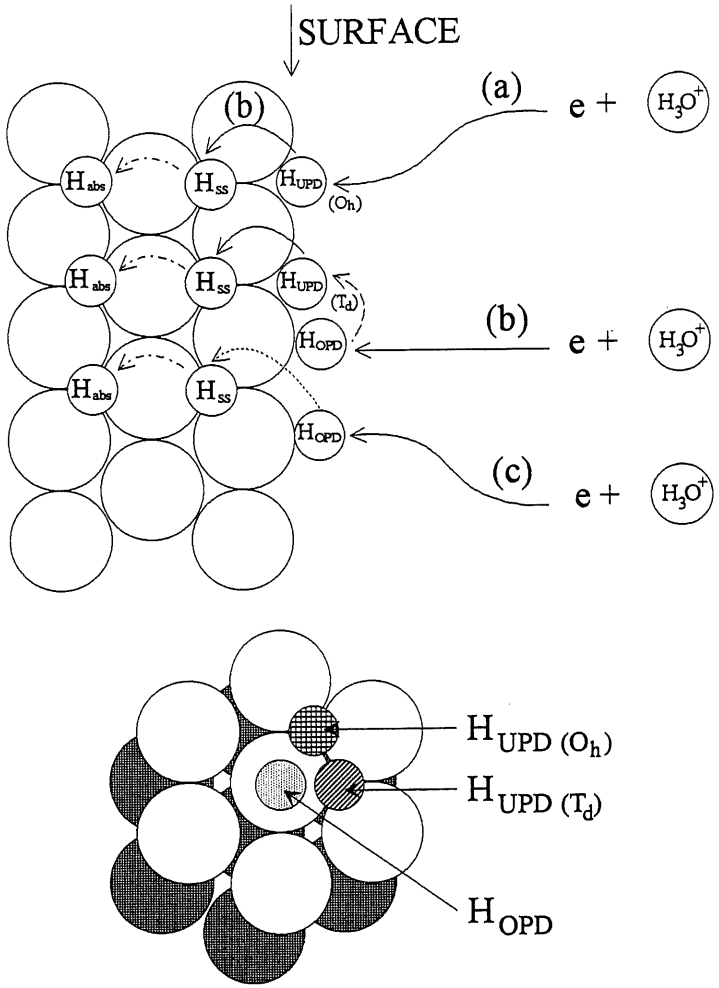

Figure 8. Visual representation of three possible pathways of H absorption into metals/alloys having the fcc crystallographic structure; the mechanisms are shown for the (111) surface. Pathway (**a**): H_{UPD} occupying a three-fold octahedral surface site undergoes interfacial transfer to a subsurface site, H_{ss}, and subsequently hops to an interstice below the second surface monolayer becoming absorbed H, H_{abs}. Pathway (**b**): H_{OPD} occupying an on-top surface site moves to a three-fold tetrahedral surface site and subsequently undergoes interfacial transfer to a subsurface site, H_{ss}, followed by transfer to an interstice below the second surface monolayer becoming absorbed H, H_{abs}. Pathway (**c**): H_{OPD} occupying an on-top surface undergoes direct interfacial transfer to a subsurface site, H_{SS}, followed by movement to an interstice below the second surface monolayer becoming absorbed H, H_{abs}.

1.2 DETERMINATION OF THE ENERGY OF THE M-H_{UPD} BOND FOR Rh ELECTRODES

G. Jerkiewicz and A. Zolfaghari, J. Phys. Chem., 100, 8454 (1996)

ABSTRACT

Investigation of the under-potential deposition of hydrogen (UPD H) on Rh electrodes in 0.05, 0.10 and 0.50 M aqueous solutions of H_2SO_4 in the 298 - 353 K temperature range by cyclic voltammetry (CV) demonstrates that upon temperature increase the CV profiles shift towards less-positive values. The CV hydrogen adsorption/desorption diagrams are symmetric with respect to the potential axis indicating that the UPD H is a reversible process. Theoretical treatment of the experimental data based on an electrochemical adsorption isotherm allows determination of the Gibbs free energy of adsorption, $\Delta G^{\circ}_{ads}(H_{UPD})$, as a function of temperature and the H surface coverage; it varies between −8 and −18 kJ mol^{-1}. Temperature dependence of $\Delta G^{\circ}_{ads}(H_{UPD})$ for a constant surface coverage of the under-potential deposited H (H_{UPD}) allows determination of the standard entropy of adsorption, $\Delta S^{\circ}_{ads}(H_{UPD})$, which is found to be between −15 and −125 J mol^{-1} K^{-1}. Subsequently, $\Delta H^{\circ}_{ads}(H_{UPD})$ is determined to be between −15 and −52 kJ mol^{-1}. An analysis of the values of $\Delta H^{\circ}_{ads}(H_{UPD})$ and $\Delta S^{\circ}_{ads}(H_{UPD})$ leads to conclusion that the UPD H is an enthalpy-driven process. Knowledge of $\Delta H^{\circ}_{ads}(H_{UPD})$ leads to determination of the bond energy between Rh and H_{UPD}, $E_{Rh-H_{UPD}}$, which is between 235 and 265 kJ mol^{-1} depending on the H_{UPD} surface coverage ($\theta_{H_{UPD}}$). The value of $E_{Rh-H_{UPD}}$ is close to that of the bond energy between Rh and the H chemisorbed from the gas phase (H_{chem}), $E_{Rh-H_{chem}}$, which equals 255 kJ mol^{-1}. Proximity of the magnitude of $E_{Rh-H_{UPD}}$ to that of $E_{Rh-H_{chem}}$ points to a similar binding mechanism of H under the conditions involving presence of the electrified solid/liquid interface. Closeness of $E_{Rh-H_{UPD}}$ to $E_{Rh-H_{chem}}$ also points to the same adsorption site of H_{UPD} and H_{chem} indicating that they are strongly embedded in the surface lattice of the Rh substrate. Finally, proximity of $E_{Rh-H_{UPD}}$ to $E_{Rh-H_{chem}}$ indicates that H_{UPD} and H_{chem} are equivalent surface species.

INTRODUCTION

The under-potential deposition (UPD) of hydrogen and certain metals of the *p* and *d* blocks of the periodic table on noble-metal electrodes has been a subject of intense studies in electrochemical surface science. [1-16] The under-potential deposition of a species A involving the transfer of z electrons and a complete discharge of the species A^{z+} to A may be represented by the following general formula: [11]

$$\underset{(1-\theta_{A_{UPD}})}{M} + \underset{a_{A^{z+}}}{A^{z+}} + ze \rightarrow \underset{(\theta_{A_{UPD}})}{M-A_{UPD}} \qquad [1]$$

where M stands for the metal substrate on which the electroadsorption of A takes place, $a_{A^{z+}}$ is the activity of A^{z+} in solution from which adsorption of A originates and $\theta_{A_{UPD}}$ is the surface coverage of A_{UPD}. A Langmuir-type electrochemical isotherm for this process may be represented by the following relation: [4,11,17]

$$\frac{\theta_{A_{UPD}}}{1-\theta_{A_{UPD}}} = a_{A^{z+}} \exp(-zEF/RT) \exp\left(-\Delta G^{\circ}_{ads}(A_{UPD})/RT\right) \qquad [2]$$

where E is the electrode potential* determining the coverage $\theta_{A_{UPD}}$ of the electroadsorbed species A, $\Delta G^{\circ}_{ads}(A_{UPD})$ is the standard Gibbs free energy of process [1] and the standard state corresponds to the Gibbs free of adsorption at $\theta_{A_{UPD}} = 0.5$, T is the temperature, and F and R are physico-chemical constants. In presence of lateral interactions between the adsorbed species, where the lateral interaction energy, g, inreases linearly with $\theta_{A_{UPD}}$, the second exponential component of equation [2] becomes $\exp\left(-\Delta G^{\circ}_{ads}(A_{UPD}) + g\,\theta_{A_{UPD}}/RT\right)$ and such a reformulated adsorption equation becomes the Frumkin electrochemical adsorption isotherm. [9,11,17] A detail discussion of the selection of standard states for electrochemical adsorption isotherms other than the Langmuir one is provided in ref. 9.

The under-potential deposition of hydrogen (UPD H) is known [1-14] to take place only on Rh, Pt, Ir and Pd, and at potentials positive to the thermodynamic reversible potential of the hydrogen evolution reaction (HER), $E^{\circ}_{HER} = 0.0$ V vs. NHE** (the normal hydrogen electrode). The UPD H from an acidic solution may be represented by the following surface reaction:

$$\underset{(1-\theta_{H_{UPD}})}{M} + \underset{a_{H_3O^+}}{H_3O^+} + e \rightarrow \underset{(\theta_{H_{UPD}})}{M-H_{UPD}} + H_2O \qquad [3]$$

---

* E measured vs. SHE.

** The UPD H is a process which takes place above the H^+ / H_2 equilibrium potential, E_{eq}.

where M represents the metal substrate on which the UPD H takes place, $a_{H_3O^+}$ is the activity of H_3O^+ species from which the under-potential deposited H (H_{UPD}) originates, $\theta_{H_{UPD}}$ is the H_{UPD} surface coverage, and E, $\Delta G^{\circ}_{ads}(H_{UPD})$, R, F and T are defined above. It is of importance to discuss the electrosorption valency, γ, of H_{UPD} upon its under-potential deposition, thus the completeness of discharge of the H^+ cation upon its adsorption (a detail description of the electrosorption valency with its definition is given in ref. 18). The adsorption of the H_{UPD} species from acidic solutions on noble-metal electrodes was studied by Schultze and Vetter, [18] and by Vetter and Klein [19] who evaluated that $\gamma_{H_{UPD}} = 0.95 \cong 1$. Based on these findings one may conclude that the UPD H leads to a complete discharge of H^+ (or H_3O^+) which is the source of the electroadsorbed H, H_{UPD}, thus the value of z for the process equals unity ($z = 1$) and the electrochemical adsorption isotherm for reaction [3] may be written according to the following equation: [4,11,17]

$$\frac{\theta_{H_{UPD}}}{1-\theta_{H_{UPD}}} = a_{H_3O^+} \exp(-EF/RT) \exp(-\Delta G^{\circ}_{ads}(H_{UPD})/RT) \qquad [4]$$

In discussion of hydrogen adsorption on Pt and Rh electrode surfaces, it is essential to distinguish between H_{UPD} and the over-potential deposited H (H_{OPD}) which is an intermediate of the HER. [6-13] The over-potential deposition of hydrogen (OPD H) takes place at potentials negative to E°_{HER}, thus at potentials negative with respect to the UPD H and H_{OPD} is bound less strongly to the metal substrate than H_{UPD}. [6-13] Spectroscopic measurements [20-22] show that the H_{OPD} interacts with a H_2O molecule forming a bond whereas H_{UPD} appears to be unavailable for forming a bond with H_2O molecules in the double-layer region. Experimental evidence [23,24] also reveals that on Pt electrodes, H_{UPD} co-exist with H_{OPD} in the negative potential region, thus the two species must occupy two distinct surface adsorption sites in order to sustain their chemical identity. Subsequently, if H_{UPD} and H_{OPD} occupy unlike adsorption sites, then their Gibbs free energies of adsorption, enthalpies of adsorption and bond energies should be distinct.

In general, fundamental studies of the enthalpies of adsorption of H_{UPD} and H_{OPD}, $\Delta H^{\circ}_{ads}(H_{UPD})$ and $\Delta H^{\circ}_{ads}(H_{OPD})$, and the bond energies between the metal substrate (M) and H_{UPD} or between M and H_{OPD} ($E_{M-H_{UPD}}$ and $E_{M-H_{OPD}}$, respectively) are of extreme importance to electrochemical surface science, materials and corrosion sciences. [25-27] They allow one to

assess which of these electroadsorbed H species undergoes interfacial entry into the host metal as well as to evaluate, on the thermodynamic basis, the adsorption sites of the H_{UPD} and H_{OPD} surface species. [23,24,28,29] Subsequently, experimentally determined values of the Gibbs free energies of the electroadsorbed H_{UPD} and H_{OPD}, $\Delta G^{\circ}_{ads}(H_{UPD})$ and $\Delta G^{\circ}_{ads}(H_{OPD})$, lead to determination of the chemical potential gradient associated with the interfacial H transfer from the adsorbed to the absorbed state, thus the thermodynamic driving force of the process. [28,29] The latter is of vital importance to the recently developing metal-hydride science because it defines the nature and strength of the $M-H$ bond on the metal surface prior to the H interfacial transfer into the metal bulk.

While there is a significant amount of data [12,30,31] on $\Delta G^{\circ}_{ads}(H_{chem})$, $\Delta H^{\circ}_{ads}(H_{chem})$, $\Delta S^{\circ}_{ads}(H_{chem})$ and $E_{M-H_{chem}}$ for dissociative H chemisorption from the gas phase, the authors are unaware of any data on $E_{M-H_{UPD}}$ which is the original contribution reported in this paper. New data is reported on $\Delta G^{\circ}_{ads}(H_{UPD})$ as a function of T and $\theta_{H_{UPD}}$, $\Delta H^{\circ}_{ads}(H_{UPD})$ and $\Delta S^{\circ}_{ads}(H_{UPD})$ in relation to the concentration of the electrolyte which gives rise to the specific anion adsorption.

EXPERIMENTAL

1. Electrode Preparation. The technique of preparing electrodes was found to be very important with respect to the reproducibility of the experimental results. [32-36] The electrode preparation procedure involved the following steps: (a) initial cleaning of the Rh wire (99.99% purity) by refluxing in acetone for 12 h; (b) flame-welding the Rh wire to a Ag wire for electrical contact (the Ag wire was not in contact with the solution); (c) sealing the Rh wire into pre-cleaned soft-glass tubing followed again by step (a); (d) cleaning the electrode in conc. H_2SO_4 for 12 h; (e) repetitive washing in "Nanopure" water, followed by soaking for 24 h. Since the heat treatment of Rh electrodes always affected the surface, prior to the measurements the electrodes were cycled 4,000 times between 0.04 and 1.40 V, NHE, in order to release any stress from the near-surface region. [37] After this procedure, the electrodes and their surfaces were found stable and did not undergo any further changes, as revealed from the CV profiles (see refs. 35-37); the shape of the UPD H CV profiles and the double layer CV charging curves were found to be consistent with those reported in earlier literature. [5,35,36] The real surface area of the Rh(poly) electrodes was determined by accepting an anodic charge value of 210 $\mu C\ cm^{-2}$ as that necessary to form a monolayer of H_{UPD} [5,35,36] allowing for double-layer charging. It was calculated to be $A_r = 0.70 \pm 0.01\ cm^2$.

Solution and Electrochemical Cell. High-purity solutions were prepared from BDH "Aristar" grade H_2SO_4 and "Nanopure" water (18 MΩ cm), and their cleanliness was verified by recording CV H_{UPD} adsorption/desorption profiles and comparing them with those in the literature. [32-37] The experiments were conducted in a standard all-Pyrex, three-compartment electrochemical cell. [32-37] The glassware was pre-cleaned according to well established previous procedure. [32-34] During the experiments H_2 gas, pre-cleaned and pre-saturated with water vapor, was bubbled through the reference electrode (RE) compartment in which a Pt/Pt-black reference electrode (RE) was immersed. Similarly, N_2 gas, pre-cleaned and pre-saturated with water vapor, was passed through the working (WE) and counter electrode (CE) compartments. [32,33]

Temperature Measurements. The electrochemical cell was immersed in a water bath (Haake W13) and the temperature was controlled to within ± 0.5 K by means of a thermostat (Haake D1); the water level in the bath was maintained above the electrolyte in the cell. The temperature in the water bath and the electrochemical cell were controlled by means of thermometers (± 0.5 K) and a K-type thermocouple (80 TK Fluke), and were found to agree to within ± 0.5 K. In order to ensure uniform temperature distribution in the cell, N_2 gas pre-heated to the temperature of the water bath was passed through the electrolyte.

Electrochemical Measurements. The experimental procedure applied in this project involved standard cyclic-voltammetry (CV) measurements of the UPD H on Rh electrodes in a 0.5 M aqueous solution of H_2SO_4 within a temperature range between 273 and 343 K. The electrochemical instrumentation included: (a) EG&G Model 263A potentiostat-galvanostat; (b) IBM-compatible 80386, 40 MHz computer; and (c) EG&G M270 Electrochemical Software. All potentials were measured with respect to the reversible hydrogen electrode (RHE) immersed in the same electrolyte. The potential of the RHE differed from that of the normal hydrogen electrode (NHE); it was evaluated according to the Nernst equation that the zero potential on the RHE scale in the 0.50, 0.10 and 0.05 M aqueous H_2SO_4 solutions corresponded to −0.021, −0.060 and −0.075 V, respectively, on the NHE scale.

Curve Fitting Procedure. The $\Delta G_{ads}(H_{UPD})$, $\Delta S_{ads}(H_{UPD})$, $\Delta H_{ads}(H_{UPD})$ and $E_{Rh-H_{UPD}}$ vs. θ_H or E plots presented in Results and Discussion were fitted into a first, second or third order polynomials using the SigmaPlot software package of Jandel Scientific. The SigmaPlot linear regression procedure uses the least squares to fit a set of (x_i, y_i) where $i = 1, \ldots, n$, to a polynomial of order p, $y = \beta_o + \beta_1 x + \beta_2 x^2 + \ldots + \beta_P x^P$. In the vector-matrix

notation, this problem is formulated as: $Y = X\beta + \varepsilon$ where the $(n \times 1)$ vector containing the y_i data is $Y = [y_1, y_2, \ldots, y_n]$ and the $n \times (p+1)$ design matrix is

$$X = \begin{bmatrix} 1 & x_1 & x_1^2 & \ldots & x_1^P \\ 1 & x_2 & x_2^2 & \ldots & x_2^P \\ & & & & \\ 1 & x_n & x_n^2 & \ldots & x_n^P \end{bmatrix}$$

β is a $(p+1) \times 1$ vector of parameters to be estimated, $\beta = [\beta_0, \beta_1, \ldots, \beta_P]$, and ε is a $(n \times 1)$ vector of residuals. The solution for the least squares estimates of the parameters β_i is given by $b = (X' \cdot X)^{-1} X' \cdot Y$. The software uses the Cholesky decomposition of the X' Y matrix and gives the regression curve expressed by $\hat{y} = b_o + b_1 x_o + b_2 x_o^2 + \ldots + b_P x_o^P$. A detail description of this procedure can be found in refs. 38,39.

RESULTS AND DISCUSSION

Temperature-Dependence of the UPD H. Fig. 1 shows a series of CV adsorption-desorption for the UPD H from a 0.50 M aqueous solution of H_2SO_4 for various temperature between 273 and 343 K, with an interval of 10 K recorded at the sweep rate of 20 mV s^{-1}. It should be added that experiments were conducted with the temperature interval of 5 K but in order not to obscure the graph fewer experimental curves are shown. The CV profiles demonstrate that the adsorption and desorption peaks shift towards less positive potentials upon the temperature increase and that they are symmetric with respect to the potential axis indicating that the surface process is reversible. An increase of the cathodic current at the lower potential limit of the CV profiles, thus prior to the sweep reversal, is due to the onset of the over-potential deposition of H. The authors conducted identical experiments in 0.05 and 0.10 M aqueous H_2SO_4 solutions in order to evaluate changes in the CV profiles brought about by the temperature variation. In order to avoid repetitions, the authors show a series of UPD H cyclic-voltammetry adsorption-desorption profiles for the three concentrations of H_2SO_4 at four different temperatures (Fig. 2). The diagrams indicate the same behavior of the UPD H adsorption-desorption profiles which may be summarized as follows: (i) the temperature increase shifts the UPD H adsorption-desorption profiles towards less-positive values; (ii) no new features are observed in the CV profiles that could result from the

temperature increase for a given concentration of H_2SO_4; (iii) upon decrease of the concentration of H_2SO_4, the UPD H adsorption-desorption peaks become less sharp (less pronounced) but the total H_{UPD} adsorption-desorption charges remain unchanged. [40-44]

Determination of $\Delta G^\circ_{ads}(H_{UPD})$, $\Delta S^\circ_{ads}(H_{UPD})$ and $\Delta H^\circ_{ads}(H_{UPD})$. In the absence of lateral interaction between adsorbed species, the standard Gibbs free energy of adsorption can be expressed by relation $\Delta G^\circ_{ads} = N\, q^\circ_{ads}$ where N is the number of adsorbed species and q°_{ads} is the standard Gibbs free energy of adsorption per adsorbed species. [45-47] However, when more species become adsorbed on the substrate, they might begin to interact and to influence each other's enthalpies of adsorption and bond energies. In this case, the values of q°_{ads} and ΔG°_{ads} change due to *lateral repulsive* or *attractive interactions*. [45] In other words, the relation between ΔG°_{ads} and the surface coverage of the adsorbed species points to the nature of their lateral interactions.

Evaluation of the Gibbs free energy of adsorption for H_{UPD}, $\Delta G^\circ_{ads}(H_{UPD})$, may not be simply based on the Langmuir or the Frumkin isotherm for it is unknown whether $\Delta G^\circ_{ads}(H_{UPD})$ is independent of the H_{UPD} surface coverage, $\theta_{H_{UPD}}$, thus $\Delta G^\circ_{ads}(H_{UPD})_{\theta_{H_{UPD}}=0} = \Delta G^\circ_{ads}(H_{UPD})_{\theta_{H_{UPD}}\neq 0}$, or whether it changes in a linear manner with $\theta_{H_{UPD}}$, thus $\Delta G^\circ_{ads}(H_{UPD})_{\theta_{H_{UPD}}\neq 0} = \Delta G^\circ_{ads}(H_{UPD})_{\theta_{H_{UPD}}=0} + g\,\theta_{H_{UPD}}$. The authors determine numerically the Gibbs free energy of adsorption for given $\theta_{H_{UPD}}$ and T based upon the following formula (see Appendix for the origin of this relation):

$$\frac{\theta_{H_{UPD}}}{1-\theta_{H_{UPD}}} = P_{H_2}^{1/2} \exp\left(-\frac{FE}{RT}\right)\exp\left(-\frac{\Delta G^\circ_{ads}(H_{UPD})}{RT}\right) \qquad [5]$$

where $\Delta G^\circ_{ads}(H_{UPD})$ includes a coverage-dependent parameter, $\omega(\theta_{H_{UPD}})$, which describes their lateral interactions, thus $\Delta G^\circ_{ads}(H_{UPD})_{\theta_{H_{UPD}}\neq 0} = \Delta G^\circ_{ads}(H_{UPD})_{\theta_{H_{UPD}}=0} + \omega(\theta_{H_{UPD}})$, $P_{H_2}^{1/2}$ is the partial pressure of H_2 in the reference electrode compartment, and E is the experimentally measured potential difference between the working electrode and the reference electrode immersed in the same solution, thus the potential, E, measured versus the RHE. Based upon the experimental data, the authors determine the potential, E, at which the H_{UPD} surface coverage, $\theta_{H_{UPD}}$, reaches a given value for a given constant temperature, T, and subsequently introduce it into formula [5] and calculate $\Delta G^\circ_{ads}(H_{UPD})$. This procedure is applied to various values of $\theta_{H_{UPD}}$ between 0.05 and 0.95 with an interval of 0.05 and it allows determination of

$\Delta G^{\circ}_{ads}(H_{UPD})$ as a function of both $\theta_{H_{UPD}}$ and T, $\Delta G^{\circ}_{ads}(H_{UPD}) = f(\theta_{H_{UPD}}, T)$. Fig. 3 shows 3D plots of $\Delta G^{\circ}_{ads}(H_{UPD})$ versus $\theta_{H_{UPD}}$ and T for the three concentrations of H_2SO_4; the data demonstrate that $\Delta G^{\circ}_{ads}(H_{UPD})$ varies between −18 and −8 kJ mol^{-1} depending on $\theta_{H_{UPD}}$ and T. The Gibbs free energy of adsorption has the most negative values at the lowest temperature and at the smallest H_{UPD} surface coverage. Augmentation of $\Delta G^{\circ}_{ads}(H_{UPD})$ with increasing $\theta_{H_{UPD}}$ for a constant temperature (T = const) indicates that the lateral interactions between the H_{UPD} species are predominantly of the repulsive nature. [2-4,23,24,30,31,45,48]

It is of interest to assess the dependence of $\Delta G^{\circ}_{ads}(H_{UPD})$ as a function of $\theta_{H_{UPD}}$ for a constant temperature (T = const). An examination of the $\Delta G^{\circ}_{ads}(H_{UPD})$ vs. $(\theta_{H_{UPD}}, T)$ plots shown in Fig. 3 for 0.05 and 0.10 M H_2SO_4 solutions indicates that the changes of $\Delta G^{\circ}_{ads}(H_{UPD})$ are pronounced the most in the $0 - 0.20$ range of $\theta_{H_{UPD}}$ and at low temperatures. When the temperature approaches high values, $\Delta G^{\circ}_{ads}(H_{UPD})$ does not vary more than some 4 kJ mol^{-1} and the $\Delta G^{\circ}_{ads}(H_{UPD})$ vs. $\theta_{H_{UPD}}$ relations become almost linear. In the 0.50 M H_2SO_4 solution, the $\Delta G^{\circ}_{ads}(H_{UPD})$ vs. $\theta_{H_{UPD}}$ dependence is slightly more complex; at low temperatures, $\Delta G^{\circ}_{ads}(H_{UPD})$ varies significantly with $\theta_{H_{UPD}}$ especially in the $0 - 0.40$ range of the surface coverage by H_{UPD}. However at high temperatures, the changes become less pronounced and $\Delta G^{\circ}_{ads}(H_{UPD})$ does not vary more than some 4 kJ mol^{-1} over the whole range of $\theta_{H_{UPD}}$. An analysis of the $\Delta G^{\circ}_{ads}(H_{UPD})$ vs. $\theta_{H_{UPD}}$ plots shown in Fig. 3 reveals that they may not be simply fitted into the Frumkin isotherm in order to evaluate the energy of lateral interactions because the dependences are non-linear, thus appraisal of the energy of lateral repulsions is not straightforward. Nevertheless, in the case of H adsorption from 0.05 and 0.10 M H_2SO_4 solutions and in the $0.20 - 0.80$ range of the H_{UPD} surface coverage, the $\Delta G^{\circ}_{ads}(H_{UPD})$ vs. $\theta_{H_{UPD}}$ relations are linear indicating applicability of the Frumkin isotherm. The authors fitted the $\Delta G^{\circ}_{ads}(H_{UPD})$ vs. $\theta_{H_{UPD}}$ relations (for T = const) for $0.20 \le \theta_{H_{UPD}} \le 0.80$ into the Frumkin isotherm and evaluated the Gibbs free energy of lateral repulsions, g, in relation to the temperature. The data shown in Fig. 4 indicate that g assumes values between 2 and 5 kJ mol^{-1} thus increasing $\Delta G^{\circ}_{ads}(H_{UPD})$ from more negative to less negative values. The experimental results also indicate that g varies with temperature, $g = f(T)$, and that it assumes the lowest values at the highest temperatures.

The entropy of the UPD H on Rh, $\Delta S^{\circ}_{ads}(H_{UPD})$, is determined based upon the temperature dependence of $\Delta G^{\circ}_{ads}(H_{UPD})$. An analysis of the $\Delta G^{\circ}_{ads}(H_{UPD})$ vs. $(\theta_{H_{UPD}}, T)$ plots shown in Fig. 3 reveals that for a given H_{UPD} surface coverage ($\theta_{H_{UPD}}$ = const) the relation

between $\Delta G^{\circ}_{ads}(H_{UPD})$ and T is linear, thus allowing determination of the entropy of adsorption from the slope of the $\Delta G^{\circ}_{ads}(H_{UPD})$ vs. T dependences, $\Delta S^{\circ}_{ads}(H_{UPD}) = -\left(\partial \Delta G^{\circ}_{ads}(H_{UPD})/\partial T\right)_{\theta_{H_{UPD}}=const}$. Fig. 5 shows the $\Delta S^{\circ}_{ads}(H_{UPD})$ vs. $\theta_{H_{UPD}}$ relations for the three concentrations of H_2SO_4. The data demonstrate that $\Delta S^{\circ}_{ads}(H_{UPD})$ varies significantly with $\theta_{H_{UPD}}$ between -125 and -15 J mol^{-1} K^{-1}; it assumes the more negative values at the lowest H_{UPD} surface coverage and it assumes less-negative values with increasing $\theta_{H_{UPD}}$. The $\Delta S^{\circ}_{ads}(H_{UPD})$ vs. $\theta_{H_{UPD}}$ relations almost follow each other for $\theta_{H_{UPD}} \geq 0.55$ and there are significant differences for $\theta_{H_{UPD}} < 0.55$. The differences between the $\Delta S^{\circ}_{ads}(H_{UPD})$ vs. $\theta_{H_{UPD}}$ relations for the 0.05 and 0.10 M H_2SO_4 solutions are small and they almost overlap each other. The $\Delta S^{\circ}_{ads}(H_{UPD})$ vs. $\theta_{H_{UPD}}$ relation for the 0.5 M H_2SO_4 solution differs from the others and $\Delta S^{\circ}_{ads}(H_{UPD})$ has more-negative values especially in the $0-0.55$ range of $\theta_{H_{UPD}}$. At this preliminary level, the $\Delta S^{\circ}_{ads}(H_{UPD})$ vs. $\theta_{H_{UPD}}$ behavior may be assigned to the specific anion adsorption being more pronounced in the more concentrated electrolyte. The $\Delta S^{\circ}_{ads}(H_{UPD})$ vs. $\theta_{H_{UPD}}$ dependences presented here indicate that the entropy of the under-potential deposition of H depends on the concentration of the electrolyte thus is associated with the anion concentration at the solid/liquid interface. In order to evaluate the entropy of the very first H_{UPD} adatom deposited on the Rh electrode, the authors fitted the $\Delta S^{\circ}_{ads}(H_{UPD})$ vs. $\theta_{H_{UPD}}$ plots into a third order polynomial and then elucidated $\Delta S^{\circ}_{ads}(H_{UPD})_{\theta_{H_{UPD}}\to 0}$ from the Y-intercept. In the case of H adsorption from the 0.05 and 0.10 M H_2SO_4 solutions, the values of $\Delta S^{\circ}_{ads}(H_{UPD})_{\theta_{H_{UPD}}\to 0}$ are the same and equal -99 J mol^{-1} K^{-1} whereas in the case of the 0.5 M H_2SO_4 solution it is -138 J mol^{-1} K^{-1}.

The enthalpy of the under-potential deposition of H on Rh electrodes, $\Delta H^{\circ}_{ads}(H_{UPD})$, from aqueous H_2SO_4 solutions is determined based on the above determined values of $\Delta G^{\circ}_{ads}(H_{UPD})$ and $\Delta S^{\circ}_{ads}(H_{UPD})$, and the well-known formula $\Delta G^{\circ} = \Delta H^{\circ} - T\,\Delta S^{\circ}$. Fig. 6 shows $\Delta H^{\circ}_{ads}(H_{UPD})$ versus $\theta_{H_{UPD}}$ relations for the three concentrations of H_2SO_4, namely 0.05, 0.10 and 0.5 M H_2SO_4. The dependences demonstrate that $\Delta H^{\circ}_{ads}(H_{UPD})$ accepts negative values between -45 and -15 kJ mol^{-1}. For the three concentrations of H_2SO_4, $\Delta H^{\circ}_{ads}(H_{UPD})$ increases towards less-negative values with increasing $\theta_{H_{UPD}}$. In order to evaluate the enthalpy change associated with deposition of the very first H_{UPD} adatom on the Rh electrode, the authors fitted the $\Delta H^{\circ}_{ads}(H_{UPD})$ vs. $\theta_{H_{UPD}}$ plots into a third order polynomial and then elucidated $\Delta H^{\circ}_{ads}(H_{UPD})_{\theta_{H_{UPD}}\to 0}$ from the Y-intercept. In the case of H adsorption

from the 0.05 and 0.10 M H_2SO_4 solutions, the values of $\Delta H^{\circ}_{ads}(H_{UPD})_{\theta_{H_{UPD}} \to 0}$ are the same and equal -45 kJ mol^{-1} whereas in the case of the 0.5 M H_2SO_4 solution it is -56 kJ mol^{-1}. Decrease of $\Delta H^{\circ}_{ads}(H_{UPD})$ with increasing $\theta_{H_{UPD}}$ points to the repulsive nature of the lateral interactions between the H_{UPD} adatoms.

It is essential to assess whether the under-potential deposition of H on Rh electrodes is an enthalpy-driven or entropy-driven process. Comparison of the experimentally determined values of $\Delta H^{\circ}_{ads}(H_{UPD})$ with the product $T\,\Delta S^{\circ}_{ads}(H_{UPD})$ for various H_{UPD} surface coverages reveals that $\left|\Delta H^{\circ}_{ads}(H_{UPD})\right| > \left|T\,\Delta S^{\circ}_{ads}(H_{UPD})\right|$, thus indicating the process in enthalpy-driven.

Determination of the $Rh-H_{UPD}$ Bond Energy, $E_{Rh-H_{UPD}}$. The energy of the $M-H_{UPD}$ bond, $E_{M-H_{UPD}}$, has never been evaluated for the electroadsorbed H on Rh, Pt, Ir or any other metal on which the UPD H takes place, thus it is one of the most significant contributions presented in this paper. Moreover, evaluation of the $E_{M-H_{UPD}}$ vs. $\theta_{H_{UPD}}$ relation is of importance in determination of the influence of the electrified solid-liquid interface on the strength and nature of the metal-hydrogen bond.

The energy of the $M-H_{UPD}$ bond, $E_{M-H_{UPD}}$, can readily be calculated once the $\Delta H^{\circ}_{ads}(H_{UPD})$ values for various H_{UPD} surface coverages have been found. Appraisal of the $M-H_{UPD}$ bond energy, $E_{M-H_{UPD}}$ (here of the $Rh-H_{UPD}$ bond energy, $E_{Rh-H_{UPD}}$) is based upon the following theoretical treatment.

The two single-electrode processes of the system studied are as follows:

working electrode: $\quad H^+ + e + M \rightarrow M-H_{UPD}$ [6]

reference electrode: $\quad 1/2\,H_2 \rightarrow H^+ + e$ [7]

and their respective Born-Haber thermodynamic cycles are:

$$\begin{array}{ccccccc} H^+_{(gas)} & + & e_{(gas)} & + & M & \xleftarrow{I_H} & H_{(gas)} + M \\ \downarrow \Delta H^{\circ}_{solv} & & \uparrow \Phi + EF & & & & \uparrow E_{M-H_{UPD}} \\ H^+ & + & e_{M(E\neq 0)} & + & M & \xrightarrow{\Delta H^{\circ}_{WE}} & M-H_{UPD} \end{array} \qquad [8]$$

and

$$\begin{array}{ccccc} H_{(gas)} & \xrightarrow{I_H} & H^+ & + & e_{(gas)} \\ \uparrow \tfrac{1}{2} D_{H_2} & & \uparrow \Delta H^\circ_{solv} & & \uparrow \Phi \\ 1/2\, H_2 & \xrightarrow{\Delta H^\circ_{RE}} & H^+ & + & e_{M(E=0)} \end{array} \qquad [9]$$

where ΔH°_{solv} is the standard enthalpy of solvation of H^+, I_H is the ionization potential of H, Φ is the metal work function and it varies linearly with the applied potential, thus $\Phi_{(E\neq 0)} = \Phi_{(E=0)} + FE$, D_{H_2} is the dissociation energy of the hydrogen molecule, ΔH°_{WE} is the enthalpy of the single-electrode process at the working electrode and ΔH°_{RE} is the enthalpy of the single-electrode process at the reference electrode. [49,50] Summation of the two single-electrode processes leads to the following total reaction:

$$1/2\, H_2 + M \xrightarrow{\Delta H^\circ_{ads}(H_{UPD})} M - H_{UPD} \qquad [10]$$

Subsequently, upon adding the respective Born-Haber cycles and bearing in mind that there is a Volta potential difference between the metal and the solution so that the H^+ and e extracted from the two solid electrodes are at different electrostatic potentials and this difference compensates exactly the work function variation shown in scheme [8] at the working electrode, thus EF, one obtains the following relation for the $M - H_{UPD}$ bond energy:

$$E_{M-H_{UPD}} = \frac{1}{2} D_{H_2} + \Delta H^\circ_{ads}(H_{UPD}) \qquad [11]$$

Fig. 7 shows the values of the $Rh - H_{UPD}$ bond energy, $E_{Rh-H_{UPD}}$, for H_{UPD} electroadsorbed from 0.05, 0.10 and 0.5 M H_2SO_4 solutions. The experimental data reveal that the values fall in the $230 - 270$ kJ mol^{-1} range and that the variation of $E_{Rh-H_{UPD}}$ versus $\theta_{H_{UPD}}$ follows the changes of $\Delta H^\circ_{ads}(H_{UPD})$ as a function of $\theta_{H_{UPD}}$. The $Rh - H_{UPD}$ bond energy varies the most in the case of the 0.5 M H_2SO_4 electrolyte whereas in the case of the 0.05 and 0.1 M H_2SO_4 solutions the plots follow each other. The variation of $E_{Rh-H_{UPD}}$ with the concentration of

H_2SO_4 is assigned to the specific anion adsorption at the electrodes surfaces which is pronounced the most for the most concentrated electrolyte. [51-53]

It is essential to compare the above determined value of $E_{Rh-H_{UPD}}$ to those for H chemisorbed dissociatively from the gas phase on Rh (H_{chem}). The values of the $Rh-H_{chem}$ bond energy, $E_{Rh-H_{chem}}$, for H chemisorbed on Rh(111) and Rh(110) single-crystal faces [30,45] are $E_{Rh(111)-H_{chem}} = 255$ and $E_{Rh(110)-H_{chem}} = 255$ kJ mol^{-1}, respectively. These data and the experimental results for $E_{Rh-H_{UPD}}$ indicate that the bond energies for the electroadsorbed H and the chemisorbed H are close to each other, say within some 25 kJ mol^{-1}. Prior to any further discussion of the relation between $E_{Rh-H_{UPD}}$ and $E_{Rh-H_{chem}}$, it is essential to elaborate on the $M-H_{chem}$ bond energy for various transition metals.

In the review article by Christmann [30], it is recognized that the values of the $M-H_{chem}$ bond energies, $E_{M-H_{chem}}$, for various transition metals fall into the $250-270$ kJ mol^{-1} range and that they are almost the same for various single-crystal faces of the transition metals. Proximity of the values of $E_{M-H_{chem}}$ and their independent of the surface geometry points to a similar surface binding mechanism on various transition metal surfaces. Thus, one may conclude that the H_{chem} adatom is strongly embedded into the metal surface lattice being coplanar with the metal topmost surface atoms or that it penetrates into the metal surface lattice occupying sites between the first and the second metal surface layer.

It has been shown above that $Rh-H_{UPD}$ bond energy, $E_{Rh-H_{UPD}}$, falls close to that for $Rh-H_{chem}$, say within the proximity of some 25 kJ mol^{-1}. Based on these data and on the discussion of the nature of the $M-H_{chem}$ surface bond, it is apparent that the binding mechanism between Rh and H_{UPD} involving the electrified double-layer is similar to that under gas-phase conditions. In other words, the under-potential deposited H, H_{UPD}, is also embedded in the surface metal lattice in a manner similar to that for the chemisorbed H. This conclusion coincides with the observation [20-22] that the H_{UPD} species is unavailable to form a bond with H_2O molecules in the double layer region. Finally, it should be added that at this point of development of the treatment presented here, the specific interaction of H adatoms with co-adsorbed anions or water molecules are not taken into account. [51-53] This important aspect is currently under experimental and theoretical investigation on Rh(111) and Pt(111), and will be reported in subsequent papers.

CONCLUSIONS

1. Temperature-dependence of the under-potential deposition of H on Rh electrodes from 0.05, 0.1 and 0.5 M aqueous H_2SO_4 solutions by cyclic-voltammetry and a theoretical approach based on an electrochemical adsorption isotherm allow determination of $\Delta G^{\circ}_{ads}(H_{UPD})$, $\Delta S^{\circ}_{ads}(H_{UPD})$ and $\Delta H^{\circ}_{ads}(H_{UPD})$ of adsorption; $\Delta G^{\circ}_{ads}(H_{UPD})$ accepts values between -8 and -18 kJ mol^{-1}, $\Delta S^{\circ}_{ads}(H_{UPD})$ between -15 and -125 J mol^{-1} K^{-1} and $\Delta H^{\circ}_{ads}(H_{UPD})$ between -15 and -52 kJ mol^{-1}.

2. The $\Delta G^{\circ}_{ads}(H_{UPD})$ is found to increase with the H_{UPD} surface coverage, $\theta_{H_{UPD}}$, indicating that the lateral interactions between H_{UPD} adatoms are of the repulsive nature.

3. Knowledge of $\Delta H^{\circ}_{ads}(H_{UPD})$ permits determination of the surface bond energy between Rh and H_{UPD}, $E_{Rh-H_{UPD}}$, which is between 235 and 265 kJ mol^{-1} depending on the H_{UPD} surface coverage ($\theta_{H_{UPD}}$). The value of $E_{Rh-H_{UPD}}$ is close to that of the bond energy between Rh and the H chemisorbed from the gas phase (H_{chem}), $E_{Rh-H_{chem}}$, which equals 255 kJ mol^{-1}. Proximity of these values points to a similar binding mechanism under the conditions involving the presence of an electric field and electrolyte and under the gas-phase conditions. Thus H_{UPD} and H_{chem} are equivalent surface species and H_{UPD} is embedded in the metal surface lattice in a manner similar to that of H_{chem}.

ACKNOWLEDGMENTS

Acknowledgment is made to the NSERC of Canada and FCAR du Québec for support of this research. The authors thank discussions with Professor B. E. Conway of the University of Ottawa and Professor R. Parsons, FRS, of the University of Southampton for comments on thermodynamics of the electrified solid/liquid interface. The junior author acknowledges a graduate fellowship from the MHE of Iran.

REFERENCES

1. Will, F.G. and Knorr, C.A. *Z. Electrochem.* **1960**, *64*, 258-269; 270-275.

2. Boeld, W. and Breiter, M. W. *Z. Elektrochem.* **1960**, *64*, 897-902; see also Breiter, M. W. and Kennel, B. *Z. Elektrochem.* **1960**, *64*, 1180-1187..

3. Breiter, M. W. in *Transactions of the Symposium on Electrode Processes*, Yeager, E. (Ed.), John Wiley and Sons, New York, 1961; see also Breiter, M. W. *Electrochim. Acta.* **1962**, *7*, 25-38; Breiter, M. W. *Ann. N. Y. Acad. Sci.* **1963**, *101*, 709-721.

4. Frumkin, A. N. in *Advances of Electrochemistry and Electrochemical Engineering*, Delahey, P. (Ed.), Vol. 3, Interscience Publishers, New York, 1963; pp 287-391.

5. Woods, R. in *Electroanalytical Chemistry*, Bard, A. (Ed.), Vol. 9, Marcel Dekker, New York, 1977; pp 27-90.

6. Conway, B. E. *Theory and Principles of Electrode Processes*; Ronald Press, London, 1965.

7. Enyo, M. in *Modern Aspects of Electrochemistry*, Conway, B. E. and Bockris, J. O'M. (Eds.), Vol. 11, Plenum Press, New York, 1975; pp 251-314.

8. Enyo, M. in *Comprehensive Treatise of Electrochemistry*, Conway, B. E. and Bockris, J. O'M. (Eds.), Vol. 7, Plenum Press, New York, 1983; pp 241-300.

9. Conway, B. E., Angerstein-Kozlowska, H. and Dhar, H. P. *Electrochim. Acta* **1974**, *19*, 455-460.

10. Conway, B. E., and Angerstein-Kozlowska, H. *Acc. Chem. Res.* **1981**, *14*, 49-56.

11. Conway, B. E., Angerstein-Kozlowska, H. and Ho, F. C. *J. Vac. Sci. Technol.* **1977**, *14*, 351-364.

12. Conway, B. E., Angerstein-Kozlowska, H. and Sharp, W. B. A. *Trans. Faraday Soc.* **1977**, *19*, 1373-1389.

13. Conway, B. E. *Sci. Prog. Oxf.* **1987**, *71*, 479-510; see also Conway, B. E. and Bai, L. J. Electroanal. Chem. **1986**, *198*, 149-175.

14. Baldauf, M. and Kolb, D. M. *Electrochim. Acta* **1993**, *38*, 2145-2153.

15. Haissinsky, M. *J. Chim. Phys.* **1946**, *43*, 21.

16. Kolb, D. M., Przasnyski, M. and Gerischer, H. *J. Electroanal. Chem.* **1974**, *54*, 25-38.

17. Gileadi, E. *Electrode Kinetics*, VCH Publishers, Inc., New York 1993.

18. Schultze, J. W. and Vetter, K. J., *J. Electroanal. Chem.*, **1973**, *44*, 63-81.

19. Vetter, K. J. and Klein, G. P., Z. Elektrochem., **1962**, *66*, 760.

20. Bewick, A. and Russell, J. W. *J. Electroanal. Chem.* **1982**, *132*, 329-343.

21. Nichols, R. J. and Bewick, A. *J. Electroanal. Chem.* **1988**, *243*, 445-453.
22. Bewick, A. and Russell, J. W., *J. Electroanal. Chem.* **1982**, *142*, 337-343.
23. Protopopoff, E. and Marcus, P. *J. Vac. Sci. Technol. A*, **1987**, 5, 944-947; see also *C. R. Acad. Sci. Paris,* **1989**, *t 308*, Serie II, 1127-1133.
24. Protopopoff, E. and Marcus, P. *J. Chim. Phys.* **1991**, *88*, 1423-1452.
25. MacKey, K.M. *Hydrogen Compounds of the Metallic Elements*, E.&F.N. Spon, London, 1966.
26. Alefeld, G. and Volkl, J. (Eds.), *Hydrogen in Metals*, Parts I and II; Springer-Verlag, New York, 1978.
27. Schlapbach, L. (Ed.), *Hydrogen in Intermetalic Compounds*; Part I, Springer-Verlag, New York, 1988; Part II, Springer-Verlag, New York, 1992.
28. Conway, B. E. and Jerkiewicz, G. *J. Electroanal. Chem.* **1993**, *357*, 47-66; see also Jerkiewicz, G., Borodzinski, J. J., Chrzanowski, W. and Conway, B. E. *J. Electrochem. Soc.* **1995**, *142*, 3755-3763.
29. Conway, B. E. and Jerkiewicz, G. *Z. Phys. Chem. Bd.* **1994**, *183*, 281-286.
30. Christman, K. *Surface Sci. Rep.* **1988**, *9*, 1-163.
31. Breiter, M. *Trans. Faraday. Soc.* **1964**, *64*, 1445-1449.
32. Angerstein-Kozlowska, H., Conway, B. E. and Sharp, W. B. A. *J. Electroanal. Chem.* **1973**, *43*, 9.
33. Angerstein-Kozlowska, H. in *Comprehensive Treatise of Electrochemistry*, Vol.9, Yeager, E., Bockris, J.O'M., Conway, B. E. and Sarangapani, S. (Eds.) Plenum Press, New York, 1984; pp. 15-59.
34. Conway, B. E., Sharp, W.B.A., Angerstein-Kozlowska, H. and Criddle, E. E. *Anal. Chem.* **1973**, *41*, 1321.
35. Jerkiewicz, G. and Borodzinski, J. J. *Langmuir*, **1993**, *9*, 2202.
36. Jerkiewicz, G. and Borodzinski, J. J. *J. Chem. Soc. Faraday Transactions*, **1994**, *90*, 3669-3675.
37. Tremiliosi-Filho, G., Jerkiewicz, G. and Conway, B. E. *Langmuir*, **1992**, *8*, 658.
38. Dongarra, J. J., Bunch, J. R., Moler, C. B. and Stewart, G. W., Linpack User's Guide, SIAM, Philidelphia (1979).
39. Draper, N. and Smith, H. *Applied Regression Analysis*, John Wiley and Sons, Inc., New York (1981).

40. Wasberg, M., Hourani, M. and Wieckowski, A. *J. Electroanal. Chem.* **1990**, *278*, 425-432.

41. Hourani, M., Wasberg, M., Rhee, C. and Wieckowski, A. *Croatica Chim. Acta.* **1990**, *63*, 373-399.

42. Zelenay, P., Horányi, G., M., Rhee, C. K. and Wieckowski, A. *J. Electroanal. Chem.* **1991**, *300*, 499-519.

43. Clavilier, J., Wasberg, M., Petit,. M. and Klein, L. H. *J. Electroanal. Chem.* **1994**, *374*, 123-131.

44. Wan, L.-J., Yan, S.-L., Swain, G. M. and Itaya, K. *J. Electroanal. Chem.* **1995**, *381*, 105-111.

45. Somorjai, G. A. *Introduction to Surface Chemistry and Catalysis*, John Wiley and Sons, Inc., New York, 1994.

46. Langmuir, I. *J. Am. Chem. Soc.* **1918**, *40*, 1361-1403.

47. Fowler, R. H. and Guggenheim, F. A. *Statistical Thermodynamics*, Cambridge University Press, London, 1939.

48. Adamson, A. W. *Physical Chemistry of Surfaces*, John Wiley and Sons, New York, 1990.

49. Lide, D. R. (Ed.), *CRC Handbook of Chemistry and Physics*, 72nd Edition, CRC Press, Boston, 1991.

50. Bard, A. J., Parsons, R. and Jordan, J. (Eds.) *Standard Potentials in Aqueous Solutions*, Marcel Dekker, Inc., New York, 1985.

51. Wieckowski, A. in *Electrochemical Interfaces*, Abruña, H. (Ed.), VCH, New York, 1991, p. 65; and refs. therein.

52. Wieckowski, A. in *Adsorption of Molecules at Metal Electrodes*, Lipkowski, J. and Ross, P. N. (Eds.), VCH, New York, 1992, p. 119; and refs. therein.

53. Shi, Z., Wu. S. and Lipkowski, J. *Electrochim. Acta* **1995**, *40*, 9-15; Shi, Z., Wu, S. and Lipkowski, J. *J. Electroanal. Chem.* **1995**, *384*, 171-177.

APPENDIX

Let's consider the two single-electrode processes taking place at the working electrode (WE), metal M_1 and the reference electrode (RE), metal M_2:

$$H^+ + e + M_1 \rightarrow M_1 - H_{UPD} \qquad \text{(WE)} \qquad [1]$$

$$H^+ + e \rightarrow 1/2\, H_2 \qquad \text{(RE)} \qquad [2]$$

Based upon reactions [1] and [2] one may propose the following Gibbs free energy cycles (B. E. Conway, *Theory and Principles of Electrode Processes*, ref. 6); for process [1]:

$$\begin{array}{ccccc} H_{(gas)} & \xrightarrow{\Delta G^\circ_{ion}(H)} & H^+_{(gas)} & + & e_{(gas)} \\ \uparrow \Delta G^\circ_{M_1-H_{ads}} & & \downarrow \Delta G^\circ_{solv}(H^+) & & \downarrow -\Phi_{M_1(E\neq 0)} \\ M_1 - H_{ads} & \xrightarrow{-\Delta G^\circ_{WE}} & H^+_{aq} & + & e_{M_1(E\neq 0)} \end{array} \qquad [3]$$

Based upon the above cycle one gets the following relation for Gibbs free energy of the process taking place at the working electrode, ΔG°_{WE}:

$$-\Delta G^\circ_{WE} = \Delta G^\circ_{M_1-H_{ads}} + \Delta G^\circ_{ion}(H) + \Delta G^\circ_{solv}(H^+) - \Phi_{M_1(E\neq 0)} \qquad [4]$$

where $\Delta G^\circ_{M-H_{UPD}}$ is the Gibbs free energy required to break the $M - H_{UPD}$ bond, $\Delta G^\circ_{solv}(H^+)$ is the Gibbs free energy of solvation of H^+, $\Delta G^\circ_{ion}(H)$ is the Gibbs free energy of ionization of H and the work function of the substrate metal varies linearly with the applied potential, thus $\Phi_{M_1(E\neq 0)} = \Phi_{M_1(E=0)} + EF$.

For process [2]:

$$\begin{array}{ccccc} H_{(gas)} & \xrightarrow{\Delta G^{\circ}_{ion}(H)} & H^{+}_{(gas)} & + & e_{(gas)} \\ \uparrow 1/2\Delta G^{\circ}_{diss}(H_2) & & \downarrow \Delta G^{\circ}_{solv}(H^{+}) & & \downarrow -\Phi_{M_2(E=0)} \\ \frac{1}{2}H_2 & \xrightarrow{-\Delta G^{\circ}_{RE}} & H^{+}_{aq} & + & e_{M_2(E=0)} \end{array} \qquad [5]$$

Based upon the above cycle one gets the following relation for the Gibbs free energy of the process taking place at the reversible hydrogen electrode, ΔG°_{RE}:

$$-\Delta G^{\circ}_{RE} = 1/2\Delta G^{\circ}_{diss}(H_2) + \Delta G^{\circ}_{ion}(H) + \Delta G^{\circ}_{solv}(H^{+}) - \Phi_{M_2(E=0)} \qquad [6]$$

For the single electrode process [1] one may write the following relations:

$$G^{\circ}_{WE} + RT\ln\frac{\theta_{H_{UPD}}}{1-\theta_{H_{UPD}}} = G^{\circ}_{H^{+}} + RT\ln a_{H^{+}} + G^{\circ}_{e(M_1)} + F(\phi_{M_1} - \phi_S) \qquad [7]$$

$$\Delta G^{\circ}_{WE} = RT\ln a_{H^{+}} - RT\ln\frac{\theta_{H_{UPD}}}{1-\theta_{H_{UPD}}} + F(\phi_{M_1} - \phi_S) \qquad [8]$$

where $\Delta G^{\circ}_{WE} = G^{\circ}_{H_{UPD}} - G^{\circ}_{H^{+}} - G^{\circ}_{e(M)}$

For the single electrode process [2] one may write the following relations:

$$1/2G^{\circ}_{diss}(H_2) + RT\ln P^{1/2}_{H_2} = G^{\circ}_{H^{+}} + RT\ln a_{H^{+}} + G^{\circ}_{e(M_2)} + F(\phi_{M_2} - \phi_S) \qquad [9]$$

$$\Delta G^{\circ}_{RE} = RT\ln a_{H^{+}} - RT\ln P^{1/2}_{H_2} + F(\phi_{M_2} - \phi_S) \qquad [10]$$

According to the first Kirchoff's law:

$$FE + F\left(\Phi_{M_2} - \Phi_{M_1}\right) + F\left(\phi_S - \phi_{M_2}\right) + F\left(\phi_{M_1} - \phi_S\right) = 0 \qquad [11]$$

In the above relation, E stands for the experimentally measured potential difference between M_1 and M_2, thus $E = E_{M_1} - E_{M_2} \equiv E_1 - E_2$. From equations [8] and [10] one may isolate formulae for $F(\phi_S - \phi_{M_2})$ and $F(\phi_{M_1} - \phi_S)$ and substitute them into relation [11]. Subsequently, one gets the following equation:

$$F(E_1 - E_2) + F(\Phi_{M_2} - \Phi_{M_1}) - \Delta G^{\circ}_{RE} - RT \ln P_{H_2}^{1/2} + \Delta G^{\circ}_{WE} + RT \ln \frac{\theta_{H_{UPD}}}{1 - \theta_{H_{UPD}}} = 0 \qquad [12]$$

Substituting relations [4] and [6] for ΔG°_{WE} and ΔG°_{RE}, one arrives at the following relation:

$$F(E_1 - E_2) + 1/2\Delta G^{\circ}_{diss}(H_2) - \Delta G^{\circ}_{M_1-H_{UPD}} - RT \ln P_{H_2}^{1/2} + RT \ln \frac{\theta_{H_{UPD}}}{1 - \theta_{H_{UPD}}} = 0 \qquad [13]$$

and after rearrangement, one gets the following relation:

$$RT \ln \frac{\theta_{H_{UPD}}}{1 - \theta_{H_{UPD}}} = -F(E_1 - E_2) - 1/2\Delta G^{\circ}_{diss}(H_2) + \Delta G^{\circ}_{M_1-H_{UPD}} + RT \ln P_{H_2}^{1/2} \qquad [14]$$

Its rearrangement leads to relation [15]:

$$\frac{\theta_{H_{UPD}}}{1 - \theta_{H_{UPD}}} = P_{H_2}^{1/2} \exp\left(-\frac{F(E_1 - E_2)}{RT}\right) \exp\left(\frac{2\Delta G^{\circ}_{M_1-H_{UPD}} - \Delta G^{\circ}_{diss}(H_2)}{2RT}\right) \qquad [15]$$

Since adsorption of one mole of hydrogen molecules leads to two moles of adsorbed hydrogen adatoms on the substrate M_1, $H_2 \xrightarrow{ads} 2H_{ads(M_1)}$, one may write that:

$$2\Delta G^{\circ}_{ads}(H_{UPD}) = \Delta G^{\circ}_{diss}(H_2) - 2\Delta G^{\circ}_{M_1-H_{UPD}} \qquad [16]$$

which after fundamental mathematics becomes:

$$\frac{\theta_{H_{UPD}}}{1 - \theta_{H_{UPD}}} = P_{H_2}^{1/2} \exp\left(-\frac{F(E_1 - E_2)}{RT}\right) \exp\left(-\frac{\Delta G^{\circ}_{ads}(H_{UPD})}{RT}\right) \qquad [17]$$

Finally, one may use the Nernst equation to replace the H_2 gas pressure (or more precisely fugacity) by an equation comprising the H^+ activity and the potential, namely $H^+ + e \rightarrow 1/2H_2$:

$$E_2 = E^\circ - \frac{RT}{F} \ln \frac{P_{H_2}^{1/2}}{a_{H^+}} \qquad [18]$$

where by the definition $E^\circ = 0.00$ V. The latter leads to the following relation:

$$P_{H_2}^{1/2} = a_{H^+} \exp\left(- \frac{F(E_2 - E^\circ_{NHE})}{RT} \right) \qquad [19]$$

and its substitution into relation [17] results in the following formula:

$$\frac{\theta_{H_{UPD}}}{1 - \theta_{H_{UPD}}} = a_{H^+} \exp\left(- \frac{F(E_1 - E^\circ_{NHE})}{RT} \right) \exp\left(- \frac{\Delta G^\circ_{ads}(H_{UPD})}{RT} \right) \qquad [20]$$

The points that have to be stressed here are as follows:
(i) both equations [17] and [20] may be used to determine the Gibbs free energy of adsorption; however, application of relation [17] requires precise knowledge of the activity coefficient of H^+, thus utilization of equation [20] is more convenient and leads to more precise results since pressure measurements are well established and data well known;
(ii) the potential difference that appears in equation [17] refers to the experimentally measured potential of the RHE immersed in the same solution;
(iii) the potential that appears in equation [20] refers to the NHE.

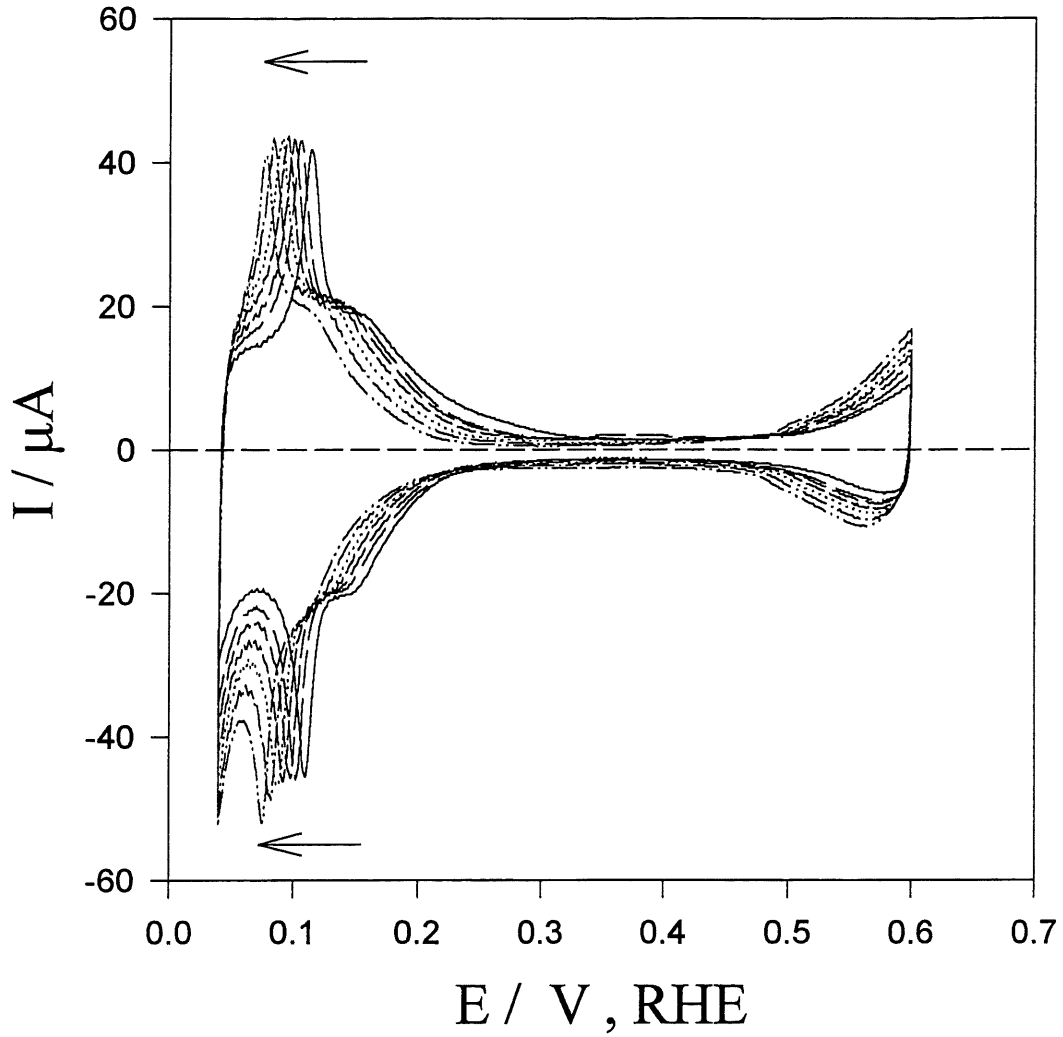

Figure 1. Series of the cyclic-voltammetry (CV) profiles for the under-potential deposition of H (UPD H) in a 0.5 M aqueous solution of H_2SO_4 for a temperature range between 273 and 343 K, with an interval of 10 K, and recorded at the sweep rate $s = 20\ mV\ s^{-1}$, the electrode surface area $A_r = 0.70 \pm 0.01\ cm^2$. The arrows indicate the shift of the adsorption and desorption peaks upon the temperature increase

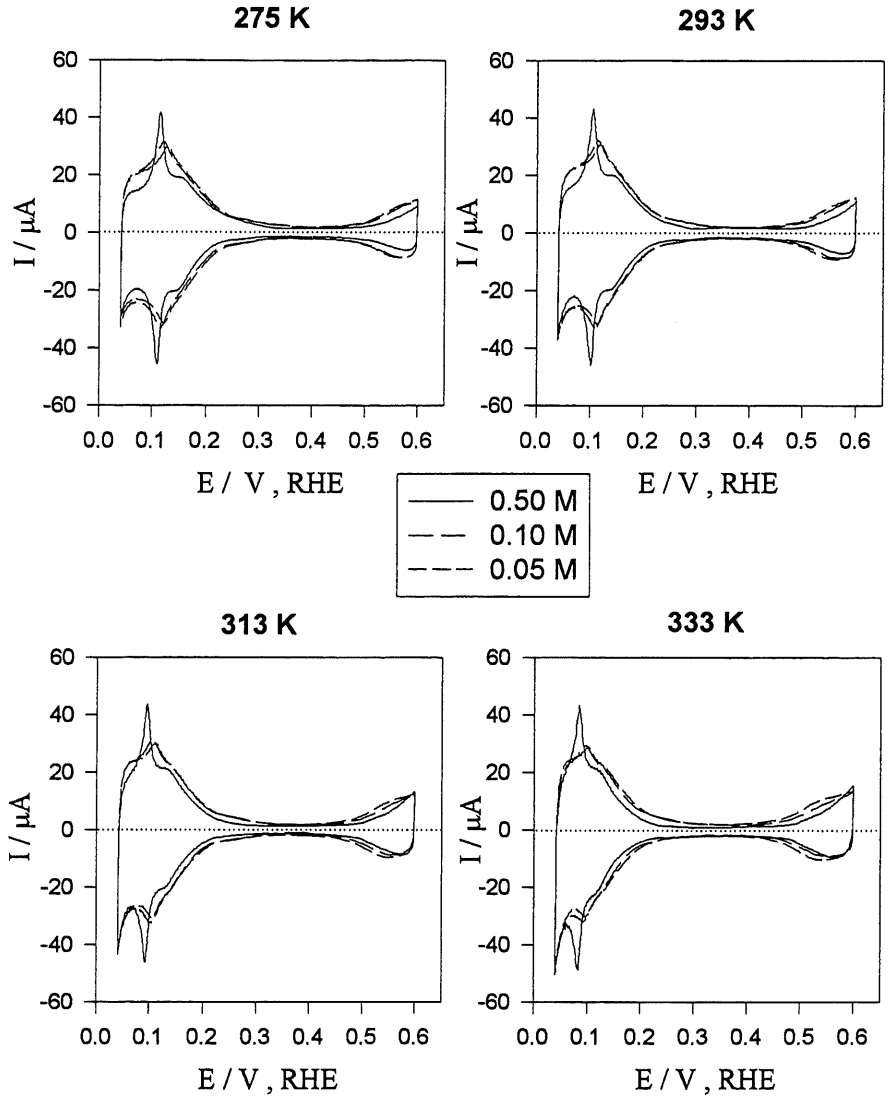

Figure 2. Four sets of cyclic-voltammetry (CV) profiles for the under-potential deposition of H (UPD H) in 0.05, 0.1 and 0.5 M aqueous solutions of H_2SO_4 at four different temperatures 275, 293, 313 and 333 K; the sweep rate $s = 20\ mV\ s^{-1}$ and the electrode surface area $A_r = 0.70 \pm 0.01\ cm^2$. The CV profiles show that upon the temperature increase the adsorption-desorption peaks shift towards less-positive values and the adsorption-desorption peak becomes less pronounced upon the concentration decrease.

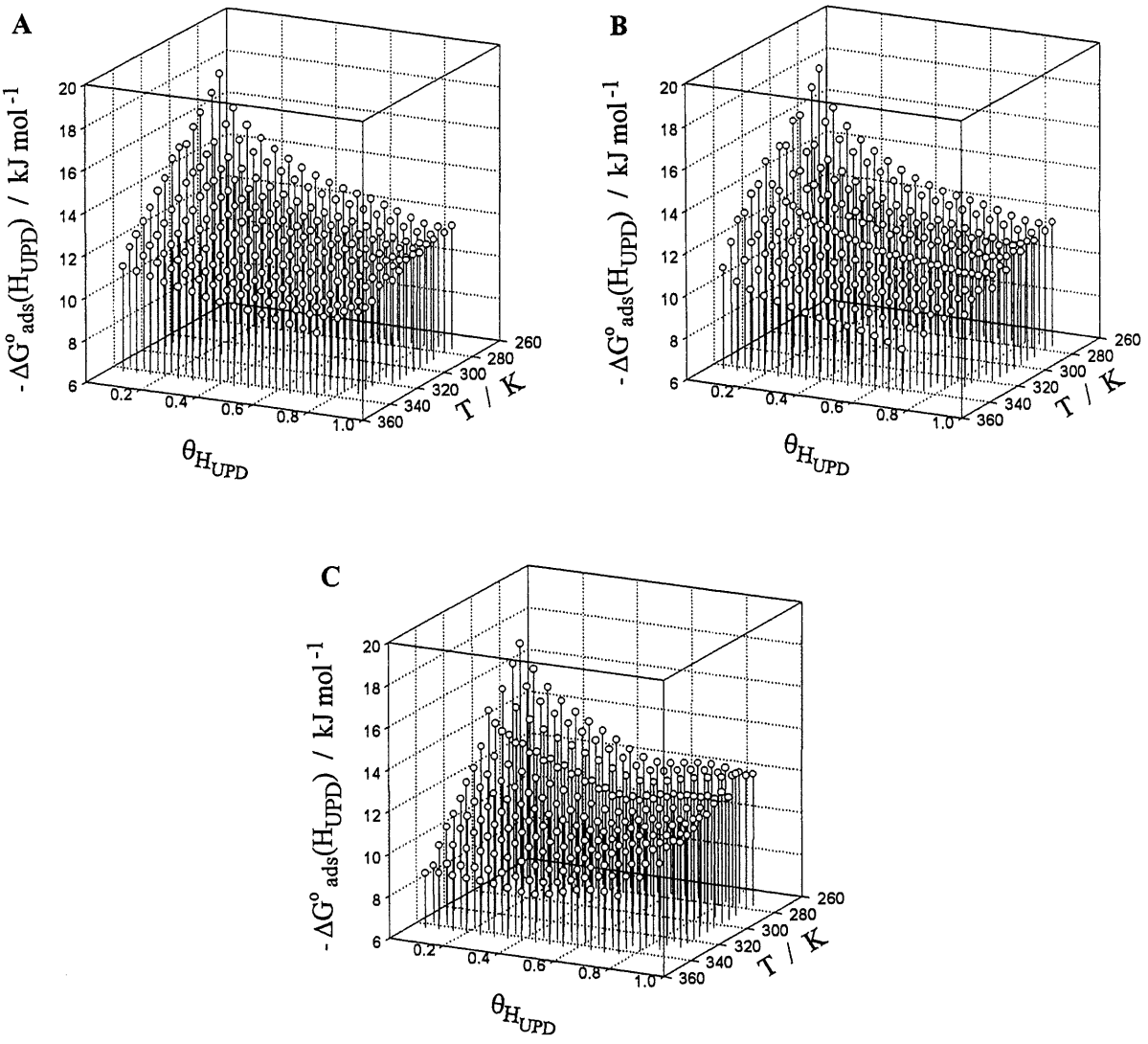

Figure 3. 3D plots showing the Gibbs free energy of the under-potential deposition of H, $\Delta G^{\circ}_{ads}(H_{UPD})$, versus $\theta_{H_{UPD}}$ and T, $\Delta G^{\circ}_{ads}(H_{UPD}) = f(\theta_{H_{UPD}}, T)$ for three concentrations of H_2SO_4, namely 0.05 0.1 and 0.5 M. $\Delta G^{\circ}_{ads}(H_{UPD})$ assumes values between −18 and −8 kJ mol^{-1} depending on $\theta_{H_{UPD}}$ and T; $\Delta G^{\circ}_{ads}(H_{UPD})$ reaches the most negative values at the lowest temperature and the smallest surface coverage, $\theta_{H_{UPD}}$. Augmentation of $\Delta G^{\circ}_{ads}(H_{UPD})$ with increasing $\theta_{H_{UPD}}$ for T = const points to the repulsive nature of lateral interactions between H_{UPD} adatoms. **(A)** 0.05 M H_2SO_4, **(B)** 0.1 M H_2SO_4, **(C)** 0.5 M H_2SO_4.

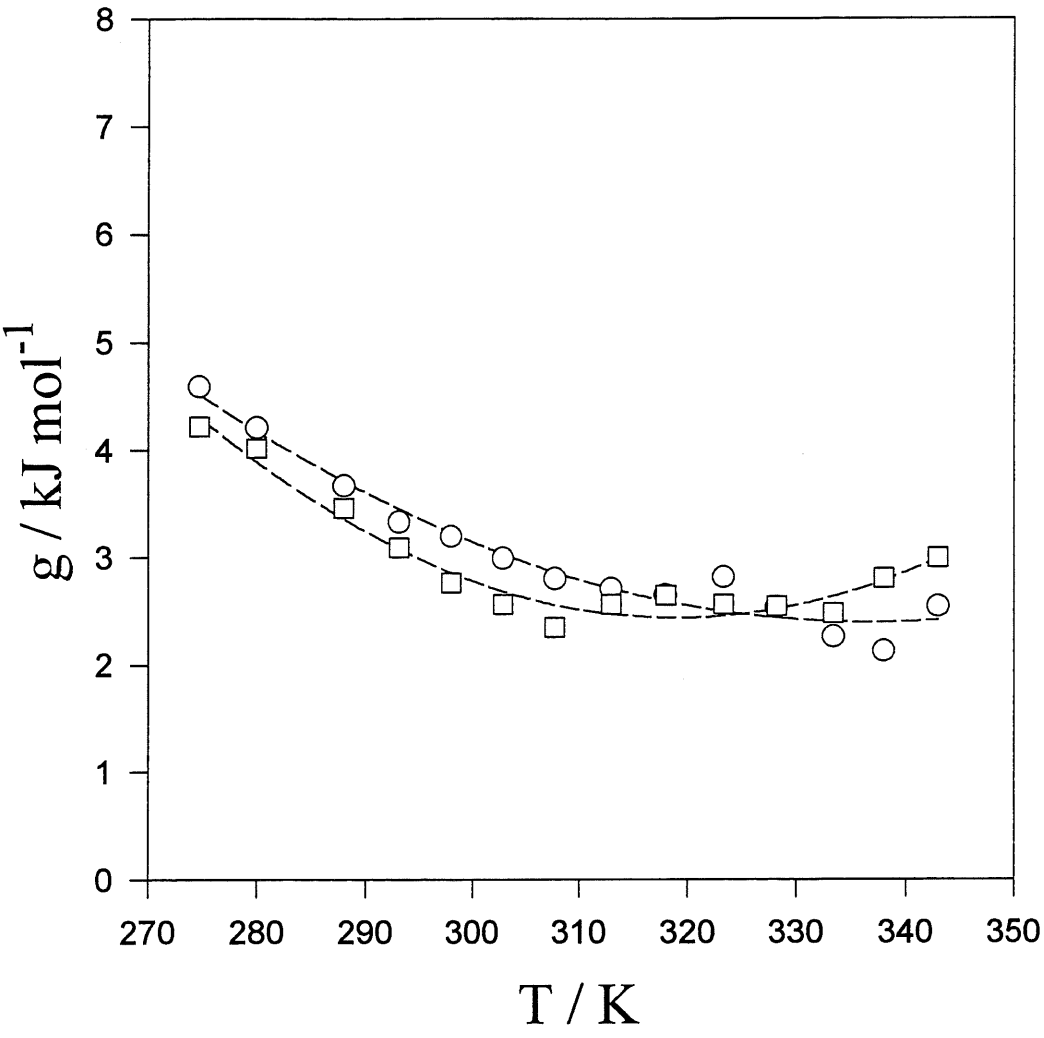

Figure 4. Relation between the energy of lateral interactions between H_{UPD} adatoms adsorbed on Rh electrodes, g, as a function of temperature, T, for the under-potential deposition of H from 0.05 and 0.1 M aqueous H_2SO_4 solutions. The parameter g assumes values between 2 and 5 kJ mol^{-1} pointing to the repulsive nature of the interactions. O refers to 0.05 M aq H_2SO_4 and □ to 0.1 M aq H_2SO_4.

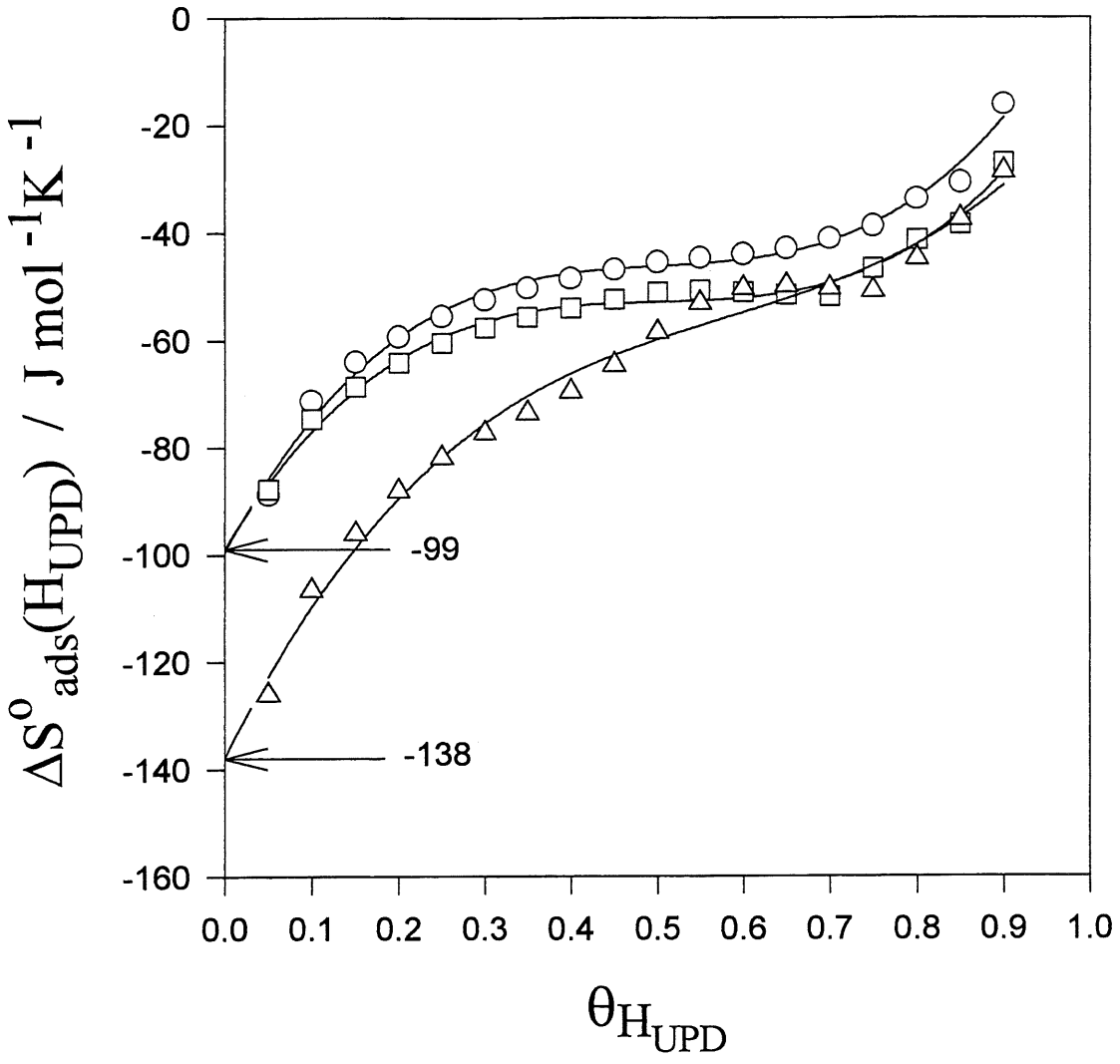

Figure 5. Dependence of $\Delta S^{\circ}_{ads}(H_{UPD})$ versus $\theta_{H_{UPD}}$ for the under-potential deposition of H from three solutions of H_2SO_4 having the 0.05 0.1 and 0.5 M concentrations; $\Delta S^{\circ}_{ads}(H_{UPD})$ assumes the more negative values at the lowest H_{UPD} surface coverage. The $\Delta S^{\circ}_{ads}(H_{UPD})$ vs. $\theta_{H_{UPD}}$ relations follow each other for $\theta_{H_{UPD}} \geq 0.55$; significant differences are pronounced for $\theta_{H_{UPD}} < 0.55$. The entropy for the under-potential deposition of the very first H_{UPD} adatom, thus $\Delta S^{\circ}_{ads}(H_{UPD})_{\theta_{H_{UPD}} \to 0}$, is evaluated from the Y-intercept of the $\Delta S^{\circ}_{ads}(H_{UPD})$ versus $\theta_{H_{UPD}}$ dependences. O refers to 0.05 M aq H_2SO_4, □ refers to 0.1 M aq H_2SO_4 and Δ refers to 0.5 M aq H_2SO_4.

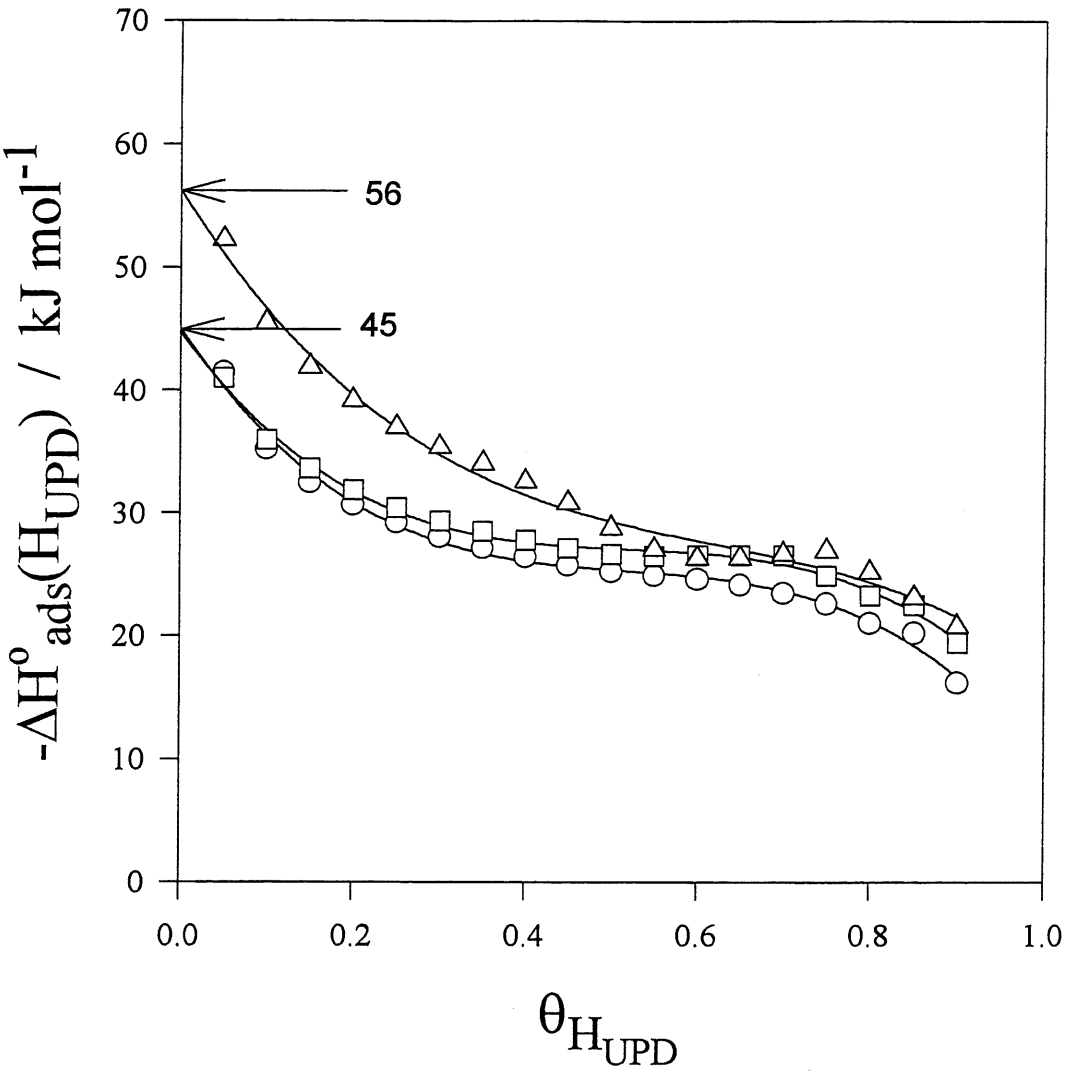

Figure 6. Dependence of $\Delta H^{\circ}_{ads}(H_{UPD})$ versus $\theta_{H_{UPD}}$ for the under-potential deposition of H from three solutions of H_2SO_4 having the 0.05 0.1 and 0.5 M concentrations; $\Delta H^{\circ}_{ads}(H_{UPD})$ accepts the more negative values at the lowest H_{UPD} surface coverage. Upon the H_{UPD} surface coverage increase, $\Delta H^{\circ}_{ads}(H_{UPD})$ increases towards less-negative values. The enthalpy for the under-potential deposition of the very first H_{UPD} adatom, thus $\Delta H^{\circ}_{ads}(H_{UPD})_{\theta_{H_{UPD}}\to 0}$, is evaluated from the Y-intercept of the $\Delta H^{\circ}_{ads}(H_{UPD})$ versus $\theta_{H_{UPD}}$ relations. O refers to 0.05 M aq H_2SO_4, □ refers to 0.1 M aq H_2SO_4 and Δ refers to 0.5 M aq H_2SO_4.

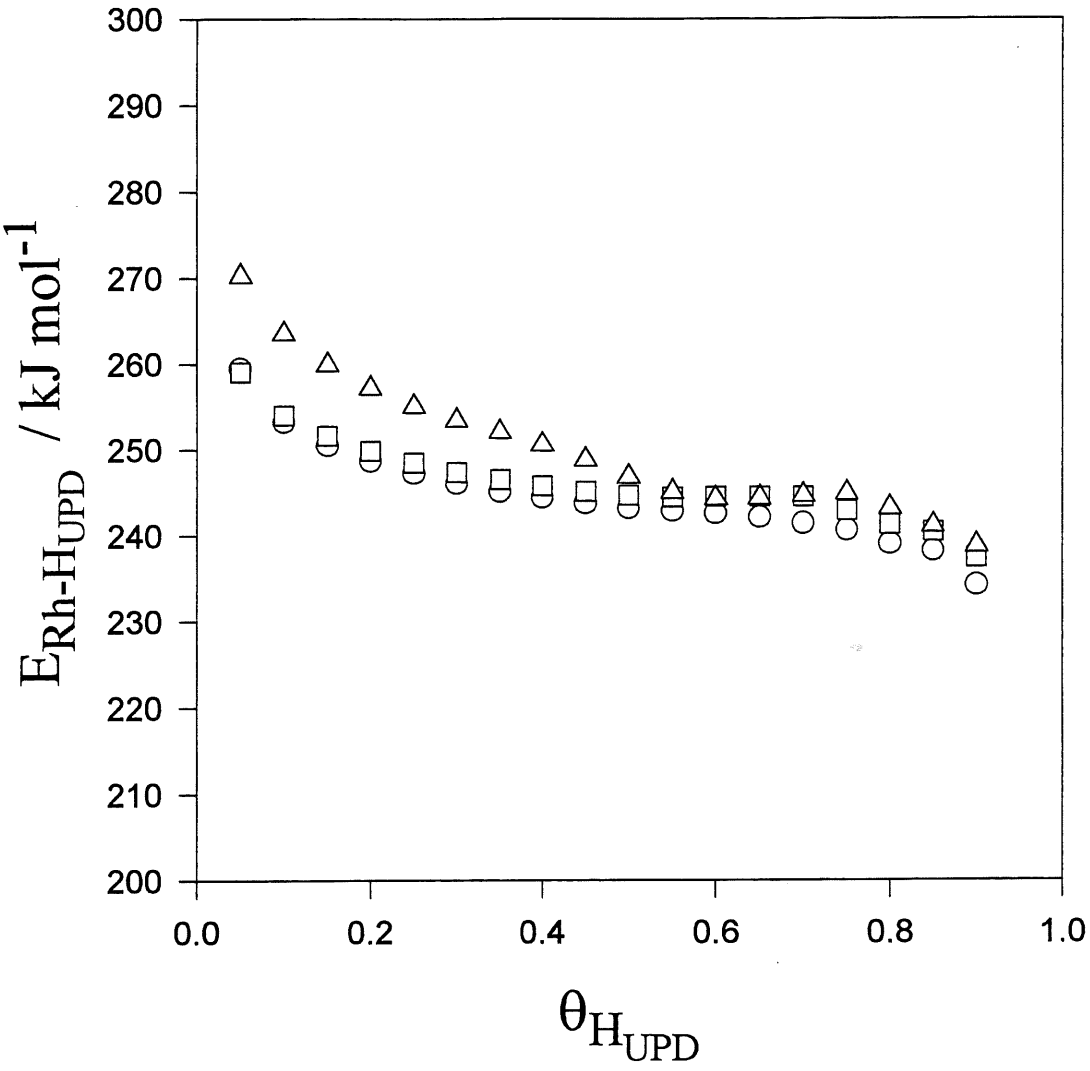

Figure 7. Dependence of $E_{Rh-H_{UPD}}$ versus $\theta_{H_{UPD}}$ for the under-potential deposited H from three solutions of H_2SO_4 having the 0.05, 0.1 and 0.5 M concentrations; $E_{Rh-H_{UPD}}$ accepts values between 230 and 270 kJ mol^{-1}; the variation of $E_{Rh-H_{UPD}}$ versus $\theta_{H_{UPD}}$ follows the changes of $\Delta H^{\circ}_{ads}(H_{UPD})$ versus $\theta_{H_{UPD}}$. O refers to 0.05 M aq H_2SO_4, □ refers to 0.1 M aq H_2SO_4 and Δ refers to 0.5 M aq H_2SO_4.

1.3 FUNDAMENTAL THERMODYNAMIC ASPECTS OF THE UNDER-POTENTIAL DEPOSITION OF HYDROGEN, SEMICONDUCTORS AND METALS

A. Zolfaghari and G. Jerkiewicz in Solid/Liquid Electrochemical Interface., Eds. G. Jerkiewicz, M. P. Soriaga, K. Uosaki and A. Wieckowski, ACS Symposium Series, ACS, Washington D.C., No. 656, Chapter 4, 45 (1997)

ABSTRACT

The paper presents theoretical methodology that allows determination of thermodynamic state functions of the under-potential deposition of hydrogen, UPD H, and semiconductor or metallic species, UPD M. The experimental approach involves temperature dependence of the UPD by application of cyclic-voltammetry or chronocoulometry. The theoretical approach is based on a general electrochemical adsorption isotherm and numerical calculations which lead to determination of the Gibbs free energy of adsorption, ΔG°_{ads}, as a function of T and θ. Temperature dependence of ΔG°_{ads} (for $\theta = \text{const}$) leads to appraisal of the entropy of adsorption, ΔS°_{ads}, whereas coverage dependence of ΔG°_{ads} (for $T = \text{const}$) allows assessment of the nature of the lateral interactions between the adsorbed species; knowledge of ΔG°_{ads} and ΔS°_{ads} leads to determination of ΔH°_{ads}. The paper presents new approach which permits elucidation of the bond energy between the substrate, S, and H_{UPD} or S and M_{UPD}, $E_{S-H_{UPD}}$ and $E_{S-M_{UPD}}$, respectively. Comprehension of $E_{S-H_{UPD}}$ is essential in assessment of the strength of the $S-H_{UPD}$ bond and the adsorption site of H_{UPD}. Knowledge of $E_{S-M_{UPD}}$ is of importance in: (i) evaluation of the strength of the cohesive forces acting between S and M_{UPD} that are responsible for the adhesion of the adsorbate to the substrate; and (ii) comparison of the $S-M_{UPD}$ bond with that observed for the 3-D bulk deposit of M. The UPD H on Rh and Pt electrodes from aqueous H_2SO_4 solution is discussed as an example of application of this methodology.

INTRODUCTION

The under-potential deposition, UPD, of hydrogen, H, and semiconductors and metals, abbreviated by M, of the *p* and *d* blocks of the periodic table on transition-metal has been a subject of intense studies in electrochemical surface science (*1-15*).

The UPD refers to the phenomenon of deposition of H or M on a foreign metallic substrate, S, at potentials positive to the equilibrium potential of the hydrogen evolution reaction, HER, E°_{HER}, or to the equilibrium potential of the bulk deposition of M, $E_{M^{z+}/M}$. The UPD of H is known (*1-13,16-19*) to take place on Rh, Pt, Ir and Pd at potentials positive roughly between 0.05 and 0.40 V versus the reversible hydrogen electrode, RHE. The UPD of M takes place on the above mentioned noble-metal substrates as well as on other transition metals such as Au, Ag and Cu on which the UPD H is not observed (*20-28*). The UPD M appears to be a more general phenomenon which precedes 3D bulk-type deposition at potentials positive with

respect to $E^{\circ}_{M^{z+}/M}$* and it always takes place at a metal substrate more noble with respect to the species undergoing the under-potential deposition. Thus the UPD adlayer acts as a precursor for the formation and growth of the 3D bulk-type phase on the foreign metal substrate. Various UPD systems are reviewed in refs. *20*, *21*, *24* and *29* with description of different substrates and metal ions deposited from aqueous or non-aqueous solutions. The UPD M is usually limited to a monolayer and the process resembles chemisorption of a submonolayer or a monolayer, ML, of a metal or a semiconductor from the gas phase. The origin of the UPD can be explained in terms of the existence of stronger attractive, chemisorptive forces between the foreign metal substrate, S, and the depositing species, here H or M, than those between like atoms within the 3D deposit of M. In other words, the $S-M_{UPD}$ bond energy, $E_{S-M_{UPD}}$, is greater than that of the $M-M$ bond in the 3D lattice of M, E_{M-M}.

Kolb et al. (*23*) observed that the potential of stripping of the bulk deposit is shifted towards lower potentials with respect to the potential of desorption of the UPD layer; this difference was defined as the underpotential shift, ΔE_P. The underpotential shift was correlated to the difference in work functions, Φ, between the substrate, S, and the UPD species, M, and expressed by the following equation:

$$\Delta E_P = \alpha \, \Delta\Phi \qquad (1)$$

where $\alpha = 0.5 \text{ V eV}^{-1}$ and $\Delta\Phi = \Phi_S - \Phi_M$. The consequence of equation 1 is that the work function of the substrate, Φ_S, should be greater the work function of the UPD species, Φ_M, thus $\Phi_S \rangle \Phi_M$ if the under-potential deposition is to occur.

It is well recognized in electrochemical surface science that anions coadsorbed on the electrode surface with the UPD species influence their cyclic-voltammetry, CV, and chronocoloumetry characteristics (*30-32*). Structural changes associated with M and anion coadsorption are investigated by electrochemical, radiochemical, and UHV techniques as well as by scanning tunneling microscopy, STM, and atomic force microscopy, AFM (*14,15,33-40*). These changes can be related to such thermodynamic state functions as the Gibbs free energy, entropy and enthalpy of adsorption (*18,19,30,32*).

---

* Equilibrium potential, E_{eq}.

Whereas the origin of the UPD H and UPD M as well as the 3D bulk deposition of M is quite well understood, there is a lack of knowledge of the $S-M_{UPD}$ bond energy, $E_{S-M_{UPD}}$, as well as thermodynamic state functions for the UPD. This paper addresses this issue and demonstrates a theoretical methodology which allows determination of the state functions and $E_{S-M_{UPD}}$ on the basis of experimental data. The experimental methodology involves application of cyclic-voltammetry over a wide temperature range, or chronocoulometry whereas the theoretical treatment is based on a general electrochemical isotherm and adsorption thermodynamics.

Under-Potential Deposition of Hydrogen

The UPD H from an acidic aqueous solution may be represented by the following single-electrode processes:

$$\textit{working electrode} \qquad H^+ + e + S \;=\; S-H_{UPD} \tag{2}$$

$$\textit{reference electrode} \qquad 1/2\,H_2 \;=\; H^+ + e \tag{3}$$

The activity of the solvated proton in the bulk of the electrolyte of the working-electrode and reference-electrode compartments is the same and it equals a_{H^+}. The pressure of the H_2 in the reference-electrode compartment is $P^r_{H_2}$. If the temperature is the same in both compartments, then the process is described by the following general electrochemical adsorption isotherm:

$$\frac{\theta_{H_{UPD}}}{1-\theta_{H_{UPD}}} = a_{H^+}\exp\left(-\frac{FE_{SHE}}{RT}\right)\exp\left(-\frac{\Delta G^\circ_{ads}(H_{UPD})}{RT}\right) \tag{4}$$

where $\theta_{H_{UPD}}$ is the surface coverage of H_{UPD}, E_{SHE} is the potential measured versus the standard hydrogen electrode, SHE, $\Delta G^\circ_{ads}(H_{UPD})$ is the standard Gibbs free energy of adsorption, T is the temperature and R and F are physico-chemical constants. The above formula is a specific form of the following general relation for the conditions mentioned above:

$$\frac{\theta_{H_{UPD}}}{1-\theta_{H_{UPD}}} = \frac{a^{w}_{H^+}}{a^{r}_{H^+}} \sqrt{P^{r}_{H_2}} \exp\left(-\frac{FE_{eq}}{RT}\right) \exp\left(-\frac{\Delta G^{\circ}_{ads}(H_{UPD})}{RT}\right) \quad (5)$$

where $a^{w}_{H^+}$ and $a^{r}_{H^+}$ are the activities of H^+ in the working-electrode and reference-electrode compartments, and E_{eq} is the equilibrium potential related to $P^{r}_{H_2}$ through the Nernst formula. When the temperatures of both compartments are the same and the activities of H^+ are equal, then equations 4 and 5 reduce to the following formula:

$$\frac{\theta_{H_{UPD}}}{1-\theta_{H_{UPD}}} = \sqrt{P^{r}_{H_2}} \exp\left(-\frac{FE_{RHE}}{RT}\right) \exp\left(-\frac{\Delta G^{\circ}_{ads}(H_{UPD})}{RT}\right) \quad (6)$$

where E_{RHE} is the potential measured versus the reversible hydrogen electrode, RHE, immersed in the same electrolyte.

It should be added that equation 4 is neither the Langmuir nor the Frumkin isotherm and $\Delta G^{\circ}_{ads}(H_{UPD})$ refers to the Gibbs free energy of adsorption at given $\theta_{H_{UPD}}$ and T (*18,19*). Assessment of the relation between $\Delta G^{\circ}_{ads}(H_{UPD})$ and $(\theta_{H_{UPD}}, T)$ may clarify whether the process follows either of the two electrochemical adsorption isotherms. However, even in the case of H chemisorption under gas-phase conditions, in absence of the electrified double layer, the relations between $\Delta G^{\circ}_{ads}(H_{UPD})$ and $\theta_{H_{UPD}}$ are more complicated and rarely follow the two most fundamental cases (*41*). Thus it is reasonable to conclude that H chemisorption does not follow the common isotherms due to presence of complex first-nearest and second-nearest neighbor lateral interactions between the adsorbed species (*41-43*).

It should be stressed that both equations 4 and 6 may be applied for determination of $\Delta G^{\circ}_{ads}(H_{UPD})$, but equation 4 requires precise knowledge of the activity coefficient of the proton whereas equation 6 demands knowledge of the hydrogen gas pressure in the reference electrode compartment which is more accessible. In other words, it is easier to apply equation 6 to determine $\Delta G^{\circ}_{ads}(H_{UPD})$ than equation 4. It is evident that experimental appraisal of E at which H_{UPD} reaches a given $\theta_{H_{UPD}}$ at a given T allows numerical determination of $\Delta G^{\circ}_{ads}(H_{UPD})$. Such calculations may be performed for a series of coverages of H_{UPD} and for various temperatures, and they results in evaluation of $\Delta G^{\circ}_{ads}(H_{UPD})$ as a function of $\theta_{H_{UPD}}$ and T, $\Delta G^{\circ}_{ads}(H_{UPD})$ versus $(\theta_{H_{UPD}}, T)$.

Cyclic-voltammetry, CV, and chronocoulometry (*44*) are experimental techniques that can be applied to evaluate the dependence of the H_{UPD} surface coverage on temperature variation and to determine $\Delta G^{\circ}_{ads}(H_{UPD})$. CV is in many respects the electrochemical equivalent of temperature programmed desorption, TPD, although CV results in determination of different thermodynamic parameters than TPD. CV allows one to study the surface coverage of the adsorbed species during potential-stimulated adsorption and desorption at various temperatures. Theoretical treatment of CV experimental results leads to elucidation of important thermodynamic state functions such as ΔG°_{ads}, ΔH°_{ads} and ΔS°_{ads}. Thus it is sensible to refer to it as *potential-stimulated adsorption-desorption*, PSAD.

Figure 1 shows two series of CV adsorption-desorption profiles for UPD H on Rh and Pt from 0.50 M aqueous H_2SO_4 solution. In the case of Rh there is only one adsorption-desorption peak where as in the case of Pt there are two peaks. Upon the temperature increase, the peaks shift towards less-positive potentials and there is a slight redistribution of the charge between the two peaks for Pt (*18,19*). These data allow calculation of $\Delta G^{\circ}_{ads}(H_{UPD})$ based on equation 5 and the results are shown in Figure 2 as 3D plots of $\Delta G^{\circ}_{ads}(H_{UPD})$ versus $(\theta_{H_{UPD}}, T)$. $\Delta G^{\circ}_{ads}(H_{UPD})$ assumes the most negative values in at the lowest T and the lowest $\theta_{H_{UPD}}$. In the case of Rh, $\Delta G^{\circ}_{ads}(H_{UPD})$ has values between −18 and −8 kJ mol^{-1} whereas in the case of Pt, it varies between -25 and -11 kJ mol^{-1}. For a given constant T, $\Delta G^{\circ}_{ads}(H_{UPD})$ increases towards less-negative values with $\theta_{H_{UPD}}$ augmentation indicating that the lateral interactions between H_{UPD} adatoms are repulsive. The $\Delta G^{\circ}_{ads}(H_{UPD})$ versus $\theta_{H_{UPD}}$ relations are non-linear indicating that the adsorption process is complex and may not be simply described by the Langmuir or the Frumkin isotherm (*18,19*). For a given constant $\theta_{H_{UPD}}$, the relation between $\Delta G^{\circ}_{ads}(H_{UPD})$ and T is linear and it describes the entropy of adsorption, $\Delta S^{\circ}_{ads}(H_{UPD})$, through the following relation:

$$\Delta S^{\circ}_{ads}(H_{UPD}) = -\left(\frac{\partial \Delta G^{\circ}_{ads}(H_{UPD})}{\partial T}\right)_{\theta_{H_{UPD}}=const} \qquad (7)$$

Figure 3 shows $\Delta S^{\circ}_{ads}(H_{UPD})$ for UPD H on Rh and Pt as a function of $\theta_{H_{UPD}}$. In the case of Rh $\Delta S^{\circ}_{ads}(H_{UPD})$ has values between −125 and −30 J mol^{-1} K^{-1} whereas in the case of Pt it varies between −75 and −40 J mol^{-1} K^{-1}. The $\Delta S^{\circ}_{ads}(H_{UPD})$ versus $\theta_{H_{UPD}}$ plot for Pt forms two waves which are associated with two peaks in the CV adsorption-desorption profiles.

The enthalpy of adsorption is readily determined based on the experimental values of $\Delta G^{\circ}_{ads}(H_{UPD})$ and $\Delta S^{\circ}_{ads}(H_{UPD})$ and equation 8:

$$\Delta H^{\circ}_{ads}(H_{UPD}) = \Delta G^{\circ}_{ads}(H_{UPD}) + T\,\Delta S^{\circ}_{ads}(H_{UPD}) \qquad (8)$$

Figure 4 shows values of $\Delta H^{\circ}_{ads}(H_{UPD})$ for UPD H on Rh and Pt as a function of $\theta_{H_{UPD}}$ determined on the basis of the experiment data presented in Figures 2 and 3. The results demonstrate that in the case of Rh, $\Delta H^{\circ}_{ads}(H_{UPD})$ varies between −52 and −20 kJ mol^{-1} whereas in the case of Pt, it falls between -45 and -28 kJ mol^{-1}. The $\Delta H^{\circ}_{ads}(H_{UPD})$ versus $\theta_{H_{UPD}}$ relation for Pt reveals two waves which again are associated with the two peaks in the CV adsorption-desorption profiles.

It is essential to elaborate on the $\Delta S^{\circ}_{ads}(H_{UPD})$ versus $\theta_{H_{UPD}}$ and $\Delta H^{\circ}_{ads}(H_{UPD})$ versus $\theta_{H_{UPD}}$ plots. An analysis of the data shown in Figures 3 and 4 reveals that the enthalpy and entropy variations are mirror images. Such thermodynamic dependences are well known in catalysis (*45-46*) and show that variation of the entropy of adsorption is always counterbalanced by alteration of the enthalpy of adsorption. This phenomenon is recognized as *a compensation effect* (*45*) and the data presented in the present paper indicate that it is also observable for electrochemical systems.

An alternative approach that may be applied to determine $\Delta H^{\circ}_{ads}(H_{UPD})$ involves combination of equation 4 with the Gibbs-Helmholtz relation which leads to the following formula (*18,19*):

$$\frac{\partial(E/T)}{\partial(1/T)} = -\left[\frac{\Delta H^{\circ}_{ads}(H_{UPD})}{F}\right]_{\theta_{H_{UPD}} = \text{const}} \qquad (9)$$

Thus by experimental determination of pairs of values of E and T at which the H_{UPD} coverage is constant, $\theta_{H_{UPD}} = \text{const}$, and by plotting E/T versus 1/T one obtains linear relations and from their slope one may evaluate $\Delta H^{\circ}_{ads}(H_{UPD})$. The authors applied this methodology and found that such determined values $\Delta H^{\circ}_{ads}(H_{UPD})$ agreed to within 1.5 kJ mol^{-1} with those shown in Figure 4.

The energy of the $S-H_{UPD}$ bond (here $Rh-H_{UPD}$ and $Pt-H_{UPD}$), $E_{S-H_{UPD}}$, may be determined on the basis of Born-Haber thermodynamic cycles for the respective single-

electrode processes (*18,19*). Summation of the two single-electrode reactions shown in equations 2 and 3 leads to the following overall process:

$$1/2\,H_2 + S \xrightarrow{\Delta H^\circ_{ads}(H_{UPD})} S-H_{UPD} \qquad (10)$$

Addition of the Born-Haber cycles (*18,19*) leads to the the following relation for the $S-H_{UPD}$ bond energy, $E_{S-H_{UPD}}$:

$$E_{S-H_{UPD}} = \frac{1}{2}D_{H_2} - \Delta H^\circ_{ads}(H_{UPD}) \qquad (11)$$

where D_{H_2} is the dissociation enerhy of the H_2 molecule. Figure 5 demonstrates relations between $E_{Rh-H_{UPD}}$ or $E_{Pt-H_{UPD}}$ and $\theta_{H_{UPD}}$ based on the values of $\Delta H^\circ_{ads}(H_{UPD})$ shown in Figure 4. The $Rh-H_{UPD}$ bond energy is between 240 and 270 kJ mol^{-1} and that of the $Pt-H_{UPD}$ bond is between 250 and 265 kJ mol^{-1}; both bond energies vary slightly with the H_{UPD} surface coverage. The results presented in Figure 5 show that $Rh-H_{UPD}$ and $Pt-H_{UPD}$ bond energies fall close to that for the respective bond energies between the same substrate and the chemisorbed H, H_{chem}, $E_{Rh-H_{chem}}$ and $E_{Pt-H_{chem}}$, respectively, which is 255 kJ mol^{-1} for Rh and $243-255$ kJ mol^{-1} for Pt (*41*). Proximity of these values indicates that H_{UPD}, is an energetic equivalent of H_{chem}. Moreover, if the bond energies for H_{UPD} and H_{chem} are so close, then it is reasonable to assume that H_{UPD} similarly to H_{chem} is strongly embedded in the surface lattice of the metal substrate.

It is apparent on the basis of equation 11 that the $E_{S-H_{UPD}}$ versus $\theta_{H_{UPD}}$ plots follow the variations of $\Delta H^\circ_{ads}(H_{UPD})$ since $1/2\,D_{H_2}$ represents a constant.

An aspect that the authors would like to emphasize is that the present treatment, being the first approach, does not take into account the specific adsorption of anions and their contribution to the overall adsorption charge. Indeed, there is a certain anion contribution and it may affect the values of $\Delta G^\circ_{ads}(H_{UPD})$ but the present approximation, which is meant to verify the validity of the theoretical treatment, does not take it into account. However, experimental research on Pt and Rh single crystals is under way and the results will be presented in subsequent papers which will take into account the anion effect.

Under-Potential Deposition of Semiconductors and Metals

The under-potential deposition of semiconductors and metals, UPD M, from an aqueous solution containing a monovalent cation, M^+, on a substrate more noble than the species undergoing the UPD may be represented by the following single-electrode processes:

$$\textit{working electrode} \qquad S + M^+ + e \;=\; S - M_{UPD} \tag{12}$$

$$\textit{reference electrode} \qquad M \;=\; M^+ + e \tag{13}$$

Summation of the above relations leads to the following overall equation which represents the formation of the UPD layer of M on S:

$$S + M \;=\; S - M_{UPD} \tag{14}$$

The treatment presented here is based on the supposition that M^+ undergoes a complete discharge to M. If the activities of M^+, a_{M^+}, in the working-electrode and reference-electrode compartments are the same and if they are maintained at the same temperature, T, then the relation between the surface coverage of M, $\theta_{M_{UPD}}$, and the applied potential, E, is described by the general electrochemical adsorption isotherm:

$$\frac{\theta_{M_{UPD}}}{1-\theta_{M_{UPD}}} = a_{M^+} \exp\left(-\frac{FE}{RT}\right)\exp\left(-\frac{\Delta G^\circ_{ads}(M_{UPD})}{RT}\right) \tag{15}$$

where E is the potential measured versus the standard potential of the M^+/M reference electrode, $\Delta G^\circ_{ads}(M_{UPD})$ is the standard Gibbs free energy of adsorption of the process, thus the formation of UPD layer of M on S as shown in equation 14, and R and F are explained above. Equation 15 is a specific form of the following relation:

$$\frac{\theta_{M_{UPD}}}{1-\theta_{M_{UPD}}} = \frac{a^w_{M^+}}{a^r_{M^+}} \exp\left(-\frac{FE_{eq}}{RT}\right)\exp\left(-\frac{\Delta G^\circ_{ads}(M_{UPD})}{RT}\right) \tag{16}$$

where $a^{w}_{M^+}$ and $a^{r}_{M^+}$ are the activities of M^+ in the working-electrode and reference-electrode compartments, and E_{eq} is the equilibrium electrode potential. When T is the same in both compartments and when $a^{w}_{M^+} = a^{r}_{M^+}$, one obtains equation 15.

There are many similarities between the theoretical treatment of the UPD H and the UPD M. For instance, it is evident on the basis of the above formula that experimental evaluation of the potential at which $\theta_{M_{UPD}}$ has a given value for a series of temperatures allows numerical determination of $\Delta G^{\circ}_{ads}(M_{UPD})$. Such calculations may be performed for all values of $\theta_{M_{UPD}}$ and T, and one may plot $\Delta G^{\circ}_{ads}(M_{UPD})$ as a function of $\theta_{M_{UPD}}$ and T, thus $\Delta G^{\circ}_{ads}(M_{UPD})$ versus $(\theta_{M_{UPD}}, T)$. Evaluation of the $\Delta G^{\circ}_{ads}(M_{UPD})$ versus $\theta_{M_{UPD}}$ relations (for $T = const$) allows one to assess the energy of lateral interactions between the M_{UPD} adatoms. The entropy of adsorption, $\Delta S^{\circ}_{ads}(M_{UPD})$, may evaluated on the basis of equations 7 and subsequently, the enthalpy of adsorption, $\Delta H^{\circ}_{ads}(M_{UPD})$, is readily determined based on equation 8.

An alternative approach that may be applied to determine $\Delta H^{\circ}_{ads}(M_{UPD})$ is similar to the one presented above for the enthalpy of adsorption of H_{UPD} (see equation 9) and it is based on the Gibbs-Helmholtz formula and the general adsorption isotherm presented in equation 15. Thus by experimental determination of pairs of values of E and T at which the M_{UPD} coverage is constant, $\theta_{M_{UPD}} = const$, and by plotting E/T versus 1/T one obtains linear relations and from their slope one may evaluate $\Delta H^{\circ}_{ads}(M_{UPD})$. It should be added that there is a limited amount of data on thermodynamics of the UPD of semiconductors and metals, and at present that authors are unaware of any temperature dependence measurements of the UPD M. The chronocoulometry methodology applied by Lipkowski et al. (*30,32,44*) results in evaluation of the surface coverage of the adsorbed metallic and anionic species and their ΔG°_{ads}. The approach proposed in this paper and based on temperature-dependence measurements followed by theoretical treatment represents an extension to the approach developed and applied by the laboratory of Lipkowski and it will allow one to assess consistency of the surface thermodynamic data.

Knowledge of the $S-M_{UPD}$ bond energy is essential in evaluation of the cohesive forces acting between the metal substrate and the under-potential deposited species that are responsible for the adhesion of the deposited monolayer to the substrate. They are of different nature than the forces acting between alike atoms in the 3D lattice of S or M. Thus, the magnitude of $E_{S-M_{UPD}}$ is a good measure of the adhesion the deposit to the substrate. The

energy of the $S-M_{UPD}$ bond, $E_{S-M_{UPD}}$, may be determined on the basis of the following Born-Haber thermodynamic cycles for the respective single-electrode processes shown in equations 12 and 13:

$$\begin{array}{ccccccc} M^{+}_{(gas)} & + & e_{(gas)} & + & S & \xleftarrow{I_M} & M_{(gas)} + S \\ \downarrow \Delta H^{\circ}_{solv} & & \uparrow \Phi + EF & & & & \uparrow E_{S-M_{UPD}} \end{array} \qquad (17)$$

$$M^{+}_{(aq)} + e_{S(E\neq 0)} + S \xrightarrow{\Delta H^{\circ}_{WE}} S-M_{UPD}$$

$$\begin{array}{ccccc} M_{(gas)} & \xrightarrow{I_M} & M^{+}_{(gas)} & + & e_{(gas)} \\ \uparrow \Delta H^{\circ}_{atom(M)} - \Delta H^{\circ}_{surf(M)}\,\sigma_m & & \downarrow \Delta H^{\circ}_{solv} & & \uparrow \Phi \end{array} \qquad (18)$$

$$M \xrightarrow{\Delta H^{\circ}_{RE}} M^{+}_{(aq)} + e_{M(E=0)}$$

where $\Delta H^{\circ}_{surf(M)}$ the standard surface enthalpy defined as the energy required to create 1 cm^2 of the surface (the unit being J cm^{-2}) and σ_m is the molar surface of M, thus the number of cm^2 occupied by 1 mole of M surface atoms (the unit being $cm^2\ mol^{-1}$); the unit of the product $\Delta H^{\circ}_{surf(M)}\,\sigma_M$ is J mol^{-1}. The surface enthalpy is related to the surface tension, γ, through the following relation (*45,46*):

$$\Delta H^{\circ}_{surf(M)} = \gamma - T\frac{\partial \gamma}{\partial T} \qquad (19)$$

Thus even if $\Delta H^{\circ}_{surf(M)}$ is not well known, one may evaluate it based on the temperature dependence of the surface tension.

By adding the above Born-Haber cycles (equations 17 and 18) and bearing in mind that there is a Volta potential difference between the metal and the solution so that M^+ and e extracted from two solid electrodes are at different electrostatic potentials and that this difference compensates exactly the work function variation shown in equation 17 for the

working electrode, EF, one obtains the following relation for the $S-M_{UPD}$ bond energy, $E_{S-M_{UPD}}$:

$$E_{S-M_{UPD}} = \Delta H^{\circ}_{atom(M)} - \Delta H^{\circ}_{surf(M)}\, \sigma_m - \Delta H^{\circ}_{ads}(M_{UPD}) \qquad (20)$$

There are several significant implications of equation 20. The above formula indicates that: (i) $E_{S-M_{UPD}}$ follows changes of $\Delta H^{\circ}_{ads}(M_{UPD})$; (ii) the surface enthalpy, $\Delta H^{\circ}_{surf(M)}$, depends on the surface structure thus it may be concluded that the value of $E_{S-M_{UPD}}$ varies with the structure of the metal substrate; and (iii) the molar surface of M, σ_m, is surface-geometry dependent at it affects the magnitude of $E_{S-M_{UPD}}$.

Recent studies on the UPD M show that the adsorption-desorption CV profiles often reveal a hysteresis whose origin has been assigned to lateral interactions between the UPD species and the coadsorbed anions, and to surface reconstruction or surface compression processes (*30,32-40*). It ought to be emphasized that the cathodic component of the CV profiles allows determination of $\Delta G^{\circ}_{ads}(M_{UPD})$ whereas the anodic one refers to $\Delta G^{\circ}_{des}(M_{UPD})$. If the CV profiles are symmetrical, thus if there is no hysteresis, then $\Delta G^{\circ}_{ads}(M_{UPD}) = -\Delta G^{\circ}_{des}(M_{UPD})$ and the adsorption and desorption processes are energetically equivalent, as it is the case of the UPD H. On the other hand, if a hysteresis effect is observable in the CV adsorption-desorption profiles, then integration of the $\Delta G^{\circ}_{ads}(M_{UPD})$ versus $\theta_{M_{UPD}}$ relation provides the Gibbs free energy of *adsorption* of one monolayer (or submonolayer, depending on the system) of the UPD species. Integration of the $\Delta G^{\circ}_{des}(M_{UPD})$ versus $\theta_{M_{UPD}}$ relation gives the Gibbs free energy of *desorption* of one monolayer (or submonolayer) of the UPD species. Considering that a hysteresis effect implies that $\Delta G^{\circ}_{ads}(M_{UPD}) \neq -\Delta G^{\circ}_{des}(M_{UPD})$, then their difference, $\delta\Delta G^{\circ}(M_{UPD})$, defined by equation 21, is a measure of the Gibbs free energy associated with the lateral interactions between M_{UPD} and the anions during the adsorption and desorption processes, as well as the surface reconstruction and surface compression processes.

$$\delta\Delta G^{\circ}(M_{UPD}) = \Delta G^{\circ}_{ads}(M_{UPD}) + \Delta G^{\circ}_{des}(M_{UPD}) \qquad (21)$$

CONCLUSIONS

The authors present thermodynamic methodology which can be applied to the phenomenon of the under-potential deposition on metal electrodes. It allows determination of the Gibbs free energy, entropy and enthalpy of adsorption, ΔG°_{ads}, ΔS°_{ads} and ΔH°_{ads}. New theoretical

approach is presented which leads to determination of the bond energy between the metal substrate and the under-potential deposited species, here H or M, $E_{S-H_{UPD}}$ and $E_{S-M_{UPD}}$, respectively. Knowledge of $E_{S-M_{UPD}}$ is essential in evaluation of the binding forces acting between the substrate and the deposit, thus the forces that are responsible for adhesion of the deposit to the substrate. The authors also discuss the hysteresis effect often observed in the CV adsorption-desorption profiles for UPD M and indicate that the difference between $\Delta G^{\circ}_{ads}(M_{UPD})$ and $\Delta G^{\circ}_{des}(M_{UPD})$ is a measure of the Gibbs free energy associated with the lateral interactions between M_{UPD} adatoms and the coadsorbed anions as well as the surface reconstruction and surface compression processes.

ACKNOWLEDGMENTS

Acknowledgment is made to the NSERC of Canada and the FCAR du Québec for support of this research project. A. Zolfaghari acknowledges a graduate fellowship from MCHE of Iran. The authors are indebted to Prof. A. Lasia of l'Université de Sherbrooke for discussions and comments on thermodynamics of the UPD.

REFERENCES

1. Will, F.G. *J. Electrochem. Soc.* **1965**, *112*, 451-455.

2. Boeld, W.; Breiter, M. W. *Z. Elektrochem.* **1960**, *64*, 897-902.

3. Breiter, M. W.; Kennel, B. *Z. Elektrochem.* **1960**, *64*, 1180-1187.

4. Frumkin, A. N. In *Advances in Electrochemistry and Electrochemical Engineering*; Delahey, P., Ed.; Interscience Publishers: New York, 1963; Vol. 3, pp 287-391.

5. Woods, R. In *Electroanalytical Chemistry*; Bard, A., Ed.; Marcel Dekker: New York, 1977; Vol. 9, pp 27-162.

6. Conway, B. E. *Theory and Principles of Electrode Processes*; Ronald Press: London, 1965.

7. Enyo, M. In *Modern Aspects of Electrochemistry*; Conway, B. E.; Bockris, J. O'M.; Eds.; Plenum Press: New York, 1975; Vol. 11, pp 251-314.

8. Enyo, M. In *Comprehensive Treatise of Electrochemistry*; Conway, B. E.; Bockris, J. O'M.; Eds.; Plenum Press: New York, 1983; Vol. 7, pp 241-300.

9. Conway, B. E.; Angerstein-Kozlowska, H.; Dhar, H. P. *Electrochim. Acta* **1974**, *19*, 455-460.

10. Conway, B. E.; Angerstein-Kozlowska, H. *Acc. Chem. Res.* **1981**, *14*, 49-56.

11. Conway, B. E.; Angerstein-Kozlowska, H.; Ho, F. C. *J. Vac. Sci. Technol.* **1977**, *14*, 351-364.
12. Conway, B. E.; Angerstein-Kozlowska, H.; Sharp, W. B. A. *J. Chem. Soc., Faraday Trans. I* **1978,** *74*, 1373-89; see also Conway, B. E.; Currie, J. C. *J. Chem. Soc., Faraday Trans. I* **1978,** *74*, 1390-1402.
13. Conway, B. E. *Sci. Prog. Oxf.* **1987**, *71*, 479-510.
14. Gregory, B. W.; Stickney, J. L. *J. Electroanal. Chem.* **1990**, *300*, 543-561.
15. Suggs, D. W.; Stickney, J. L. *Surface Sci.* **1993**, *290*, 362-374; 375-387.
16. Conway, B. E.; Jerkiewicz, G. *J. Electroanal. Chem.* **1993**, *357*, 47-66; see also Conway, B. E.; Jerkiewicz, G. *Zeit. Phys. Chem. Bd.* **1994**, *183*, 281-286.
17. Jerkiewicz, G.; Borodzinski, J. J.; Chrzanowski, W.; Conway, B. E. *J. Electroanal. Soc.* **1995**, *142*, 3755-3763.
18. Jerkiewicz, G.; Zolfaghari, A. *J. Electrochem. Soc.* **1996**, *143*, 1240-1248.
19. Jerkiewicz, G.; Zolfaghari, A. *J. Phys. Chem.* **1996**, *100*, 8454-8461.
20. Kolb, D. M. In *Advances in Electrochemistry and Electrochemical Engineering*; Gerischer, H.; Tobias, C. W.; Eds.; Wiley Interscience: New York, 1978, Vol. 11, pp 125-271.
21. Despic, A. R. In *Comprehensive Treatise of Electrochemistry*; Conway, B. E.; Bockris, J. O'M.; Yeager, E.; Khan, S. U. M.; White, R. E.; Eds.; Plenum Press: New York, 1983, Vol. 7, pp 451-528.
22. Conway, B. E.; Chacha, J. S. *J. Electroanal. Chem.* **1990**, *287*, 13-41.
23. Kolb, D. M; Przasnycki, M.; Gerischer, H. *J. Electroanal. Chem.* **1974**, *54*, 25-38.
24. Adzic, R. R. In *Advances in Electrochemistry and Electrochemical Engineering*; Gerischer, H.; Tobias, C. W.; Eds.; Wiley Interscience: New York, 1978, Vol. 13, pp 159-260.
25. Van der Eerden, J. P.; Staikov, G.; Kashchiev, D.; Lorenz, W. J. *Surface Sci.* **1979**, *82*, 364-382.
26. Jüttner, K.; Lorenz, W. J. *Z. Phys. Chem.* **1980**, *122*, 163-185
27. Hanson, M. E.; Yeager, E. In *Electrochemical Surface Science*; Soriaga, M. P.; Ed.; ACS Symposium Series: Washington, 1988, Vol. 378, pp 141-153.
28. Gileadi, E. *Electrode Kinetics*; VCH: New York, 1993.
29. Budevski, E. B.; Staikov, G. T.; Lorenz, W. J. *Electrochemical Phase Formation and Growth*; VCH: New York, 1996.

30. Lipkowski, J. Stolberg, L., Yang, D.-F., Pettinger, B., Mirwald, S., Henglein, F.; Kolb, D. M. *Electrochim. Acta* **1994**, *39*, 1045-1056.
31. Mrozek, P.; Sung, Y.-E.; Han, M.; Gamboa-Aldeco, M.; Wieckowski, A.; Chen, C.-H.; Gewirth, A. A. *Electrochim. Acta* **1995**, *40*, 17-28.
32. Shi. Z.; Lipkowski, J. *J. Phys. Chem.* **1995**, *99*, 4170-4175; see also Savich, W.; Sun, S.-G.; Lipkowski, J.; Wieckowski, J. *J. Electroanal. Chem.* **1995**, *388*, 233-237.
33. Zelenay, P.; Rice-Jackson, L. M.; Wieckowski, A.; Gawlowski, J. *Surface Sci.* **1991**, *256*, 253-263; see also Varga, K.; Zelenay, P.; Wieckowski, A. *J. Electroanal. Chem.* **1992**, *330*, 453-467.
34. Zelenay, P; Wieckowski, A. In *Electrochemical Interfaces*; Abruña, H.; Ed.; VCH: New York, 1991, pp 479-527.
35. Zelenay, P.; Gamboa-Aldeco, M.; Horanyi, G.; Wieckowski, A. *J. Electroanal. Chem.* **1993**, *357*, 307-326.
36. Gamboa-Aldeco, M.; Herrero, E.; Zelenay, P. S.; Wieckowski, A. *J. Electroanal. Chem.* **1993**, *348*, 451-457.
37. Krauskopf, E. K.; Wieckowski, A. In *Adsorption of Molecules at Metal Electrodes*; Lipkowski, J.; Ross, P. N.; Eds.; VCH: New York, 1992, pp 119-169.
38. Sawaguchi, T.; Yamada, T.; Okinaka, Y.; Itaya, K. *J. Phys. Chem.* **1995**, *99*, 14149-14155.
39. Wan, L.-J.; Yau, S.-L.; Itaya, K. *J. Phys. Chem.*, **1995**, *99*, 9507-9513.
40. Manne, S.; Hansma, P. K.; Massie, J.; Elings, V. B.; Gewirth, A. A. *Science*, **1991**, *251*, 183-186; see also Chen, C.; Gewirth, A. A. *J. Am. Chem. Soc.*, **1992**, *114*, 5439-5440.
41. Christman, K. *Surface Sci. Rep.* **1988**, *9*, 1-163.
42. Langmuir, I. *J. Am. Chem. Soc.* **1918**, *40*, 1361-1403.
43. Fowler, R. H.; Guggenheim, F. A. *Statistical Thermodynamics*; Cambridge University Press: London, 1939.
44. Lipkowski, J.; Stolberg, L. In *Adsorption of Molecules at Metal Electrodes*; Lipkowski, J.; Ross, P. N., Eds.; VCH: New York, 1992, pp 171-238.
45. Adamson, A. W. *Physical Chemistry of Surfaces*; John Wiley and Sons: New York, 1990.
46. Somorjai, G. A. *Introduction to Surface Chemistry and Catalysis*; John Wiley and Sons: New York, 1994.

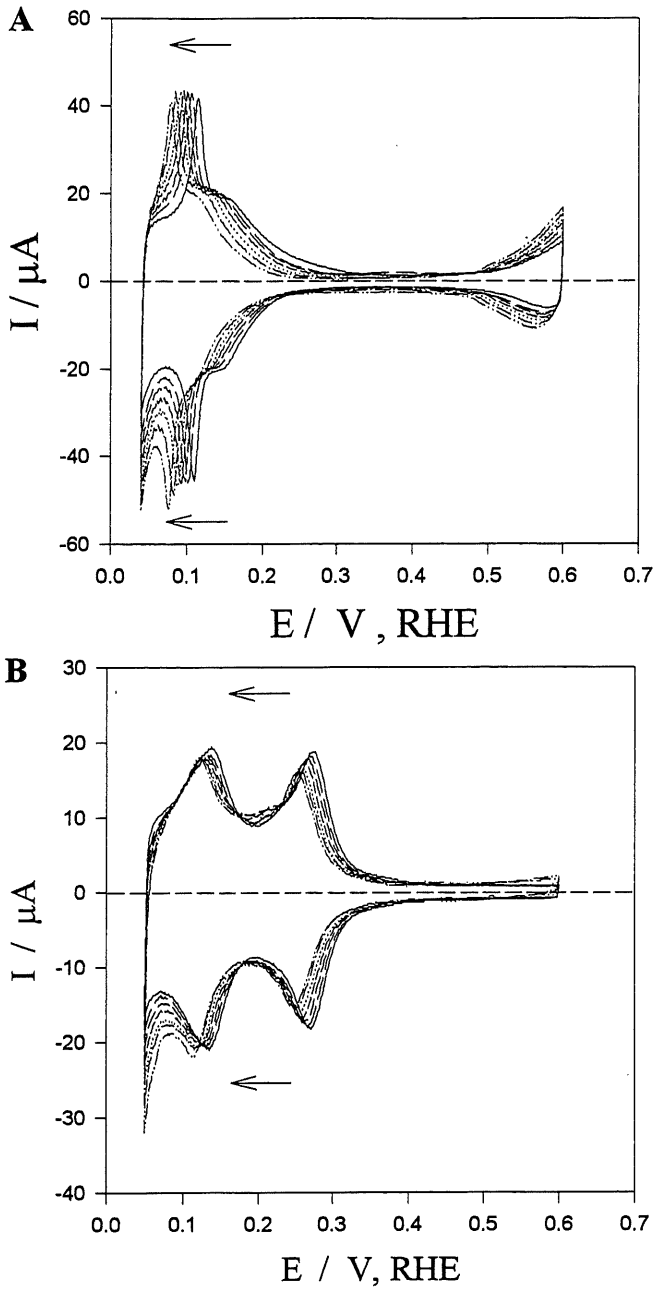

Figure 1. Series of cyclic-voltammetry, CV, profiles for the under-potential deposition of H, UPD H, from 0.50 M aqueous solution of H_2SO_4 for a temperature range between 273 and 343 K, with an interval of 10 K, and recorded at the sweep rate $s = 20\ mV\ s^{-1}$. **A.** For Rh; the electrode surface area $A_r = 0.70 \pm 0.01\ cm^2$. **B.** For Pt; the electrode surface area $A_r = 0.72 \pm 0.01\ cm^2$. The arrows indicate the shift of the adsorption and desorption peaks upon the temperature increase.

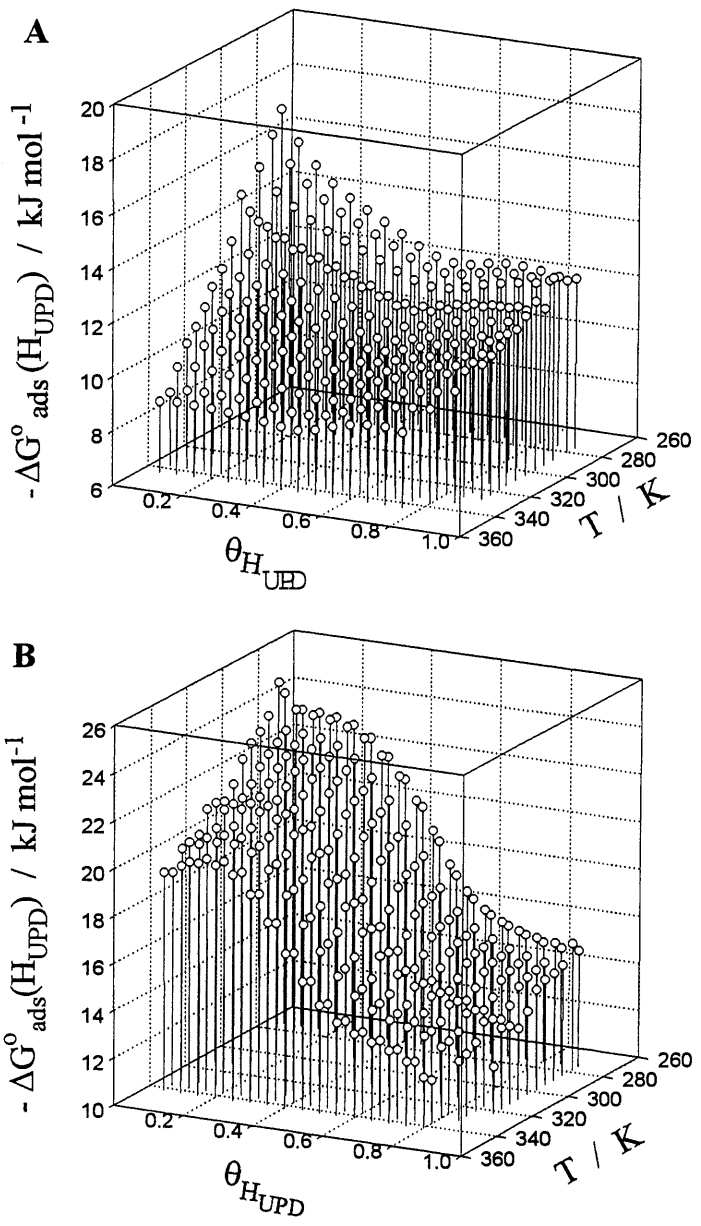

Figure 2. 3D plots showing the Gibbs free energy of the under-potential deposition of H, $\Delta G^{\circ}_{ads}(H_{UPD})$, versus $\theta_{H_{UPD}}$ and T, $\Delta G^{\circ}_{ads}(H_{UPD}) = f(\theta_{H_{UPD}}, T)$, for adsorption from 0.50 M aqueous solution of H_2SO_4. **A.** Rh. **B.** Pt. Augmentation of $\Delta G^{\circ}_{ads}(H_{UPD})$ with increase of $\theta_{H_{UPD}}$ for T = const points to the repulsive nature of lateral interactions between H_{UPD} adatoms. The $\Delta G^{\circ}_{ads}(H_{UPD})$ versus T relations for $\theta_{H_{UPD}}$ = const allow elucidation of the entropy of adsorption, $\Delta S^{\circ}_{ads}(H_{UPD})$.

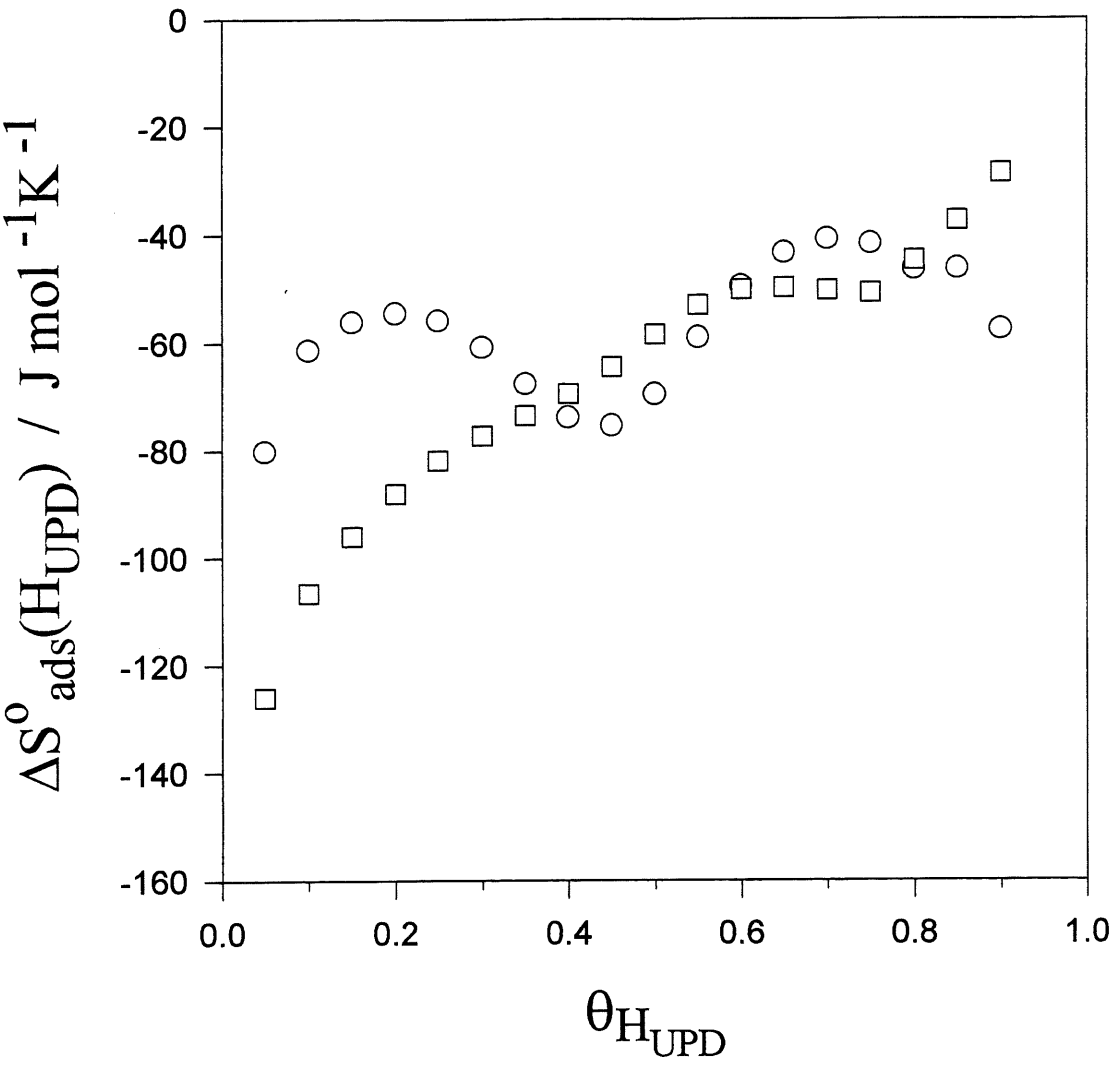

Figure 3. Dependence of $\Delta S^{\circ}_{ads}(H_{UPD})$ on $\theta_{H_{UPD}}$ for the under-potential deposition of H, UPD H, from 0.50 M aqueous H_2SO_4 solution. □ refers to Rh; $\Delta S^{\circ}_{ads}(H_{UPD})$ has values between −125 and −30 J mol^{-1} K^{-1}. ○ refers to Pt; $\Delta S^{\circ}_{ads}(H_{UPD})$ has values between −75 and −40 J mol^{-1} K^{-1}.

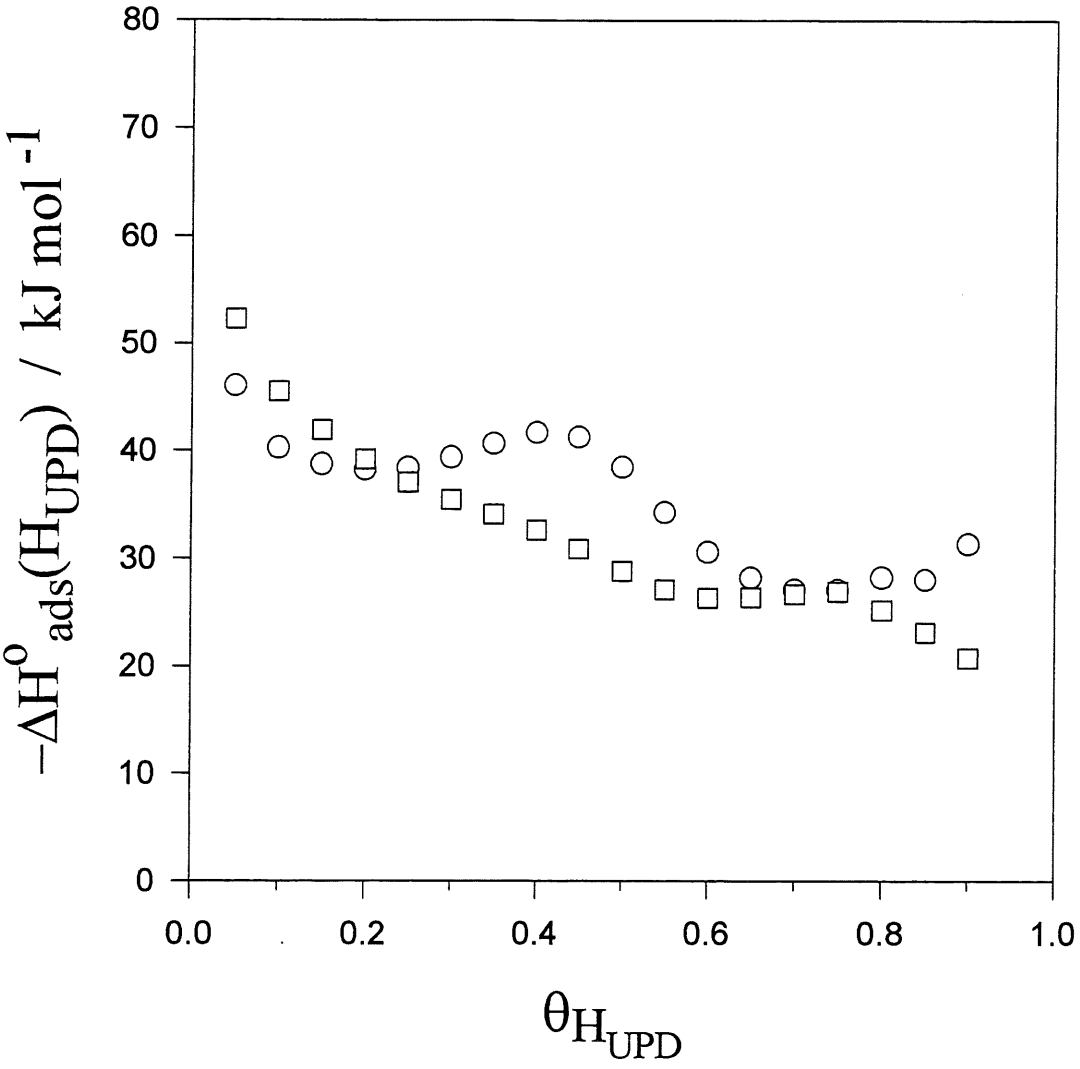

Figure 4. Dependence of $\Delta H^{\circ}_{ads}(H_{UPD})$ on $\theta_{H_{UPD}}$ for the under-potential deposition of H, UPD H, from 0.50 M aqueous H_2SO_4 solution. □ refers to Rh; $\Delta H^{\circ}_{ads}(H_{UPD})$ has values between −52 and −20 kJ mol^{-1}. ○ refers to Pt; $\Delta H^{\circ}_{ads}(H_{UPD})$ has values between −45 and −28 kJ mol^{-1}.

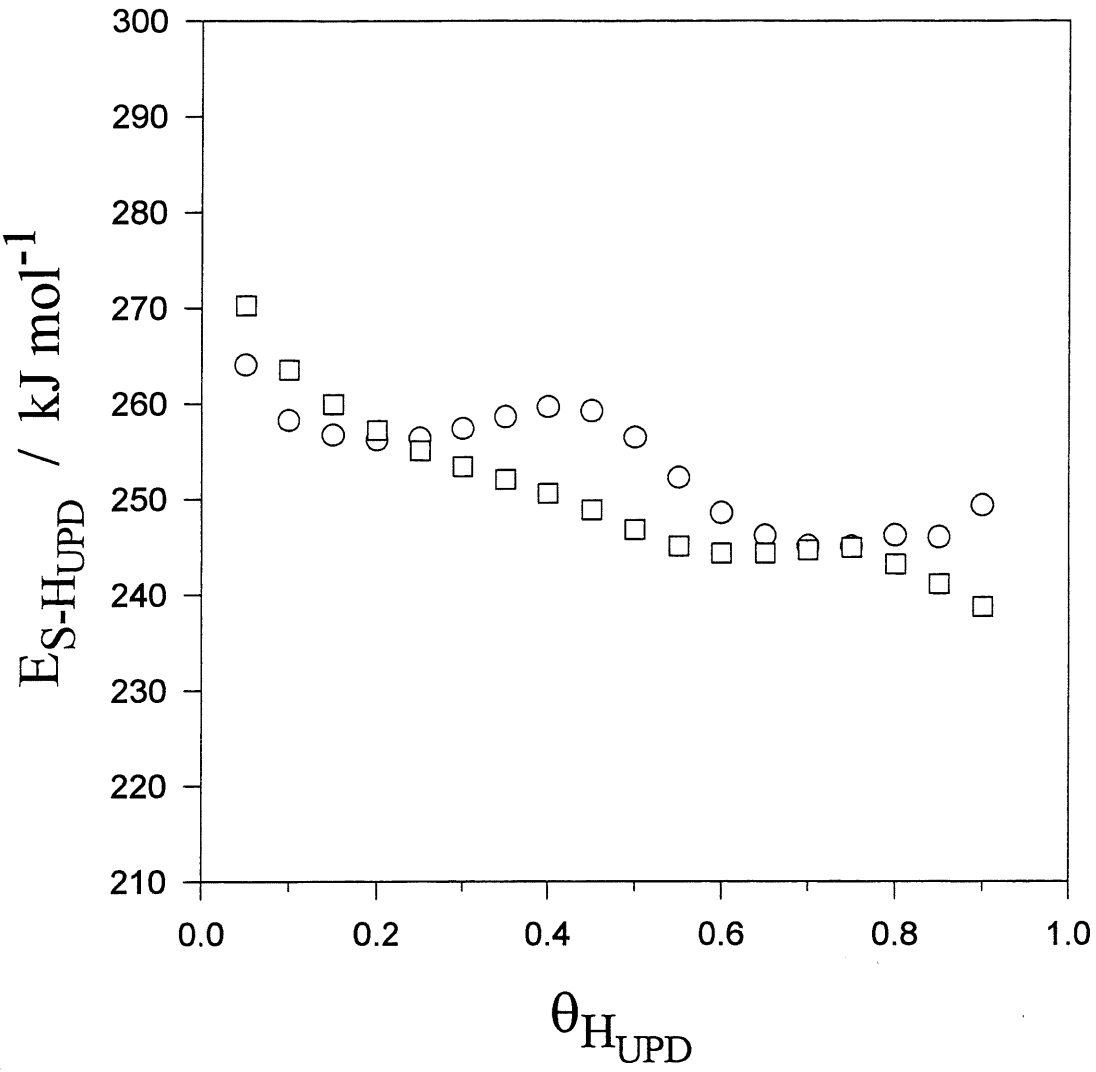

Figure 5. Dependence of $E_{S-H_{UPD}}$ on $\theta_{H_{UPD}}$ for the under-potential deposition of H, UPD H, from 0.50 M aqueous H_2SO_4 solution. □ refers to the $Rh-H_{UPD}$ bond energy, $E_{Rh-H_{UPD}}$, which have values between 240 and 270 kJ mol^{-1}. ○ refers to the $Pt-H_{UPD}$ bond energy, $E_{Pt-H_{UPD}}$, which assumes values between 250 and 265 kJ mol^{-1}. The variation of $E_{S-H_{UPD}}$ versus $\theta_{H_{UPD}}$ follows the $\Delta H^{\circ}_{ads}(H_{UPD})$ versus $\theta_{H_{UPD}}$ relations.

CHAPTER 2

COMPREHENSIVE RESEARCH ON THE UNDER POTENTIAL DEPOSITION OF HYDROGEN ON Pt AND Rh ELECTRODES IN ABSENCE/PRESENCE OF CHEMISORBED SULFUR

Chapter 2, which comprises two papers, examines in detail thermodynamic parameters of the under-potential deposition of hydrogen on polycrystalline Pt and Rh electrodes and compares the thermodynamic data for the two substrates. It also examines thermodynamics of the UPD H on Pt in presence of chemisorbed S. The paper in section 2.1 (*A. Zolfaghari, M. Chayer and G. Jerkiewicz, J. Electrochem. Soc., 144, 3034 (1997)*) demonstrates new data on $\Delta G_{ads}(H_{UPD})$, $\Delta S^{\circ}_{ads}(H_{UPD})$ and $\Delta H^{\circ}_{ads}(H_{UPD})$ for Pt and Rh electrodes with respect to the concentration of supporting electrolyte, thus the surface concentration of the specifically adsorbed anions. For the first time, the $Pt-H_{UPD}$ and $Rh-H_{UPD}$ surface bond energies, $E_{Pt-H_{UPD}}$ and $E_{Rh-H_{UPD}}$ respectively, are determined. On the thermodynamic ground, the authors relate H_{UPD} to H_{chem} and discuss its surface adsorption site. The values of $E_{Pt-H_{UPD}}$ and $E_{Rh-H_{UPD}}$ fall close to those of the respective bond energies between Pt or Rh and H_{chem}, $E_{Pt-H_{chem}}$ and $E_{Rh-H_{chem}}$, respectively. Proximity of $E_{M-H_{UPD}}$ to $E_{M-H_{chem}}$ (where M = Pt or Rh) indicates that H_{UPD} and H_{chem} might have a similar binding mechanism in presence of the electrified solid/liquid interface and under gas-phase conditions; it shows that H_{UPD} and H_{chem} might occupy the same adsorption sites, thus indicating that H_{UPD} alike H_{chem} is strongly embedded in the surface lattice of the Pt or Rh substrate.

Sulfur chemisorption and its ability to modify surface-catalytic properties of metallic electrodes is broadly recognized (52-54,52,62,93,97,102,126-136). The paper in section 2.2 presents new results on S chemisorption on Pt electrodes and its impact on the UPD H. The UPD H on Pt can be completely suppressed by a monolayer, ML, of chemisorbed sulfur, S_{chem}, or partially by submonolayers of S_{chem} having their surface coverage less than 0.33, $\theta_S < 0.33$. A relation between S_{chem} surface coverage, θ_S, and the coverage by H_{UPD}, $\theta_{H_{UPD}}$, is demonstrated. Temperature-dependent experimental studies followed by comprehensive theoretical treatment result in determination of ΔG_{ads}, ΔS°_{ads} and ΔH°_{ads} in absence and presence of S_{chem}. Changes of the $Pt-H_{UPD}$ surface bond energy brought about by a S_{chem} submonolayer having its coverage of 0.10 ($\theta_S = 0.10$) are evaluated. The submonolayer of

S_{chem} affects ΔG_{ads}, ΔS°_{ads} and ΔH°_{ads} as well as the $Pt-H_{UPD}$ bond energy, $E_{Pt-H_{UPD}}$, which becomes weaker in presence of the S_{chem} submonolayer than in its absence. The lateral interactions between H_{UPD} and S_{chem} are brought about by local electron withdrawing effects that propagate through the underlying metal which acts as a mediator. The papers presented section 2.1 (*A. Zolfaghari, M. Chayer and G. Jerkiewicz, J. Electrochem. Soc., 144, 3034 (1997)*) and section 2.2 (*A. Zolfaghari, F. Villiard, M. Chayer and G. Jerkiewicz, J. Alloys and Compounds, 235-254, 481 (1997)*) are a result of my essential contribution in experimental, theoretical and writing parts. The contributions of F. Villiard and M. Chayer were in experimental part which were done as student term projects under my experimental supervision. The contribution of Dr. G. Jerkiewicz was in theoretical and writing constituent.

2.1 ENERGETICS OF THE UNDER-POTENTIAL DEPOSITION OF HYDROGEN ON PLATINUM ELECTRODES. PART I: ABSENCE OF COADSORBED SPECIES

A. Zolfaghari, M. Chayer and G. Jerkiewicz, J. Electrochem. Soc., 144, 3034 (1997)

ABSTRACT

Research on the under-potential deposition of hydrogen, UPD H, on Pt electrodes by cyclic-voltammetry in 0.05, 0.10 and 0.50 M aqueous H_2SO_4 solutions at T from 273 to 343 K shows that the adsorption-desorption profiles shift towards less-positive values upon T increase. Treatment of the experimental results based on a general electrochemical adsorption isotherm allows determination of $\Delta G^{\circ}_{ads}(H_{UPD})$ as a function of T and the H_{UPD} surface coverage, $\theta_{H_{UPD}}$; $\Delta G^{\circ}_{ads}(H_{UPD})$ varies from −11 to −25 kJ mol^{-1}. The relation between $\Delta G^{\circ}_{ads}(H_{UPD})$ and T for $\theta_{H_{UPD}}$ = const allows determination of $\Delta S^{\circ}_{ads}(H_{UPD})$ which is from −40 to −90 J mol^{-1} K^{-1}. Subsequently, $\Delta H^{\circ}_{ads}(H_{UPD})$ is determined and it varies from −27 to −46 kJ mol^{-1}. An analysis of the values of $\Delta H^{\circ}_{ads}(H_{UPD})$ and $\Delta S^{\circ}_{ads}(H_{UPD})$ leads to conclusion that the UPD H on Pt electrodes is an enthalpy-driven process. Knowledge of $\Delta H^{\circ}_{ads}(H_{UPD})$ permits determination of the bond energy between Pt and H_{UPD}, $E_{Pt-H_{UPD}}$, which is from 245 to 265 kJ mol^{-1}. The value of $E_{Pt-H_{UPD}}$ falls close to that of the bond energy between Pt and H_{chem}, $E_{Pt-H_{chem}}$, which varies from 243 to 247 kJ mol^{-1}. Proximity of $E_{Pt-H_{UPD}}$ to $E_{Pt-H_{chem}}$ indicates that H_{UPD} and H_{chem} have a similar binding mechanism in presence of the electrified solid/liquid interface and under gas-phase conditions; it shows that H_{UPD} and H_{chem} might occupy the same adsorption sites, thus indicating that H_{UPD} alike H_{chem} is strongly embedded in the surface lattice of the Pt substrate.

INTRODUCTION

The electro-adsorption of hydrogen, H, is one of the most extensively studied electrochemical surface science systems due to its relevance to H adsorption at and absorption into host metals, metal-hydride (M-H) batteries, H-based fuel cells and H-induced corrosion referred to as H embrittlement. [1-20] Knowledge of the physico-chemical nature of the adsorbed H and the basic steps involved in its interfacial transfer into the metal bulk is of significance in corrosion research and in design of M-H batteries. In materials science, the entry of H into the host metal is highly undesirable and leads to formation of a metal hydride which possesses inferior mechanical properties with respect to the H-free metal; the process causes subsequent deterioration of mechanical properties of the metal and disintegration of its structure through internal fracturing. In M-H batteries, fast H entry into the host metal, followed by the metal-hydride formation, is the key objective of the process in order to employ such formed a metal hydride as an anode. It is recognized that the H transfer from the adsorbed to the absorbed state can be either suppressed or enhanced by smart selection of

coadsorbates which act either as surface poisons or as surface promoters. [15,16,20] In electrochemical surface science, two kinds of electroadsorbed H species are known: the under-potential deposited H, H_{UPD}, and the over-potential deposited H, H_{OPD}. The under-potential deposition of H, UPD H, takes place at potentials positive with respect to the thermodynamic reversible potential of the hydrogen evolution reaction, HER, E°_{HER}, and it is known to occur at Pt, Rh, Pd and Ir electrodes. The over-potential deposition of H, OPD H, takes place at negative potentials with respect to the E°_{HER} because H_{OPD} is an intermediate of the HER. Thus H_{OPD} exists on all metal electrode surfaces at negative potentials. [10-16,20] Both these surface species, namely H_{UPD} and H_{OPD}, are known to absorb into Pd but absorption of H_{UPD} is quantitative whereas absorption of H_{OPD} is not. [21] In the case of metals which do not reveal the under-potential deposition of hydrogen, it is obviously H_{OPD} which becomes absorbed in the lattice of the host metal.

The UPD H on Pt from acidic solution may be represented by the following single-electrode surface electrochemical process:

$$\underset{1-\theta_{H_{UPD}}}{Pt} + \underset{a_{H_3O^+}}{H_3O^+} + e \rightarrow \underset{\theta_{H_{UPD}}}{Pt-H_{UPD}} + H_2O \qquad [1]$$

where Pt represents the substrate at which the UPD H takes place, $a_{H_3O^+}$ is the activity of H_3O^+ species from which H_{UPD} originates and $\theta_{H_{UPD}}$ is the H_{UPD} surface coverage. In the course of the UPD H, the hydrated proton undergoes discharge and the electrosorption valency, γ, of H_{UPD} upon the deposition equals 0.95, $\gamma_{H_{UPD}} = 0.95 \cong 1$. [22,23] Based on these findings one may conclude that the UPD H leads to a complete discharge of H^+ (or H_3O^+) which is the source of H_{UPD}, thus the value of z for the process equals unity, $z = 1$. The electrochemical adsorption isotherm for Eq. 1 coupled with the respective single-electrode process occurring at the hydrogen reference electrode ($H^+ + e \rightarrow 1/2\, H_2$) may be written according to the following equation: [4,10-13,20,24]

$$\frac{\theta_{H_{UPD}}}{1-\theta_{H_{UPD}}} = a_{H_3O^+} \exp(-EF/RT) \exp\left(-\Delta G^{\circ}_{ads}(H_{UPD})/RT\right) \qquad [2]$$

where E is the electrode potential measured *versus the standard hydrogen electrode*, SHE, and it determines the surface coverage of H_{UPD}, $\Delta G^{\circ}_{ads}(H_{UPD})$ is the standard Gibbs free energy of adsorption, T is the temperature and R, F are physico-chemical constants. It should be added that Eq. 2 is a general electrochemical adsorption isotherm and $\Delta G^{\circ}_{ads}(H_{UPD})$ refers to the value of the Gibbs free energy of adsorption at given T and $\theta_{H_{UPD}}$. Depending on the relationship between $\Delta G^{\circ}_{ads}(H_{UPD})$ at $\theta_{H_{UPD}} = 0$ and at $\theta_{H_{UPD}} \neq 0$, the isotherm becomes the Langmuir one ($\Delta G^{\circ}_{ads}(H_{UPD}) = \text{const}$ at all $\theta_{H_{UPD}}$) or the Frumkin one ($\Delta G^{\circ}_{ads}(H_{UPD})$ varies linearly with $\theta_{H_{UPD}}$). Subsequently, selection of the standard states depends on the presence/absence of lateral interactions. [9,10,24] A detail discussion of the selection of standard states for the adsorption isotherms is provided in ref. 9.

Spectroscopic evidence reveals that H_{OPD} adsorbed on Pt and Rh electrodes interacts with water molecules forming a bond whereas H_{UPD} appears to be unavailable for binding H_2O molecules in the double-layer region. [25-27] This observation indicates that H_{OPD} is bonded less strongly to the metal substrate than H_{UPD}. [9-13,20] Experimental data [28,29] also reveal that on Pt electrodes, H_{UPD} co-exist with H_{OPD} in the negative potential region, thus the two species must occupy distinct surface adsorption sites in order to sustain their physico-chemical identity. Subsequently, if H_{UPD} and H_{OPD} occupy different adsorption sites, then their Gibbs free energies of adsorption, enthalpies of adsorption and bond energies should be discrete. In general, knowledge of the Gibbs free energies of adsorption for the electroadsorbed H_{UPD} and H_{OPD}, $\Delta G^{\circ}_{ads}(H_{UPD})$ and $\Delta G^{\circ}_{ads}(H_{OPD})$, respectively, leads to determination of the chemical potential gradient associated with the interfacial H transfer from the adsorbed to the absorbed state, thus it leads to elucidation of the thermodynamic driving force of the process. [15,16,20] The latter is of vital importance to the recently developing metal-hydride science because it defines the nature and strength of the $M-H$ bond on the metal surface prior to the H interfacial transfer into the metal bulk. Studies on the enthalpies of adsorption of H_{UPD} and H_{OPD}, $\Delta H^{\circ}_{ads}(H_{UPD})$ and $\Delta H^{\circ}_{ads}(H_{OPD})$, respectively, and the bond energies between Pt and H_{UPD} or between Pt and H_{OPD}, $E_{Pt-H_{UPD}}$ and $E_{Pt-H_{OPD}}$, respectively, are of importance to electrochemical surface science because they allow assessment, on the thermodynamic basis, of the adsorption sites of the H_{UPD} and H_{OPD} surface species. [20,25-29]

Despite significant amount of thermodynamic data [12,17-19] on the H chemisorbed from the gas phase (H_{chem}), thus $\Delta G^{\circ}_{ads}(H_{chem})$, $\Delta H^{\circ}_{ads}(H_{chem})$, $\Delta S^{\circ}_{ads}(H_{chem})$ and $E_{M-H_{chem}}$, there is a limited amount on data on thermodynamics of the UPD H. This paper is an extension to the important, early research of Breiter et al. [2,3] who studied $\Delta H^{\circ}_{ads}(H_{UPD})$ on Pt-group metals by

application of the Gibbs-Helmholtz relation. The authors of the present paper demonstrate a new theoretical approach which allows determination of $\Delta G^{\circ}_{ads}(H_{UPD})$ versus $\left(T, \theta_{H_{UPD}}\right)$, in the form of 3D plots, and evaluation of $\Delta S^{\circ}_{ads}(H_{UPD})$ and $\Delta H^{\circ}_{ads}(H_{UPD})$ as a function of $\theta_{H_{UPD}}$. New data are reported on $\Delta G^{\circ}_{ads}(H_{UPD})$, $\Delta S^{\circ}_{ads}(H_{UPD})$ and $\Delta H^{\circ}_{ads}(H_{UPD})$ for Pt electrodes with respect to the concentration of the supporting electrolyte, thus the surface concentration of the specifically adsorbed anions. The authors determine, for the first time, the $Pt-H_{UPD}$ surface bond energy, $E_{Pt-H_{UPD}}$. On the thermodynamic ground, they relate H_{UPD} to H_{chem} and discuss its surface adsorption site.

EXPERIMENTAL

Electrode Preparation. The technique of preparing electrodes was found to be important with respect to the reproducibility of the experimental results. [30-34] The electrode preparation procedure involved the following steps: (a) initial cleaning of the Pt wire (99.998% purity) by refluxing in acetone for 12 h; (b) flame-welding the Pt wire to a Ag wire for electrical contact (the Ag wire was not in contact with the solution); (c) sealing the Pt wire into pre-cleaned soft-glass tubing followed again by step (a); (d) cleaning the electrode in conc. H_2SO_4 for 12 h; (e) repetitive washing in "Nanopure" water, followed by soaking for 24 h. Since the heat treatment of Pt electrodes always affected the surface, the electrodes were cycled 4,000 times between 0.05 and 1.50 V versus the reversible hydrogen electrode, RHE, prior to the measurements in order to release any stress from the near-surface region. [33,34] After this procedure, the electrodes and their surfaces were found stable and did not undergo any further changes, as revealed from the CV profiles; the shape of the UPD H CV profiles and the double layer CV charging curves were found to be consistent with those reported in earlier literature. [30-32] The real surface area of the Pt electrodes was determined by accepting an anodic charge value of 220 $\mu C\ cm^{-2}$ as that necessary to form a monolayer of H_{UPD} [5,30] allowing for double-layer charging. It was calculated to be $A_r = 0.720 \pm 0.005\ cm^2$.

Solution and Electrochemical Cell. High-purity solutions were prepared from BDH "Aristar" grade H_2SO_4 and "Nanopure" water, and their cleanliness was verified by recording CV H_{UPD} adsorption-desorption profiles and comparing them with those in the literature. [30-32] The experiments were conducted in a standard all-Pyrex, two-compartment electrochemical cell. [33-36] The glassware was pre-cleaned according to the well established procedure. [31] During the experiments H_2 gas, pre-cleaned and pre-saturated with water vapor, was bubbled

through the reference electrode, RE, compartment in which a Pt/Pt-black reference electrode was immersed. N_2 gas, pre-cleaned and pre-saturated with water vapor, was passed through the working, WE, compartment. [31]

Temperature Measurements. The cell was immersed in a water bath (Haake W13) and the temperature was controlled to within ± 0.5 K by means of a thermostat (Haake D1); the water level in the bath was maintained above the electrolyte in the cell. The temperature in the water bath and the electrochemical cell were controlled by means of thermometers (± 0.5 K) and a K-type thermocouple (80 TK Fluke), and were found to agree to within ± 0.5 K. In order to ensure uniform temperature distribution in the cell, N_2 gas pre-heated to the temperature of the water bath was passed through the electrolyte.

Electrochemical Measurements. The experimental procedure applied in this project involved standard cyclic-voltammetry measurements of the UPD H on Pt electrodes in 0.05, 0.10 and 0.50 M aqueous solutions of H_2SO_4 within a temperature range between 273 and 343 K. The electrochemical instrumentation included: (a) EG&G Model 263A potentiostat-galvanostat; (b) IBM-compatible 80386, 40 MHz computer; and (c) EG&G M270 Electrochemical Software. All potentials were measured with respect to the reversible hydrogen electrode, RHE, immersed in the same electrolyte.

RESULTS AND DISCUSSION

Temperature-Dependence of the UPD H. Figure 1 shows a series of CV adsorption-desorption for the UPD H from 0.50 M aqueous solution of H_2SO_4 for various temperature between 273 and 343 K, with an interval of 10 K recorded at the sweep rate of 20 mV s^{-1}. The experiments were conducted with a temperature interval of 5 K but in order not to obscure the graph fewer experimental curves are shown. The authors conducted identical experiments in 0.05 and 0.10 M aqueous H_2SO_4 solutions in order to evaluate changes in the CV profiles brought about by the temperature and concentration variation and selected results are shown in Figure 2. The features of Figures 1 and 2 may be summarized as follows: (i) upon the temperature increase, the UPD H adsorption-desorption profiles shift towards less-positive values; they are symmetric with respect to the potential axis indicating that the surface electrochemical process is reversible; (ii) the third anodic peak which appears between the two main ones decreases when the temperatures rises and gradually disappears; (iii) redistribution of the UPD H adsorption-desorption charges is observed with the temperature increase as indicated by arrows in the CV profiles; (iv) apart from the

redistribution of the adsorption-desorption charges, no new features are observed in the CV profiles that could result from the temperature increase for a given concentration of H_2SO_4; (v) upon decrease of the concentration of H_2SO_4, the UPD H adsorption-desorption peaks become less sharp (less pronounced); (vi) an increase of the cathodic current at the lower potential limit of the CV profiles, thus prior to the sweep reversal, is due to the onset of the OPD H. [11,12]

It is of interest to briefly discuss the increase of the cathodic current at the lower limit of the CV profiles, an aspect not scrutinized in previous literature. At first, it might be surprising to observe a cathodic current at positive potentials due to onset of adsorption of H_{OPD}, the latter being an intermediate of the HER. Indeed, the thermodynamic reversible potential of the HER, E°_{HER}, equals zero but it refers to a thermodynamic equilibrium involving the hydrogen gas evolved at the standard pressure of 1 atm. Because the hydrogen pressure in the working-electrode compartment is very small, the equilibrium potential of the HER is displaced towards positive values as expected on the basis of the Nernst equation.

Determination of $\Delta G^{\circ}_{ads}(H_{UPD})$, $\Delta S^{\circ}_{ads}(H_{UPD})$ and $\Delta H^{\circ}_{ads}(H_{UPD})$. Evaluation of $\Delta G^{\circ}_{ads}(H_{UPD})$ as a function of $\theta_{H_{UPD}}$ is essential in determination of the nature of lateral interactions between the H_{UPD} adatoms. Generally, in absence of lateral interactions, the standard Gibbs free energy of adsorption for any surface species may be expressed by relation $\Delta G^{\circ}_{ads} = N\, q^{\circ}_{ads}$ where N is the number of adsorbed species and q°_{ads} is the standard Gibbs free energy of adsorption per adsorbed species. [37-40] However, it is seldom observed that adsorbed species do not interact with each other. When lateral interactions set in, they affect the Gibbs free energy of adsorption and the values of q°_{ads} and ΔG°_{ads} change. [37,40] In other words, the relation between ΔG°_{ads} and the surface coverage of the adsorbed species points to the nature of their lateral interactions; increase of ΔG°_{ads} from more-negative to less-negative values demonstrates the repulsive nature of the lateral interactions and vice versa.

Evaluation of the Gibbs free energy of adsorption of H_{UPD} $\Delta G^{\circ}_{ads}(H_{UPD})$ as a function of $\theta_{H_{UPD}}$ is not trivial because it is unknown whether the process follows the Langmuir or the Frumkin isotherm. In other words the relation between $\Delta G^{\circ}_{ads}(H_{UPD})$ and the H_{UPD} surface coverage, $\theta_{H_{UPD}}$, is unknown prior to experimental evaluation of $\Delta G^{\circ}_{ads}(H_{UPD})$ for a series of T and $\theta_{H_{UPD}}$. It is the subsequent theoretical treatment of the $\Delta G^{\circ}_{ads}(H_{UPD})$ versus $\theta_{H_{UPD}}$ experimental relations which allows one to determine which adsorption isotherm, if any, describes the best the system under investigation. In the Langmuir case, $\Delta G^{\circ}_{ads}(H_{UPD})$ is

independent of $\theta_{H_{UPD}}$, thus $\Delta G^{\circ}_{ads}(H_{UPD})_{\theta_{H_{UPD}}=0} = \Delta G^{\circ}_{ads}(H_{UPD})_{\theta_{H_{UPD}}\neq 0}$; in the Frumkin case, $\Delta G^{\circ}_{ads}(H_{UPD})$ changes with $\theta_{H_{UPD}}$ in a linear manner, thus $\Delta G^{\circ}_{ads}(H_{UPD})_{\theta_{H_{UPD}}\neq 0} = \Delta G^{\circ}_{ads}(H_{UPD})_{\theta_{H_{UPD}}=0} + g\,\theta_{H_{UPD}}$, where g is an energetic component describing the lateral interactions. It is worthwhile adding that H chemisorption from the gas phase on single-crystal surfaces of transition metals rarely follows simple adsorption isotherms and even if so, this behavior is often limited to a narrow H coverage range (see ref. 19). Quantitative explanation of complex ΔG°_{ads} versus $\theta_{H_{UPD}}$ relations is accomplished based on numerical calculations of the lateral interactions with respect to the surface adsorption sites and the H surface coverage.

It is of utmost importance to emphasize that the electrochemical adsorption isotherm for H_{UPD} may be represented in two forms: the first as in Eq. 2 or as in Eq. 3 obtained through application of the Nernst formula (see ref. 20):

$$\frac{\theta_{H_{UPD}}}{1-\theta_{H_{UPD}}} = P_{H_2}^{1/2} \exp\left(-\frac{EF}{RT}\right)\exp\left(-\frac{\Delta G^{\circ}_{ads}(H_{UPD})}{RT}\right) \qquad [3]$$

where $P_{H_2}^{1/2}$ is the partial pressure of H_2 in the reference electrode compartment, and E is the experimentally measured potential difference between the working electrode and the reference electrode immersed in the same solution, thus the potential measured *versus the reversible hydrogen electrode*. [20] It should be emphasized that $\Delta G^{\circ}_{ads}(H_{UPD})$ in Eq. 3 already includes a coverage-dependent parameter, $\omega(\theta_{H_{UPD}})$, which describes their lateral interactions, thus $\Delta G^{\circ}_{ads}(H_{UPD})_{\theta_{H_{UPD}}\neq 0} = \Delta G^{\circ}_{ads}(H_{UPD})_{\theta_{H_{UPD}}=0} + \omega(\theta_{H_{UPD}})$, and no assumption is made with respect to the nature of the relation between $\Delta G^{\circ}_{ads}(H_{UPD})$ and $\theta_{H_{UPD}}$. The parameter $\omega(\theta_{H_{UPD}})$ is not a linear function of the H_{UPD} surface coverage, thus the above formula does not represent the well-known Frumkin isotherm but rather a general electrochemical adsorption isotherm.

In the course of research, the authors determined numerically $\Delta G^{\circ}_{ads}(H_{UPD})$ as a function of $\theta_{H_{UPD}}$ for various T between 273 and 343 K based on the above formula and the experimental data are presented in Figures 1 and 2. From the anodic component of CV profiles (the cathodic component is obscured by co-adsorbed H_{OPD} at the least-positive potentials), they evaluated the potential at which the H_{UPD} surface coverage, $\theta_{H_{UPD}}$, reached a given value for a given temperature, T, and subsequently introduced the data into Eq. 3 and evaluated $\Delta G^{\circ}_{ads}(H_{UPD})$. This procedure was applied to various values of $\theta_{H_{UPD}}$ between 0.05

and 0.90, with an interval of 0.05, and it led to evaluation of $\Delta G^{\circ}_{ads}(H_{UPD})$ as a function of both $\theta_{H_{UPD}}$ and T, $\Delta G^{\circ}_{ads}(H_{UPD}) = f(\theta_{H_{UPD}}, T)$, for the three concentrations of the aqueous H_2SO_4 solution; the results of the numerical calculations are shown in Figure 3 as 3D plots of $\Delta G^{\circ}_{ads}(H_{UPD})$ versus $(\theta_{H_{UPD}}, T)$. Examination of the $\Delta G^{\circ}_{ads}(H_{UPD})$ versus $(\theta_{H_{UPD}}, T)$ relations leads to the following general observations: (i) $\Delta G^{\circ}_{ads}(H_{UPD})$ varies from −11 to −25 kJ mol^{-1}; (ii) $\Delta G^{\circ}_{ads}(H_{UPD})$ has the most negative values at the lowest temperature and at the smallest H_{UPD} surface coverage; (iii) changes of $\Delta G^{\circ}_{ads}(H_{UPD})$ are pronounced the most in the $0.20 - 0.80$ range of $\theta_{H_{UPD}}$; (iv) increase of $\Delta G^{\circ}_{ads}(H_{UPD})$ towards less-negative values with increasing $\theta_{H_{UPD}}$ (for $T = const$) indicates that the lateral interactions between H_{UPD} adatoms are predominantly of the repulsive nature; [2-4,19,20,37-41] the lateral repulsions are the most noticeable, thus the strongest, in the $0.20 - 0.80$ range of $\theta_{H_{UPD}}$; (v) for a given, constant H_{UPD} surface coverage, $\Delta G^{\circ}_{ads}(H_{UPD})$ assumes less-negative values when the temperature increases; (vi) for a given, constant temperature, T, $\Delta G^{\circ}_{ads}(H_{UPD})$ has less-negative values when the H_{UPD} surface coverage increases.

An important aspect that should be discussed is the anion adsorption on Pt, here sulfate of bisulfate, attained by discharge which is represented by the following equation:

$$Pt + A^{-} \rightarrow Pt - A_{ads} + e \qquad [4]$$

Recent data [42-45] demonstrate that the anion adsorption can overlap the potential region corresponding to the UPD H. At present, the charge associated with the anion adsorption on Pt from the 0.05, 0.10 and 0.50 M aqueous solutions of H_2SO_4 is not well established, thus the authors are unable to account for it. The anion surface coverage depends on its bulk concentration and already at low concentrations of the order of 0.001 or 0.01 M it reaches a maximal (saturation) value. In the case of the results presented in the paper, the sulfate surface coverage is not affected significantly by the change of the bulk concentration of H_2SO_4. Thus the experimentally evaluated value of $\Delta G^{\circ}_{ads}(H_{UPD})$ may contain an anion contribution, $\Delta G^{\circ}_{ads}(A_{ads})$, but it seems reasonable to consider it constant for the three concentrations of H_2SO_4. Hence, even if the $\Delta G^{\circ}_{ads}(H_{UPD})$ values are obscured by a certain anion contribution, it is sensible to assume that it is almost constant and that the $\Delta G^{\circ}_{ads}(H_{UPD})$ versus $(\theta_{H_{UPD}}, T)$ variations are meaningful. The recent interest in anion adsorption has led to new and interesting data on the anion surface concentration. Future advancement of

experimental approaches into temperature dependence measurements followed by theoretical treatment will result in precise determination of $\Delta G^{\circ}_{ads}(A_{ads})$, $\Delta S^{\circ}_{ads}(A_{ads})$ and $\Delta H^{\circ}_{ads}(A_{ads})$.

The standard entropy of the UPD H on Pt, $\Delta S^{\circ}_{ads}(H_{UPD})$, was determined based on the temperature dependence of $\Delta G^{\circ}_{ads}(H_{UPD})$. An analysis of the $\Delta G^{\circ}_{ads}(H_{UPD})$ versus $(\theta_{H_{UPD}}, T)$ plots (Figure 3) shows that for $\theta_{H_{UPD}} = \text{const}$ the relation between $\Delta G^{\circ}_{ads}(H_{UPD})$ and T is linear and it allows evaluation of the entropy of adsorption on the basis of the slope of the $\Delta G^{\circ}_{ads}(H_{UPD})$ versus T dependences, thus $\Delta S^{\circ}_{ads}(H_{UPD}) = -(\partial \Delta G^{\circ}_{ads}(H_{UPD}) / \partial T)_{\theta_{H_{UPD}}=\text{const}}$. Figure 4 shows $\Delta S^{\circ}_{ads}(H_{UPD})$ versus $\theta_{H_{UPD}}$ relations for the three concentrations of H_2SO_4. The main observations of the examination of the data may be summarized as follows: (i) $\Delta S^{\circ}_{ads}(H_{UPD})$ varies significantly with $\theta_{H_{UPD}}$ and it has values from –40 to –90 J mol^{-1} K^{-1}; (ii) the $\Delta S^{\circ}_{ads}(H_{UPD})$ versus $\theta_{H_{UPD}}$ relations reveal two waves which the authors associate with two adsorption-desorption peaks in the CV profiles; (iii) the $\Delta S^{\circ}_{ads}(H_{UPD})$ versus $\theta_{H_{UPD}}$ relations have a local minimum at $\theta_{H_{UPD}} = 0.45$ and the minimal value of $\Delta S^{\circ}_{ads}(H_{UPD})$ varies from –75 to –90 J mol^{-1} K^{-1}, depending on the H_2SO_4 concentration; this local minimum of $\Delta S^{\circ}_{ads}(H_{UPD})$ corresponds to the potential between the two CV adsorption-desorption peaks (Figures 1 and 2); (iv) $\Delta S^{\circ}_{ads}(H_{UPD})$ has the least-negative values for the UPD H from 0.50 M aq. H_2SO_4; (v) the $\Delta S^{\circ}_{ads}(H_{UPD})$ versus $\theta_{H_{UPD}}$ relations for H adsorption from 0.05 and 0.10 M aq. H_2SO_4 solutions almost follow each other throughout the whole $\theta_{H_{UPD}}$ range; (vi) the $\Delta S^{\circ}_{ads}(H_{UPD})$ versus $\theta_{H_{UPD}}$ relations are complex and fitting them into an n-th order polynomial does not provide any new insight. At this preliminary level, changes of the $\Delta S^{\circ}_{ads}(H_{UPD})$ versus $\theta_{H_{UPD}}$ behavior brought about by varying the H_2SO_4 concentration may be assigned to the anion adsorption. The $\Delta S^{\circ}_{ads}(H_{UPD})$ versus $\theta_{H_{UPD}}$ plots presented in Figure 4 show that the entropy of the UPD H depends on the concentration of the electrolyte, thus it is associated with the anion concentration at the solid/liquid interface. [42-45]

The enthalpy of the under-potential deposition of H on Pt electrodes, $\Delta H^{\circ}_{ads}(H_{UPD})$, from aqueous H_2SO_4 solutions can be readily calculated based on the experimentally determined values of $\Delta G^{\circ}_{ads}(H_{UPD})$ and $\Delta S^{\circ}_{ads}(H_{UPD})$, and the well-known formula $\Delta G^{\circ} = \Delta H^{\circ} - T\,\Delta S^{\circ}$. Figure 5 shows $\Delta H^{\circ}_{ads}(H_{UPD})$ versus $\theta_{H_{UPD}}$ relations for the three concentrations of H_2SO_4 and the data demonstrate that $\Delta H^{\circ}_{ads}(H_{UPD})$ varies from –27 to –46 kJ mol^{-1}. The $\Delta H^{\circ}_{ads}(H_{UPD})$ versus $\theta_{H_{UPD}}$ plots show two waves, the first one in the $0 - 0.45$ range of $\theta_{H_{UPD}}$ and the second one for $\theta_{H_{UPD}} > 0.45$; the enthalpy of adsorption

reaches a local minimum of some -40 or -45 kJ mol^{-1} (depending on the electrolyte concentration) at $\theta_{H_{UPD}} \cong 0.45$.

At this point of the discussion it is important to elaborate on the theoretical approach used in determination of $\Delta H^{\circ}_{ads}(H_{UPD})$ presented here and that applied by Breiter et al. [2,3,41] The theoretical methodology used by the present authors is based on Eq. 3 [20] whereas Breiter et al. determined $\Delta H^{\circ}_{ads}(H_{UPD})$ through application of the Gibbs-Helmholtz formula. The current authors also applied the latter approach and found that their results agreed to within 2 kJ mol^{-1}. Thus it ought to be emphasized that both the theoretical methodologies are applicable to determination of $\Delta H^{\circ}_{ads}(H_{UPD})$.

It is essential to assess whether the under-potential deposition of H on Pt electrodes is an enthalpy-driven or an entropy-driven process, an aspect that has never been investigated so far. Comparison of the experimentally determined values of $\Delta H^{\circ}_{ads}(H_{UPD})$ with the product $T\,\Delta S^{\circ}_{ads}(H_{UPD})$ for various H_{UPD} surface coverages reveals that $\left|\Delta H^{\circ}_{ads}(H_{UPD})\right| > \left|T\,\Delta S^{\circ}_{ads}(H_{UPD})\right|$, thus indicating the process in enthalpy-driven.

Determination of the $Pt-H_{UPD}$ Bond Energy, $E_{Pt-H_{UPD}}$. The energy of the $Pt-H_{UPD}$ bond, $E_{Pt-H_{UPD}}$, has never been evaluated, thus it is one of the most significant and new contributions presented in the paper. Knowledge of $E_{Pt-H_{UPD}}$ is essential for assessment of the strength of the forces acting between the Pt surface and the H_{UPD} adatom, and to appraisal of the surface adsorption site occupied by H_{UPD} on the basis of thermodynamic consideration. Moreover, evaluation of the $E_{Pt-H_{UPD}}$ versus $\theta_{H_{UPD}}$ relation is of importance in determination of the influence of the adsorbed anions, whose surface excess is potential dependent, [42-45] on the strength and nature of the $Pt-H_{UPD}$ bond, thus the impact of the electrified solid-liquid interface. The energy of the $Pt-H_{UPD}$ bond can be determined based on the experimentally calculated values of $\Delta H^{\circ}_{ads}(H_{UPD})$ for various $\theta_{H_{UPD}}$ (Figure 5). Appraisal of $E_{Pt-H_{UPD}}$ is based on the following theoretical treatment. The two single-electrode processes of the system are as follows:

working electrode: $\quad H^{+} + e + Pt \rightarrow Pt - H_{UPD}$ [4]

reference electrode: $\quad 1/2\,H_2 \rightarrow H^{+} + e$ [5]

and their summation gives the following total reaction:

$$1/2\,H_2 + Pt \xrightarrow{\Delta H^{\circ}_{ads}(H_{UPD})} Pt - H_{UPD} \qquad [6]$$

Addition of the two respective thermodynamic Born-Haber cycles for the two single-electrode processes leads to the following formula for the bond energy (details of this theoretical treatment is provided in ref. 20):

$$E_{Pt-H_{UPD}} = \frac{1}{2} D_{H_2} - \Delta H^{\circ}_{ads}(H_{UPD}) \qquad [7]$$

where D_{H_2} is the dissociation energy of the H_2 molecule and $D_{H_2} = 435.93$ kJ mol^{-1}. The authors evaluated $E_{Pt-H_{UPD}}$ in the three aqueous solutions of H_2SO_4 based on the experimental values of $\Delta H^{\circ}_{ads}(H_{UPD})$ and the results are shown in Figure 6. The data reveal that the values of $E_{Pt-H_{UPD}}$ fall in the $245-265$ kJ mol^{-1} range and that the variation of $E_{Pt-H_{UPD}}$ versus $\theta_{H_{UPD}}$ follows changes of $\Delta H^{\circ}_{ads}(H_{UPD})$ versus $\theta_{H_{UPD}}$ plot as expected on the ground of Eq. 7. The $Pt-H_{UPD}$ bond energy varies the most in the case of the 0.50 M H_2SO_4 electrolyte whereas in the case of the 0.05 and 0.10 M H_2SO_4 solutions the plots follow each other, however these differences are small and of the order of some 10 kJ mol^{-1}, thus some 4% of the value of $E_{Pt-H_{UPD}}$. At this preliminary stage, the dependence of $E_{Pt-H_{UPD}}$ on the concentration of H_2SO_4 is assigned to the anion interaction with the electrode surface and the water molecules at the solid/liquid interface. [42-45]

It is essential to elaborate on the two waves of the $\Delta H^{\circ}_{ads}(H_{UPD})$ versus $\theta_{H_{UPD}}$ and $E_{Pt-H_{UPD}}$ versus $\theta_{H_{UPD}}$ relations (Figures 5 and 6). Spectroscopic data from the laboratory of Bewick [25-27] lead to distinction of two kinds of adsorbed H: the weakly bonded H and the strongly bonded H; these two surface species interact with the substrate in a distinct manner giving rise to different physico-chemical properties as revealed by electroreflectance studies. The authors associate these two electroadsorbed H species with the two waves of the $\Delta H^{\circ}_{ads}(H_{UPD})$ versus $\theta_{H_{UPD}}$ and $E_{Pt-H_{UPD}}$ versus $\theta_{H_{UPD}}$ relations; the wave in the $0-0.45$ range of $\theta_{H_{UPD}}$ represents the strongly bonded H whereas that for $\theta_{H_{UPD}} > 0.45$ refers to the weakly bonded H.

It is fundamental to compare the values of $E_{Pt-H_{UPD}}$ to those for H_{chem} on well-defined Pt surfaces. The values of the $Pt-H_{chem}$ bond energy, $E_{Pt-H_{chem}}$, for H chemisorbed on three low-index surfaces, namely (111), (110) and (100) single-crystal faces [19] are 255, 243 and 247 kJ mol^{-1}, respectively. These data and the experimental results for $E_{Pt-H_{UPD}}$ indicate that the

bond energies for the electroadsorbed H and the chemisorbed H are very close to each other, say within some 10 kJ mol^{-1}. In the review article by Christmann [19], it is recognized that the values of the $M-H_{chem}$ bond energies, $E_{M-H_{chem}}$, for various transition metals fall into the $240-270$ kJ mol^{-1} range. It is also discussed that they do not differ much for various single-crystal faces of the transition metals. Proximity of the values of $E_{M-H_{chem}}$ and their relative independence of the surface geometry points to a similar surface binding mechanism on various transition metals. Thus one may conclude that the H_{chem} adatom is strongly embedded in the surface lattice of the metal substrate being coplanar with the topmost surface atoms of the metal substrate or that it penetrates into the metal surface lattice occupying sites between the first and the second surface layer. In the light of these observations and the experimentally determined values of $E_{Pt-H_{UPD}}$ the authors conclude that the binding mechanism between Pt and H_{UPD} involving the electrified double-layer is similar to that under the gas-phase conditions. In other words, the under-potential deposited H, H_{UPD}, might also be embedded in the surface lattice of Pt in a manner similar to that for the chemisorbed H. This conclusion coincides with the observation [25-27] that the H_{UPD} adsorbed on Pt electrodes is unavailable to form a bond with H_2O molecules in the double layer region. The authors wish to add that at this point of the development of the treatment presented in the paper, the specific interaction of H_{UPD} adatoms with co-adsorbed anions is not taken into account although the anion effect is observed through the concentration dependence of $\Delta G^{\circ}_{ads}(H_{UPD})$, $\Delta S^{\circ}_{ads}(H_{UPD})$, $\Delta H^{\circ}_{ads}(H_{UPD})$ and $E_{Pt-H_{UPD}}$. This aspect is presently under experimental investigation on Pt(111) and Pt(100).

CONCLUSIONS

1. Temperature-dependence of the UPD H on Pt electrodes in 0.05, 0.10 and 0.50 M aqueous H_2SO_4 solutions studied by cyclic-voltammetry followed by theoretical treatment allows determination of $\Delta G^{\circ}_{ads}(H_{UPD})$, $\Delta S^{\circ}_{ads}(H_{UPD})$ and $\Delta H^{\circ}_{ads}(H_{UPD})$; $\Delta G^{\circ}_{ads}(H_{UPD})$ varies from -11 to -25 kJ mol^{-1}, $\Delta S^{\circ}_{ads}(H_{UPD})$ from -40 to -90 J mol^{-1} K^{-1}, and $\Delta H^{\circ}_{ads}(H_{UPD})$ from -27 to -46 kJ mol^{-1}.

2. $\Delta G^{\circ}_{ads}(H_{UPD})$ increases towards less-negative values with the increasing H_{UPD} surface coverage, $\theta_{H_{UPD}}$, indicating that the lateral interactions between H_{UPD} adatoms are of the repulsive nature.

3. Knowledge of $\Delta H^{\circ}_{ads}(H_{UPD})$ leads to determination of the surface bond energy between Pt and H_{UPD}, $E_{Pt-H_{UPD}}$, which varies from 245 to 265 kJ mol^{-1}, depending on the

H_{UPD} surface coverage, $\theta_{H_{UPD}}$. The value of $E_{Pt-H_{UPD}}$ is within 10 kJ mol^{-1} of the bond energy between Pt and the H chemisorbed from the gas phase, H_{chem}, $E_{Pt-H_{chem}}$, which is in the $243-255$ kJ mol^{-1} range for the low-index single-crystal faces. Proximity of $E_{Pt-H_{UPD}}$ to $E_{Pt-H_{chem}}$ points to a similar binding mechanism under the conditions involving presence of the electrified solid/liquid interface and the gas-phase conditions. Closeness of $E_{Pt-H_{UPD}}$ to $E_{Pt-H_{chem}}$ leads to the important observation that H_{UPD} and H_{chem} are energetically equivalent surface species, thus H_{UPD} alike H_{chem} might be embedded in the surface lattice of the Pt substrate.

ACKNOWLEDGMENTS

Acknowledgment is made to the NSERC of Canada and the FCAR du Québec for support of this research. The authors thank Professor B. E. Conway of the University of Ottawa and Professor R. Parsons, FRS, of the University of Southampton for comments on thermodynamics of the electrified solid/liquid interface. They acknowledge discussion with Professor A. Lasia on the displacement of the thermodynamic reversible potential of the HER. A. Zolfaghari acknowledges a graduate fellowship from the MCHE of Iran. M. Chayer conducted this research as her B.Sc. last term project.

REFERENCES

1. F. G. Will and C. A. Knorr, *Z. Electrochem.*, **64**, 258; 270 (1960); see also F. G. Will, *J. Electrochem. Soc.*, **112**, 451 (1965).

2. W. Boeld and M. W. Breiter, *Z. Elektrochem.*, **64**, 897 (1960); see also M. W. Breiter and B. Kennel, *Z. Elektrochem.*, **64**, 1180 (1960).

3. M. W. Breiter, in *Transactions of the Symposium on Electrode Processes*, Ed. E. Yeager, John Wiley and Sons, New York (1961); see also M. W. Breiter, *Electrochim. Acta.*, 7, 25 (1962); M. W. Breiter, *Ann. N. Y. Acad. Sci.*, **101**, 709 (1963); M. W. Breiter, *Electrochemical Processes in Fuel Cells*, Springer-Verlag, New York (1969).

4. A. N. Frumkin, in *Advances of Electrochemistry and Electrochemical Engineering*, Ed. P. Delahey, Vol. 3, p. 287, Interscience Publishers, New York (1963).

5. R. Woods, in *Electroanalytical Chemistry*, Ed. A. Bard, Vol. 9, p. 27, Marcel Dekker, New York (1977).

6. B. E. Conway, *Theory and Principles of Electrode Processes*; Ronald Press, London (1965).

7. M. Enyo, in *Modern Aspects of Electrochemistry*, Eds. B. E. Conway and J. O'M. Bockris, Vol. 11, p. 251, Plenum Press, New York (1975).
8. M. Enyo, in *Comprehensive Treatise of Electrochemistry*, Eds. B. E. Conway and J. O'M. Bockris, Vol. 7, p. 241, Plenum Press, New York (1983).
9. B. E. Conway, H. Angerstein-Kozlowska and H. P. Dhar, *Electrochim. Acta*, **19**, 455 (1974).
10. B. E. Conway and H. Angerstein-Kozlowska, *Acc. Chem. Res.*, **14**, 49 (1981).
11. B. E. Conway, H. Angerstein-Kozlowska and F. C. Ho, *J. Vac. Sci. Technol.*, **14**, 351 (1977).
12. B. E. Conway, H. Angerstein-Kozlowska and W. B. A. Sharp, *J. Chem. Soc., Faraday Trans. I*, **74**, 1373 (1978).
13. B. E. Conway, *Sci. Prog. Oxf.*, **71**, 479 (1987); see also B. E. Conway and L. Bai, *J. Electroanal. Chem.*, **198**, 149 (1986).
14. M. Baldauf and D. M. Kolb, *Electrochim. Acta*, **38**, 2145 (1993).
15. B. E. Conway, and G. Jerkiewicz, *Electroanal. Chem.*, **357**, 47 (1993); see also G. Jerkiewicz, J. J. Borodzinski, W. Chrzanowski and B. E. Conway, B. E. *J. Electrochem. Soc.*, **142**, 3755 (1995).
16. B. E. Conway and G. Jerkiewicz, *Z. Phys. Chem. Bd.*, **183**, 281 (1994).
17. Eds. G. Alefeld and J. Volkl, *Hydrogen in Metals*, Parts I and II; Springer-Verlag, New York (1978).
18. Ed. L. Schlapbach, *Hydrogen in Intermetalic Compounds*; Part I, Springer-Verlag, New York (1988); Part II, Springer-Verlag, New York (1992).
19. K. Christman, *Surface Sci. Rep.*, **9**, 1 (1988).
20. G. Jerkiewicz and A. Zolfaghari, *J. Electrochem. Soc.*, **143**, 1240 (1996); G. Jerkiewicz and A. Zolfaghari, *J. Phys. Chem.*, **100**, 8454 (1996).
21. J. McBreen, *J. Electroanal. Chem.*, **287**, 279 (1990).
22. J. W. Schultze and K. J. Vetter, *J. Electroanal. Chem.*, **44**, 63 (1973).
23. K. J. Vetter and G. P. Klein, Z. Elektrochem., **66**, 760 (1962).
24. E. Gileadi, *Electrode Kinetics*, VCH Publishers, Inc., New York (1993).
25. A. Bewick and A. M. Taxford, *J. Electroanal. Chem.*, **47**, 255 (1973); see also A. Bewick and J. W. Russell, *J. Electroanal. Chem.*, **132**, 329 (1982).
26. A. Bewick and J. W. Russell, *J. Electroanal. Chem.*, **142**, 337 (1982).
27. R. J. Nichols and A. Bewick, *J. Electroanal. Chem.*, **243**, 445 (1988).

28. E. Protopopoff and P. Marcus, *J. Vac. Sci. Technol. A*, **5**, 944 (1987); see also *C. R. Acad. Sci. Paris,* **t 308**, Serie II, 1127 (1989).
29. E. Protopopoff and P. Marcus, *J. Chim. Phys.*, **88**, 1423 (1991).
30. H. Angerstein-Kozlowska, B. E. Conway and W. B. A. Sharp, *J. Electroanal. Chem.*, **43**, 9 (1973).
31. H. Angerstein-Kozlowska, in *Comprehensive Treatise of Electrochemistry*, Eds. E. Yeager, J. O'M. Bockris, B. E. Conway and S. Sarangapani, Vol. 9, p. 15, Plenum Press, New York (1984).
32. B. E. Conway, W. B. A. Sharp, H. Angerstein-Kozlowska and E. E. Criddle, *Anal. Chem.*, **41**, 1321 (1973).
33. G. Tremiliosi-Filho, G. Jerkiewicz and B. E. Conway, *Langmuir*, **8**, 658 (1992).
34. G. Jerkiewicz, G. Tremiliosi-Filho and B. E. Conway, *J. Electroanal. Chem.*, **334**, 359 (1992).
35. B. E. Conway, G. Tremiliosi-Filho and G. Jerkiewicz, *J. Electroanal. Chem.*, **297**, 435 (1991).
36. G. Jerkiewicz and J. J. Borodzinski, *Langmuir*, **9**, 2202 (1993).
37. G. A. Somorjai, A. *Introduction to Surface Chemistry and Catalysis*, John Wiley and Sons, Inc., New York (1994).
38. I. Langmuir, *J. Am. Chem. Soc.*, **40**, 1361 (1918).
39. R. H. Fowler and F. A. Guggenheim, *Statistical Thermodynamics*, Cambridge University Press, London (1939).
40. A. W. Adamson, *Physical Chemistry of Surfaces*, John Wiley and Sons, New York (1990).
41. M. Breiter, *Trans. Faraday. Soc.*, **64**, 1445 (1964).
42. A. Wieckowski, in *Electrochemical Interfaces*, Ed. H. Abruña, p. 65, VCH, New York (1991); and refs. therein.
43. A. Wieckowski, in *Adsorption of Molecules at Metal Electrodes*, Eds. J. Lipkowski and P. N. Ross, p. 119, VCH, New York (1992); and refs. therein.
44. Z. Shi, S. Wu and J. Lipkowski, *Electrochim. Acta*, **40**, 9 (1995); Z. Shi, S. Wu and J. Lipkowski, *J. Electroanal. Chem.*, **384**, 171 (1995).
45. B. E. Conway, *Electrochim. Acta*, **40**, 1501 (1995).

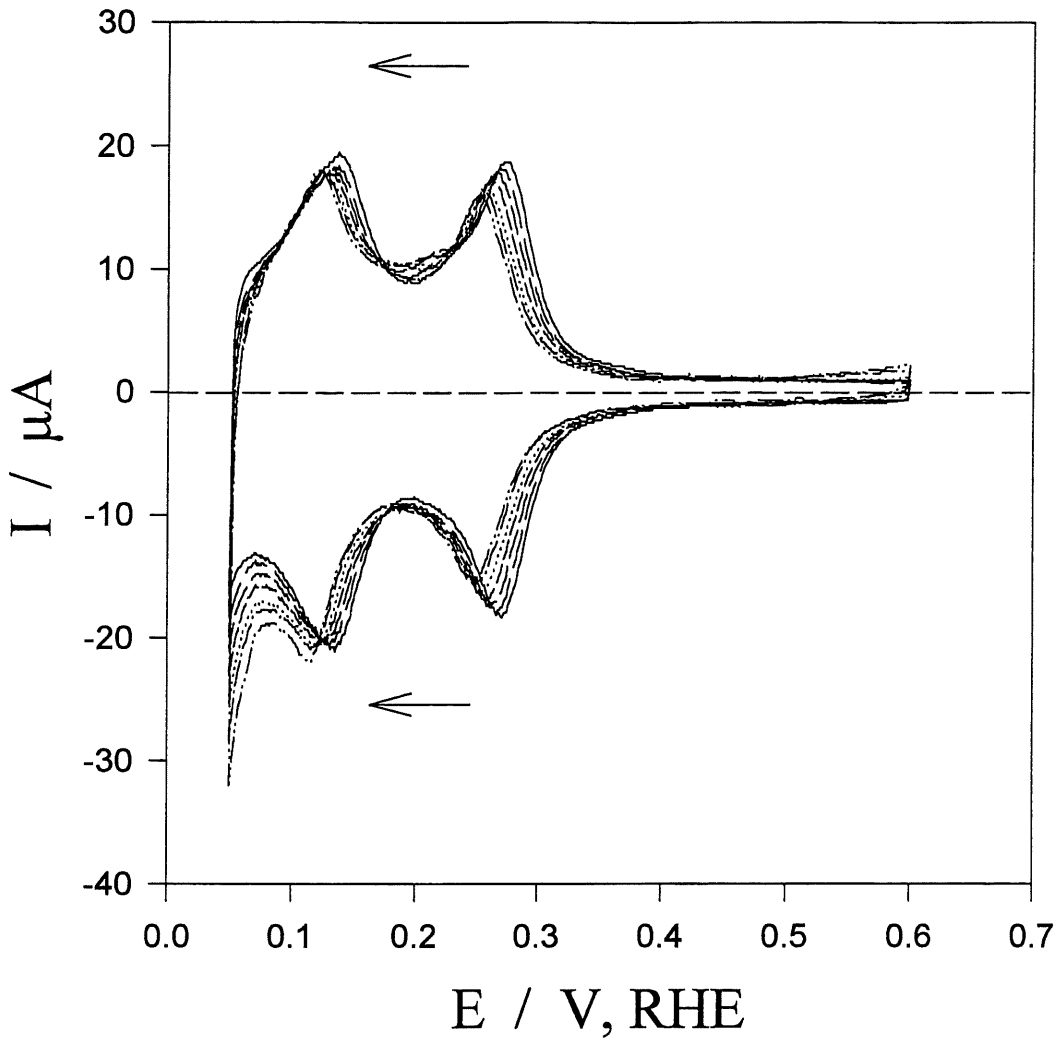

Figure 1. Series of the cyclic-voltammetry (CV) profiles for the under-potential deposition of H (UPD H) on Pt from 0.50 M aq. H_2SO_4 solution for a temperature range between 273 and 343 K, with an interval of 10 K, and recorded at the sweep rate $s = 20\ mV\ s^{-1}$; the electrode surface area $A_r = 0.720 \pm 0.005\ cm^2$. The arrows indicate changes in the adsorption and desorption profiles upon the temperature increase.

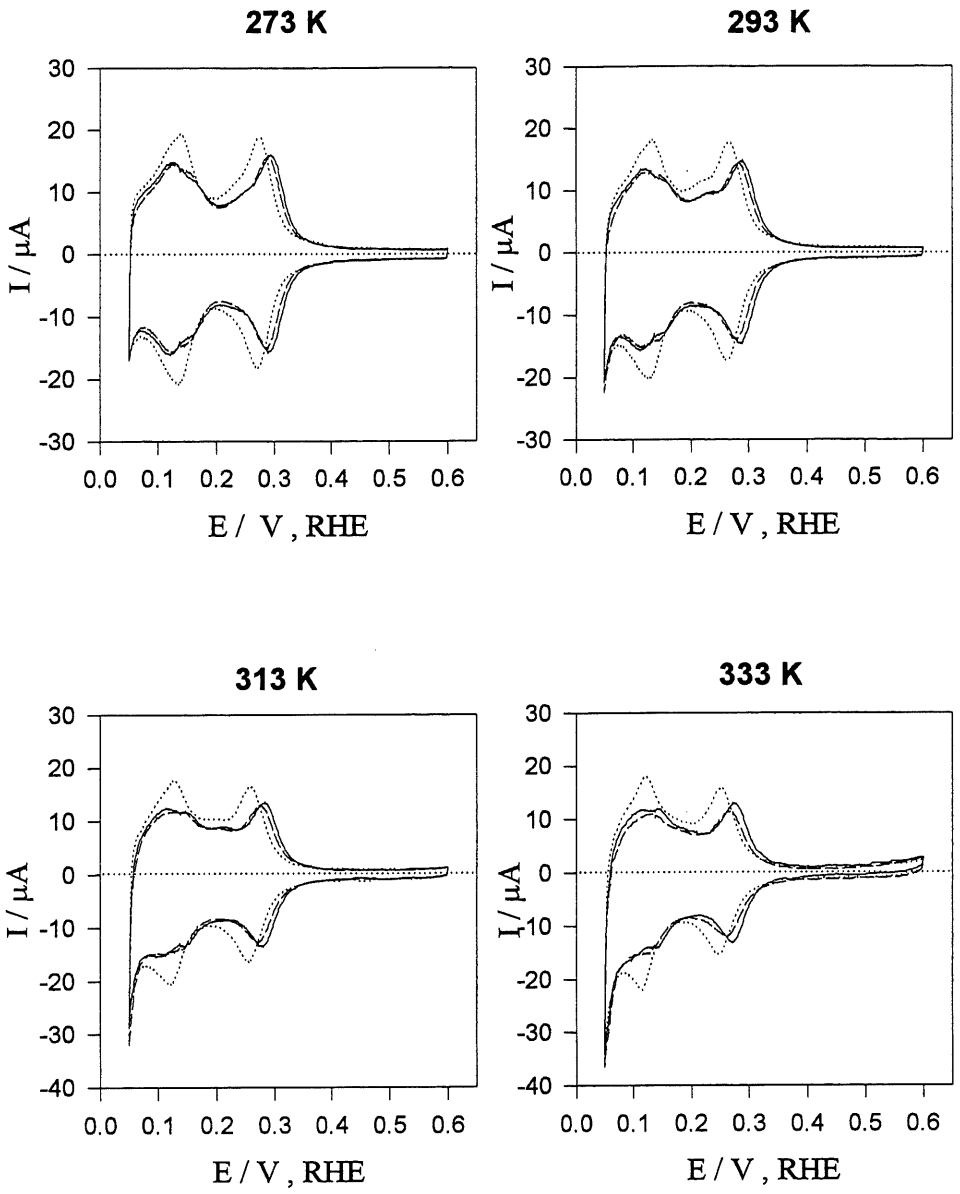

Figure 2. Four sets of cyclic-voltammetry (CV) profiles for the under-potential deposition of H (UPD H) on Pt from 0.05, 0.10 and 0.50 M aq. H_2SO_4 solutions at four different temperatures, 273, 293, 313 and 333 K; the sweep rate $s = 20\ mV\ s^{-1}$; the electrode surface area $A_r = 0.720 \pm 0.005\ cm^2$. The CV profiles reveal redistribution of the adsorption and desorption charges upon the temperature and concentration variation. Upon the concentration decrease, the adsorption and desorption peaks becomes less pronounced; solid line 0.05 M aq. H_2SO_4; dashed line 0.10 M aq. H_2SO_4; dotted line 0.50 M aq. H_2SO_4.

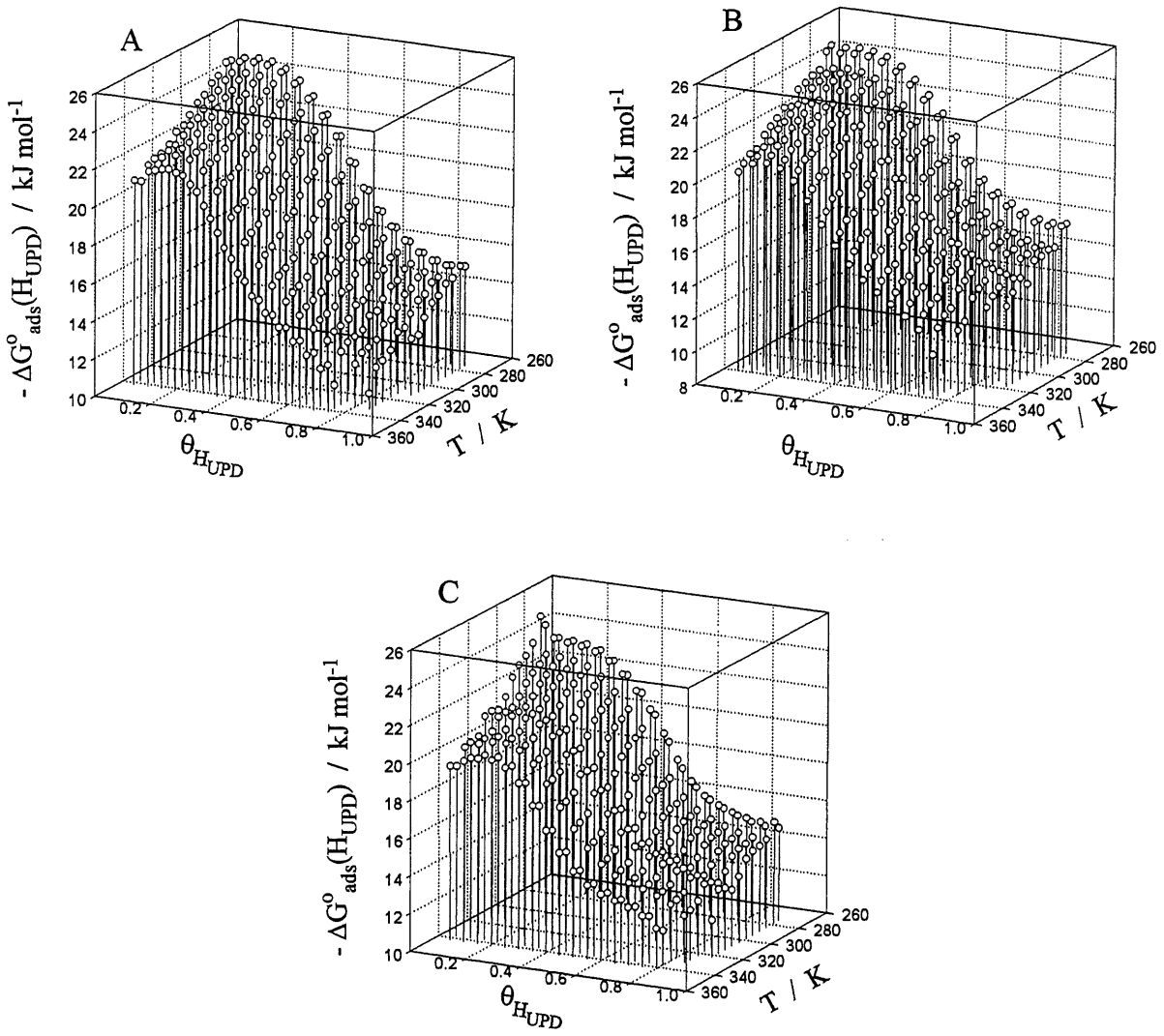

Figure 3. 3D plots showing the Gibbs free energy of adsorption of H_{UPD} on Pt, $\Delta G^{\circ}_{ads}(H_{UPD})$ versus $\theta_{H_{UPD}}$ and T, $\Delta G^{\circ}_{ads}(H_{UPD}) = f(\theta_{H_{UPD}}, T)$, from 0.05, 0.10 and 0.50 M aq. H_2SO_4 solutions; $\Delta G^{\circ}_{ads}(H_{UPD})$ has values between −11 and −25 kJ mol^{-1} depending on $\theta_{H_{UPD}}$ and T; $\Delta G^{\circ}_{ads}(H_{UPD})$ reaches the most negative values at the lowest temperature and the smallest H_{UPD} surface coverage, $\theta_{H_{UPD}}$. Increase of $\Delta G^{\circ}_{ads}(H_{UPD})$ with $\theta_{H_{UPD}}$ for T = const points to the repulsive nature of lateral interactions between H_{UPD} adatoms. (**A**) 0.05 M H_2SO_4, (**B**) 0.10 M H_2SO_4, (**C**) 0.50 M H_2SO_4. The experimental error of $\Delta G^{\circ}_{ads}(H_{UPD})$, $\delta\,\Delta G^{\circ}_{ads}(H_{UPD})$, is ± 1 kJ mol^{-1}.

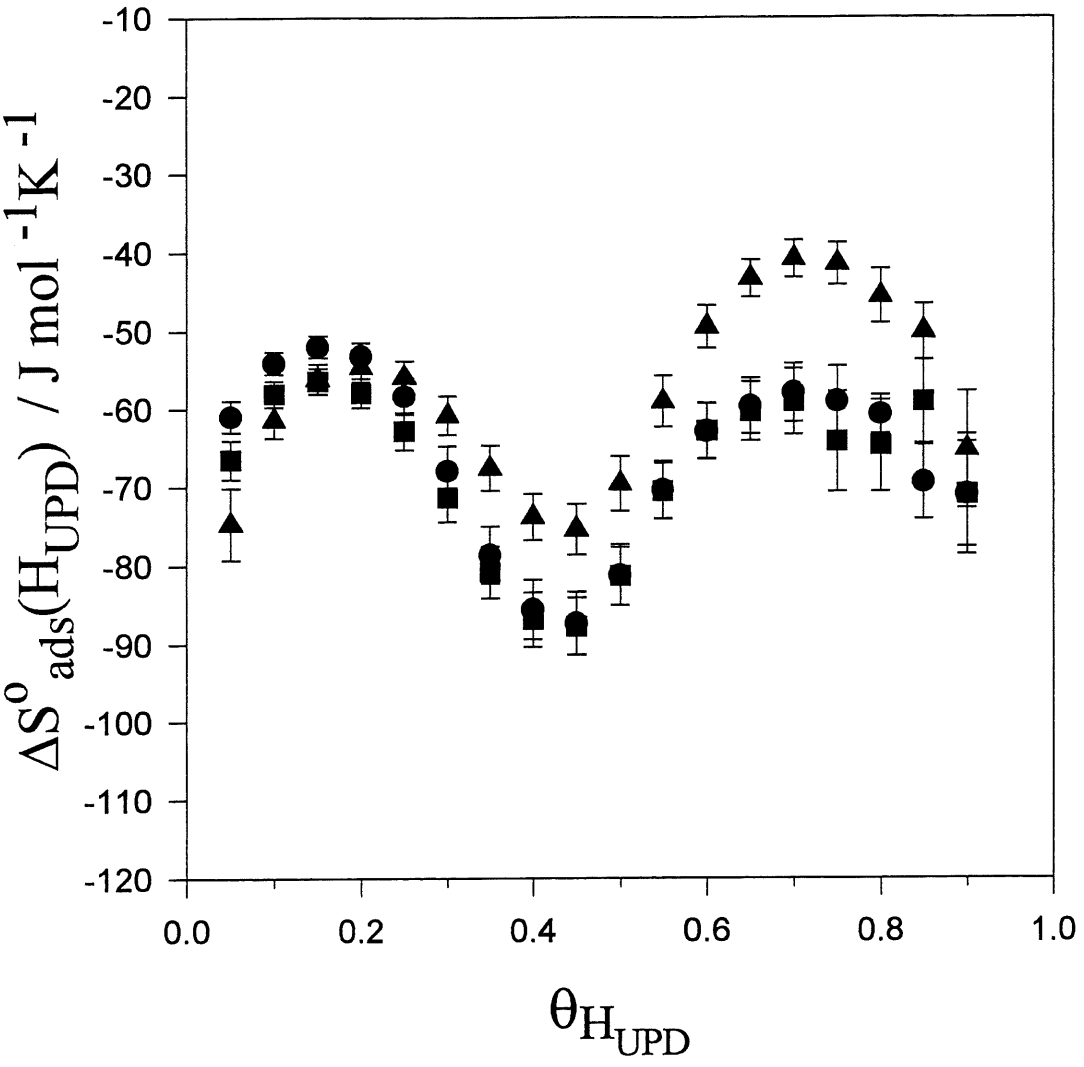

Figure 4. $\Delta S^{\circ}_{ads}(H_{UPD})$ versus $\theta_{H_{UPD}}$ relations for the under-potential deposition of H on Pt from 0.05, 0.10 and 0.50 M aq. H_2SO_4 solutions; the relations reveal two waves with a local minimum at $\theta_{H_{UPD}} = 0.45$; $\Delta S^{\circ}_{ads}(H_{UPD})$ has the least-negative values in 0.50 M aq. H_2SO_4 solution and at large values of the H_{UPD} surface coverage, $\theta_{H_{UPD}}$; the $\Delta S^{\circ}_{ads}(H_{UPD})$ versus $\theta_{H_{UPD}}$ plots for H adsorption from 0.05 and 0.10 M aq. H_2SO_4 solutions almost follow each other throughout the whole H_{UPD} surface coveragerange. ● refers to 0.05 M aq H_2SO_4, ■ refers to 0.10 M aq H_2SO_4, and Δ refers to 0.50 M aq H_2SO_4.

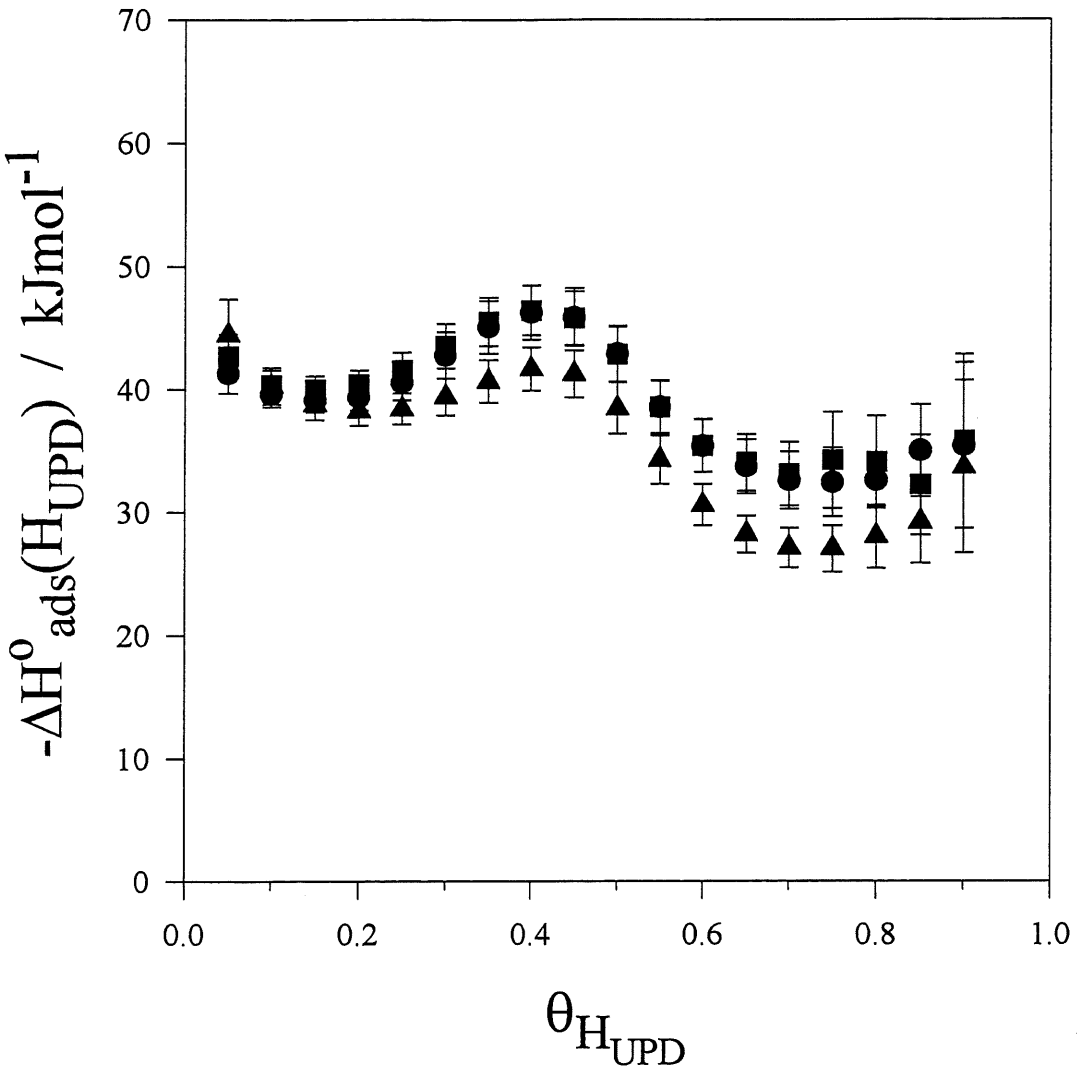

Figure 5. $\Delta H^{\circ}_{ads}(H_{UPD})$ versus $\theta_{H_{UPD}}$ relations for the under-potential deposition of H from 0.05, 0.10 and 0.50 M aq. H_2SO_4 solutions; $\Delta H^{\circ}_{ads}(H_{UPD})$ reveals two waves and it has more negative values for $0 < \theta_{H_{UPD}} < 0.45$; the $\Delta H^{\circ}_{ads}(H_{UPD})$ versus $\theta_{H_{UPD}}$ relations for H adsorption from 0.05 and 0.10 M aq. H_2SO_4 solutions almost follow each other throughout the whole H_{UPD} surface coverage range. ● refers to 0.05 M aq H_2SO_4, ■ refers to 0.1 M aq H_2SO_4, and Δ refers to 0.5 M aq H_2SO_4.

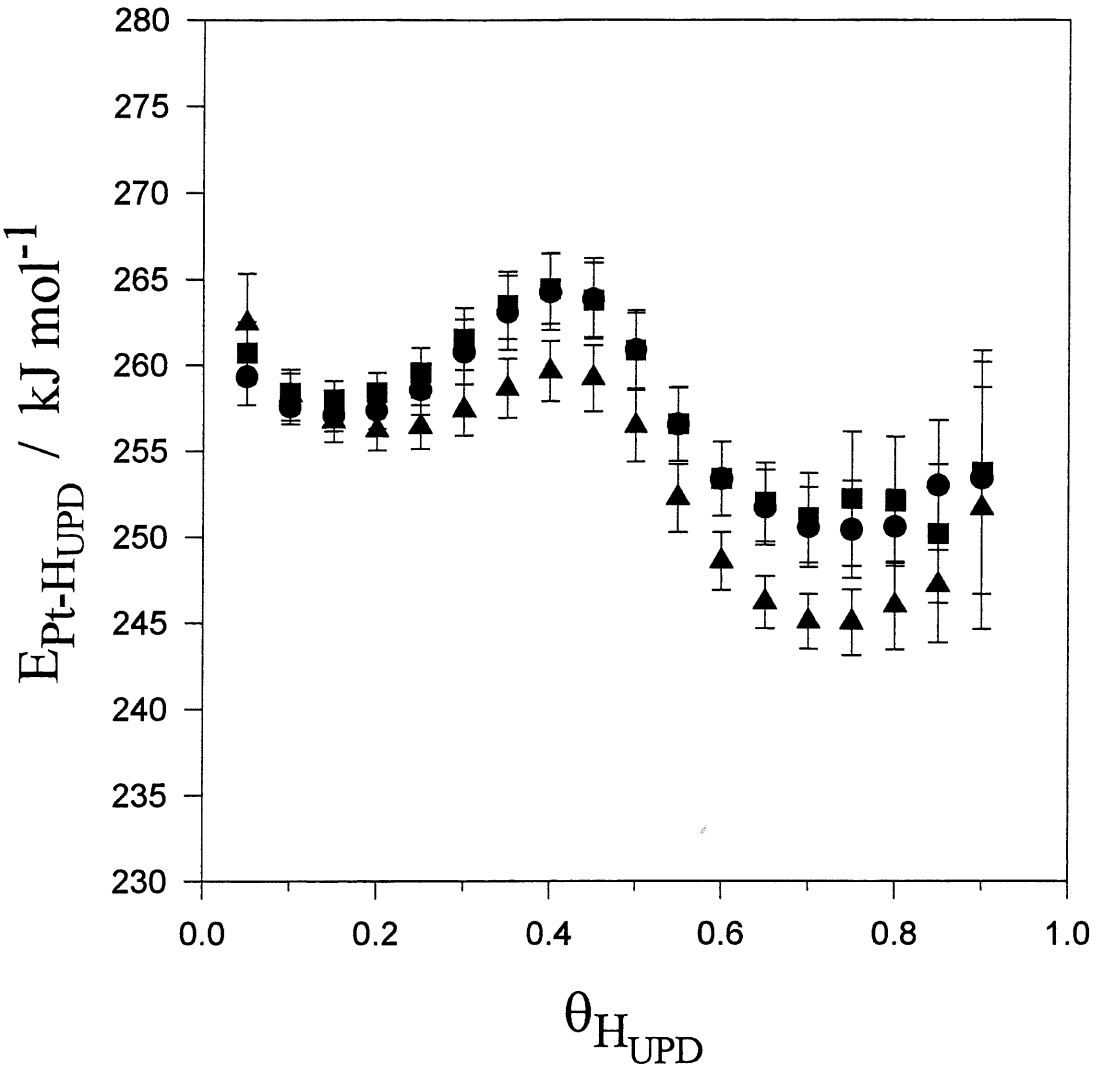

Figure 6. $E_{Pt-H_{UPD}}$ versus $\theta_{H_{UPD}}$ relations for the under-potential deposited H from 0.05, 0.10 and 0.50 M aq. H_2SO_4 solutions; $E_{Pt-H_{UPD}}$ has values between 245 and 265 kJ mol^{-1}; the variation of $E_{Pt-H_{UPD}}$ versus $\theta_{H_{UPD}}$ follows the changes of $\Delta H^{\circ}_{ads}(H_{UPD})$ as expected on the basis of Eq. 7, $E_{Pt-H_{UPD}} = 1/2D_{H_2} - \Delta H^{\circ}_{ads}(H_{UPD})$. ● refers to 0.05 M aq H_2SO_4, ■ refers to 0.1 M aq H_2SO_4, and Δ refers to 0.5 M aq H_2SO_4.

2.2 HYDROGEN ADSORPTION ON Pt AND Rh ELECTRODES AND BLOCKING OF ADSORPTION SITES BY CHEMISORBED SULFUR

A. Zolfaghari, F. Villiard, M. Chayer and G. Jerkiewicz, J. Alloys and Comp., 235, 481 (1997)

ABSTRACT

Research on the under-potential deposition of H, UPD H, on Pt and Rh electrodes in aqueous H_2SO_4 solution at temperatures between 273 and 343 K by cyclic-voltammetry, CV, followed by theoretical treatment leads to determination of ΔG°_{ads}, ΔS°_{ads} and ΔH°_{ads} and the bond energy between the metal substrate, M, and H_{UPD}, $E_{M-H_{UPD}}$. Knowledge of $E_{M-H_{UPD}}$ results in elucidation of the surface adsorption site of H_{UPD} based on thermodynamic deliberation. The UPD H on Pt can be completely suppressed by a monolayer, ML, of chemisorbed S, S_{chem}, or partially by submonolayers of S_{chem} having their surface coverage less than 0.33, $\theta_S < 0.33$. A submonolayer of S_{chem} having $\theta_S = 0.10$ affects ΔG°_{ads}, ΔS°_{ads} and ΔH°_{ads} as well as the $Pt-H_{UPD}$ bond energy, $E_{Pt-H_{UPD}}$, which becomes weaker in presence of the S_{chem} submonolayer than in its absence. The lateral interactions between H_{UPD} and S_{chem} are brought about by local electron withdrawing effects that propagate through the underlying metal which acts as a mediator.

1. INTRODUCTION

In recent years the electrochemical surface science of hydrogen, H, has been undergoing renewed interest due to application of metal-hydride batteries and hydrogen-based fuel cells as power sources for emission-free electric vehicles, EV [1-12]. Hydrogen absorption into host metals can be accomplished either by electrochemical or gas-phase techniques. In electrochemistry, two types of adsorbed H are recognized: (i) the under-potential deposited H, H_{UPD}; and (ii) the over-potential deposited H, H_{OPD} [13]. The species occupy distinct surface adsorption sites and both can undergo entry into the host metal becoming absorbed H, H_{abs} [14]. In the case of charging at high negative potentials H absorption and the hydrogen evolution reaction, HER, occur concurrently and the amount of H_{abs} can be related to the overpotential, η, of the HER and the mechanism of the process [15-18]. It is recognized that certain elements or compounds adsorbed on the metal surface and referred to as *site blocking elements*, SBE, possess the ability of enhancing or decreasing the H transfer from the *adsorbed* to the *absorbed* state [8,17,19-21]. The SBE's chemisorbed on the metal surface reveal a *dual action* and behave either as *surface poisons* or as *surface promoters* depending on their physico-chemical nature [17]. The surface promoters can effectively enhance the rate of H interfacial transfer and increase the amount of H absorbed in the host metal, thus increasing its capacity. The latter is of vital importance to high energy-density M-H batteries which are an alternative to the Ni-Cd ones. On the other, hand surface

poisons which suppress the H interfacial transfer are excellent inhibitors of H embrittlement of metal structures. Experimental evidence indicates that chemical species such as CO, urea, thiourea, compounds of As, Se, S and P as well as heterocycles are known to affect the adsorption of H in the region corresponding to the under-potential deposition of H, UPD H, and the kinetics of the HER [19-24]. Their action was a subject of thorough theoretical research and numerical simulations based on the lateral interactions between the electroadsorbed H and the coadsorbed SBE's [17]. SBE's affect catalytic properties of the electrified solid/liquid interface through the following action: (i) they can block surface adsorption sites; (ii) they affect energetics of the reaction at the double-layer; (iii) they change the work function of the substrate; (iv) they influence the charge transfer at the electrode/solution interface; and (v) they affect adsorption behavior of the reaction products and intermediates. Sulfur, S, is of vital interest to electrochemical surface science, metal hydride science and technology, and corrosion science because it is a model SBE. The species undergoes strong chemisorption and sustains its chemical identity on the metal electrode surface. Cathodic polarization does not lead to its desorption through formation of a reduced derivative and it can be desorbed only through oxidation at high positive potentials [25,26].

In this paper, the authors present new thermodynamic data the UPD H which lead to elucidation of the surface adsorption sites of H_{UPD} on Pt and Rh electrodes. They also present results on S chemisorption on Pt electrodes and its influence on the UPD H. They determine a relation between the S surface coverage, θ_S, and the coverage by H_{UPD}, $\theta_{H_{UPD}}$. Temperature dependence experimental studies followed by comprehensive theoretical treatment result in determination of ΔG°_{ads}, ΔS°_{ads} and ΔH°_{ads} in absence and presence of S. They evaluate changes of the $Pt-H_{UPD}$ bond energy brought by the S submonolayer.

2. EXPERIMENTAL DETAILS

The Pt and Rh electrode preparation procedure and the electrochemical cell applied were identical to those described elsewhere [13,24,25,27,28]. The 0.5 M aqueous H_2SO_4 solution was prepared from BDH Aristar grade H_2SO_4 and Nanopure water. The cell was immersed in a water bath (Haake W13) and the temperature was controlled to within ± 0.5 K by means of a thermostat (Haake D1). The temperature in the bath and the cell was controlled by means of thermometers and a K-type thermocouple (80 TK Fluke) and were found to agree to within ± 0.5 K. The experimental procedure applied in this project involved standard cyclic-voltammetry, CV, measurements of the UPD H on Pt and Rh electrodes at

temperatures between 273 and 343 K with an interval of 5 K. The instrumentation included: (a) EG&G Model 263A potentiostat-galvanostat; (b) IBM-compatible 80386, 40 MHz computer; and (c) EG&G M270 Electrochemical Software. All potentials were measured with respect to the reversible hydrogen electrode, RHE, immersed in the same electrolyte. The potential of the RHE differed from that of the normal hydrogen electrode, NHE, and according to the Nernst equation zero potential on the RHE scale corresponded to −0.021 on the NHE one.

Formation of a monolayer of chemisorbed S, S_{chem}, on Pt was accomplished by electrode immersion in 0.01 M aqueous Na_2S (Aldrich) solution followed by rinsing in Nanopure water. Appraisal of influence of S_{chem} on the H adsorption behavior was accomplished by recording CV profiles in the potential regions corresponding to UPD H and the surface oxide formation.

3. RESULTS AND DISCUSSION

3.1 Temperature Dependence and Thermodynamics of the UPD H

Fig. 1 shows a series of CV adsorption-desorption for the UPD H on Pt and Rh from 0.5 M aqueous H_2SO_4 solution for temperature between 273 and 343 K with an interval of 10 K recorded at the sweep rate of 20 mV s^{-1} (experiments were conducted with an interval of 5 K but in order not to obscure the graphs fewer experimental curves are shown). Both metals have different cyclic-voltammograms (CV's), namely Pt reveals two peaks whereas Rh only one. The CV's show that the adsorption-desorption peaks shift towards less-positive potentials upon the temperature increase and that they are symmetric with respect to the potential axis indicating reversibility of the surface process. An increase of the cathodic current at the lower potential limit of the CV's, thus prior to the sweep reversal, is due to the onset of the over-potential deposition of H, OPD H. The UPD H adsorption-desorption behavior may be summarized as follows: (i) the temperature increase shifts the UPD H adsorption-desorption CV's towards less-positive values; (ii) no new features are observed in the CV's that could result from the temperature increase. Theoretical treatment of the experimental data based on eq. (1) allows determination of the Gibbs free energy of adsorption, $\Delta G^{\circ}_{ads}(H_{UPD})$, as a function of the H_{UPD} surface coverage, $\theta_{H_{UPD}}$, and temperature, T, thus 3D $\Delta G^{\circ}_{ads}(H_{UPD})$ versus $\left(\theta_{H_{UPD}}, T\right)$ plots [14,24].

$$\frac{\theta_{H_{UPD}}}{1-\theta_{H_{UPD}}} = P_{H_2}^{1/2} \exp\left(-\frac{E F}{R T}\right) \exp\left(-\frac{\Delta G^{\circ}_{ads}(H_{UPD})}{R T}\right) \qquad (1)$$

where $\Delta G^{\circ}_{ads}(H_{UPD})$ includes a coverage-dependent parameter, $\omega(\theta_{H_{UPD}})$, which describes their lateral interactions, thus $\Delta G^{\circ}_{ads}(H_{UPD})_{\theta_{H_{UPD}} \neq 0} = \Delta G^{\circ}_{ads}(H_{UPD})_{\theta_{H_{UPD}}=0} + \omega(\theta_{H_{UPD}})$, $P_{H_2}^{1/2}$ is the partial pressure of H_2 in the reference electrode compartment, E is the experimentally measured potential difference between the working electrode and the reference electrode immersed in the same solution, thus the potential, E, measured versus the RHE, and R and F are physico-chemical constants. The results of these calculations are shown in Fig. 2 and they indicate that in the case of Pt $\Delta G^{\circ}_{ads}(H_{UPD})$ has values between −25 and −12 kJ mol^{-1} and in case of Rh $\Delta G^{\circ}_{ads}(H_{UPD})$ has values between −17 and −8 kJ mol^{-1}. Thus it may be concluded that the driving force of the UPD H on Pt is larger than in the case of Rh. In both cases $\Delta G^{\circ}_{ads}(H_{UPD})$ has the most-negative values at the lowest T and the smallest $\theta_{H_{UPD}}$. For a given T, $\Delta G^{\circ}_{ads}(H_{UPD})$ increases with $\theta_{H_{UPD}}$ indicating that the lateral interactions between the H_{UPD} adatoms are predominantly of the repulsive nature [29-32]. Because the slope of these relations are a measure of the strength of the lateral interactions, it may be concluded (Fig. 2) that the lateral repulsions between the H_{UPD} adatoms are stronger on Pt than on Rh. The $\Delta G^{\circ}_{ads}(H_{UPD})$ versus T relations for a given $\theta_{H_{UPD}}$ are linear and allow determination of the entropy of adsorption, $\Delta S^{\circ}_{ads}(H_{UPD})$, based on eq. (2):

$$\Delta S^{\circ}_{ads}(H_{UPD}) = -\left[\frac{\partial \Delta G^{\circ}_{ads}(H_{UPD})}{\partial T}\right]_{\theta_{H_{UPD}} = const} \qquad (2)$$

The results shown in Fig. 3 indicate that $\Delta S^{\circ}_{ads}(H_{UPD})$ has values between −80 and −41 J mol^{-1} K^{-1} for Pt and between −126 and −29 J mol^{-1} K^{-1} for Rh, thus $\Delta S^{\circ}_{ads}(H_{UPD})$ is more negative for Rh than for Pt. In the case of Pt, the $\Delta S^{\circ}_{ads}(H_{UPD})$ versus $\theta_{H_{UPD}}$ relation reveals two waves which can be associated with the two CV peaks whereas in the case of Rh $\Delta S^{\circ}_{ads}(H_{UPD})$ increases monotonously towards less-negative values. The enthalpy of adsorption, $\Delta H^{\circ}_{ads}(H_{UPD})$, is readily determined based on the experiment values of $\Delta G^{\circ}_{ads}(H_{UPD})$ and $\Delta S^{\circ}_{ads}(H_{UPD})$ and the well-known formula $\Delta G^{\circ} = \Delta H^{\circ} - T\,\Delta S^{\circ}$. The results shown in Fig. 4 demonstrate that $\Delta H^{\circ}_{ads}(H_{UPD})$ has values between −46 and −27 kJ mol^{-1} for Pt and between −52 and −21 kJ mol^{-1} for Rh and that changes of $\Delta H^{\circ}_{ads}(H_{UPD})$ versus $\theta_{H_{UPD}}$

are more pronounced for Rh than for Pt. Finally, knowledge of $\Delta H^{\circ}_{ads}(H_{UPD})$ leads to evaluation of the bond energy between the metal substrate, M (here M is Pt or Rh), and H_{UPD}, $E_{M-H_{UPD}}$, based on eq. (3):

$$E_{M-H_{UPD}} = \frac{1}{2}D_{H_2} - \Delta H^{\circ}_{ads}(H_{UPD}) \qquad (3)$$

where D_{H_2} is the dissociation energy of the hydrogen molecule and $D_{H_2} = 436$ kJ mol^{-1}. Such determined values of $E_{Pt-H_{UPD}}$ and $E_{Rh-H_{UPD}}$ as a function of $\theta_{H_{UPD}}$ are shown in Fig. 5 and they demonstrate that $E_{Pt-H_{UPD}}$ is between 245 and 264 kJ mol^{-1} and those of $E_{Rh-H_{UPD}}$ between 239 and 270 kJ mol^{-1}. The values of $E_{Pt-H_{UPD}}$ and $E_{Rh-H_{UPD}}$ fall close to those for the bond between Pt or Rh and chemisorbed H, H_{chem}, which are $243 \le E_{Pt-H_{chem}} \le 255$ kJ mol^{-1} and $E_{Rh-H_{chem}} = 255$ kJ mol^{-1}, respectively [33]. Proximity of these values leads to the conclusion that H_{chem} and H_{UPD} are thermodynamic equivalents. Subsequently, if $M-H_{UPD}$ and $M-H_{chem}$ bond energies are close to each other, then it is rational to conclude that H_{UPD} occupies the same surface adsorption site as H_{chem} thus that it is embedded in the surface lattice of the metal substrate.

3.2 Sulfur Chemisorption on Pt Electrodes

A layer of chemisorbed S, S_{chem}, on Pt was formed by its immersion in 0.01 M aqueous Na_2S solution. The surface coverage of such a formed S_{chem} layer was 1.2; it exceeded the value of unity because the electrode was of polycrystalline nature and on the average more S_{chem} atom were adsorbed at the grain boundaries and surface imperfections resulting in the S/Pt ration greater than unity. This layer of S_{chem} suppressed completely the UPD H on Pt [19,20] as it was revealed by CV measurements (Fig. 6). Coupled FTIR, AES, CEELS and electrochemical measurements [25,26,34,35] indicate that S_{chem} is in its atomic form, thus it is not bonded to the surface in the form of S oxides or sulfides. The S_{chem} layer can be removed by the electrode cycling into the oxide formation region [36,37], thus it may be concluded that the surface oxidation and the S_{chem} oxidative desorption overlap. Complete removal of the S_{chem} layer cannot be accomplished within one CV and it requires several cycles (Fig. 6). FTIR and UHV data [25,26,38] indicate that the oxidative desorption of S_{chem} at $E \ge 1.1$ V, RHE, results in formation of sulfate and its desorption:

$$S_{chem} + 4H_2O \xrightarrow{E \geq 1.1\,V} SO_4^{2-} + 8H^+ + 6e \qquad (4)$$

Because the Pt surface oxidation commences at 0.85 V, RHE, and the oxidative desorption of S_{chem} at $E \geq 1.1$ V, RHE, the total anodic charge equals $q_{AN(i)} = q_{OX(i)} + q_{S(i)}$ ($q_{OX(i)}$ is the charge of oxide formation, $q_{S(i)}$ is the charges of S_{chem} desorption and the subscript *i* represents the *i-th cycle*). The cathodic charge $q_{CATH(i)}$, at $0.5 \leq E \leq 1.2$ V, RHE, corresponds to reduction of the surface oxide film [35]. Clearly, their difference for every CV allows one to evaluate the charge of the sulfur oxidative desorption per cycle, $q_{S(i)}$. Summation of these charges for all CV's leads to precise determination of the overall charge of the S_{chem} oxidative desorption, $q_S = \sum q_{S(i)}$, and when divided by the number of electrons transferred during the oxidation, it results in the total number of S_{chem} adatoms on the Pt electrode prior to the oxidative desorption.

$$N_S = \frac{q_S}{6e} \qquad (5)$$

An analysis of the CV's (Fig. 6) allows one to establish a relation between the H_{UPD} surface coverage, $\theta_{H_{UPD}}$, the S_{chem} surface coverage, θ_S, and the surface oxide coverage, θ_O, with respect to the number of cycles for the S_{chem} oxidative desorption (Fig. 7). Examination of the results leads to two important observations: (i) less than 1 ML of S_{chem} is required for complete suppression of the UPD H; (ii) the $\theta_{H_{UPD}}$ and θ_S relations intersect at the coverage of 0.33; and (iii) presence of S_{chem} suppresses the Pt surface oxidation. Elsewhere, the authors demonstrate results on the effectiveness of the S_{chem} oxidative desorption by cycling to other potential limits higher than 1.2 V [35]; those findings indicate the higher the potential limit, the more effective the oxidative desorption of the S_{chem} layer. It has to stressed that formation of a monolayer of S_{chem} followed by cycling to $E = 1.2$ V, RHE, leads to formation of submonolayers of S_{chem} whose coverage can be controlled with the accuracy of some 2% of a ML especially in the range of $\theta_S \leq 0.4$.

3.3 Thermodynamics of the UPD H at Pt in Presence of a Submonolayer of Chemisorbed S

The idea which was the guided the project was elucidation of the influence of S_{chem} on thermodynamics of the UPD H and on the bond $Pt - H_{UPD}$ energy. The authors presumed that S_{chem} adatoms, forming a submonolayer and coadsorbed with H_{UPD}, can withdraw electron gas

from the Pt atoms with which they form a surface bond. This electron withdrawal gives rise to a localized electron deficit which is compensated by withdrawing electron gas from the neighboring Pt atoms as well as those involving the $Pt-H_{UPD}$ bond [17,35]. The Pt substrate acts as a mediator bringing about lateral $S_{chem}-H_{UPD}$ interactions. It was assumed that the electron density of the $Pt-H_{UPD}$ bond should be decreases by the coadsorbed S_{chem} adatoms, thus the $Pt-H_{UPD}$ bond should be weaker in presence of a submonolayer of S_{chem} that in its absence. This concept was tested experimentally and theoretically and the results are presented below.

A submonolayer of S_{chem} having $\theta_S = 0.1$ was preadsorbed on Pt according to the according to the procedure described above. CV's for the UPD H on Pt in 0.5 M aqueous H_2SO_4 solution at temperature between 273 and 343 K, with an interval of 10 K at the sweep rate of 20 mV s^{-1} (Fig. 8). The results indicate that $\theta_{H_{UPD}}$ is strongly affected by the S_{chem} submonolayer as well as by temperature variation and the higher the temperature, the more H_{UPD} adsorbed on Pt. The Gibbs free energy of adsorption in presence of S_{chem}, $\Delta G^{\circ}_{ads(S)}(H_{UPD})$, is evaluated on the basis eq. (6) and the results shown in Fig. 8 [17].

$$\frac{\theta_{H_{UPD}}}{1-\theta_{H_{UPD}}-\theta_S} = P_{H_2}^{1/2} \exp\left(-\frac{E\,F}{R\,T}\right) \exp\left(-\frac{\Delta G^{\circ}_{ads\,(S)}(H_{UPD})}{R\,T}\right) \qquad (6)$$

In presence of the S_{chem} submonolayer having $\theta_S = 0.1$, $\Delta G^{\circ}_{ads(S)}(H_{UPD})$ has values between −22 and −9 kJ mol^{-1} (Fig. 9), thus values less negative than those in absence of S_{chem}; it assumes the most negative values at the lowest T and the lowest $\theta_{H_{UPD}}$. It has been mentioned above that for T = const, $\Delta G^{\circ}_{ads}(H_{UPD})$ increases towards less negative values with increase of $\theta_{H_{UPD}}$ (Figs. 2 and 9). This change of $\Delta G^{\circ}_{ads}(H_{UPD})$ with $\theta_{H_{UPD}}$ indicates that the lateral interactions between the H_{UPD} adatoms are repulsive and the slope of the $\Delta G^{\circ}_{ads}(H_{UPD})$ versus $\theta_{H_{UPD}}$ plots is a measure of their strength [24,29-33]. In the case of the UPD H in presence of S_{chem}, the variations of $\Delta G^{\circ}_{ads(S)}(H_{UPD})$ with $\theta_{H_{UPD}}$ are more pronounced at low T than at high T whereas in absence of S_{chem} they are roughly of the same magnitude. Thus one may conclude that in presence of the S_{chem} submonolayer the lateral repulsions between the H_{UPD} adatoms are stronger at low T than at high T.

The entropy of adsorption in presence of the S_{chem} submonolayer, $\Delta S^{\circ}_{ads(S)}(H_{UPD})$, was evaluated based on the $\Delta G^{\circ}_{ads(S)}(H_{UPD})$ versus T relations for $\theta_{H_{UPD}} = \text{const}$; it has values between −46 and 41 J mol^{-1} K^{-1} (Fig. 3). The results show that the slope of the

$\Delta G^{\circ}_{ads(S)}(H_{UPD})$ versus T relations varies from negative values at low $\theta_{H_{UPD}}$ to positive ones at high $\theta_{H_{UPD}}$ thus indicating that $\Delta S^{\circ}_{ads(S)}(H_{UPD})$ increases with $\theta_{H_{UPD}}$. Comparison of $\Delta S^{\circ}_{ads}(H_{UPD})$ with $\Delta S^{\circ}_{ads(S)}(H_{UPD})$ reveals that presence of the S_{chem} submonolayer significantly increases the entropy of the UPD.

The enthalpy of adsorption in presence of S_{chem}, $\Delta H^{\circ}_{ads(S)}(H_{UPD})$, is determined based on the values of $\Delta G^{\circ}_{ads(S)}(H_{UPD})$ and $\Delta S^{\circ}_{ads(S)}(H_{UPD})$, and formula $\Delta G^{\circ} = \Delta H^{\circ} - T\,\Delta S^{\circ}$. The results (Fig. 4) indicate that $\Delta H^{\circ}_{ads(S)}(H_{UPD})$ has values between -34 and 3 kJ mol^{-1}. An analysis of the data indicates that presence of the submonolayer of S_{chem} significantly increases the enthalpy of adsorption with respect to its values in absence of S_{chem}.

Determination $\Delta H^{\circ}_{ads(S)}(H_{UPD})$ allowed evaluation of the influence of presence of the S_{chem} submonolayer on the $Pt-H_{UPD}$ bond energy, $E_{Pt-H_{UPD}(S)}$. The values of $E_{Pt-H_{UPD}(S)}$ for various $\theta_{H_{UPD}}$ were evaluated according to eq. (3) and they are between 214 and 252 kJ mol^{-1} (Fig. 5). The results demonstrate that presence of the S_{chem} submonolayer decreases the $Pt-H_{UPD}$ bond energy by some $12-31$ kJ mol^{-1} depending on $\theta_{H_{UPD}}$. The decrease of the $Pt-H_{UPD}$ bond energy indicates that the S_{chem} adatoms create an electron deficit at the $Pt-H_{UPD}$ bond giving rise to a weaker $Pt-H_{UPD}$ bond.

The authors believe that the results represent an important contribution to comprehension of the atomic-level mechanism of the action of SBE's and their impact on coadsorbed H_{UPD} adatoms and that they will serve in subsequent development of criteria for selection and design of surface species which could act selectively either as surface poisons or surface poisons of H adsorption and absorption.

4. CONCLUSIONS

1. Immersion of Pt in aqueous Na_2S solution leads to formation of a monolayer of S_{chem} which completely suppressed the UPD H; a submonolayer of S_{chem} having its surface coverage less than 0.33 blocks the UPD H but only partially. The S_{chem} monolayer can be gradually desorbed by oxidative desorption at E = 1.2 V and the S_{chem} coverage can be controlled with an precision of 2% of a ML.

2. $\Delta G^{\circ}_{ads}(H_{UPD})$ has the following values: (i) between -25 and -12 kJ mol^{-1} for Pt; (ii) between -17 and -8 kJ mol^{-1} for Rh; and (iii) between -22 and -9 kJ mol^{-1} for Pt with a submonolayer of S_{chem} ($\theta_S = 0.1$).

3. $\Delta S^{\circ}_{ads}(H_{UPD})$ has the following values: (i) between −80 and −41 J mol^{-1} K^{-1} for Pt; (ii) between −126 and −29 J mol^{-1} K^{-1} for Rh; and (iii) between −46 and 41 J mol^{-1} K^{-1} for Pt with a submonolayer of S_{chem} ($\theta_S = 0.1$).

4. $\Delta H^{\circ}_{ads}(H_{UPD})$ has the following values: (i) between −46 and −27 kJ mol^{-1} for Pt; (ii) between −52 and −21 kJ mol^{-1} for Rh; and (iii) between −34 and 3 kJ mol^{-1} for Pt with a submonolayer of S_{chem} ($\theta_S = 0.1$).

5. The $M - H_{UPD}$ bond energy has the following values: (i) between 245 and 264 kJ mol^{-1} for Pt; (ii) between 239 and 270 kJ mol^{-1} for Rh; and (iii) between 214 and 252 kJ mol^{-1} for Pt with a submonolayer of S_{chem} ($\theta_S = 0.1$). The S_{chem} adatoms adsorbed on Pt create an electron deficit at the Pt surface atoms to which they are bonded. This deficit propagates through the Pt substrate and gives rise to electron withdrawal from the $Pt - H_{UPD}$ bond, thus to a weaker $Pt - H_{UPD}$ bond.

6. The H_{UPD} adatoms have repulsive lateral interactions which become stronger in presence of the S_{chem} submonolayer than in its absence.

ACKNOWLEDGMENTS

Acknowledgment is made to the NSERC of Canada and le FCAR du Québec for support of this research project. A. Zolfaghari gratefully acknowledges a graduate fellowship from the MCHE of Iran. F. Villiard and M. Chayer conducted this research as their last term projects.

REFERENCES

1. K. M. Mackay, *Hydrogen Compounds of the Metallic Elements*, E.&F.N. Spon, London (1966).

2. G. Alefeld and J. Volkl, Editors, *Hydrogen in Metals*, Parts I and II, Springer-Verlag, New York (1978).

3. L. Schlapbach, Editor, *Hydrogen in Intermetalic Compounds*, Part I, Springer-Verlag, New York (1988); Part II, Springer-Verlag, New York (1992).

4. P.K. Subramanyan, in *Comprehensive Treatise of Electrochemistry*, Vol. 4, Ch.8, J.O'M. Bockris, B.E. Conway, E. Yeager and R.E. White, Editors, Plenum Press, New York (1981).

5. J. J. G. Willems, *Ph.D. Thesis*, Eindhoven, The Netherland (1984).

6. A. F. Andersen and A. J. Maeland, Editors, *Hydrides for Energy Storage*, Pergamon Press, Oxford (1978).

7. B. E. Conway and G. Jerkiewicz, Editors, *Electrochemistry and Materials Science of Cathodic Hydrogen Absorption and Adsorption*, The Electrochemical Society, PV 94-21, Pennington, NJ (1995).

8. R. A. Oriani, J. P. Hirth and M. Smialowski, Editors, *Hydrogen Degradation of Ferrous Metals*, Noyes Publications, Park Ridge, NJ (1985).

9. S. R. Ovshinsky, M. A. Fetcenko and J. Ross, *Science*, **260** (1993) 176.

10. S. R. Ovshinsky, K. Sapru, B. Reichman and A. Reger, US Patents No. 4,623,597 (1986); see also S. R. Ovshinsky and M. A. Fetcenko, US Patent No. 5,096,667 (1992); No. 5,104,617 (1992); No. 5,135,589 (1992); No. 5,238,756 (1993); No. 5,277,999 (1994).

11. M. Ciureanu, D. Moroz, R. Ducharme, D. H. Ryan, J. Ström-Olsen and M. Trudeau, *Zeit. Phys. Chem. Bd.*, **183**, 365 (1994); Q. M. Yang, M. Ciureanu, D. H. Ryan and J. Ström-Olsen, *J. Electrochem. Soc.*, **141** (1994) 2108; 2113; **141** (1994) 2430.

12. O. Savadogo, P. R. Roberge and T. N. Veziroglu, Editors, *New Materials for Fuel Cell Systems I*, Proceedings of the First International Symposium on New Materials for Fuel Cell Systems, Édition de l'École Polytechnique de Montréal, Montréal (1995).

13. B.E. Conway and L. Bai, J. Chem. Soc., *Faraday Trans. I*, **81** (1985) 1841.

14. G. Jerkiewicz and A. Zolfaghari, *J. Electrochem. Soc.*, **143** (1996) 1240.

15. B. E. Conway and G. Jerkiewicz, *J. Electroanal. Chem.*, **357** (1993) 47.

16. B. E. Conway and G. Jerkiewicz, *Z. Phys. Chem., Bd.*, **183** (1994) 281.

17. G. Jerkiewicz, J. J. Borodzinski, W. Chrzanowski and B. E. Conway, *J. Electrochem. Soc.*, **142** (1995) 3705.

18. A. Lasia and D. Grégoire, *J. Electrochem. Soc.*, **142** (1995) 3393.

19. P. Marcus and E. Protopopoff, *Surface Sci.*, **161** (1985) 533; *Surface Sci. Letters*, **169** (1986) L237; *J. Vac. Sci. Technol.*, **A5** (1986) 944.

20. E. Protopopoff and P. Marcus, *J. Electrochem. Soc.*, **135** (1988) 3073; J. Chim. Phys. **88** (1991) 1423; *C. R. Acad. Sci. Paris*, **t. 308**, Série II, (1989) 1685.

21. J. McBreen, *J. Electroanal. Chem.*, **287** (1990) 279.

22. S. Morin and B. E. Conway, *J. Electroanal. Chem.*, **376** (1994) 135.

23. D. Zurawski, K. Chan and A. Wieckowski, *J. Electroanal. Chem.*, **210** (1986) 315; see also D. Zurawski and A. Wieckowski, *Langmuir*, **8** (1992) 2317.

24. G. Jerkiewicz and A. Zolfaghari, *J. Phys. Chem.*, **100** (1996) 8454.

25. C. Quijada, A. Rodes, J. L. Vázquez, J. M. Pérez and A. Aldaz, *J. Electroanal. Chem.*, **394** (1995) 217.

26. C. Quijada, A. Rodes, J. L. Vázquez, J. M. Pérez and A. Aldaz, *J. Electroanal. Chem.*, **398** (1995) 105.

27. H. Angerstein-Kozlowska, B. E. Conway and W. B. A. Sharp, *J. Electroanal. Chem.*, **43** (1973) 9.

28. H. Angerstein-Kozlowska, in *Comprehensive Treatise of Electrochemistry*, Vol. 9, Ch. 9, E. Yeager, J. O'M. Bockris, B. E. Conway and S. Sarangapani, Editors, Plenum Press, New York (1984).

29. Langmuir, I., *J. Am. Chem. Soc.*, **40** (1918) 1361.

30. R. H. Fowler and F. A. Guggenheim, *Statistical Thermodynamics*, Cambridge University Press, London (1939).

31. A. W. Adamson, *Physical Chemistry of Surfaces*, John Wiley and Sons, New York (1990).

32. G. A. Somorjai, *Introduction to Surface Chemistry and Catalysis*, John Wiley and Sons, New York (1994).

33. K. Christman, *Surface Sci. Rep.*, **9** (1988) 1.

34. Y.-E. Sung, W. Chrzanowski, A. Zolfaghari, G. Jerkiewicz and A. Wieckowski, *J. Am. Chem. Soc.*, submitted (1996).

35. A. Zolfaghari, G. Jerkiewicz, Y.-E. Sung and A. Wieckowski, in K. Itaya and A. Wieckowski, Editors, *Electrode Processes VI*, The Electrochemical Society, PV 96-8, Pennington, NJ, in press (1996).

36. G. Tremiliosi-Filho, G. Jerkiewicz and B. E. Conway, *Langmuir*, **6** (1992) 658.

37. G. Jerkiewicz, G. Tremiliosi-Filho and B. E. Conway, *J. Electroanal. Chem.*, **344** (1992) 359.

38. N. Batina, J. W. McCargar, L. Laguren-Davidson, C.-H. Lin and A. T. Hubbard, *Langmuir*, **5** (1989) 123.

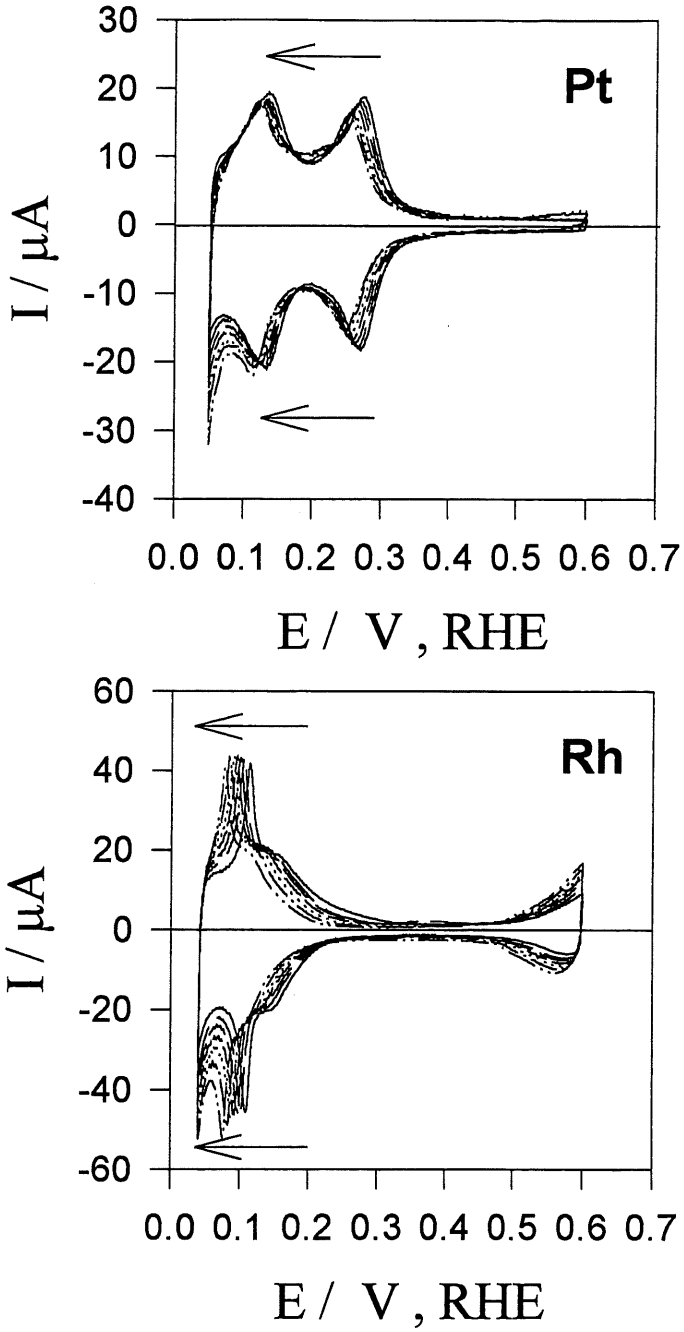

Figure 1. Series of CV profiles for the UPD H on Pt and Rh electrodes in 0.5 M aqueous H_2SO_4 solution for a temperature range between 273 and 343 K, with an interval of 10 K; the sweep rate $s = 20\ mV\ s^{-1}$, the electrode surface area is $A_r = 0.72 \pm 0.01\ cm^2$ for Pt and $A_r = 0.70 \pm 0.01\ cm^2$ for Rh; the arrows indicate shift of the adsorption-desorption peaks upon the temperature increase.

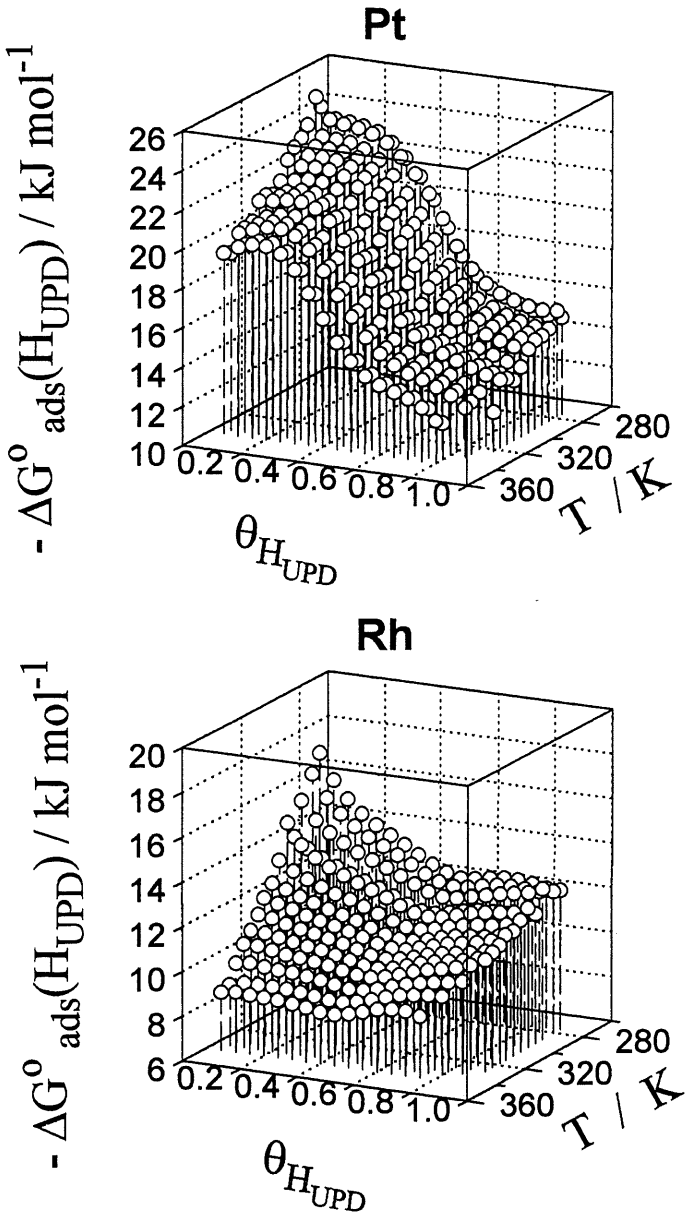

Figure 2. 3D plots showing $\Delta G^{\circ}_{ads}(H_{UPD})$ versus $\theta_{H_{UPD}}$ and T for the UPD H on Pt and Rh electrodes in 0.5 M aqueous H_2SO_4. $\Delta G^{\circ}_{ads}(H_{UPD})$ assumes values between −25 and −12 kJ mol^{-1} for Pt and between −17 and −8 kJ mol^{-1} for Rh; $\Delta G^{\circ}_{ads}(H_{UPD})$ reaches the most negative values at the lowest T and the smallest $\theta_{H_{UPD}}$. Increase of $\Delta G^{\circ}_{ads}(H_{UPD})$ with $\theta_{H_{UPD}}$ for T = const points to the repulsive nature of lateral interactions between H_{UPD} adatoms.

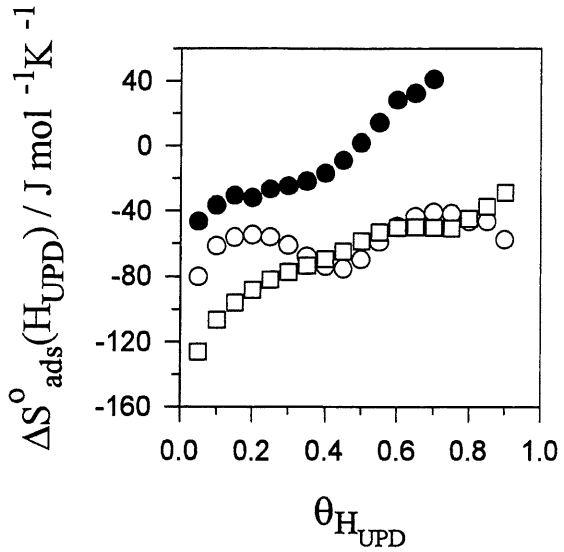

Figure 3. $\Delta S^{\circ}_{ads}(H_{UPD})$ versus $\theta_{H_{UPD}}$ relations for the UPD H from 0.5 M aqueous H_2SO_4 on: (i) Pt in absence of S_{chem} (○); (ii) Rh in absence of S_{chem} (□); and (iii) Pt in presence of S_{chem}, $\theta_S = 0.1$, (●); $\Delta S^{\circ}_{ads}(H_{UPD})$ has values between −80 and −4 J mol^{-1} K^{-1} for Pt in absence of S_{chem}, values between −126 and −29 J mol^{-1} K^{-1} for Rh and values between −46 and 41 J mol^{-1} K^{-1} for Pt with a submonolayer of S_{chem}.

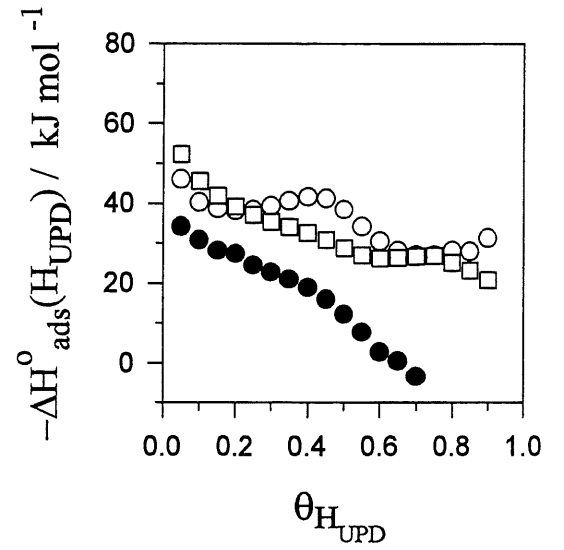

Figure 4. $\Delta H^{\circ}_{ads}(H_{UPD})$ versus $\theta_{H_{UPD}}$ relations for the UPD H from 0.5 M aqueous H_2SO_4 on: (i) Pt in absence of S_{chem} (○); (ii) Rh in absence of S_{chem} (□); and (iii) Pt in presence of S_{chem}, $\theta_S = 0.1$, (●); $\Delta H^{\circ}_{ads}(H_{UPD})$ has values between −46 and −27 kJ mol^{-1} for Pt in absence of S_{chem}, values between −52 and −21 kJ mol^{-1} for Rh and values between −34 and 3 kJ mol^{-1} for Pt with a submonolayer of S_{chem}.

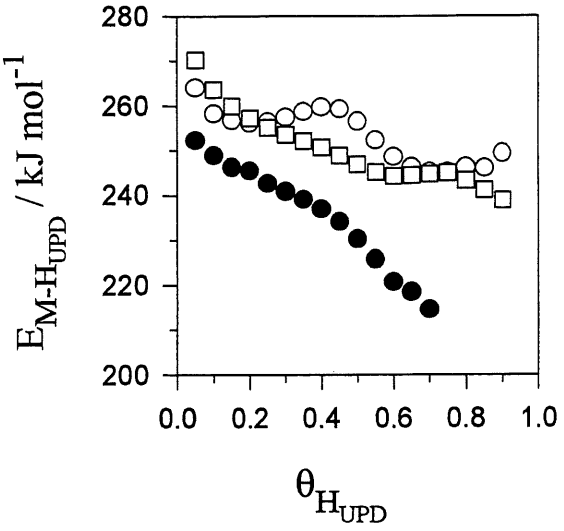

Figure 5. $E_{M-H_{UPD}}$ versus $\theta_{H_{UPD}}$ relations for the UPD H from 0.5 M aqueous H_2SO_4 on: (i) Pt in absence of S_{chem} (O); (ii) Rh in absence of S_{chem} (□); and (iii) Pt in presence of S_{chem}, $\theta_S = 0.1$, (●); $E_{M-H_{UPD}}$ has values between 245 and 264 kJ mol^{-1} for Pt in absence of S_{chem}, values between 239 and 270 kJ mol^{-1} for Rh and values between 214 and 252 kJ mol^{-1} for Pt with a submonolayer of S_{chem}.

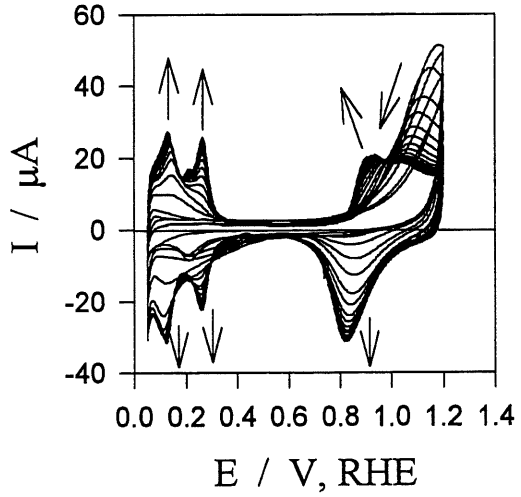

Figure 6. Series of CV profiles for Pt electrode covered with a layer of S_{chem} in 0.5 M aqueous H_2SO_4 solution at 298 K; the sweep rate $s = 20$ mV s^{-1} and the electrode surface area $A_r = 0.72 \pm 0.01$ cm^2. Upon potential cycling to 1.20 V, RHE, the S_{chem} layer undergoes oxidative desorption; unblocked surface sites become available to H_{UPD}. Presence of S_{chem} also affects the surface oxidation of Pt.

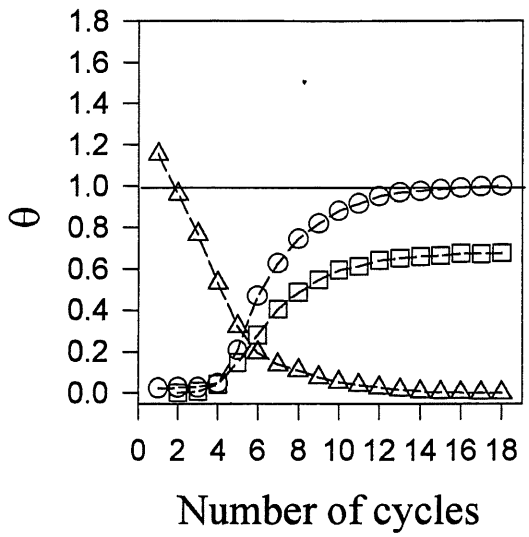

Figure 7. Relation between the H_{UPD} surface coverage, $\theta_{H_{UPD}}$, the S_{chem} surface coverage, θ_S, the surface oxide coverage, θ_O, and the number of respective cycles to 1.2 V for S_{chem} oxidative desorption determined on the basis of results presented in Fig. 10.

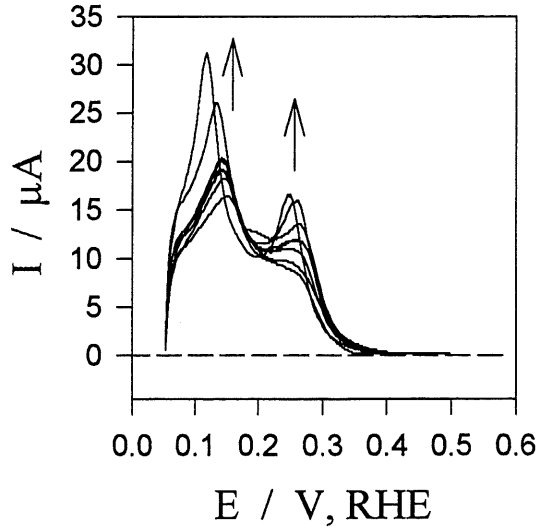

Figure 8. Series of the CV profiles for the UPD H on Pt electrode in 0.5 M aqueous H_2SO_4 solution in presence of a S_{chem} submonolayer ($\theta_S = 0.1$) for a temperature range between 273 and 343 K, with an interval of 10 K; the sweep rate $s = 20$ mV s^{-1} and the electrode surface area $A_r = 0.72 \pm 0.01\ cm^2$. The arrows indicate changes in the profile brought about by T increase.

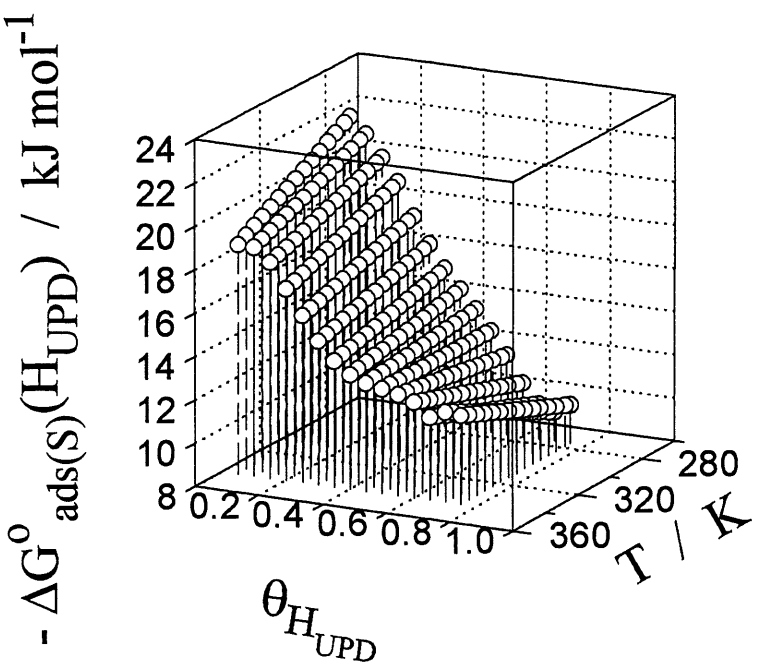

Figure 9. 3D plots showing the Gibbs free energy of the UPD H, $\Delta G^{\circ}_{ads(S)}(H_{UPD})$, versus $\theta_{H_{UPD}}$ and T, for adsorption in presence of a S_{chem} submonolayer ($\theta_S = 0.1$) from 0.5 M aqueous H_2SO_4. $\Delta G^{\circ}_{ads(S)}(H_{UPD})$ has values between –22 and –9 kJ mol^{-1} depending on $\theta_{H_{UPD}}$ and T; $\Delta G^{\circ}_{ads(S)}(H_{UPD})$ reaches the most negative values at the lowest T and the smallest $\theta_{H_{UPD}}$. Increase of $\Delta G^{\circ}_{ads(S)}(H_{UPD})$ with $\theta_{H_{UPD}}$ for T = const points to the repulsive nature of lateral interactions between H_{UPD} adatoms.

CHAPTER 3

TEMPERATURE-DEPENDENT STUDIES ON Pt SINGLE-CRYSTAL ELECTRODES AND ELUCIDATION OF THERMODYNAMICS OF THE UPD H IN ABSENCE/PRESENCE OF CHEMISORBED SULFUR

Despite tremendous efforts devoted to research on the UPD of hydrogen and metals as well as to the anion adsorption on Pt single-crystal electrodes, practically nothing is known about the T-dependence of the UPD H and anion adsorption on Pt(hkl). Chapter 3 presents new results on the subject and examines thermodynamics of the UPD H on Pt(111) by application of the theoretical methodology introduced in Chapter 1. These studies elucidate thermodynamic parameters of the UPD H on Pt(111) in absence/presence of chemisorbed sulfur. The papers presented in section 3.1 and in section 3.2 demonstrate the first experimental data which demonstrate changes in the CV profiles for Pt(100) and Pt(111), respectively, in 0.5 M aqueous H_2SO_4 solution brought about by temperature modification. Variation of the CV profiles is discussed in terms of changes of the surface coverage by the under-potential deposited H, H_{UPD}, and the adsorbed anions. The data lead to the observation that the H_{UPD} and anion adsorption on Pt(100) is strongly affected by temperature variation and this effect may be assigned to lateral repulsive interactions. However, in the case of Pt(111), H_{UPD} and anion adsorption is not strongly affected by temperature variation. This effect may be assigned to lateral interactions between the adsorbed species being of repulsive nature. In the case of Pt(111), the potential of the sharp peak in the potential region corresponding to the anion adsorption shifts towards more-positive values upon T increase and the peak current density shifts towards lower values. The behavior of the third, asymmetric peak in the double-layer region is complex; the anodic and cathodic components shift towards less-positive potentials but the displacement of the anodic one is more pronounced. A detail discussion of the changes in the CV profiles for Pt(100) and Pt(111) caused by temperature variation is presented discussed in sections 3.1 and 3.2, respectively. The paper presented in section 3.1 (*A. Zolfaghari and G. Jerkiewicz, J. Electroanal. Chem., 420, 11 (1997)*) and the paper in section 3.2 (*A. Zolfaghari and G. Jerkiewicz, J. Electroanal. Chem., 422, 1 (1997)*) are the result of my essential contribution in experimental, theoretical and writing parts. The contribution of Dr. G. Jerkiewicz was in theoretical and writing constituent.

Section 3.3 is an extension of the work presented in sections 3.1 and 3.2. It demonstrates further interpretation of the data of two last sections as well as new CV results and thermodynamics parameters for the UPD H on Pt(111) in 0.05 M aq. H_2SO_4. The H_{UPD} and anion adsorption regions on Pt(111) in 0.05 M aq. H_2SO_4 are separated therefore one can determine $\Delta G_{ads}(H_{UPD})$, $\Delta S^{\circ}_{ads}(H_{UPD})$, $\Delta H^{\circ}_{ads}(H_{UPD})$ and the $Pt(111)-H_{UPD}$ surface bond energy, $E_{Pt(111)-H_{UPD}}$. An analysis of the $\Delta G_{ads}(H_{UPD})$ versus $\theta_{H_{UPD}}$ plots for T=constant reveal that the UPD H follows the Frumkin isotherm and the energy of lateral interactions is determined. The value of $E_{Pt(111)-H_{UPD}}$ is close to that for the surface bond energy between the chemisorbed H, H_{chem}. The paper presented in section 3.3 (*Alireza Zolfaghari and Gregory Jerkiewicz, Electrochim. Acta, Submitted (1997)*) is a result of my essential contribution in experimental, theoretical and writing parts. The contribution of Dr. G. Jerkiewicz was in theoretical and writing constituent.

In section 3.4, new data on the structures of S_{chem} on the Pt(111) electrode surface in relation to its coverage. Structural data on electrochemical oxidative desorption of S_{chem} from LEED with those for temperature-stimulated desorption are compared. It is demonstrated how $\theta_{S_{chem}}$ can be controlled by selecting the positive potential limit and the number of anodic desorption scans. The temperature variation effect on the anodic desorption behavior of S_{chem} and its coverage, $\theta_{S_{chem}}$, is shown. LEED data reveal that S_{chem} forms well-defined structures on Pt(111) for $0.50 \geq \theta_{S_{chem}} \geq 0.25$: (*i*) $c(2\times2)$ at $\theta_{S_{chem}} = 1/2$, (*ii*) $\left(\sqrt{3}\times\sqrt{3}\right)R30^{\circ}$ at $\theta_{S_{chem}} = 1/3$, and (*iii*) $p(2\times2)$ at $\theta_{S_{chem}} = 1/4$. When $\theta_{S_{chem}} \leq 0.20$, structured islands of S_{chem} are observed. AES and CEELS data indicate that the chemisorbed S is not present in an oxidized or reduced state; it is almost of atomic character with an incomplete negative charge due to partial charge transfer between S_{chem} and the Pt(111) substrate. Using the methodology presented in Chapter 1 and Chapter 2, thermodynamic state functions for the UPD H in presence of S_{chem} with $\theta_{S_{chem}}$=0.1 are determined. Presence of S_{chem} influences thermodynamics of the UPD H on Pt(111) resulting in less-negative values of $\Delta G_{ads(S)}(H_{UPD})$. In absence of S_{chem}, the UPD H is enthalpy driven whereas in presence of S_{chem} it becomes entropy driven. The $Pt(111)-H_{UPD}$ bond energy is weaker in presence of S_{chem} than in its absence, and this bond energy diminution may be assigned to local electronic effects arising from the presence of S_{chem}. The paper presented in section 3.4 (*Y.-E. Sung , W. Chrzanowski and A. Wieckowski, A. Zolfaghari, S. Blais and G. Jerkiewicz, Electrochim. Acta, Submitted*

(1997)) is a result of my essential contribution in experimental, theoretical and writing parts. The contribution of S. Blais was in some experimental part. The contribution of Y.-E. Sung , Dr. W. Chrzanowski and Prof. A. Wieckowski was in surface analysis of S_{chem} on Pt(111), using Auger, LEED and CEELS techniques at the Department of Chemistry, University of Illinois at Urbana-Champaign, Urbana-Champaign IL 61801 USA. Such experimental facilities are not available at Sherbrooke. The contribution of Dr. G. Jerkiewicz was in theoretical and writing constituent.

3.1 THE TEMPERATURE DEPENDENCE OF HYDROGEN AND ANION ADSORPTION AT A Pt(100) ELECTRODE IN AQUEOUS H_2SO_4 SOLUTION

A. Zolfaghari and G. Jerkiewicz, J. Electroanal. Chem., 420, 11 (1997)

ABSTRACT

Research on the under-potential deposition of H, UPD H, and anion adsorption on Pt(100) in 0.5 M aqueous H_2SO_4 solution by cyclic-voltammetry, CV, indicate that the overall adsorption/desorption charge density is strongly affected by temperature, T, variation and that it decreases by about 1/3 when T is raised from 293 to 328 K. The sharp peak at 0.375 V vs RHE assigned to the anion adsorption decreases its potential, current density and charge density. The CV feature assigned to the UPD H, a wide shoulder overlapping the sharp peak, also decreases with T augmentation but the decline of its charge density is less pronounced. The results indicate that the H_{UPD} and anion surface coverages, $\theta_{H_{UPD}}$ and θ_{AN} respectively, are strongly temperature-dependent. This behavior may be assigned to lateral repulsive interactions.

Keywords: Hydrogen under-potential deposition, Anion adsorption, Temperature effect, Pt(100)

1. INTRODUCTION

It was demonstrated in the 1950's that single crystals of Cu and Pt could be prepared by melting the tip of a Cu or Pt wire followed by careful formation of a monocrystalline bead [1,2]. Clavilier et al. [3,4] further mastered this technique and successfully developed a procedure for preparing Pt and Rh single crystals that could be used in electrochemical measurements without expensive UHV equipment. This experimental progress led to numerous studies on single-crystal electrodes which have resulted in atomic-level understanding of the electrified solid-liquid interface and surface electrocatalysis [5-9]. Investigation of the under-potential deposition of hydrogen, UPD H, and adsorption of anions on Pt(111) and Pt(100) have been a subject of intense research and scientific discussion for over ten years [4,5,10-21]. At present, it is quite well understood that the potential regions of the UPD H and the anion adsorption overlap and that the adsorption charge as determined from cyclic-voltammetry, CV, measurements provides the total charge which corresponds to both the H adsorption/desorption and anion desorption/adsorption. Deconvolution of the charge that is assigned to the UPD H or the anion adsorption can be accomplished by performing either CO-displacement experiments [22-24] or by chronocoulometry measurements [25].

Despite tremendous effort devoted to research on the UPD of hydrogen and metals as well as to the anion adsorption on Pt single-crystal electrodes, practically nothing is known about the temperature dependence of the CV profiles for Pt(100) or Pt(111). In the present paper, the authors present the first experimental data which demonstrate changes in the CV profile for Pt(100) in 0.5 M aqueous H_2SO_4 solution brought about by temperature variation. Alteration of the CV profile is discussed in terms of changes of the surface coverage by the under-potential deposited H, H_{UPD}, and the adsorbed anions. The data lead to the observation that H_{UPD} and anion adsorption is strongly affected by temperature variation and the effect may be assigned to lateral repulsive interactions.

2. EXPERIMENTAL

1. Pt(100) Electrode Preparation

The Pt(100) single-crystal electrode was prepared and oriented according to the procedure developed by Clavilier [3,4] and further advanced by Hamelin [26,27]. It was subsequently polished with Alumina (0.05 μm) to a mirror-like finish. The quality of the Pt(100) surface was verified by recording a cyclic-voltammetry profile, CV, in 0.5 M aqueous H_2SO_4 solution at potentials between 0.06 and 0.80 V vs RHE (Fig. 1). Agreement between our results and those reported in the literature [9,16,17] indicate that the crystal was of good quality and properly oriented and that the surface was well ordered. The electrode diameter, d, was measured with a Vernier microscope and was found to be 0.219 ± 0.002 cm; the surface area, A, was 0.038 ± 0.001 cm^2.

2.2. Solution and Electrochemical Cell

The 0.5 M aqueous H_2SO_4 solution was prepared from BDH Aristar grade H_2SO_4 and Nanopure water (18 MΩ cm). The experiments were conducted in a Pyrex, two-compartment electrochemical cell. The glassware was pre-cleaned according to a well-established procedure [28-30]. During the experiments, H_2 gas, pre-cleaned and pre-saturated with water vapor, was bubbled through the reference electrode compartment in which a Pt/Pt-black electrode was immersed. It served as the reversible hydrogen electrode, RHE, and its potential was −0.021 V versus the standard hydrogen electrode, SHE. High-

purity Ar gas, pre-saturated with water vapor, was passed through the working electrode, WE, compartment. The counter electrode, CE, was a Pt wire (99.998% purity, Aesar).

2.3. Temperature Measurements

The electrochemical cell was immersed in a water bath (Haake W13) and the temperature was controlled to within ± 0.5 K by means of a thermostat (Haake D1); the water level in the bath was maintained above the electrolyte in the cell. The temperature in the water bath and the electrochemical cell were controlled by means of thermometers (± 0.5 K) and a K-type thermocouple (80 TK Fluke), and were found to agree to within ± 0.5 K. The experiments were conducted at $293 \leq T \leq 328$ K with an interval of 5 K. Measurements at Pt(100) using the hanging meniscus methodology were difficult to perform below 293 K or above 328 K because of electrolyte condensation or its creeping along the crystal surface.

2.4. Electrochemical Measurements

The experiments involved CV measurements in the potential range corresponding to the UPD H and anion adsorption in 0.5 M aqueous H_2SO_4, thus between 0.06 and 0.80 V vs RHE. The CV experiments were conducted at a sweep rate of 50 mV s^{-1}. The electrochemical instrumentation included: (a) EG&G Model 263A potentiostat-galvanostat; (b) IBM-compatible 80486 computer, and (c) EG&G M270 Electrochemical Software. All potentials were measured with respect to RHE immersed in the same electrolyte.

3. RESULTS AND DISCUSSION

3.1. Temperature-Dependence of the Pt(100) Cyclic-Voltammetry Profile in 0.5 M H_2SO_4

Fig. 1 shows a CV profile for Pt(100) cooled in $H_2 + Ar$ in 0.5 M aqueous H_2SO_4 solution at 298 K at potentials between 0.06 and 0.80 V vs RHE [9,16,17]. It reveals the following features whose behavior as a function of T will be discussed below: (i) a sharp peak at 0.375 V; (ii) a small peak at 0.267 V; and (iii) a shoulder at 0.305 V vs RHE. The shape of the CV profile indicates that the Pt(100) electrode was well ordered and that the electrolyte was free of impurities. The CV profile is symmetric with respect to the potential axis indicating that the surface electrochemical process is reversible. Integration of the anodic and cathodic components of the CV profiles between 0.15 and 0.50 V vs RHE allowing for the double-layer charging, leads the authors to the evaluation of the average charge density corresponding to both the UPD H and the anion adsorption (the total charge density,

$q_T = q_{H_{UPD}} + q_{AN}$, where $q_{H_{UPD}}$ is the charge density for the UPD H and q_{AN} is the charge density for the anion adsorption) which is 220 $\mu C\,cm^{-2}$. This value differs only slightly from that observed by Clavilier et al. [9,16,17] who observed values between 212 and 214 $\mu C\,cm^{-2}$. It should be emphasized that if the profile corresponded to a complete monolayer (ML) of H_{UPD}, then the charge density would be expected to match the theoretical value for 1 ML of H_{UPD}, thus 208 $\mu C\,cm^{-2}$. However, because the CV profile corresponds to both H_{UPD} and anion adsorption, the charge density does not have to match the theoretical one for 1 monolayer of H_{UPD} because it depends on the surface coverage of H_{UPD} and anion as well as on its chemical identity at the surface (sulfate versus bisulfate).

Fig. 2 shows a series of CV profiles for the same potential range as in Fig. 1, namely $0.06 \le E \le 0.80$ V vs RHE for eight temperatures between 293 and 328 K with an interval of 5 K. The finding of these experiments may be summarized as follows: (i) upon T increase, the sharp peak at 0.375 V vs RHE decreases and shifts towards less-positive potentials; (ii) the small peak at 0.267 V vs RHE becomes less pronounced and the potential shifts towards lower values; (iii) the shoulder at 0.305 V vs RHE becomes less pronounced upon T increase and finally disappears at $T \ge 313$ K; and (iv) no new features are observed in the CV profiles that could be assigned to T increase. An analysis of the CV profiles clearly demonstrates that the principle characteristic of the adsorption-desorption CV profiles is the decline of the peat at 0.375 V vs RHE. The changes in the CV peak area reported in Fig. 2 are completely reversible in that decreasing the temperature back to 298 K reproduced entirely the voltammetric intensities reported in Fig. 1. It should be added that there was no effect of temperature on the geometry of the meniscus between electrode and electrolyte and the electrode contact area remained constant over the temperature range studied. In order to provide a comprehensive examination of the temperature-dependence of the CV profile for Pt(100) and to analyze it in detail, the authors evaluated: (i) the value of the peak potential, E_P, of the sharp peak; (ii) the change of its current density, i_P; and (iii) the variation of the total adsorption-desorption charge density, q_T. Fig. 3 shows the experimentally determined variation of E_P as a function of T and the results indicate that the E_P versus T relation is linear and its slope, $\partial E_P / \partial T$, equals $-0.50 \times 10^{-3}\ V\,K^{-1}$. Thus on average an increase of the temperature by 10 K decreases the peak potential by 5 mV. Fig. 4. shows the i_P versus T relation and the results presented here reveal that the dependence is linear and that its slope, $\partial i_P / \partial T$, equals $-2.50\ \mu A\,cm^{-2}\,K^{-1}$. Fig. 5 shows the relation between the total adsorption/desorption charge density, q_T, and T as determined on the basis of the

experimental data presented in Fig. 2. The q_T versus T dependence is non-linear and q_T decreases from 220 to 150 $\mu C\,cm^{-2}$, thus by 70 $\mu C\,cm^{-2}$, when T is raised by 35 K. This change of q_T is very large and it accounts for some 32% of the total charge at 298 K; it clearly indicates that the amount of the adsorbed species, namely H_{UPD} and anions, decreases significantly. Preliminary interpretation of the diminution of q_T is provided in the subsequent section.

3.2. Preliminary Interpretation of the Temperature-Dependence of the Pt(100) Cyclic-Voltammetry Profile

It is well understood that the CV profile at $0.15 \le E \le 0.50$ V vs RHE for Pt(100) corresponds to the UPD H and the adsorption of sulfate/bisulfate, thus $q_T = q_{H_{UPD}} + q_{AN}$. Because q_T decreases upon T extension to higher values, it is apparent that the total surface coverage of both adsorbed species, θ_T (where $\theta_T = \theta_{H_{UPD}} + \theta_{AN}$, and $\theta_{H_{UPD}}$ is the H_{UPD} surface coverage and θ_{AN} is the anion coverage) diminishes. The variation of the individual contributions to the total charge density, $q_{H_{UPD}}$ and q_{AN} respectively, requires further explanation. Clavilier et al. [22-24] concluded based on the CO-displacement measurements that the sharp peak at 0.375 V vs RHE corresponds to the anion adsorption, and the wide shoulder at 0.305 V vs RHE overlapping the sharp peak can be assigned to the UPD H. Thus one may conclude that the anion adsorption takes place at higher potentials than the UPD H. Because the data shown in Fig. 2 reveal that the sharp peak and its charge decrease upon T augmentation, one may conclude that the surface concentration of the adsorbed anions, θ_{AN}, decreases. An analysis of the shoulder at 0.305 V vs RHE indicates that its charge density also decreases with increasing T but this behavior is less pronounced than that of the anion. Bearing in mind that this potential region corresponds to the UPD H, one may conclude that the surface coverage by H_{UPD}, $\theta_{H_{UPD}}$, decreases with rising T but to a smaller extent than that of the anions. The results presented in the paper indicate that the surface coverage by H_{UPD} and anions is strongly temperature-dependent and a rise in T lowers their respective coverages. This behavior points to the nature of the lateral interactions between H_{UPD} and anions, i.e. repulsive and temperature-dependent [31].

In this preliminary note, the authors present new and important data on the temperature-dependence of the UPD H and anion adsorption on the Pt(100) single-crystal electrode surface prepared according to the Clavilier procedure. They believe it is the first paper which demonstrates that the CV profile is strongly affected by temperature variation. In

a subsequent full-length paper, they will show results of deconvolution of the CV profiles into two separate components that can be assigned to both surface processes. This theoretical treatment will lead to quantitative analysis of the results shown in this paper.

CONCLUSIONS

Studies of the UPD H and anion adsorption on Pt(100) in 0.5 M aqueous H_2SO_4 solution by cyclic-voltammetry indicate that the overall adsorption/desorption charge density decreases by about 1/3. The sharp peak at 0.375 V vs RHE assigned to the anion adsorption decreases its potential, current density and charge density. The CV feature assigned to the UPD H, a wide shoulder overlapping the sharp peak, also decreases with T augmentation but the decline of its charge density is less pronounced. The results indicate that the H_{UPD} and anion surface coverages ($\theta_{H_{UPD}}$ and θ_{AN}), are strongly temperature-dependent. This behavior may be assigned to lateral repulsive interactions.

ACKNOWLEDGMENTS

Acknowledgment is made to the NSERC of Canada and FCAR du Québec for support of this research. A. Zolfaghari acknowledges a graduate fellowship from the MCHE of Iran.

REFERENCES

1. E. Menzel, Rept. Progr. Phys., 10 (1953) 407.
2. R. Kaishew and B. Mutaftschiew, Z. Phys. Chem., 204 (1955) 334.
3. J. Clavilier, R. Faure, G. Guinet and R. Durand, J. Electroanal. Chem., 107 (1980) 205.
4. J. Clavilier, J. Electroanal. Chem., 107 (1980) 211.
5. C. L. Scortichini and C. N. Reilley, J. Electroanal. Chem., 139 (1982) 233; 247.
6. C. L. Scortichini, F. E. Woodward and C. N. Reilley, J. Electroanal. Chem., 139 (1982) 265.
7. D. Aberdam, R. Durand, R. Faure and F. El-Omar, Surface Sci., 171 (1986) 303.
8. C. Lamy, J. M. Leger, J. Clavilier and R. Parsons, J. Electroanal. Chem., 150 (1983) 71.
9. J. Clavilier, K. El Achi, M. Petit, A. Rodes and M. A. Zamakhchari, J. Electroanal. Chem., 295 (1990) 333.
10. J. Clavilier, R. Durand, G. Guinet and R. Faure, J. Electroanal. Chem., 127 (1981) 281.
11. J. Clavilier, D. Armand and B. L. Wu, J. Electroanal. Chem., 135 (1982) 159.
12. J. Clavilier and D. Armand, J. Electroanal. Chem., 199 (1986`) 187.

13. A. Bewick and J. W. Russell, J. Electroanal. Chem., 142 (1982) 337.
14. R. J. Nichols and A. Bewick, J. Electroanal. Chem, 243 (1988) 445.
15. P. W. Faguy, N. Markovic, R. R. Adzic, C. A. Fierro and E. B. Yeager, J. Electroanal. Chem., 289 (1990) 245.
16. A. Rodes, M. A. Zamakhchari, K. El Achi and J. Clavilier, J. Electroanal. Chem., 305 (1991) 115.
17. A. Rodes, J. Clavilier, J. M. Orts, J. M. Feliu and A. Aldaz, J. Electroanal. Chem., 338 (1992) 317.
18. A. Wieckowski, P. Zelenay and K. Varga, J. Chim. Phys., 88 (1991) 1247.
19. G. Jerkiewicz and B. E. Conway, J. Chim. Phys., 88 (1991) 1381.
20. A. Peremans and A. Tadjeddine, Phys. Rev. Lett., 73 (1994) 3010.
21. A. Tadjeddine and A. Peremans, J. Chim. Phys., 93 (1996) 662.
22. J. Clavilier, R. Albalat, R. Gómez, J. M. Orts and J. M. Feliu, J. Electroanal. Chem., 360 (1992) 325.
23. R. Gómez and J. Clavilier, J. Electroanal. Chem., 354 (1993) 189.
24. J. Clavilier, J. M. Orts, R. Gómez, J. M. Feliu and A. Aldaz, in B. E. Conway and G. Jerkiewicz (Eds.), Electrochemistry and Materials Science of Cathodic Hydrogen Absorption and Adsorption, The Electrochemical Society, PV 94-21, Pennington, NJ, 1995, p. 167.
25. W. Savich, S.-G. Sun, J. Lipkowski and A. Wieckowski, J. Electroanal. Chem., 388 (1995) 233.
26. A. Hamelin, in J. O'M. Bockris, B. E. Conway and R. E. White (Eds.), Modern Aspects of Electrochemistry, Vol. 16, Plenum Press, New York, 1985; Ch. 1.
27. A. Hamelin, S. Morin, J. Richer and J. Lipkowski, J. Electroanal. Chem., 285 (1990) 249.
28. B. E. Conway, H. Angerstein-Kozlowska and W. B. A. Sharp, Trans. Faraday Soc., 19 (1977) 1373.
29. H. Angerstein-Kozlowska, in E. Yeager, J.O'M. Bockris, B. E. Conway and S. Sarangapani (Eds.), Comprehensive Treatise of Electrochemistry, Vol.9, Plenum Press, New York, 1984; Ch. 1.
30. B. E. Conway, W. B. A. Sharp, H. Angerstein-Kozlowska and E. E. Criddle, Anal. Chem., 41 (1973) 1321.
31. G. Jerkiewicz and A. Zolfaghari, J. Phys. Chem., 100 (1996) 8454.

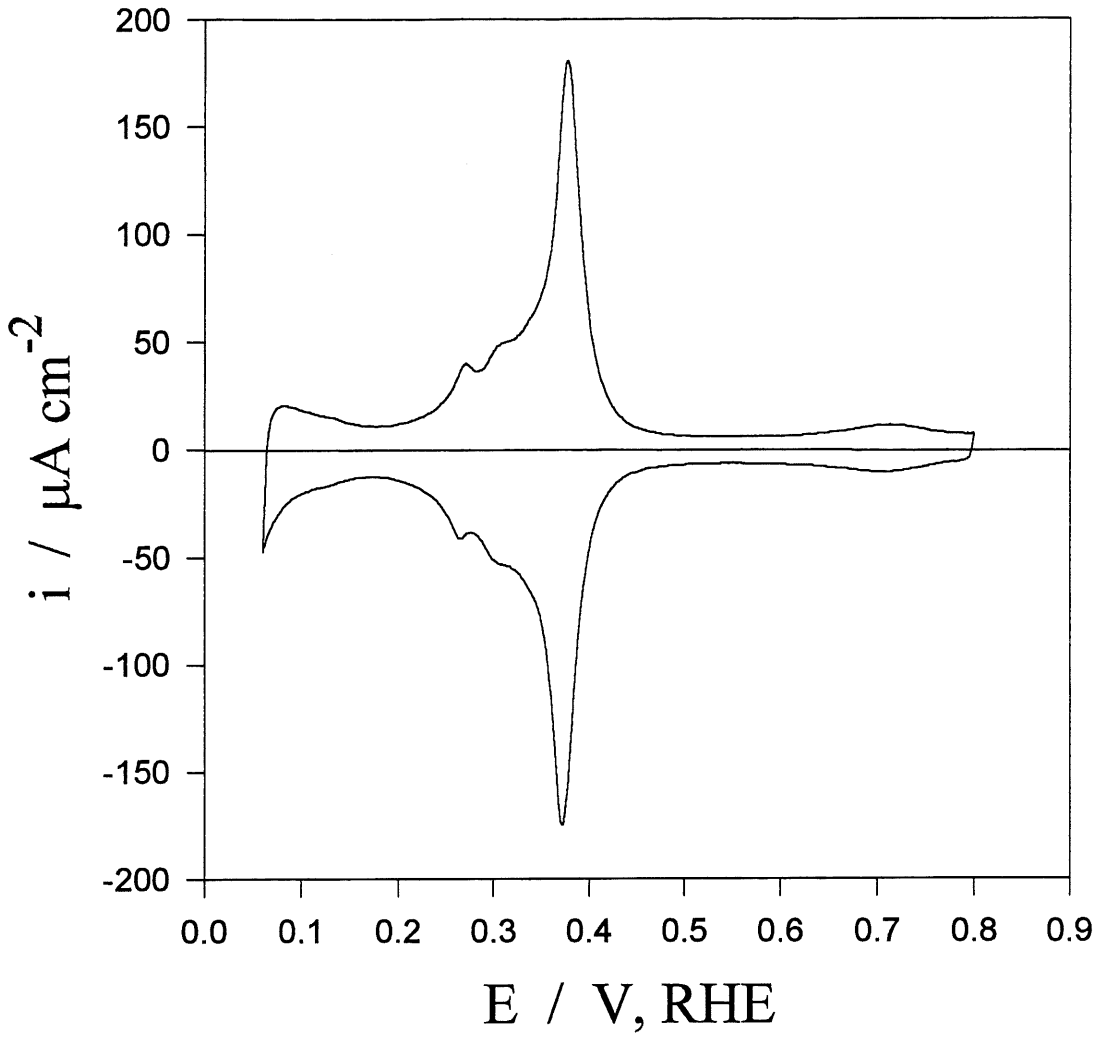

Figure 1. CV profile for Pt(100) cooled in $H_2 + Ar$ in 0.5 M aqueous H_2SO_4 solution; $A = 0.038\ cm^2$, $T = 298\ K$ and $s = 50\ mV\ s^{-1}$. It reveals the following features: (i) a sharp peak at 0.375 V; (ii) a small peak at 0.267 V; and (iii) a shoulder at 0.305 V vs RHE.

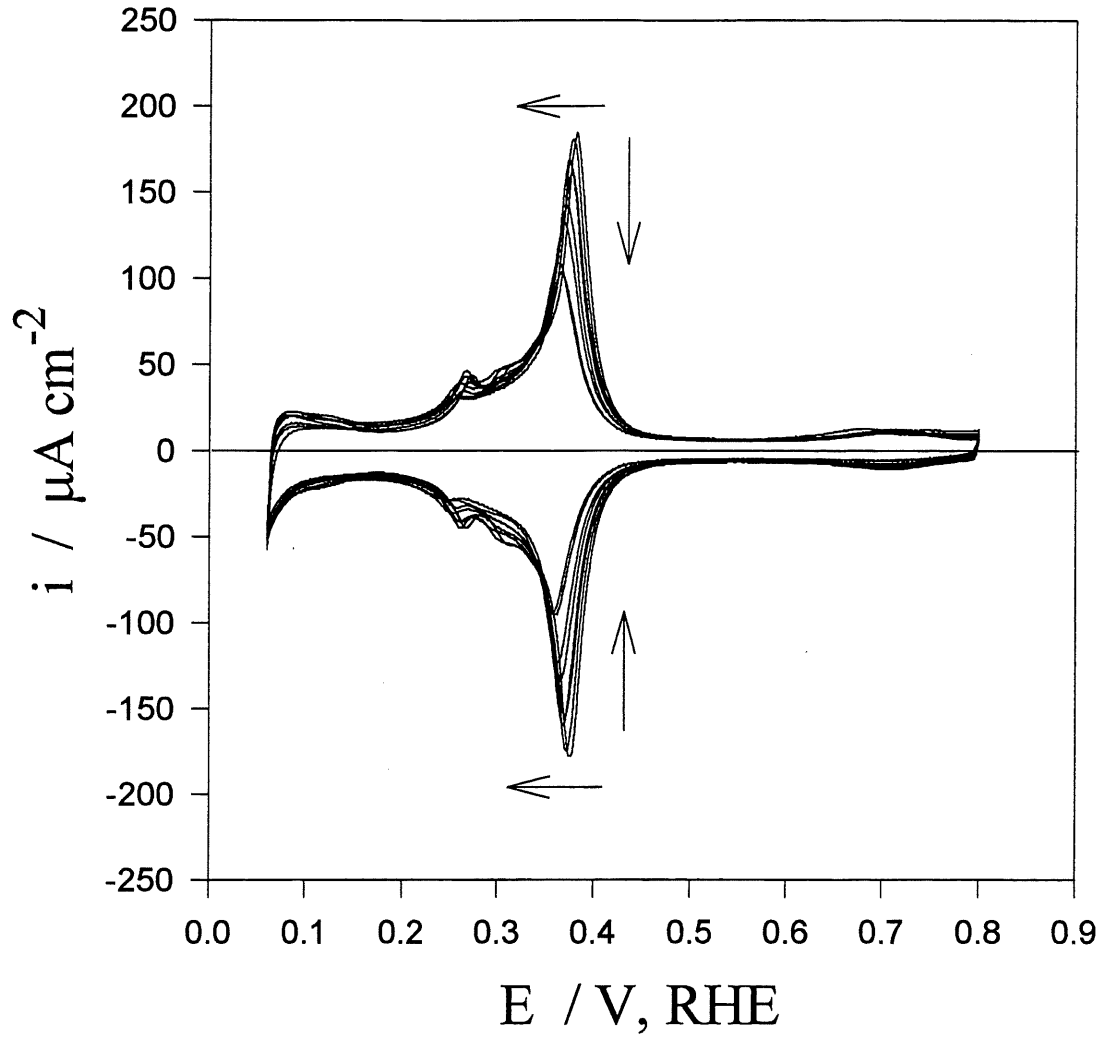

Figure 2. Series of CV profiles for Pt(100) cooled in $H_2 + Ar$ in 0.5 M aqueous H_2SO_4 solution at $293 \leq T \leq 328$ K with an interval of 5 K; $A = 0.038\ cm^2$ and $s = 50\ mV\ s^{-1}$. Arrows indicate changes in the CV profile associated with T increase.

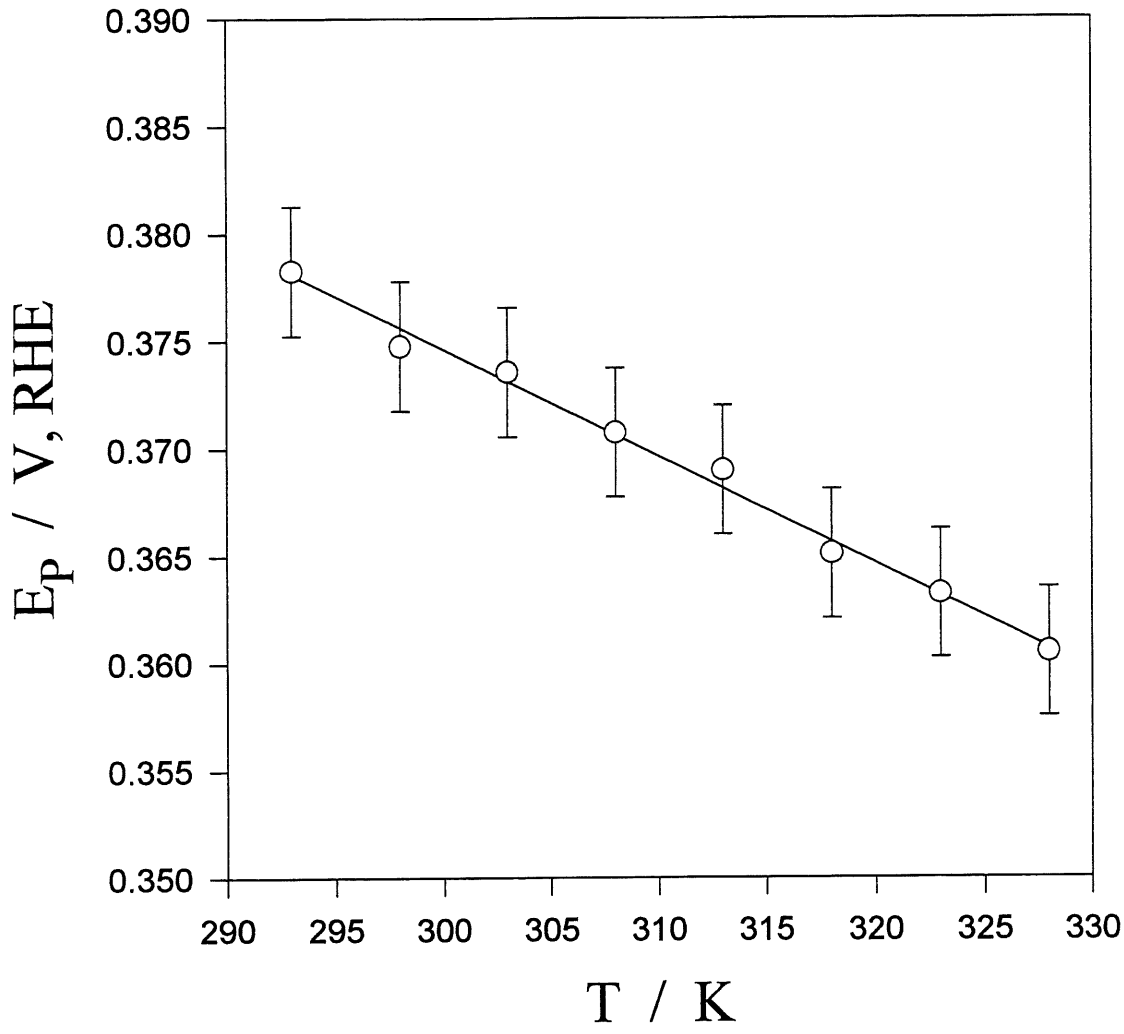

Figure 3. Relation between the potential of the sharp peak, E_P, and T. The E_P versus T dependence is linear and its slope, $\partial E_P / \partial T$, equals -0.50×10^{-3} V K^{-1}.

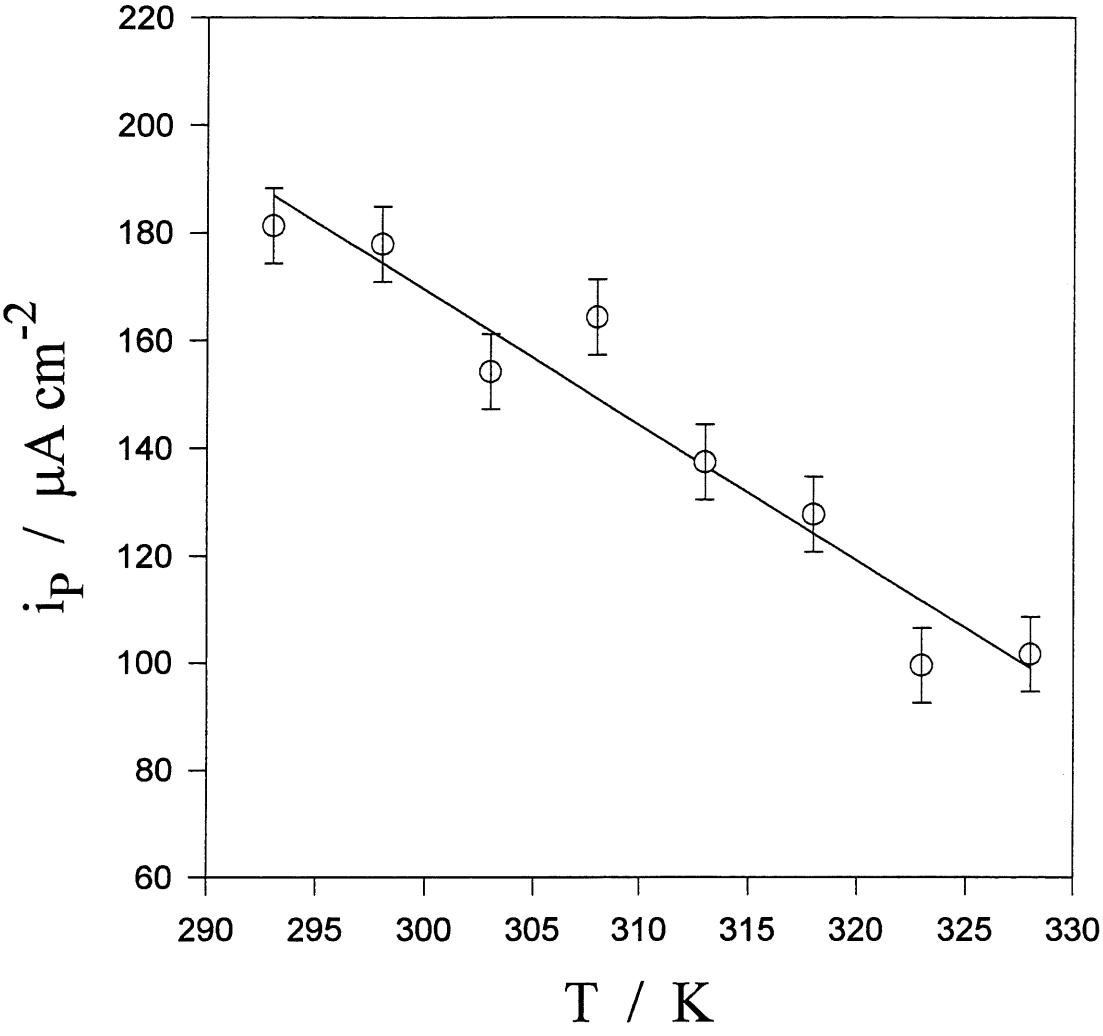

Figure 4. Relation between the current density of the sharp peak, i_P, and T. The i_P versus T dependence is linear and its slope, $\partial i_P / \partial T$, equals -2.50 μA cm^{-2} K^{-1}.

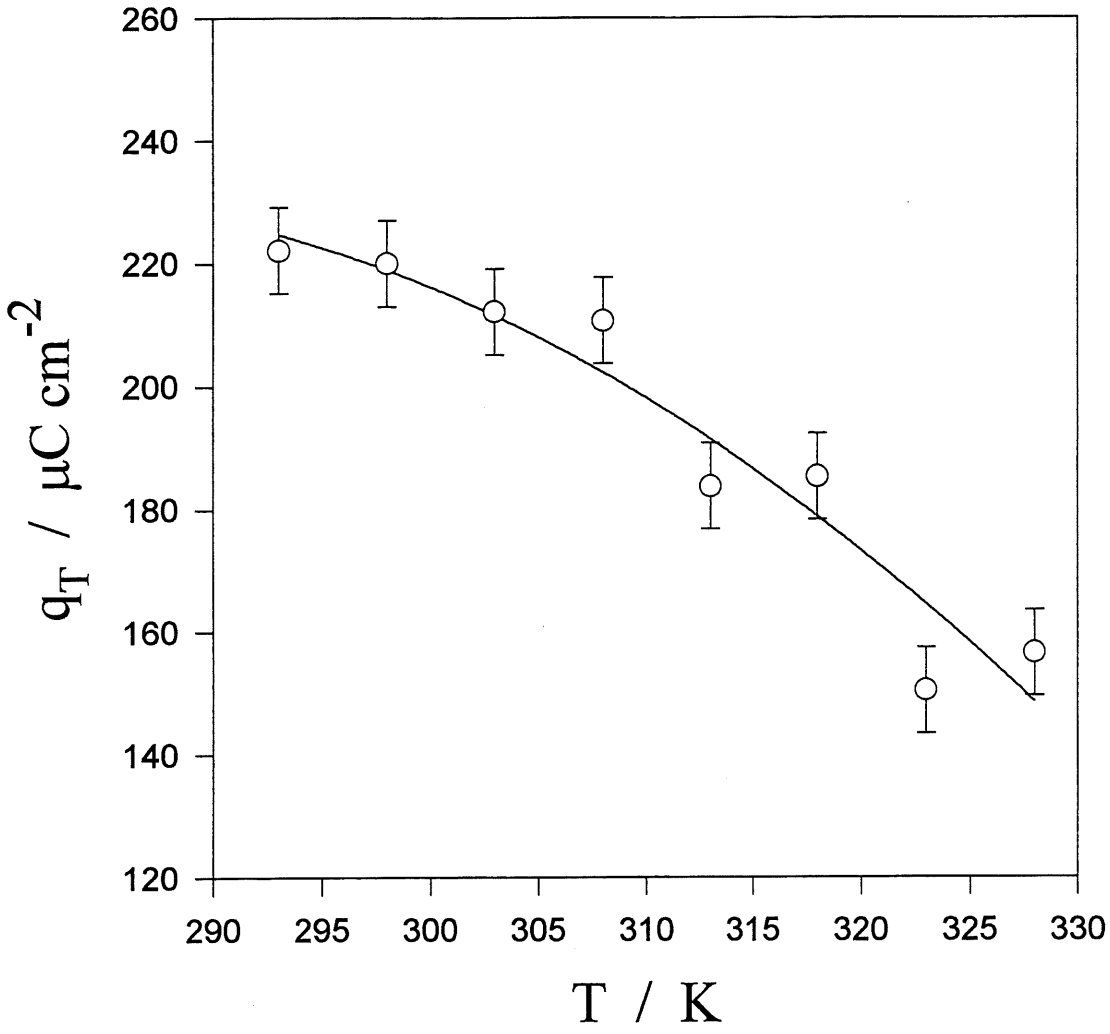

Figure 5. Relation between the total charge density between 0.15 and 0.50 V vs RHE q_T, and T ($q_T = q_{H_{UPD}} + q_{AN}$, where $q_{H_{UPD}}$ is the charge density for the UPD H and q_{AN} is the charge density for the anion adsorption). The q_T versus T dependence is non-linear and the charge density decreases by 70 μC cm^{-2} when T is raised 35 K.

3.2 NEW FINDINGS ON HYDROGEN AND ANION ADSORPTION AT A Pt(111) ELECTRODE IN AQUEOUS H_2SO_4 SOLUTION GENERATED BY TEMPERATURE VARIATION

A. Zolfaghari and G. Jerkiewicz, J. Electroanal. Chem., 422, 1 (1997)

ABSTRACT

Temperature dependence studies of the under-potential deposition of H, UPD H, and anion adsorption on Pt(111) in 0.5 M aqueous H_2SO_4 solution by cyclic-voltammetry, CV, indicate that the overall adsorption-desorption charge density is only slightly affected by temperature, T, variation and that it decreases by 25 $\mu C\,cm^{-2}$ when T is raised from 275 to 338 K. Introductory deconvolution of the CV into two components assigned to the UPD H and the anion adsorption indicates that the charge density associated with the UPD H decreases by 20 $\mu C\,cm^{-2}$ whereas that of the anion adsorption decreases by only 5 $\mu C\,cm^{-2}$. The potential of the sharp peak in the potential region corresponding to the anion adsorption shifts towards more-positive values upon T increase and the peak current density shifts towards lower values. The behavior of the third, asymmetric peak in the double-layer region is complex; the anodic and cathodic components shift towards less-positive potentials but the displacement of the anodic one is more pronounced. The results indicate that the H_{UPD} and anion surface coverages, $\theta_{H_{UPD}}$ and θ_{AN}, respectively, are slightly temperature-dependent and this behavior may be assigned to weak lateral repulsive interactions.

Keywords: Hydrogen under-potential deposition, Anion adsorption, Temperature effect, Pt(111)

1. INTRODUCTION

The significance of the cyclic-voltammetry, CV, profile for the under-potential deposition of hydrogen, UPD H, on a Pt(111) electrode surface in aqueous H_2SO_4 solution has been a subject of profound discussion for over a decade [1-19]. At present, it is well understood that the CV profile corresponds both to the UPD H and to the anion adsorption, and the CO and I-displacement [20-23] as well as chonocoulometry [24] measurements dispelled any doubts about the interpretation of the CV characteristics. In other words, the overall adsorption-desorption charge, as determined on the basis of CV profiles, represents the total charge of hydrogen and anion adsorption. Moreover, the CO or I-displacement experiments and chronocoulometry measurements allow one to determine the charge associated with the UPD H and the anion adsorption. Nevertheless, despite numerous experiments on the UPD H on the Pt(111) electrodes, essentially nothing is known about the temperature, T, dependence of the CV profile, thus about the influence of T variation on the overall adsorption charge as well as on the surface coverage by the under-potential deposited H, H_{UPD}, or the anion, $\theta_{H_{UPD}}$ and θ_{AN}, respectively. Such studies are of great importance

because they provide a direct insight into the nature of lateral interactions between the adsorbed species.

In the present paper, the authors present the new experimental data which demonstrate changes in the CV profile for a Pt(111) electrode in 0.5 M aqueous H_2SO_4 solution brought about by temperature variation. Alteration of the CV profile characteristics is discussed in terms of changes of the surface coverage by the H_{UPD} adatoms and the adsorbed anions. The results indicate that H_{UPD} and anion adsorption is not strongly affected by temperature variation and that the lateral interactions between the adsorbed species are of weak repulsive nature.

2. EXPERIMENTAL

1. Pt(111) Electrode Preparation

The Pt(111) single-crystal electrode used in this research was prepared and oriented according to the procedure developed by Clavilier [1,2] and further advanced by Hamelin [25,26]. The electrode surface was polished with Alumina (0.05 μm) to a mirror-like finish. The quality of the Pt(111) surface was verified by recording a CV in 0.5 M aqueous H_2SO_4 solution at potentials between 0.06 and 0.90 V vs. RHE (Fig. 1). Agreement between the CV profile shown in Fig. 1 and the results reported in literature [5,6,14,22,23] indicate that the crystal was of good quality and properly oriented, and that the surface was well ordered. The electrode diameter, d, was measured with a Vernier microscope and was found to be 0.271 ± 0.002 cm; the surface area, A, was 0.058 ± 0.001 cm^2.

2.2. Solution and Electrochemical Cell

The 0.5 M aqueous H_2SO_4 solution was prepared from BDH Aristar grade H_2SO_4 and Nanopure water (18 MΩ cm). The experiments were conducted in a Pyrex, two-compartment electrochemical cell. The glassware was pre-cleaned according to a well-established procedure [27-29]. During the experiments, H_2 gas, pre-cleaned and pre-saturated with water vapor, was bubbled through the reference electrode compartment in which a Pt/Pt-black electrode was immersed. It served as the reversible hydrogen electrode, RHE, and its potential was −0.021 V versus the standard hydrogen electrode, SHE. High-purity Ar gas, pre-saturated with water vapor, was passed through the working electrode, WE, compartment. The counter electrode, CE, was a Pt wire (99.998% purity, Aesar).

2.3. Cyclic-Voltammetry Temperature-Dependence Measurements

The electrochemical cell was immersed in a water bath (Haake W13) and the temperature was controlled to within ± 0.5 K by means of a thermostat (Haake D1); the water level in the bath was maintained above the electrolyte in the cell. The temperature in the water bath and the electrochemical cell were controlled by means of thermometers (± 0.5 K) and a K-type thermocouple (80 TK Fluke), and were found to agree to within ± 0.5 K. The experiments were conducted at $275 \leq T \leq 338$ K with the first interval being 13 K and the subsequent ones 10 K. Measurements at Pt(111) using the hanging meniscus methodology were difficult to perform above 338 K because of the electrolyte condensation or its creeping along the crystal surface, thus obscuring the CV profile. However, the authors were successful in conducting experiments over a 63 K temperature range.

2.4. Electrochemical Measurements

The experiments involved CV measurements in the potential range corresponding to the UPD H and anion adsorption in 0.5 M aqueous H_2SO_4, thus between 0.06 and 0.90 V vs. RHE. The CV experiments were conducted at a sweep rate of 50 mV s^{-1}. The electrochemical instrumentation employed in the course of research was standard and included: (a) EG&G Model 263A potentiostat-galvanostat; (b) IBM-compatible 80486 computer, and (c) EG&G M270 Electrochemical Software. All potentials were measured with respect to RHE immersed in the same electrolyte and at the same temperature as the Pt(111) working electrode.

3. RESULTS AND DISCUSSION

3.1. Temperature-Dependence of the Pt(111) Cyclic-Voltammetry Profile in 0.5 M H_2SO_4

Fig. 1 shows a CV profile for Pt(111) cooled in $H_2 + Ar$ in 0.5 M aqueous H_2SO_4 solution at 298 K and at potentials between 0.06 and 0.90 V vs. RHE [5,6,14,22,23]. As discussed in the above cited references, the CV profile shows the following features whose behavior as a function of T will be discussed below: (i) the anomalous wave at potentials between 0.06 and 0.30 V; (ii) the so-called butterfly with a sharp peak between 0.32 and 0.55 V; and (iii) a small, asymmetric wave between 0.62 and 0.76 V vs. RHE. The shape of the CV profile indicates that the Pt(111) electrode surface was well ordered and that the electrolyte was free of impurities. Apart from the small asymmetric wave between 0.62 and 0.76 V vs. RHE the CV profile is symmetric with respect to the potential axis indicating that

the surface electrochemical process is reversible. Integration of the anodic and cathodic components of the CV profiles between 0.06 and 0.90 V vs. RHE, allowing for the double-layer charging, leads the authors to evaluation of the average charge density corresponding to both the UPD H and the anion adsorption (the total charge density, $q_T = q_{H_{UPD}} + q_{AN}$, where $q_{H_{UPD}}$ is the charge density for the UPD H and q_{AN} is the charge density for the anion adsorption) which is 253 ± 5 $\mu C\,cm^{-2}$ at 298 K. This charge density differs slightly from the values reported by Clavilier et al., 243 $\mu C\,cm^{-2}$ [6] and 241 $\mu C\,cm^{-2}$ [30]. The authors wish to emphasize that the total charge as determined on the basis of the CV profile does not have to match the theoretical charge of formation of one monolayer (1 ML) of H_{UPD}, thus 240.3 $\mu C\,cm^{-2}$, because the total charge density corresponds both to the UPD H and anion adsorption. In other words, the total charge density, as determined from the CV profile, depends on the surface coverage by H_{UPD} and the adsorbed anion, $\theta_{H_{UPD}}$ and θ_{AN}, respectively. Moreover, the charge density is affected by the chemical identity and the degree of discharge upon adsorption of the anionic species. Thus sulfate and bisulfate might be discharged to a different extent, thus having their unique contributions to the overall adsorption-desorption charge density [24].

Fig. 2 shows a series of CV profiles for the same potential range as in Fig. 1, namely $0.06 \leq E \leq 0.90$ V vs. RHE, for seven temperatures between 275 and 338 K with the first interval being 13 K and the following ones 10 K. The CV profiles are divided into three components whose behavior as a function of T variation is discussed below; the component I corresponds to the UPD H, the components II, which slightly overlaps the first one, is assigned to the anion adsorption and the component III, whose origin is not well understood yet. The results of T-dependence measurements can be outlined as follows: (i) T increase causes small qualitative changes in the region I, the UPD H region; the anomalous wave shifts slightly towards less-positive potentials and the small peak at ca. 0.28 V (which is assigned to a small degree of surface defects, see ref. 30) becomes less pronounced; (ii) the region II, the anion adsorption region (the butterfly), reveals a different behavior; the whole profile and the sharp peak (the spike) shift towards more-positive potentials; (iii) changes in the region III are the most surprising; the T increase causes shift of the wave towards less-positive values however, the displacement of the anodic component is more pronounced than that of the cathodic one. Finally, it should be added that no new features are observed in the CV profiles that could be assigned to T variation in the range reported in this paper.

It should be added that the changes in the CV profiles reported in Fig. 2 are entirely reversible in that decreasing T back to 298 K reproduced the voltammetric intensities reported in Fig. 1 and that decreasing T down to 275 duplicates the original CV profile for this particular temperature. The only CV feature which seems to be very sensitive to the temperature treatment is the current density of the spike. However, Clavilier et al. [6,30] have demonstrated that it depends on the Pt(111) long-range surface order, thus that small degree of surface defects can decrease its sharpness. The authors wish to add that there was no effect of temperature on the geometry of the meniscus between electrode and electrolyte and the electrode contact area remained constant over the temperature range studied, thus that there was no solution creeping along the side wall of the Pt(111) crystal. Such an effect would normally increase the overall current density due to augmentation of the electrode surface area being in direct contact with the electrolyte.

In order to provide a comprehensive but not exhaustive yet examination of the temperature-dependence of the CV profile for Pt(111) in 0.5 M aqueous H_2SO_4, the authors evaluated: (i) variation of the total charge density (regions I, II and III), q_T, as well as the charge density of the UPD H and the anion adsorption, $q_{H_{UPD}}$ and q_{AN}, respectively; (ii) the shift of the potential, E_P, of the spike; and (iii) the changes of the anodic and cathodic component of the wave in the double-layer region (the region III). The deconvolution of the charge density of the regions I and II was carried out as follows. The charge of the UPD H (region I) was determined by integrating the current density between 0.06 V vs. RHE and the minimal current density of the CV profile between the region I and the region II, thus around 0.32 V vs. RHE (this limit shifts by some 20 mV when T is raised 63 K). The charge density of the anion adsorption was evaluated by integrating the current density between the latter limit (close to 0.32 V) and the upper potential limit corresponding to the anion adsorption, thus a potential close to 0.55 V vs. RHE; at this limit, the current density drops to values characteristic of the double layer charging. In performing the integration, the authors allowed for the double layer charging. Fig. 3 shows results of the integration of the charge densities determined according to the above described procedure. The total adsorption charge density, q_T, varies between 253 ± 5 to 228 ± 5 $\mu C\,cm^{-2}$, depending on T; the charge density corresponding to the UPD H decreases from 157 ± 5 to 137 ± 5 $\mu C\,cm^{-2}$ whereas that of the anion adsorption diminishes from 90 ± 5 to 85 ± 5 $\mu C\,cm^{-2}$ upon T augmentation. The results indicate that T increase from 275 to 338 K has almost no impact on the anion adsorption charge density and that the charge density of the H_{UPD} adsorption decreases by 20 $\mu C\,cm^{-2}$.

Thus it is reasonable to conclude that the CV profile alteration associated with T increase is noticeable but that it is not very pronounced. It is of interest to direct the reader's attention to the behavior of a Pt(100) electrode in the same electrolyte [31]; in this case, the anion adsorption was significantly decreased when T was raised whereas the H_{UPD} adsorption charge density was only slightly affected. Finally it ought to be stressed that the above presented results of deconvolution of the CV profiles into the H_{UPD} and anion adsorption components are only an estimation and that they carry some uncertainty because the UPD H and the anion adsorption potential regions overlap. However, the authors believe that at this preliminary level the above results provide new and important data on the temperature-dependence of the UPD H and the anion adsorption on the Pt(111) electrode.

Fig. 4 shows the experimentally determined variation of E_P of the spike as a function of T on the basis of results shown in Fig. 2. The data indicate that the E_P versus T relation is linear and its slope, $\partial E_P / \partial T$, equals 0.57×10^{-3} V K^{-1}. Thus on average an increase of the temperature by 10 K increases the peak potential by almost 6 mV. Again, it is of interest to compare the Pt(111) behavior with that of Pt(100) under the same experimental conditions. The results presented in ref. 31 indicate that the $\partial E_P / \partial T$ parameter for the Pt(100) electrode has negative values, thus demonstrating that the peak potential corresponding to the anion adsorption shifts towards less-positive values when T is raised whereas the Pt(111) electrode reveals exactly an opposite behavior. Thus one may conclude that thermodynamic of the anion adsorption on these two single-crystal electrode surfaces are divergent. The CV profiles presented in Fig. 2 also indicate that the current density of the spike is affected by T variation and that it tends to decrease when T is raised. However, it should be added that the sharpness of the spike, thus its maximal current density, is influenced by the thermal treatment, the so-called annealing and quenching, and even small modification of the procedure can bring about a tiny percentage of surface defects which affect the spike's sharpness.

Fig. 5 shows the peak potential of the anodic and the cathodic component of the wave in the double-layer region (region III) based on the CV profiles shown in Fig. 2. These results are probably the most surprising and most unexpected because they divulge that the anodic and cathodic components reveal qualitatively the same behavior but quantitative results are distinct. Both components shift towards less-positive values upon T augmentation but the displacement of the anodic one is more pronounced and linear in T whereas the shift of the cathodic one is less noticeable and the E_P vs. T relation is non-linear. More interestingly, upon T increase, the gap between the two peaks decreases and at 338 K the wave maxima

differ by only 20 mV. This is a new observation which has not been reported in previous literature and it might be of importance in subsequent interpretation of this anomalous behavior of the Pt(111) CV profile.

3.2. Preliminary Interpretation of the Temperature-Dependence of the Pt(111) Cyclic-Voltammetry Profile

On the basis of the CO or I-displacement measurements as well as chronocoulometry data [20-24] it is apparent that the CV profile at $0.06 \leq E \leq 0.55$ V vs. RHE for Pt(111) corresponds to the UPD H and the anion adsorption, thus $q_T = q_{H_{UPD}} + q_{AN}$. Because q_T decreases upon T extension towards higher values, it is apparent that the total surface coverage by both the adsorbed species, θ_T (where $\theta_T = \theta_{H_{UPD}} + \theta_{AN}$, and $\theta_{H_{UPD}}$ is the H_{UPD} surface coverage and θ_{AN} is the anion coverage), diminishes but only slightly. Preliminary deconvolution of the CV profiles into individual components assigned to the UPD H and the anion adsorption shows that the H_{UPD} surface coverage slightly decreases upon T increase. This observation points to the repulsive nature of the lateral interactions between the H_{UPD} adatoms [32] however it should be emphasized that they are not very strong because in presence of powerful repulsions, the H_{UPD} surface coverage, $\theta_{H_{UPD}}$, would decrease more than observed in the experiments. The temperature-dependence of the anion surface coverage, θ_{AN}, is even less affected by T increase indicating that the lateral interactions between the adsorbed species are weakly repulsive.

In this preliminary note, the authors present new and hitherto unreported data on the temperature-dependence of the UPD H and anion adsorption on a Clavilier-type Pt(111) single-crystal electrode surface. They believe, the current paper is the first contribution which demonstrates how the CV profile is affected by the temperature variation. At present, they are involved in similar research on a Pt(111) electrode but in less-concentrated solutions of H_2SO_4. They believe that temperature dependence studies of the UPD H in diluted solutions, where the UPD H and anion adsorption regions are well separated, followed by theoretical treatment [32] will lead to elucidation, for the first time, of thermodynamic state functions of adsorption, namely $\Delta G^{\circ}_{ads}(H_{UPD})$, $\Delta S^{\circ}_{ads}(H_{UPD})$ and $\Delta H^{\circ}_{ads}(H_{UPD})$, as well as the bond energy between the Pt(111) substrate and H_{UPD}, $E_{Pt(111)-H_{UPD}}$.

CONCLUSIONS

Studies of the UPD H and anion adsorption on a Pt(111) electrode in 0.5 M aqueous H_2SO_4 solution by cyclic-voltammetry indicate that the adsorption-desorption charge density decreases slightly (by 25 $\mu C\ cm^{-2}$) when T is raised 63 K. The CV component corresponding to the UPD H shifts towards less-positive values when T is increased whereas that of the anion adsorption towards more-positive ones. The surface coverage by the H_{UPD} adatoms and the adsorbed anions decreases slightly upon T extension indicating that the lateral interactions between alike species are weakly repulsive. The asymmetric wave in the double-layer region reveals a complex comportment; its anodic and cathodic components reveal qualitatively similar but quantitatively different behavior upon T augmentation.

ACKNOWLEDGMENTS

Acknowledgment is made to the NSERC of Canada and FCAR du Québec for support of this research. A. Zolfaghari acknowledges a graduate fellowship from the MCHE of Iran.

REFERENCES

1. J. Clavilier, R. Faure, G. Guinet and R. Durand, J. Electroanal. Chem., 107 (1980) 205.
2. J. Clavilier, J. Electroanal. Chem., 107 (1980) 211.
3. C. L. Scortichini and C. N. Reilley, J. Electroanal. Chem., 139 (1982) 233; 247.
4. C. L. Scortichini, F. E. Woodward and C. N. Reilley, J. Electroanal. Chem., 139 (1982) 265.
5. D. Aberdam, R. Durand, R. Faure and F. El-Omar, Surface Sci., 171 (1986) 303.
6. J. Clavilier, K. El Achi, M. Petit, A. Rodes and M. A. Zamakhchari, J. Electroanal. Chem., 295 (1990) 333.
7. D. Armand and J. Clavilier, J. Electroanal. Chem., 270 (1989) 331.
8. J. Clavilier, D. Armand and B. L. Wu, J. Electroanal. Chem., 135 (1982) 159.
9. J. Clavilier and D. Armand, J. Electroanal. Chem., 199 (1986`) 187.
10. A. Bewick and J. W. Russell, J. Electroanal. Chem., 142 (1982) 337.
11. R. J. Nichols and A. Bewick, J. Electroanal. Chem, 243 (1988) 445.
12. N. Markovic, N. Marinkovic and R. R. Adzic, J. Electroanal. Chem, 241 (1988) 309.
13. P. W. Faguy, N. Markovic, R. R. Adzic, C. A. Fierro and E. B. Yeager, J. Electroanal. Chem., 289 (1990) 245.

14. K. Itaya, S. Sugawara, K. Sashikata and N. Furuya, J. Vac. Sci. Technol. A8 (1), (1990) 515.
15. N. M. Markovic, N. Marinkovic and R. R. Adzic, J. Electroanal. Chem, 314 (1991) 289.
16. A. Wieckowski, P. Zelenay and K. Varga, J. Chim. Phys., 88 (1991) 1247.
17. G. Jerkiewicz and B. E. Conway, J. Chim. Phys., 88 (1991) 1381.
18. A. Peremans and A. Tadjeddine, Phys. Rev. Lett., 73 (1994) 3010.
19. A. Tadjeddine and A. Peremans, J. Chim. Phys., 93 (1996) 662.
20. J. Clavilier, R. Albalat, R. Gómez, J. M. Orts and J. M. Feliu, J. Electroanal. Chem., 360 (1992) 325.
21. R. Gómez and J. Clavilier, J. Electroanal. Chem., 354 (1993) 189.
22. J. Clavilier, J. M. Orts, R. Gómez, J. M. Feliu and A. Aldaz, in B. E. Conway and G. Jerkiewicz (Eds.), Electrochemistry and Materials Science of Cathodic Hydrogen Absorption and Adsorption, The Electrochemical Society, PV 94-21, Pennington, NJ, 1995, p. 167.
23. E. Herrero, J. M. Feliu, A. Wieckowski and J. Clavilier, Surface Sci., 325 (1995) 131.
24. W. Savich, S.-G. Sun, J. Lipkowski and A. Wieckowski, J. Electroanal. Chem., 388 (1995) 233.
25. A. Hamelin, in J. O'M. Bockris, B. E. Conway and R. E. White (Eds.), Modern Aspects of Electrochemistry, Vol. 16, Plenum Press, New York, 1985; Ch. 1.
26. A. Hamelin, S. Morin, J. Richer and J. Lipkowski, J. Electroanal. Chem., 285 (1990) 249.
27. B. E. Conway, H. Angerstein-Kozlowska and W. B. A. Sharp, Trans. Faraday Soc., 19 (1977) 1373.
28. H. Angerstein-Kozlowska, in E. Yeager, J.O'M. Bockris, B. E. Conway and S. Sarangapani (Eds.), Comprehensive Treatise of Electrochemistry, Vol.9, Plenum Press, New York, 1984; Ch. 1.
29. B. E. Conway, W. B. A. Sharp, H. Angerstein-Kozlowska and E. E. Criddle, Anal. Chem., 41 (1973) 1321.
30. J. Clavilier, A. Rodes, K. El Achi and M. A. Zamakhchari, J. Chim. Phys., 88 (1991) 1291.
31. A. Zolfaghari and G. Jerkiewicz, J. Electroanal. Chem., in press (1996).
32. G. Jerkiewicz and A. Zolfaghari, J. Phys. Chem., 100 (1996) 8454.

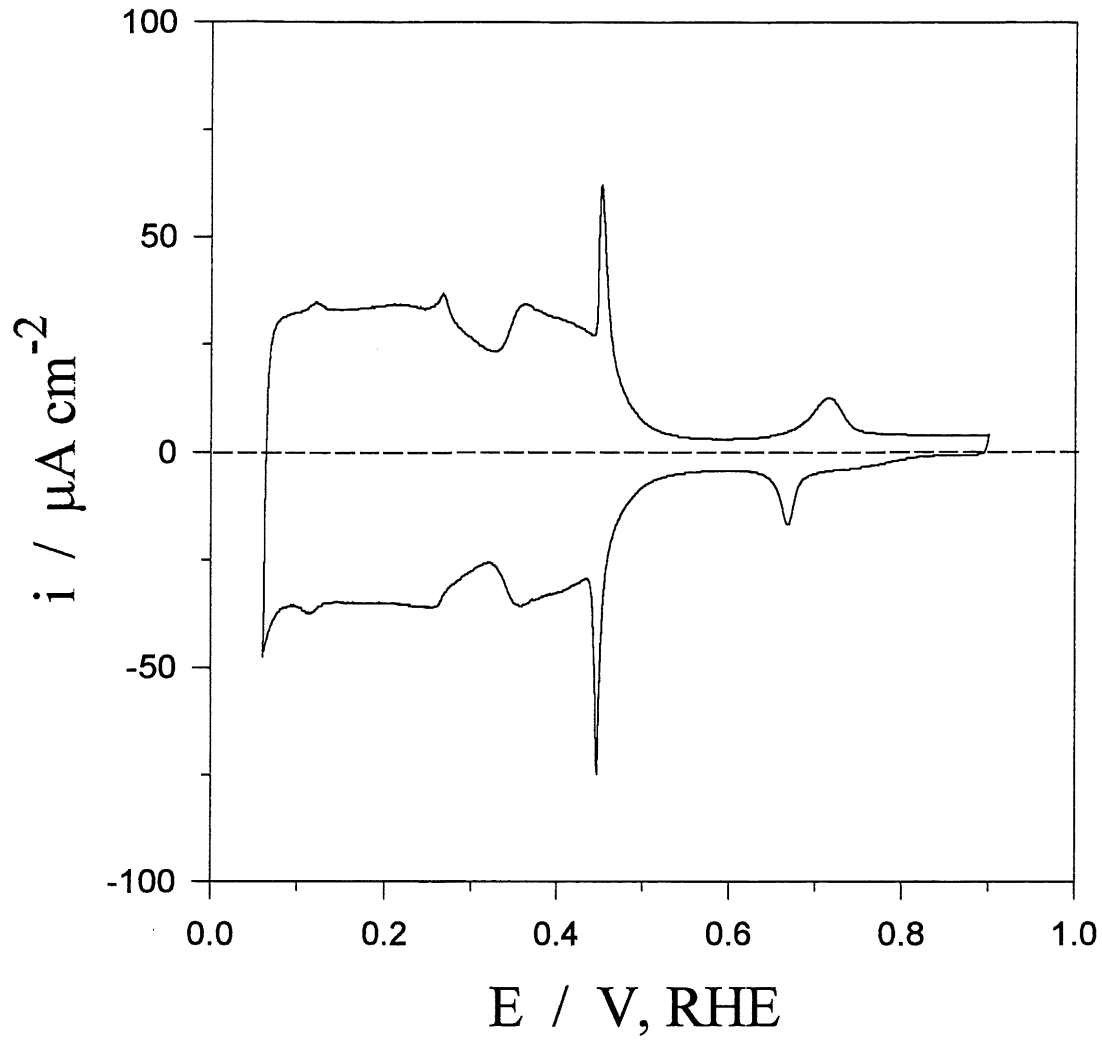

Figure 1. CV profile for a Pt(111) electrode cooled in $H_2 + Ar$ in 0.5 M aqueous H_2SO_4 solution; $A = 0.058\ cm^2$, $T = 298\ K$ and $s = 50\ mV\ s^{-1}$. The CV diagram reveals the following features: (i) the anomalous wave between 0.06 and 0.30 V vs. RHE; (ii) the so-called butterfly with a sharp peak potentials between at 0.32 and 0.55 V vs. RHE; (iii) a small, asymmetric wave between 0.62 and 0.76 V vs. RHE.

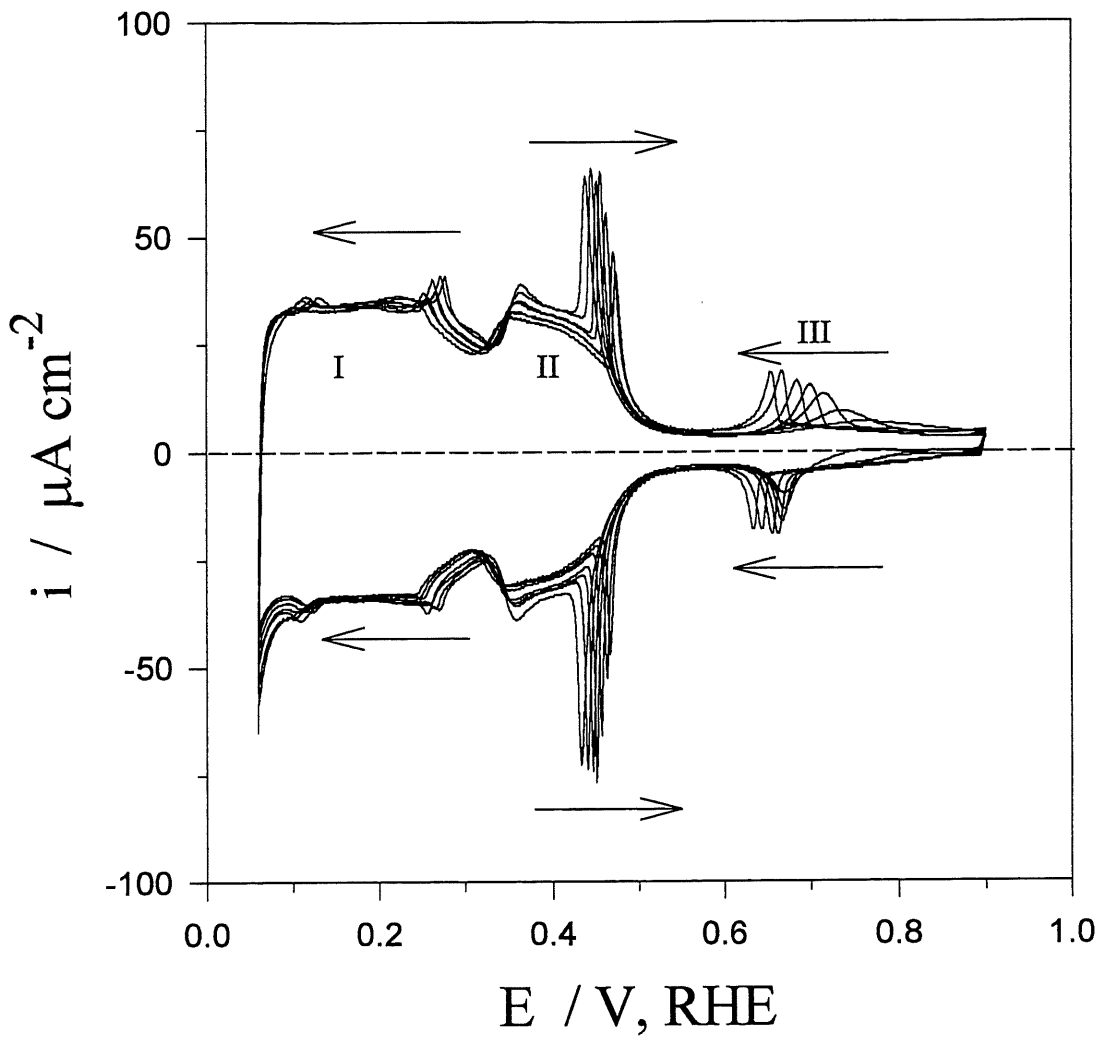

Figure 2. Series of CV profiles for a Pt(111) electrode cooled in H_2 + Ar in 0.5 M aqueous H_2SO_4 solution at $275 \leq T \leq 338$ K with the first interval being 13 K and the subsequent ones 10 K; $A = 0.058$ cm^2 and $s = 50$ mV s^{-1}. Arrows indicate changes in the CV profile associated with T increase. The CV diagrams are divided into three parts; the region I corresponding to the UPD H, the region II associated with the anion adsorption and the region III.

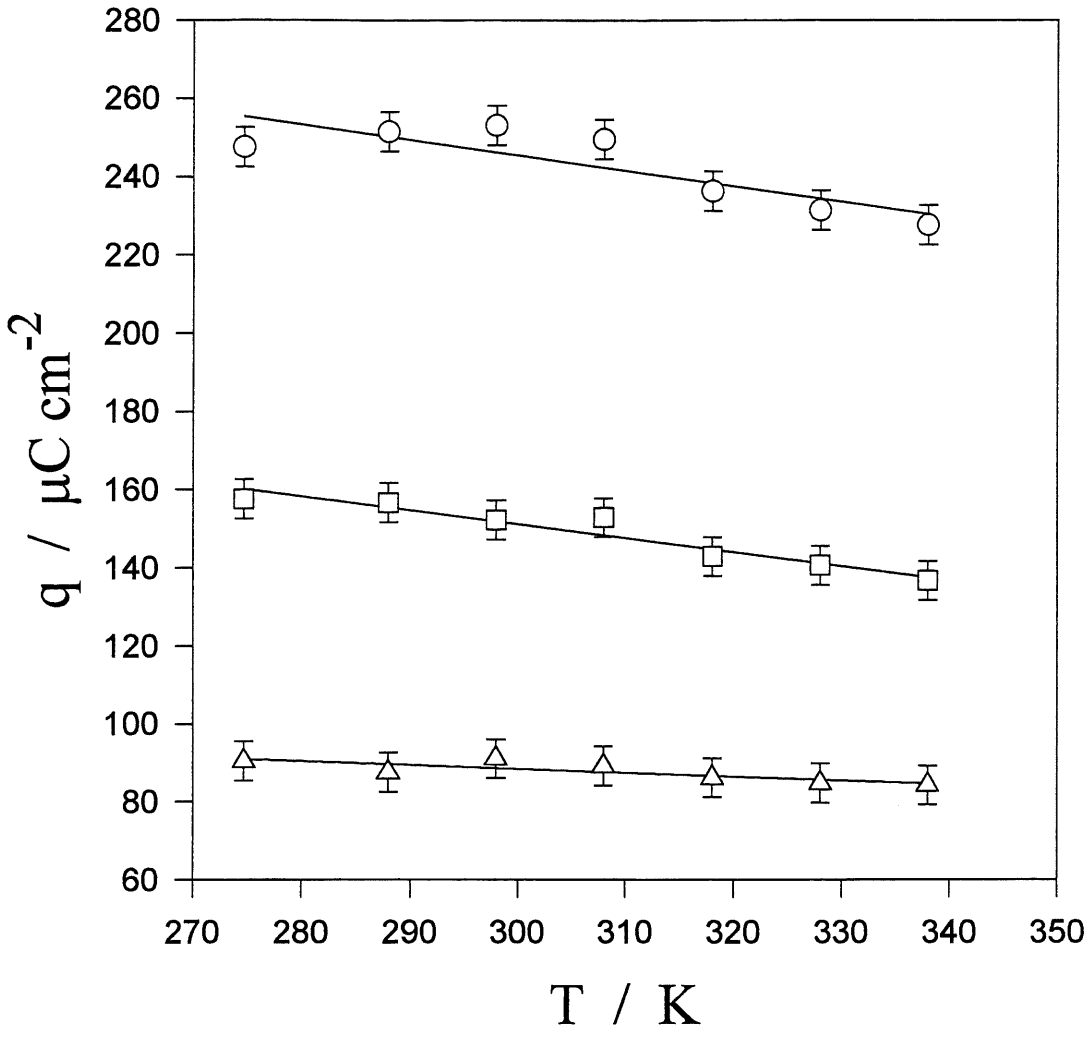

Figure 3. Relation between the total adsorption charge density, q_T (O), the UPD H charge density, $q_{H_{UPD}}$ (□), and the anion adsorption charge density, q_{AN} (Δ), as a function of temperature, T.

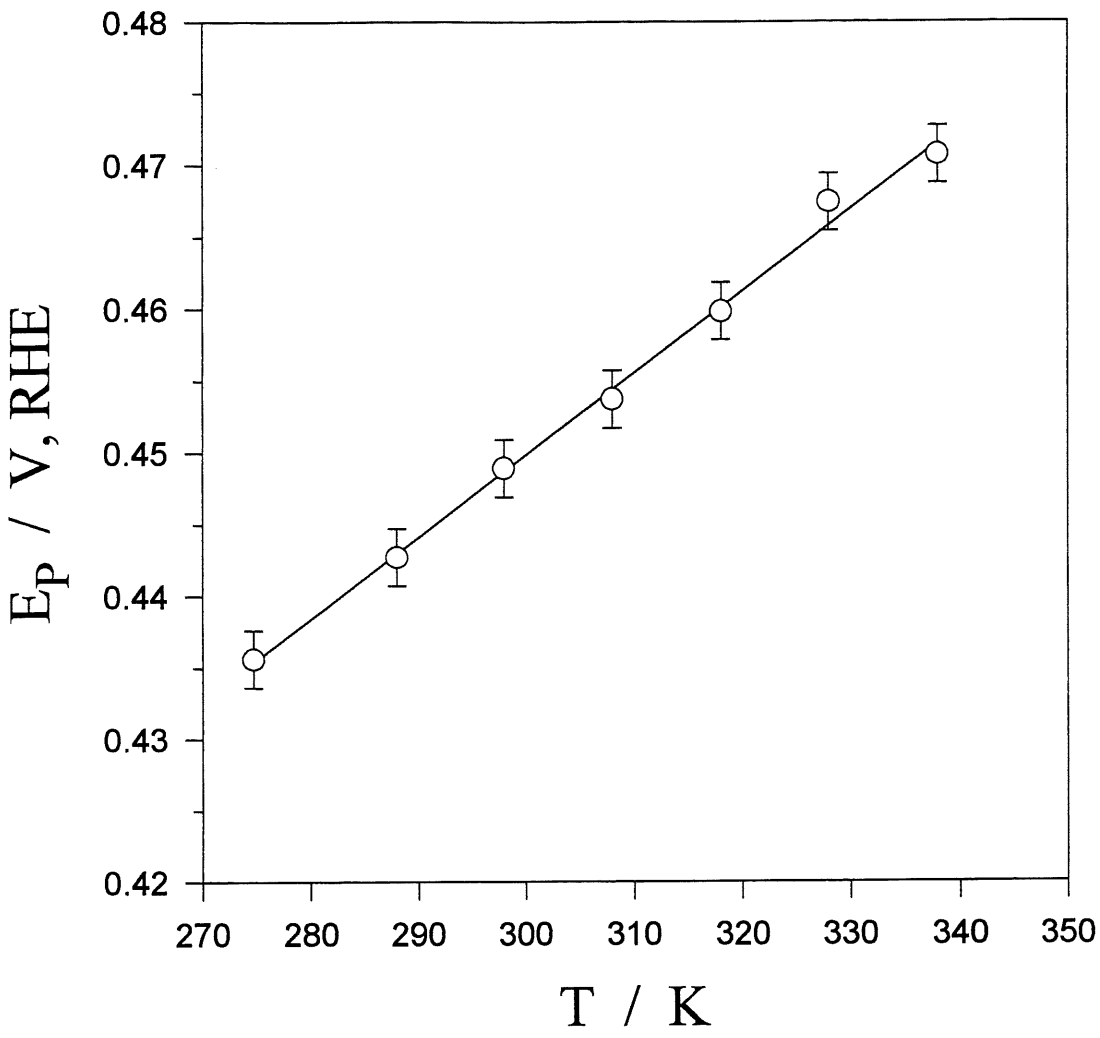

Figure 4. Relation between the potential of the sharp peak (the spike), E_P, and T. The E_P vs. T dependence is linear and its slope, $\partial E_P / \partial T$, equals 0.57×10^{-3} V K^{-1}.

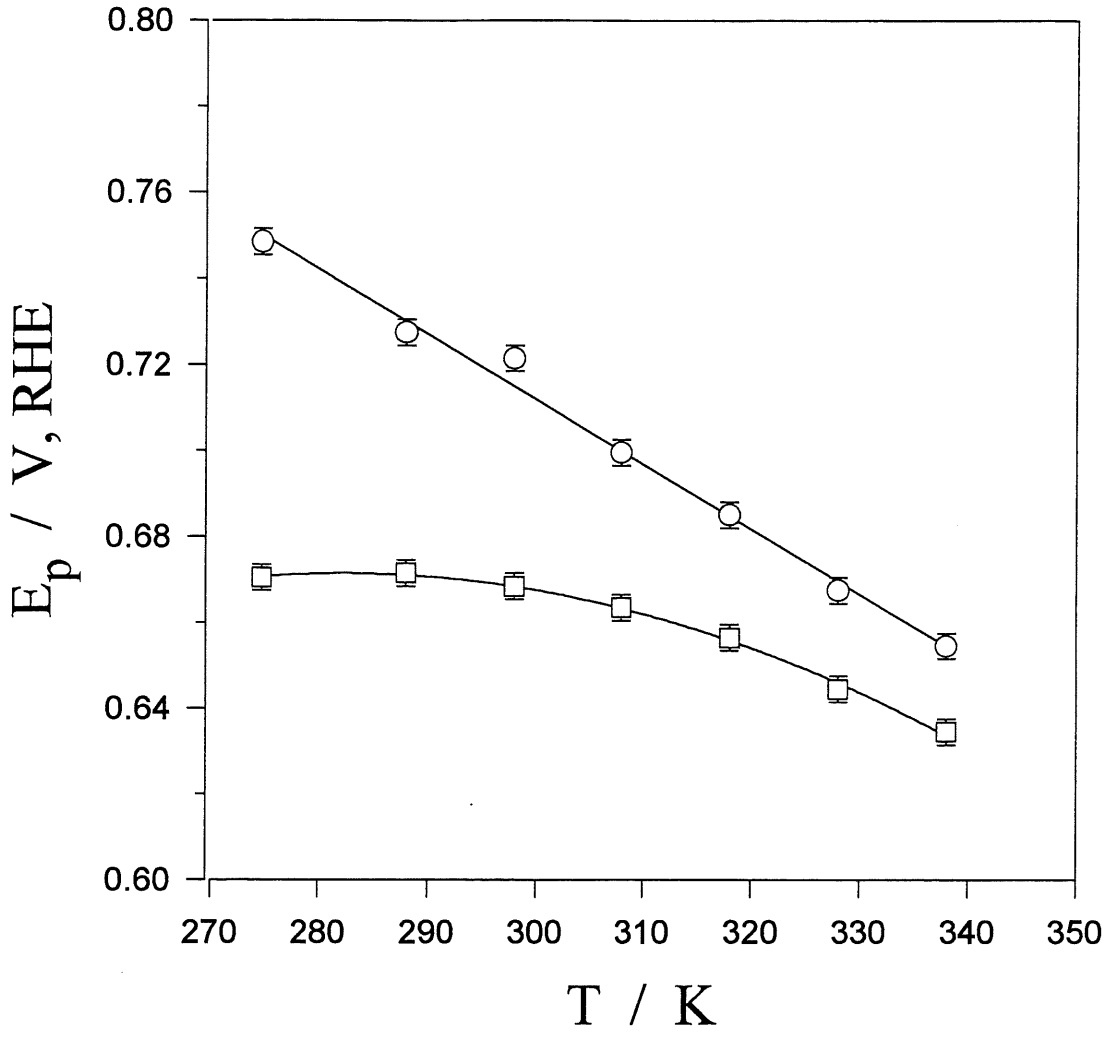

Figure 5. Relation between the maximal potential of the anodic (O) and the cathodic (□) component of the anomalous wave in the double-layer region (between 0.62 and 0.76 V vs. RHE) and T. The gap between the wave's maxima decreases when T is raised.

3.3 NEW FINDINGS ON THE TEMPERATURE DEPENDENCE OF H AND ANION ADSORPTION ON Pt(111) AND Pt(100) ELECTRODES IN AQUEOUS H_2SO_4

A. Zolfaghari and G. Jerkiewicz, Electrochim. Acta, Submitted (1997)

ABSTRACT

The temperature dependence of the under-potential deposition of hydrogen, UPD H, and anion adsorption on Pt(111) and Pt(100) in aq. solutions of H_2SO_4 was studied by application of cyclic-voltammetry, CV. An analysis of the CV profiles for Pt(111) and Pt(100) shows that the UPD H and anion adsorption regions shift towards less-positive potentials when T is raised. Integration of the CV's for Pt(111) discloses that the overall adsorption-desorption charge density decreases from 255 to 230 $\mu C\,cm^{-2}$ when T is raised from 275 to 328 K. In the case of Pt(100), the overall adsorption-desorption charge density decreases from 220 to 150 $\mu C\,cm^{-2}$, thus by 70 $\mu C\,cm^{-2}$ when T is raised from 293 to 328 K. Because the H_{UPD} and anion adsorption regions on Pt(111) in 0.05 M aq. H_2SO_4 are separated, one may determine $\Delta G_{ads}(H_{UPD})$, $\Delta S^{\circ}_{ads}(H_{UPD})$, $\Delta H^{\circ}_{ads}(H_{UPD})$ and the $Pt(111)-H_{UPD}$ surface bond energy, $E_{Pt(111)-H_{UPD}}$. The data show that $\Delta G_{ads}(H_{UPD})$ varies from -26 to -8 $kJ\,mol^{-1}$, $\Delta S^{\circ}_{ads}(H_{UPD})$ from -80 to -62 $J\,mol^{-1}\,K^{-1}$, $\Delta H^{\circ}_{ads}(H_{UPD})$ from -44 to -33 $kJ\,mol^{-1}$, and $E_{Pt(111)-H_{UPD}}$ from 262 to 250 $kJ\,mol^{-1}$. An analysis of the $\Delta G_{ads}(H_{UPD})$ versus $\theta_{H_{UPD}}$ plots reveal that the UPD H follows the Frumkin isotherm and the energy of lateral repulsions, ω, is 27 ± 2 $kJ\,mol^{-1}$, and the respective dimensionless parameter g is close to 11. The value of $E_{Pt(111)-H_{UPD}}$ is close to the surface bond energy between the chemisorbed H, H_{chem}, and Pt(111), $E_{Pt(111)-H_{chem}}$, the later being 255 $kJ\,mol^{-1}$.

INTRODUCTION

Two events marked the origin of electrochemical surface science: introduction of UHV-based techniques to electrochemistry [1,2], and incorporation of spherical and rod-shaped single crystals of Pt and Au [3-5]. Introduction of monocrystalline Pt beads [3,4,6] and their protection without expensive UHV equipment resulted in abundant research on well-defined electrode surfaces and in molecular-level comprehension of the electrified solid-liquid interface and surface electrocatalysis [7-11]. Originally, research on the under-potential deposition of hydrogen, UPD H, and adsorption of anions on Pt(111) and Pt(100) was a subject of intense research and scientific discussion for many years and it resulted in foundation of standard CV profiles which are characteristic of well-ordered surfaces [4,10-20]. At the current stage of knowledge, it is apparent that in many cases the potential regions of the UPD H and the anion adsorption on Pt(hkl) and Rh(hkl) electrodes overlap and that the adsorption charge density determined from cyclic-voltammetry, CV, provides the total charge which corresponds to both the H_{UPD} adsorption-desorption and anion desorption-adsorption.

The CO-displacement experiments [21-23] were essential in proving the nature of the adsorbed species and producing indisputable evidence on the occurrence of the two electrode processes in the same potential range.

Much research has been done on the UPD of H and metals as well as anion adsorption on Pt single-crystal electrodes but little is known about the T-dependence of the UPD H and anion adsorption on Pt(hkl). There are only two preliminary notes which provide a qualitative insight into the behavior of the adsorbed species when T is varied [24,25]. The present paper is an extension to the previous work and it presents further interpretation of the previously published data as well as new results CV data and thermodynamics parameters on the UPD H on Pt(111) in 0.05 M aq. H_2SO_4.

EXPERIMENTAL

Pt(111) and Pt(100) Electrode Preparation

The Pt(111) and Pt(100) single crystals were prepared and oriented according to the procedure developed by Clavilier [3,4] and subsequently advanced by Hamelin [5,26]. They were polished with Alumina (0.25 μm, Struers) to a mirror-like finish and the quality of the Pt(111) and Pt(100) surfaces was verified by recording CV profiles in aq. H_2SO_4 solution at potentials between 0.06 and 0.90 V, RHE, for Pt(111) and between 0.06 and 0.80 V, RHE, for Pt(100) (see Figs. 1 and 2). Agreement the results presented in Figs. 1 and 2 and those reported in the literature [6,16,17] reveals that the Pt single crystals were of good quality and that the surfaces were well ordered. The electrode diameter, d, was measured with a Vernier microscope and was found to be 0.271 ± 0.002 cm and 0.219 ± 0.002 cm for Pt(111) and Pt(100), respectively. The surface areas, A, were $0.058 \pm 0.001\ cm^2$ and $0.038 \pm 0.001\ cm^2$, respectively. Prior to each measurement, the crystals were annealed in a hydrogen flame (at around 1100 °C) and cooled in $H_2 + Ar$.

Solution and Electrochemical Cell

The 0.5 M and 0.05 M aq. H_2SO_4 solutions were prepared from BDH Aristar grade H_2SO_4 and Nanopure water (18 MΩ cm). The experiments were conducted in a Pyrex, two-compartment electrochemical cell. The glassware was pre-cleaned according to a well-established procedure [27-29]. During the experiments, H_2 gas, pre-cleaned and pre-saturated with water vapor, was bubbled through the reference electrode compartment in which a Pt/Pt-black electrode was immersed. It served as the reversible hydrogen electrode,

RHE. High-purity Ar gas, pre-saturated with water vapor, was passed through the working electrode, WE, compartment through and above solution. The counter electrode, CE, was a Pt wire (99.998% purity, Aesar).

Temperature-Dependence Measurements

The electrochemical cell was immersed in a water bath (Haake W13) and the temperature was controlled to within ± 0.5 K by means of a thermostat (Haake D1); the water level in the bath was maintained above the electrolyte in the cell. The temperature in the water bath and the electrochemical cell were controlled by means of thermometers (± 0.5 K) and a K-type thermocouple (80 TK Fluke), and were found to agree to within ± 0.5 K. The experiments were conducted with an interval of 5 K.

Electrochemical Measurements

The experiments involved CV measurements in the potential range corresponding to the UPD H and anion adsorption in 0.5 M and 0.05 M aq. H_2SO_4. The CV experiments were conducted at a sweep rate of 20 and 50 mV s^{-1}. The electrochemical instrumentation included: (a) EG&G Model 263A potentiostat-galvanostat; (b) IBM-compatible 80486 computer, and (c) EG&G M270 Electrochemical Software. All potentials were measured with respect to RHE immersed in the same electrolyte. The potential of the Pt/Pt black RHE in 0.05 and 0.5 M aq. H_2SO_4 solutions shifts towards more-positive values when T is raised. In order to correct the potential referred to the RHE scale at $T = 298$ K, it is necessary to introduce the $\partial E / \partial T$ correction factor which equals 8.4×10^{-4} V K^{-1} [30]. The conversion of the RHE at 298 K to the SHE is accomplished by application of the following relations: $E_{SHE} = E_{RHE(0.05\,M)} + 0.021$ V and $E_{SHE} = E_{RHE(0.5\,M)} + 0.075$ V. The above formulae may be derived on the basis of the Nernst and Davis equations [31]; the Davis relation allows examination of the activity coefficient of the hydrated proton as a function of the ionic strength of electrolyte.

RESULTS AND DISCUSSION

Temperature Dependence of UPD H and Anion Adsorption on Pt(111)

Fig. 1 shows a CV profile for Pt(111) in 0.5 M aq. H_2SO_4 at 298 K at potentials between 0.06 and 0.90 V, RHE; Pt(111) had been cooled in H_2 + Ar prior to conducting CV measurements [6,7,32]. The authors distinguish the potential region of the UPD H (region I) and the anion adsorption characterized by a sharp spike (region II). The shape of the CV indicates that the Pt(111) surface was well ordered and that the electrolyte was free of impurities. Apart from the small peak/wave in the double-layer region, the profile is symmetric with respect to the potential axis indicating that the surface electrochemical processes are kinetically reversible. In Fig. 3, the authors show a series of CV profiles for Pt(111) in 0.5 M aq. H_2SO_4 for $275 \leq T \leq 328$ K with the first temperature interval, ΔT, equal to 13 K and the subsequent ones being 10 K. Unlike in the preliminary note [25], the potentials corresponding to the UPD H and anion adsorption are shown with respect to the SHE; the potential of the RHE was converted to the SHE scale according to the methodology described in *Experimental*. Upon T increase, the CV characteristics corresponding to the UPD H and anion adsorption shift towards less-positive potentials but the displacement of the UPD H profiles (region I) is more pronounced than that of the anion one (region II). In ref. 25, the authors showed that integration of the CV profiles led to determination of the total adsorption charge density, q_T, as a function of T ($q_T = q_{H_{UPD}} + q_{AN}$ where $q_{H_{UPD}}$ is the charge density for the UPD H and q_{AN} is the charge density for the anion adsorption). At 298 K, the values of q_T is 252 ± 5 $\mu C\,cm^{-2}$ and it does not have to give the theoretical value of one monolayer (ML) H_{UPD} (240.3 $\mu C\,cm^{-2}$) because the profile corresponds to both the surface-electrochemical processes, namely the UPD H and anion adsorption [21-23]. Since the charge density does not have to equal to that of 1 ML of H_{UPD}, the overall charge density depends on the surface coverage by H_{UPD} and the adsorbed anion, $\theta_{H_{UPD}}$ and θ_{AN}, respectively, and it may vary its value accordingly. Furthermore, since the charge density of the adsorbed species is affected by their chemical identity and the degree of discharge upon adsorption of the ionic species, at the present state of knowledge it is difficult to predict any "theoretical charge density" of adsorption that the integration of the CV profile should provide.

An analysis of the data shown in ref. 25 leads to the following summary of the T-dependence of charge densities for the surface electrochemical processes occurring on Pt(111) in 0.5 M aq. H_2SO_4 in the 0.06 0.90 V, RHE, potential range (Table I).

Table I. Summary of the T-dependence of charge densities for the adsorption processes on Pt(111).

T / K	q_T / μC cm^{-2}	$q_{H_{UPD}}$ / μC cm^{-2}	q_{AN} / μC cm^{-2}
275	262 ± 5	179 ± 5	75 ± 5
328	222 ± 5	146 ± 5	68 ± 5

The authors examined the shift of the peak potential, E_P, of the sharp peak (the "spike") in the potential region corresponding to anions adsorption (region II) as well as the changes of the anodic and cathodic component of the wave in the double-layer region (the region III). Fig. 4 shows the experimentally determined variation of E_P of the sharp peak as a function of T on the basis of results shown in ref. 25 and Fig. 3; the graph reveals two linear plots, one corresponding to the RHE potential scale and the other to the SHE one. The results testify that the E_P versus T relation is linear in both cases and that the slope, $\partial E_P / \partial T$, equals 0.57×10^{-3} V K^{-1} for the RHE scale and -0.27×10^{-3} V K^{-1} for the SHE one. The wave/peak in the double-layer region is asymmetric with respect to the E axis but the difference between the peak potentials decreases upon T increase [25].

Temperature Dependence of UPD H and Anion Adsorption on Pt(100)

The CV profile for Pt(100) in 0.5 M aq. H_2SO_4 at 298 K at potentials between 0.06 and 0.80 V, RHE (Pt(100) had been cooled in H_2 + Ar prior to conducting electrochemical measurements) shown in Fig. 2 is characteristic of a well-ordered Pt(100) surface; it reveals that the UPD H and anion adsorption processes occur within two potential regions which overlap, thus q_T as determined on the basis of CV measurements.

In Fig. 5, the authors demonstrate a series of CV profiles for Pt(100) in 0.5 M aq. H_2SO_4 for $293 \leq T \leq 328$ K with a temperature interval, ΔT, equal to 5 K; the potentials corresponding to the electro-adsorption phenomena are quoted with respect to the SHE (in ref. 24, the potential are given with respect to the RHE). The profiles are symmetric with respect to E axis, thus testifying that the surface electrochemical processes taking place in this potential range are kinetically reversible. Upon T increase, the CV characteristics corresponding to the UPD H and anion adsorption shift towards less-positive potentials [21-23]; the current density of the sharp peak which corresponds to the anion adsorption significantly decreases [21-24]. Integration of the CV's allowed the authors to conclude that

q_T decreases from 220 to 150 $\mu C\,cm^{-2}$, thus by 70 $\mu C\,cm^{-2}$, when T is raised by only 35 K, namely from 293 to 328 K. It was impossible to determine $q_{H_{UPD}}$ and q_{AN} because the profiles may not be easily deconvoluted into two components representing two distinct surface electrochemical processes (interesting deconvolution of the CV profile for Pt(100) in 0.5 M aq. H_2SO_4 followed by theoretical treatment based on the three-state lattice gas model is presented in ref. 33). The remarkable decrease of q_T (by 32% of the total charge at 298 K) for such a narrow T range is indicative of a very strong T-dependence of the surface electrode processes. However, at present one may not conclude how much of the diminished charge density is associated with the UPD H and how much with anion adsorption.

Fig. 6 shows the experimentally determined variation of E_P of the sharp peak (representing the anion adsorption) as a function of T on the basis of results shown in ref. 24 and Fig. 5. The graph reveals two linear plots, one corresponding to the RHE potential scale and the other to the SHE one. The results testify that the E_P versus T relation is linear in both cases and that the slope, $\partial E_P / \partial T$, equals $-0.50 \times 10^{-3}\ V\,K^{-1}$ for the RHE scale and $-1.34 \times 10^{-3}\ V\,K^{-1}$ for the SHE one. It is interesting to notice that the intercept of the two sets of linear plots shown in Figs. 4 and 6 falls at $T = 323$ K for a reason that remains unclear at the present time and calls for further theoretical research.

Thermodynamics of the UPD H on Pt(111)

Thermodynamics of the UPD H on well-defined Pt(hkl) electrodes had ever been examined before and the authors focused their effort on determination of thermodynamic state functions of the process and the $Pt(111)-H_{UPD}$ surface bond energy [34-37]. Some work had been performed on energetics of the UPD H on Pt electrodes claimed to be of single-crystal nature [38,39] but an analysis of the CV profiles discloses that the electrodes were disordered, thus that they were of polycrystalline nature [38].

Research on thermodynamics of the UPD H on Pt(111) by application of CV as an experimental tool followed by theoretical treatment of the experimental data [34-37] is feasible only in a diluted aq. H_2SO_4 solution because the two components of the CV profile corresponding to the UPD H and anion adsorption are separated. In Fig. 7, the authors show a set of CV's for Pt(111) in 0.05 M aq. H_2SO_4. Their scrutiny discloses that the H_{UPD} and anion adsorption slightly overlap, therefore the deconvolution of the profiles into two components representing the two processes carries some uncertainty (less than 2%; it is resolved on the basis of the charge under the overlapping components) because the form of

their adsorption isotherms for H_{UPD} and anion is not well defined. Nevertheless, even with an uncertainty of some 2%, the current interpretation is of importance and it represents an substantial contribution. Elsewhere [40], the authors will demonstrate simulations of the CV profile for H_{UPD} and anion adsorption on Pt(111).

On the basis of these CV profiles for the entire range of T studied and equation 1, the authors examined energetics of the UPD H [34-37].

$$\frac{\theta_{H_{UPD}}}{1-\theta_{H_{UPD}}} = f_{H_2}^{1/2} \exp\left(-\frac{E_{RHE}F}{RT}\right)\exp\left(-\frac{\Delta G_{ads}(H_{UPD})}{RT}\right) \qquad (1)$$

where E_{RHE} is the potential measured versus the RHE in the same electrolyte and at the same T, f_{H_2} is the fugacity of molecular hydrogen in the RHE compartment (under normal conditions $f_{H_2} \cong P_{H_2}$; it is corrected for the vapor pressure of the electrolyte at T), and $\Delta G_{ads}(H_{UPD})$ is the Gibbs free energy of adsorption at T and at the potential, E_{RHE}, at which the H_{UPD} coverage reaches the value of $\theta_{H_{UPD}}$. Equation 1 is a different form of equation 2 which describes the UPD H on the SHE scale (for derivation, see ref. 35).

$$\frac{\theta_{H_{UPD}}}{1-\theta_{H_{UPD}}} = a_{H^+} \exp\left(-\frac{E_{SHE}F}{RT}\right)\exp\left(-\frac{\Delta G^{\circ}_{ads}(H_{UPD})}{RT}\right) \qquad (2)$$

where E_{SHE} is the potential versus the SHE at which the H_{UPD} coverage reaches the value of $\theta_{H_{UPD}}$, $\Delta G^{\circ}_{ads}(H_{UPD})$ is the standard Gibbs energy of adsorption, a_{H^+} is the activity of proton in electrolyte, and F and R are standard physico-chemical constants.

Elsewhere [35,36], the authors stressed that equations 1 and 2 represent a general electrochemical adsorption isotherm for the UPD H, not the Langmuir or the Frumkin one, and no hypothesis is made with regard to presence/absence of lateral interactions between the H_{UPD} adatoms. Thus $\Delta G_{ads}(H_{UPD})$, as determined on the basis of equation 1 or 2, already contains the H_{UPD} coverage and temperature dependent energy of lateral interactions, $\omega(\theta_{H_{UPD}}, T)$. An analysis of the experimentally examined 3D $\Delta G_{ads}(H_{UPD})$ vs. $(\theta_{H_{UPD}}, T)$ plots allows one to assess the applicability of any of the adsorption isotherms to the system under study. If the $\Delta G_{ads}(H_{UPD})$ vs. $\theta_{H_{UPD}}$ relation is linear (equation 3), then one may say that the

Frumkin isotherm is applicable. On the other hand, if $\Delta G_{ads}(H_{UPD})$ is constant and does not vary with $\theta_{H_{UPD}}$, then the Langmuir isotherm applies (equation 4).

$$\Delta G^{\circ}_{ads}(H_{UPD})_{\theta_{H_{UPD}}\neq 0} = \Delta G^{\circ}_{ads}(H_{UPD})_{\theta_{H_{UPD}}=0} + \theta_{H_{UPD}}\,\omega \qquad (3)$$

$$\Delta G^{\circ}_{ads}(H_{UPD})_{\theta_{H_{UPD}}\neq 0} = \Delta G^{\circ}_{ads}(H_{UPD})_{\theta_{H_{UPD}}=0} \qquad (4)$$

On the ground of the data shown in Fig. 7 and equation 1, the authors determined E_{RHE} at which $\theta_{H_{UPD}}$ had various but well-defined values, namely from 0.05 to 0.65 with an interval of 0.05, for a series of T from 273 to 328 K, with an interval of 5 K. Such determined sets of values of $\theta_{H_{UPD}}$, E_{RHE} and T were introduced into equation 1 and $\Delta G_{ads}(H_{UPD})$ was determined. The numerically assessed values of $\Delta G_{ads}(H_{UPD})$ are shown in Fig. 8 versus $\theta_{H_{UPD}}$ and T. The data show that $\Delta G_{ads}(H_{UPD})$ has values from -26 to -8 kJ mol^{-1} and that it has the most negative values at the smallest $\theta_{H_{UPD}}$ and the lowest T.

The standard entropy of adsorption, $\Delta S^{\circ}_{ads}(H_{UPD})$, is obtained by analysis of the experimental $\Delta G_{ads}(H_{UPD})$ versus T relations for every $\theta_{H_{UPD}} = \text{const}$ (equation 5). Because the $\Delta G_{ads}(H_{UPD})$ versus T plots are linear (Fig. 8) for every $\theta_{H_{UPD}}$ studied, one may easily determine $\Delta S^{\circ}_{ads}(H_{UPD})$ as a function of $\theta_{H_{UPD}}$ (Fig. 9). The data show that $\Delta S^{\circ}_{ads}(H_{UPD})$ has values from -63 to -79 J mol^{-1} K^{-1}.

$$\Delta S^{\circ}_{ads}(H_{UPD}) = -\left(\frac{\partial \Delta G_{ads}(H_{UPD})}{\partial T}\right)_{\theta_{H_{UPD}}=\text{const}} \qquad (5)$$

Examination of $\Delta G_{ads}(H_{UPD})$ versus $\theta_{H_{UPD}}$ (for $T = \text{const}$) leads to appraisal of the nature and strength of the energy of lateral interactions, $\omega(H_{UPD})$, acting between the H_{UPD} adatoms (equation 6), and to estimation of the adsorption isotherm which governs the process.

$$\omega(H_{UPD}) = -\left(\frac{\partial \Delta G_{ads}(H_{UPD})}{\partial \theta_{H_{UPD}}}\right)_{T=\text{const}} \qquad (6)$$

The values of $\omega(H_{UPD})$ for various T are shown in Fig. 10 and they reveal that $\omega(H_{UPD})$ is scattered over a narrow range, namely between 25 and 29 kJ mol^{-1}, the average value of lateral interactions, $\bar{\omega}(H_{UPD})$, being 27 kJ mol^{-1}. In order to examine if $\omega(H_{UPD})$ is a function of T, the authors fitted the points into a linear relation and determined that the slope of the $\omega(H_{UPD})$ versus T plot was 2.2×10^{-2} kJ mol^{-1} K^{-1}, thus there was practically no T-dependence of $\omega(H_{UPD})$ because an increase of T by 100 K would result in a very small (2.2 kJ mol^{-1}) variation of $\omega(H_{UPD})$. Thus the points are scattered over a narrow range and this is related to the experimental uncertainty which will be discussed in a subsequent paper. Positive values of $\omega(H_{UPD})$ indicate that *the lateral interactions are repulsive*. It is essential to emphasize, for the first time, that the UPD H on Pt(111) in 0.05 M aq. H_2SO_4 follows *the Frumkin electrochemical isotherm*. This conclusion is of importance in comprehension of the nature of H_{UPD} and in analysis of its adsorption site by combining spectroscopic [41-44] and thermodynamic results. Knowledge of the average value of $\omega(H_{UPD})$ allows one to determine value of the dimensionless interaction parameter *g* which appears in the Frumkin isotherm (see refs. 45,46 and equation 7) and which is defined by equation 8. In order to avoid confusion, the authors wish to add that the parameter *g* appears on the left-hand side of equation 7.

$$\frac{\theta_{H_{UPD}}}{1-\theta_{H_{UPD}}} \exp\left(g\,\theta_{H_{UPD}}\right) = a_{H^+} \exp\left(-\frac{E_{SHE}F}{RT}\right) \exp\left(-\frac{\Delta G^{\circ}_{ads}(H_{UPD})_{\theta_{H_{UPD}}=0}}{RT}\right) \qquad (7)$$

$$g = \frac{\omega(H_{UPD})}{RT} \qquad (8)$$

The average value of the interaction parameter equals to 11 and it indicates that the lateral interaction between the H_{UPD} adatoms on Pt(111) are strongly repulsive.

The enthalpy of adsorption for the UPD H on Pt(111) in 0.05 M aq. H_2SO_4, $\Delta H^{\circ}_{ads}(H_{UPD})$, is evaluated based on the above determined values of $\Delta G_{ads}(H_{UPD})$ at 298 K, thus $\Delta G^{\circ}_{ads}(H_{UPD})$, and $\Delta S^{\circ}_{ads}(H_{UPD})$, and the well-known formula $\Delta G^{\circ} = \Delta H^{\circ} - T\,\Delta S^{\circ}$. Fig. 11 shows a $\Delta H^{\circ}_{ads}(H_{UPD})$ vs. $\theta_{H_{UPD}}$ relation and demonstrates that $\Delta H^{\circ}_{ads}(H_{UPD})$ accepts negative values between -44 and -32 kJ mol^{-1}.

The $Pt(111)-H_{UPD}$ surface bond energy, $E_{Pt(111)-H_{UPD}}$, had never been evaluated for H_{UPD} on a well-defined single-crystal electrode albeit its values were available for Rh(poly)

and Pt(poly) electrodes [34-39]. Also, evaluation of the $E_{Pt(111)-H_{UPD}}$ versus $\theta_{H_{UPD}}$ relation is of importance in determination of the influence of the electrified solid-liquid interface on the strength and nature of the $Pt(111)-H_{UPD}$ surface bond. The energy of the $Pt(111)-H_{UPD}$ bond was determined based on the values of $\Delta H^{\circ}_{ads}(H_{UPD})$ for various H_{UPD} surface coverages (Fig. 11) and equation 9 [35-37].

$$E_{M-H_{UPD}} = \frac{1}{2} D_{H_2} - \Delta H^{\circ}_{ads}(H_{UPD}) \qquad (9)$$

Fig. 12 shows values of $E_{Pt(111)-H_{UPD}}$ for various H_{UPD} coverages, $\theta_{H_{UPD}}$, for the UPD H in 0.05M aq. H_2SO_4. The data reveal that the $Pt(111)-H_{UPD}$ bond energy falls in the fall in $250-262$ kJ mol^{-1} range and that its variation with $\theta_{H_{UPD}}$ is rather negligible.

It is essential to relate the values of $E_{Pt(111)-H_{UPD}}$ with that for H chemisorbed dissociatively under gas-phase conditions on Pt(111), $E_{Pt(111)-H_{chem}}$. The values of the $Pt(111)-H_{chem}$ bond energy is 255 kJ mol^{-1} [47]; the datum for $E_{Pt(111)-H_{chem}}$ and the data for $E_{Pt(111)-H_{UPD}}$ indicate that the respective bond energies for H_{UPD} and H_{chem} are close to each other, say within some less than 10 kJ mol^{-1}. In his review article, Christmann [47] recognized that the values of the $M-H_{chem}$ bond energies, $E_{M-H_{chem}}$, fall into the $250-270$ kJ mol^{-1} range for various transition metals and that it is almost unaffected by the surface structure of the substrate. Proximity of the values of $E_{M-H_{chem}}$ and their independent of the surface geometry points to a similar surface binding mechanism on various transition metals [47]. It is tempting to state that H_{UPD} should occupy the same surface adsorption site as H_{chem} based on the consistency of the respective bond energies [35-37]. However, the SFG IR experimental results of Tadjeddine and Peremans [43,44] do not support the viewpoint and the authors conclude that H_{UPD} occupies the on-top surface adsorption site. Thus, the issue of the adsorption site of H_{UPD} still remains open albeit the surface bond energy is known at the present time. Confirmation of the SFG IR data by another technique would lead to conclusion that the electrochemical interface selects a different adsorption site for H_{UPD} on Pt(111), yet still results in a bond being energetically equivalent to H_{chem}. Should this be correct, one would have to consider the surface electronic structure of the top-most layer by taking into account local electronic effects associated with the metal surface geometry and respective density of surface states.

Relation of H_{UPD} to H_{chem} and the Volcano Relation

It is essential to elaborate on the meaning of the widely-accepted volcano relation [46,48] which relates log of the exchange current density for the hydrogen evolution reaction, HER, i_o, to the Gibbs free energy of adsorption of the adsorbed H being an intermediate of the reaction. It is well established in electrochemistry that the onset of the UPD H takes place at positive potentials with respect to E°_{HER} while the HER occurs at negative ones and it is the over-potential deposited H, H_{OPD}, that is an intermediate of the process. It must be stressed that the values of $\Delta G^{\circ}_{ads,H}$ (after ref. 46) refer to H_{chem} (values for H_{OPD} are not available) whereas i_o is related to H_{OPD}, thus one compares thermodynamic and kinetic data for two distinct species. Interestingly, the relation does work and allows one to explain the kinetic results. In the present context, it remains puzzling that one obtains meaningful interpretation of kinetic data for the HER using thermodynamic values of the Gibbs free energy of adsorption for the chemisorbed H. This observation which at the present state seems inconsistent calls for careful reexamination of the state of knowledge on H_{UPD}, H_{OPD}, and H_{chem} as well as on their mutual connection.

ACKNOWLEDGMENTS

Acknowledgments is made to the NSERC of Canada, le FCAR du Québec and l'Université de Sherbrooke for support of this research project. A. Zolfaghari gratefully acknowledges a fellowship from the MCHE of Iran and an Energy Research Summer Fellowship of the US DOE, administered by The Electrochemical Society, Inc. The authors thank Professor Juan M. Feliu of Universidad de Alicante for his precious advice in setting up the system for preparation and orientation of Pt single crystals. They also gratefully acknowledge stimulating discussion with Dr. Jean Clavilier of CNRS Muedon.

REFERENCES

1. R. M. Ishikawa, J. Y. Katekaru and A. T. Hubbard, J. Electroanal. Chem., 86 (1978) 271.

2. A. T. Hubbard, Chem. Rev., 88 (1988) 633.

3. J. Clavilier, R. Faure, G. Guinet and R. Durand, J. Electroanal. Chem., 107 (1980) 205.

4. J. Clavilier, J. Electroanal. Chem., 107 (1980) 211.

5. A. Hamelin, Ch. 1 in "Modern Aspects of Electrochemistry", J. O'M. Bockris, B. E. Conway and R. E. White, Eds., Vol. 16, Plenum Press, New York (1985).

6. J. Clavilier, K. El Achi, M. Petit, A. Rodes and M. A. Zamakhchari, J. Electroanal. Chem., 295 (1990) 333.

7. D. Aberdam, R. Durand, R. Faure and F. El-Omar, Surface Sci., 171 (1986) 303.

8. C. Lamy, J. M. Leger, J. Clavilier and R. Parsons, J. Electroanal. Chem., 150 (1983) 71.

9. J. Clavilier, R. Durand, G. Guinet and R. Faure, J. Electroanal. Chem., 127 (1981) 281.

10. J. Clavilier, D. Armand and B. L. Wu, J. Electroanal. Chem., 135 (1982) 159.

11. J. Clavilier and D. Armand, J. Electroanal. Chem., 199 (1986`) 187.

12. C. L. Scortichini and C. N. Reilley, J. Electroanal. Chem., 139 (1982) 233; 247.

13. A. Bewick and J. W. Russell, J. Electroanal. Chem., 142 (1982) 337.

14. R. J. Nichols and A. Bewick, J. Electroanal. Chem, 243 (1988) 445.

15. P. W. Faguy, N. Markovic, R. R. Adzic, C. A. Fierro and E. B. Yeager, J. Electroanal. Chem., 289 (1990) 245.

16. A. Rodes, M. A. Zamakhchari, K. El Achi and J. Clavilier, J. Electroanal. Chem., 305 (1991) 115.

17. A. Rodes, J. Clavilier, J. M. Orts, J. M. Feliu and A. Aldaz, J. Electroanal. Chem., 338 (1992) 317.

18. G. Jerkiewicz and B. E. Conway, J. Chim. Phys., 88 (1991) 1381.

19. A. Peremans and A. Tadjeddine, Phys. Rev. Lett., 73 (1994) 3010.

20. A. Tadjeddine and A. Peremans, J. Chim. Phys., 93 (1996) 662.

21. J. Clavilier, R. Albalat, R. Gómez, J. M. Orts and J. M. Feliu, J. Electroanal. Chem., 360 (1992) 325.

22. R. Gómez and J. Clavilier, J. Electroanal. Chem., 354 (1993) 189.

23. J. Clavilier, J. M. Orts, R. Gómez, J. M. Feliu and A. Aldaz, in "Electrochemistry and Materials Science of Cathodic Hydrogen Absorption and Adsorption", B. E. Conway and G. Jerkiewicz, Eds., The Electrochemical Society, PV 94-21, Pennington, NJ (1995).

24. A. Zolfaghari and G. Jerkiewicz, J. Electroanal. Chem., 420 (1997) 11.

25. A. Zolfaghari and G. Jerkiewicz, J. Electroanal. Chem., 422 (1997) 1.

26. A. Hamelin, S. Morin, J. Richer and J. Lipkowski, J. Electroanal. Chem., 285 (1990) 249.

27. B. E. Conway, H. Angerstein-Kozlowska and W. B. A. Sharp, Trans. Faraday Soc., 19 (1977) 1373.

28. H. Angerstein-Kozlowska, Ch. 1 in "Comprehensive Treatise of Electrochemistry", E. Yeager, J.O'M. Bockris, B. E. Conway and S. Sarangapani, Eds., Vol.9, Plenum Press, New York (1984).

29. B. E. Conway, W. B. A. Sharp, H. Angerstein-Kozlowska and E. E. Criddle, Anal. Chem., 41 (1973) 1321.

30. B. E. Conway, H. Angerstein-Kozlowska and W. B. A. Sharp, J. Chem. Soc., Faraday Trans. I, 74 (1978) 1373.

31. J. Lurie, "Handbook of Analytical Chemistry", Mir Publishers, Moscow, 1975.

32. K. Itaya, S. Sugawara, K. Sashikata and N. Furuya, J. Vac. Sci. Technol. A8, 1, (1990) 515.

33. D. Armand and M.-L. Rosinberg, J. Electroanal. Chem., 302 (1991) 191.

34. G. Jerkiewicz and A. Zolfaghari, J. Electrochem. Soc., 143 (1996) 1240.

35. G. Jerkiewicz, and A. Zolfaghari, J. Phys. Chem., 100 (1996) 8454.

36. A. Zolfaghari, F. Villiard, M. Chayer and G. Jerkiewicz, J. Alloy Comp., 253-254 (1997) 481.

37. A. Zolfaghari, M. Chayer and G. Jerkiewicz, J. Electrochem. Soc., 144 (1997) 3034.

38. E. Protopopoff and P. Marcus, J. Vac. Sci. Technol. A5, 5 (1987) 944.

39. E. Protopopoff and P. Marcus, J. Chim. Phys. 88 (1991) 1423.

40. A. Zolfaghari, A. Lasia and G. Jerkiewicz, paper in preparation.

41. A. Bewick and J.W. Russell, J. Electroanal. Chem., 132 (1982) 329; 142 (1982) 337.

42. R.J. Nichols and A. Bewick, J. Electroanal. Chem., 243 (1988) 445.

43. A. Peremans and A. Tadjeddine, Phys. Rev. Lett., 73 (1994) 3010.

44. A. Tadjeddine and A. Peremans, J. Chim. Phys., 93 (1996) 662.

45. A. N. Frumkin, in "Advances of Electrochemistry and Electrochemical Engineering", P. Delahey, P. Ed., Vol. 3, Interscience Publishers, New York (1963).

46. B.E. Conway, "Theory and Principles of Electrode Processes", Ronald Press, London (1965).

47. K. Christman, Surface Sci. Rep., 9 (1988), 1.

48. R. Parsons, Trans. Faraday Soc., 54 (1958) 1053.

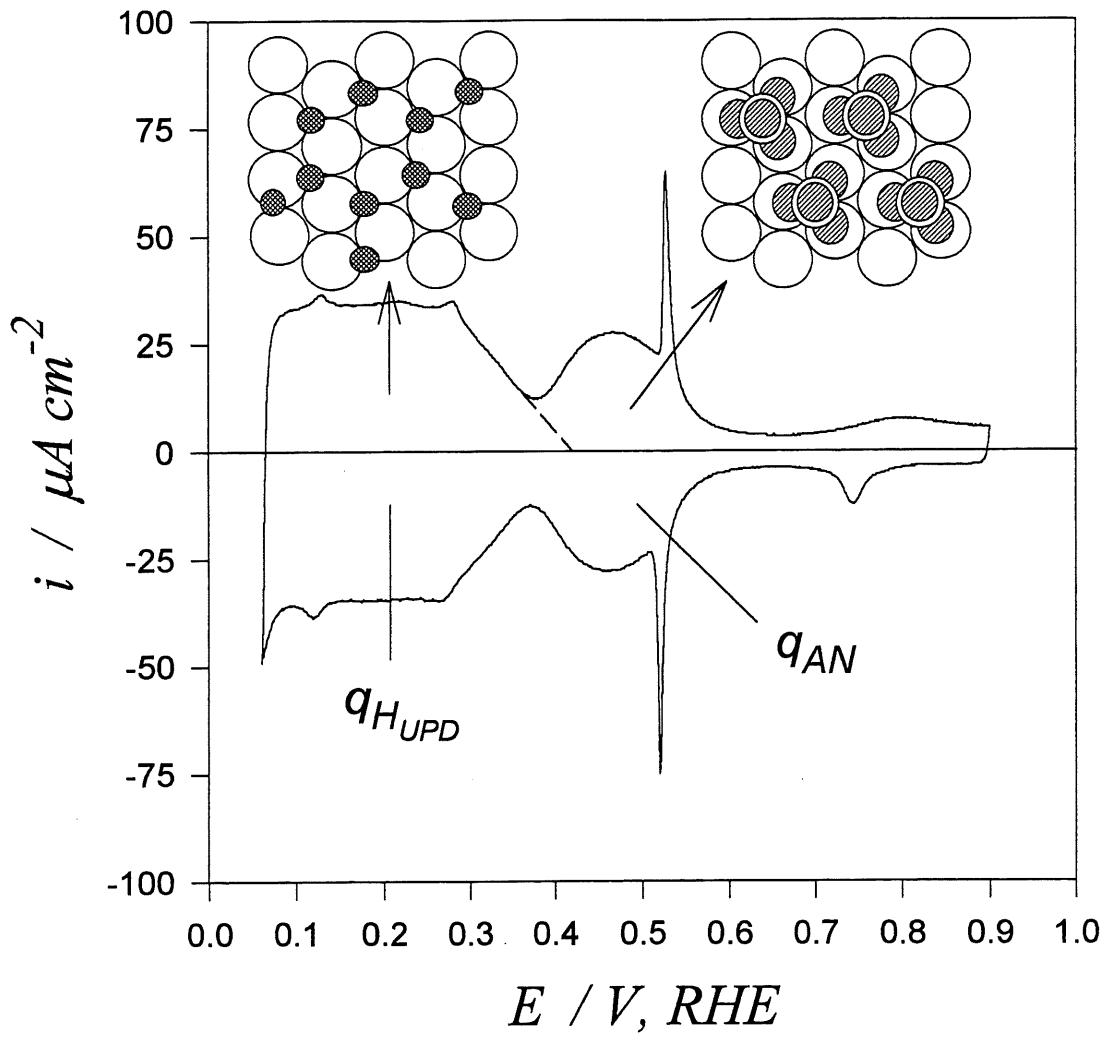

Figure 1. CV profile for a Pt(111) electrode, cooled in $H_2 + Ar$, in 0.05 M aq. H_2SO_4 solution; $A = 0.058\ cm^2$, $T = 298\ K$ and $s = 50\ mV\ s^{-1}$. The profile shows two potential regions: (i) one corresponding to the UPD H; and (ii) one being characteristic of the anion adsorption and comprising a sharp peak ("spike").

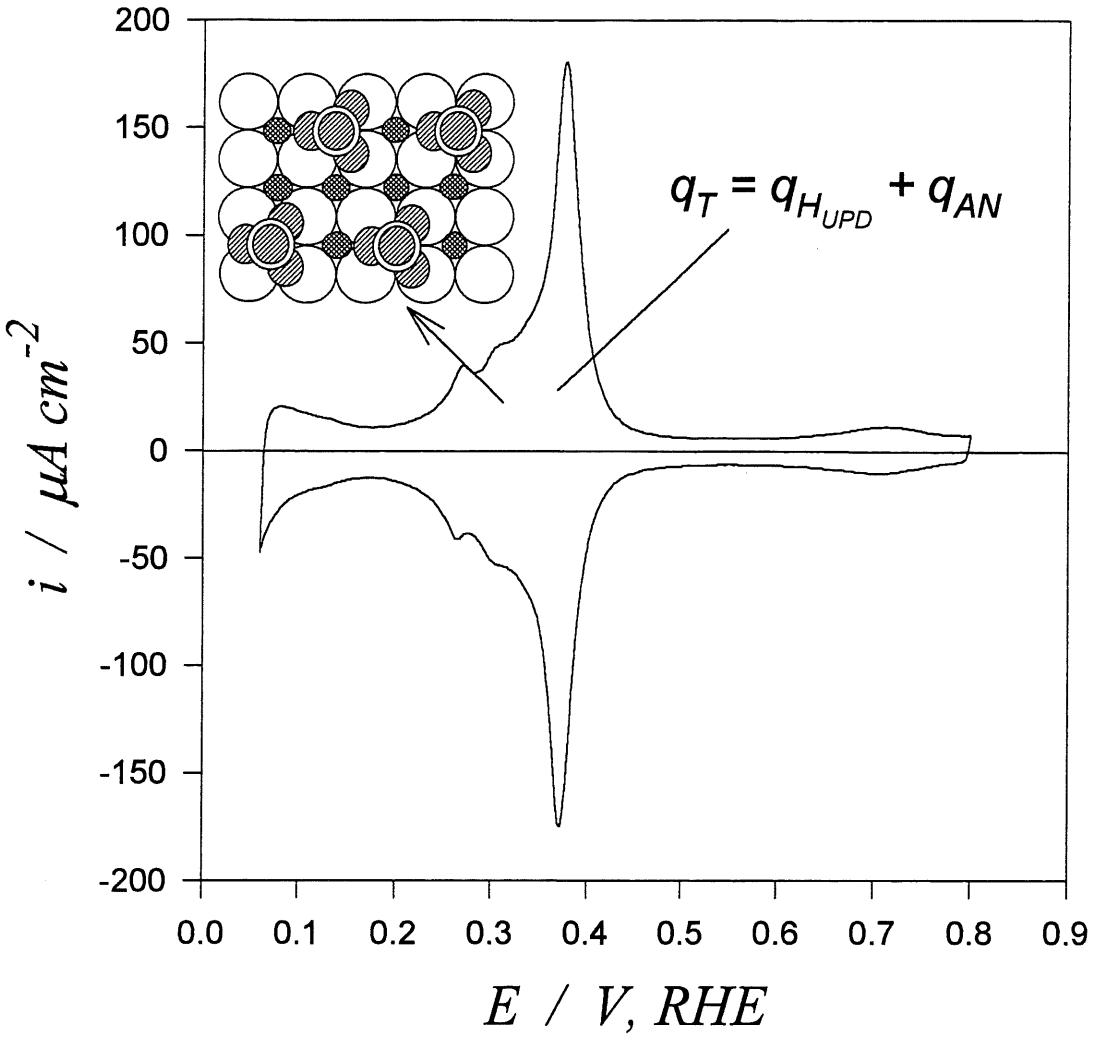

Figure 2. CV profile for Pt(100), cooled in $H_2 + Ar$, in 0.5 M aqueous H_2SO_4 solution; $A = 0.038\ cm^2$, $T = 298\ K$ and $s = 50\ mV\ s^{-1}$. It reveals the following features: (i) a sharp peak at 0.375 V; (ii) a small peak at 0.267 V; and (iii) a shoulder at 0.305 V, RHE. The schematic representation indicates that the UPD H and anion adsorption occur concurrently.

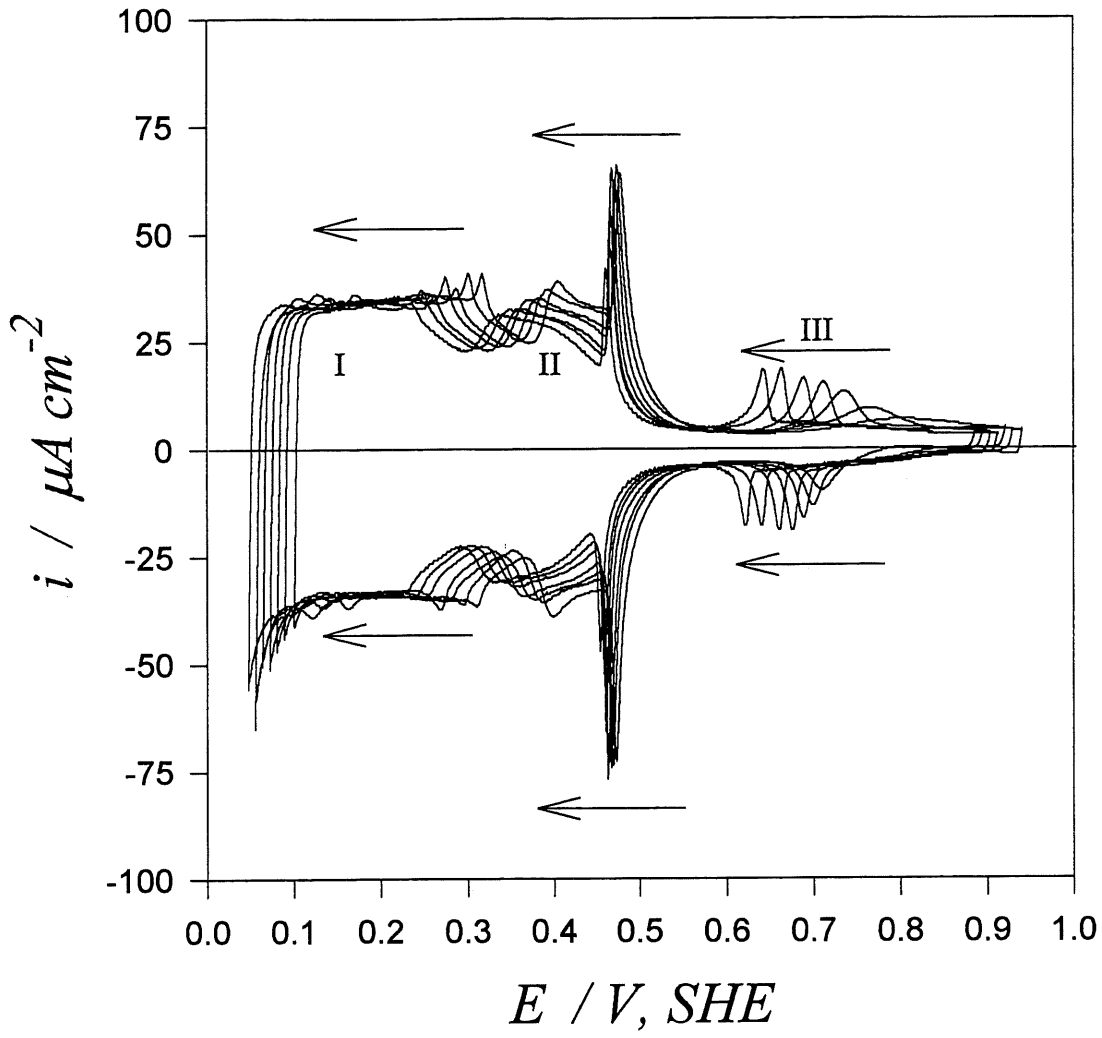

Figure 3. CV profiles for Pt(111), cooled in $H_2 + Ar$, in 0.5 M aq. H_2SO_4 solution at $275 \leq T \leq 328$ K with the first interval equal to 13 K and the subsequent ones being 10 K; $A = 0.058\ cm^2$ and $s = 50\ mV\ s^{-1}$. Arrows indicate changes in the CV's associated with T increase. The potentials are quoted with respect to the SHE. The CV's are divided into three potential regions; the region I corresponding to the UPD H, the region II associated with the anion adsorption and the region III.

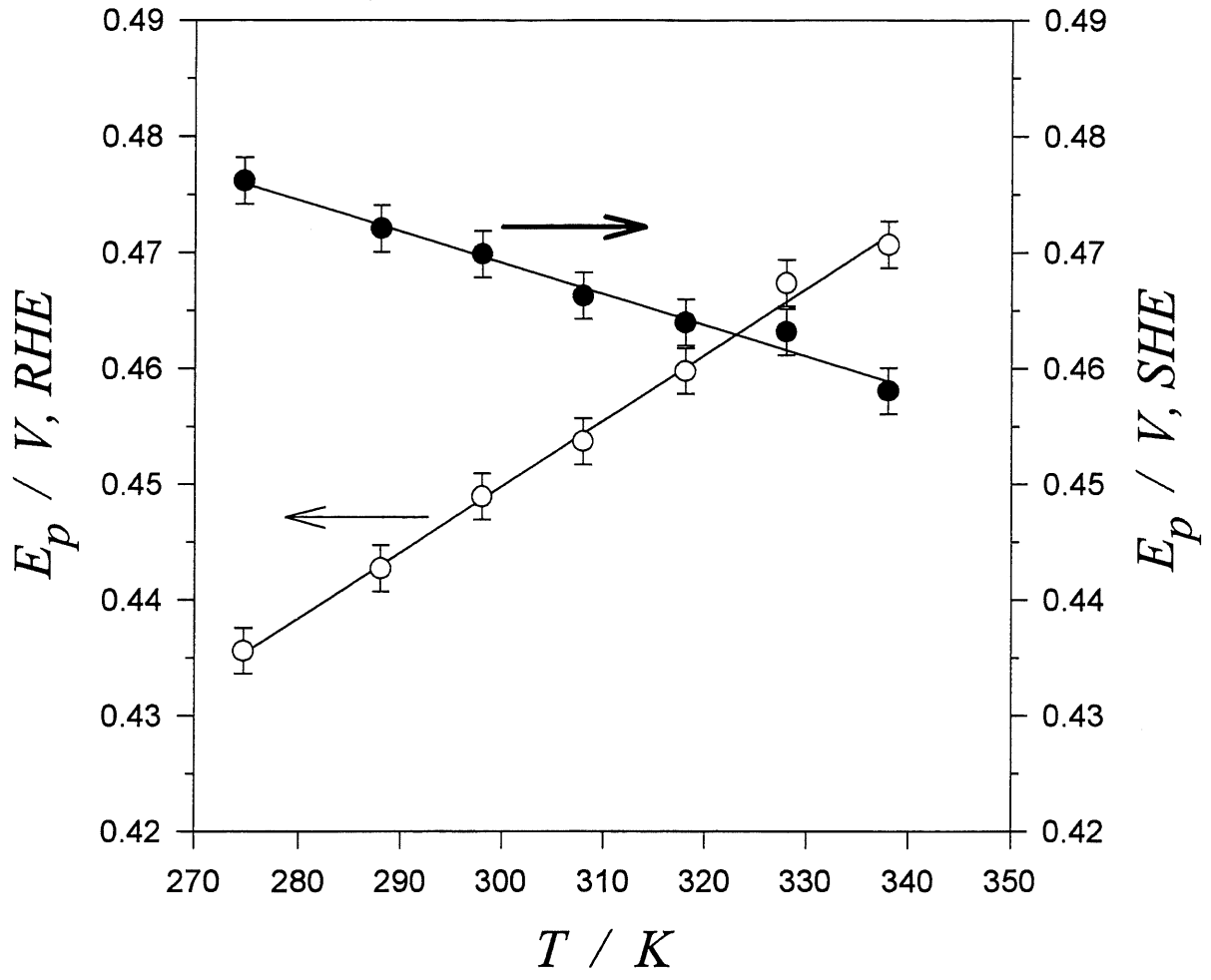

Figure 4. Relation between the potential of the sharp peak (the so-called spike), E_P, expressed on the RHE and the SHE scale, as a function of T. The E_P versus T dependences are linear and their slope, $\partial E_P / \partial T$, equals 0.57×10^{-3} V K^{-1} on the RHE scale and -0.27×10^{-3} V K^{-1} on the SHE one.

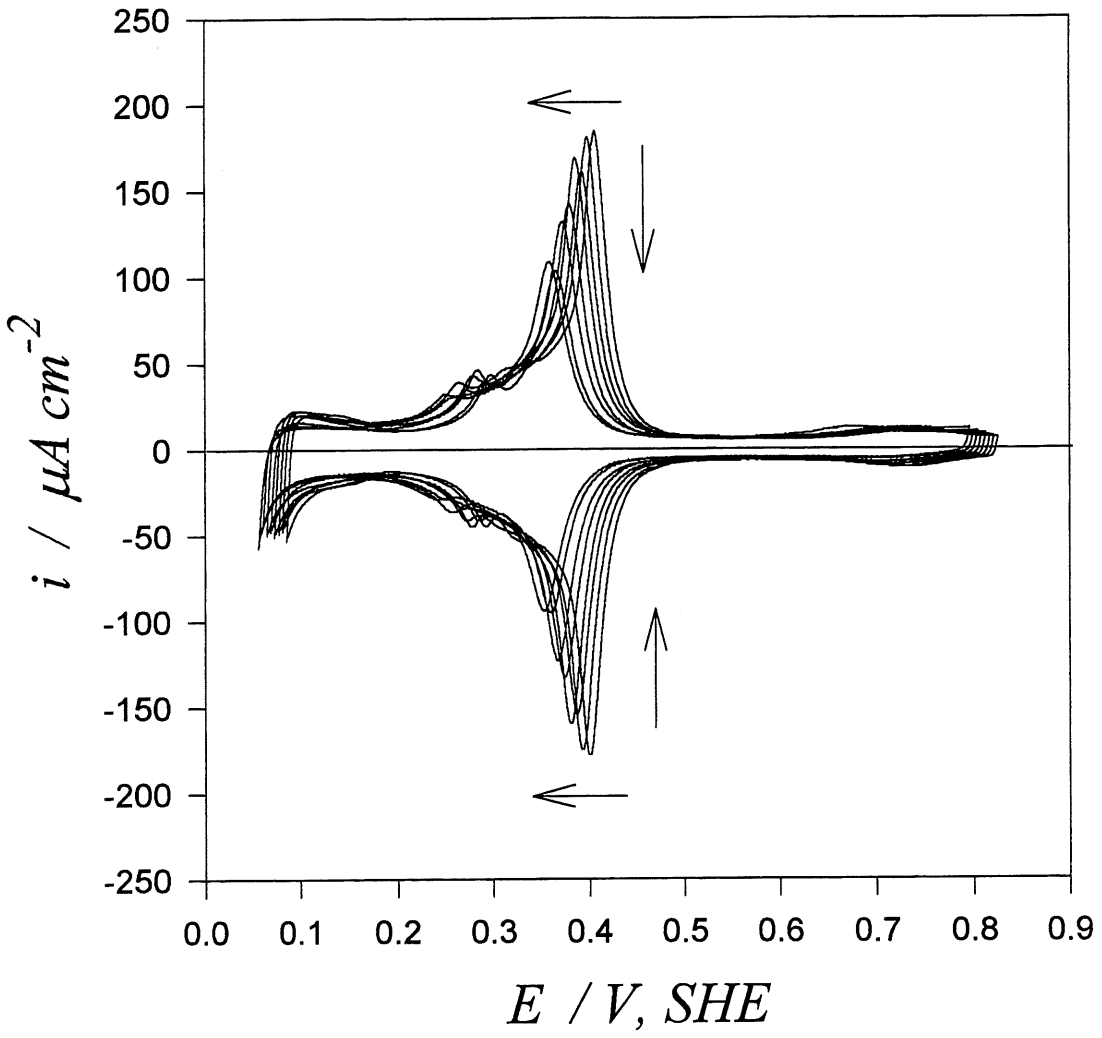

Figure 5. CV profiles for Pt(100), cooled in $H_2 + Ar$, in 0.5 M aq. H_2SO_4 solution at $293 \leq T \leq 328$ K with an interval equal to 5 K; $A = 0.038\ cm^2$ and $s = 50\ mV\ s^{-1}$. Arrows indicate changes in the CV's associated with T increase. The potentials are quoted with respect to the SHE.

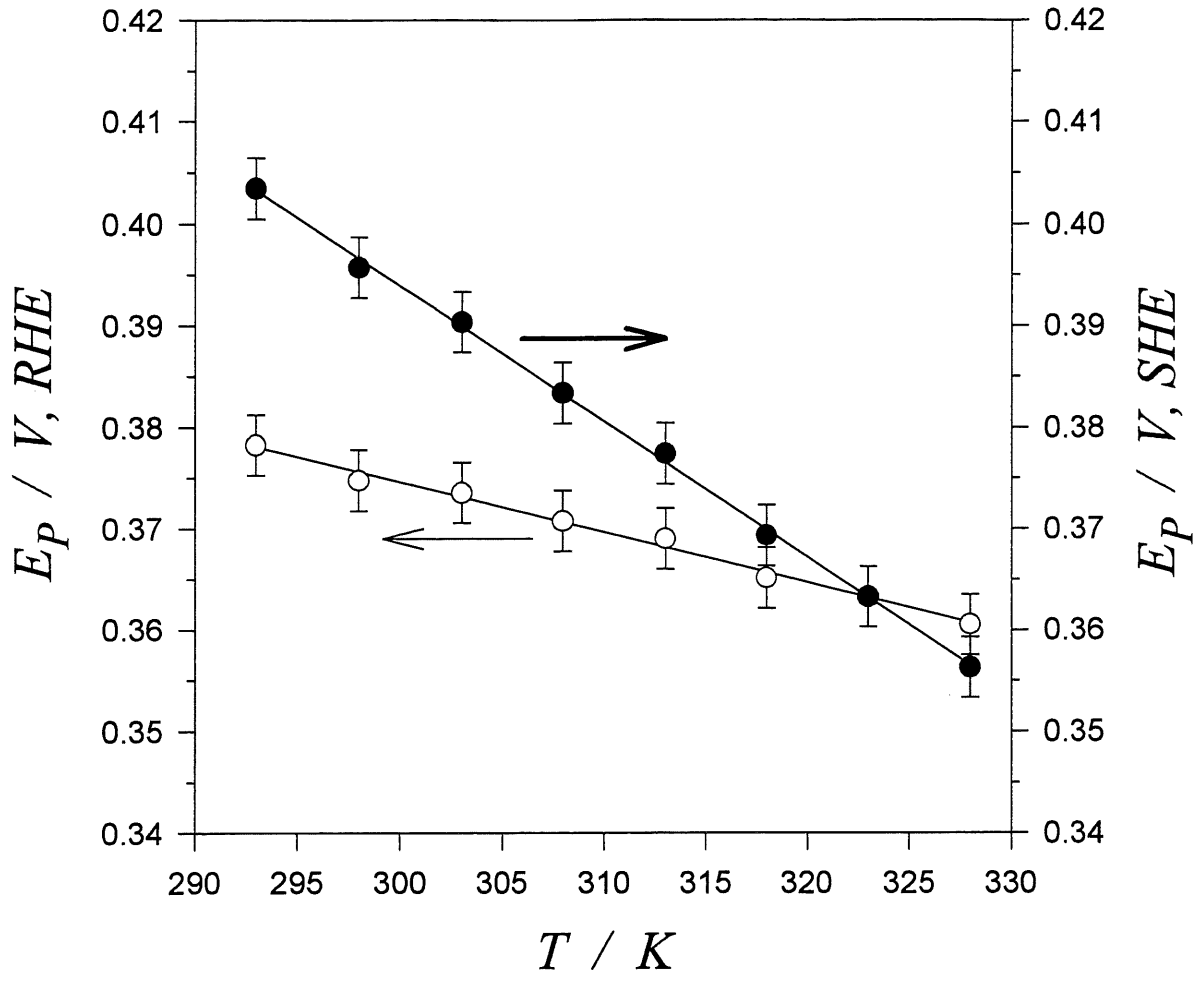

Figure 6. Relation between the potential of the sharp peak, E_P, expressed on the RHE and the SHE scale, as a function of T. The E_P versus T dependences are linear and their slope, $\partial E_P / \partial T$, equals -0.50×10^{-3} V K^{-1} on the RHE scale and -1.34×10^{-3} V K^{-1} on the SHE one.

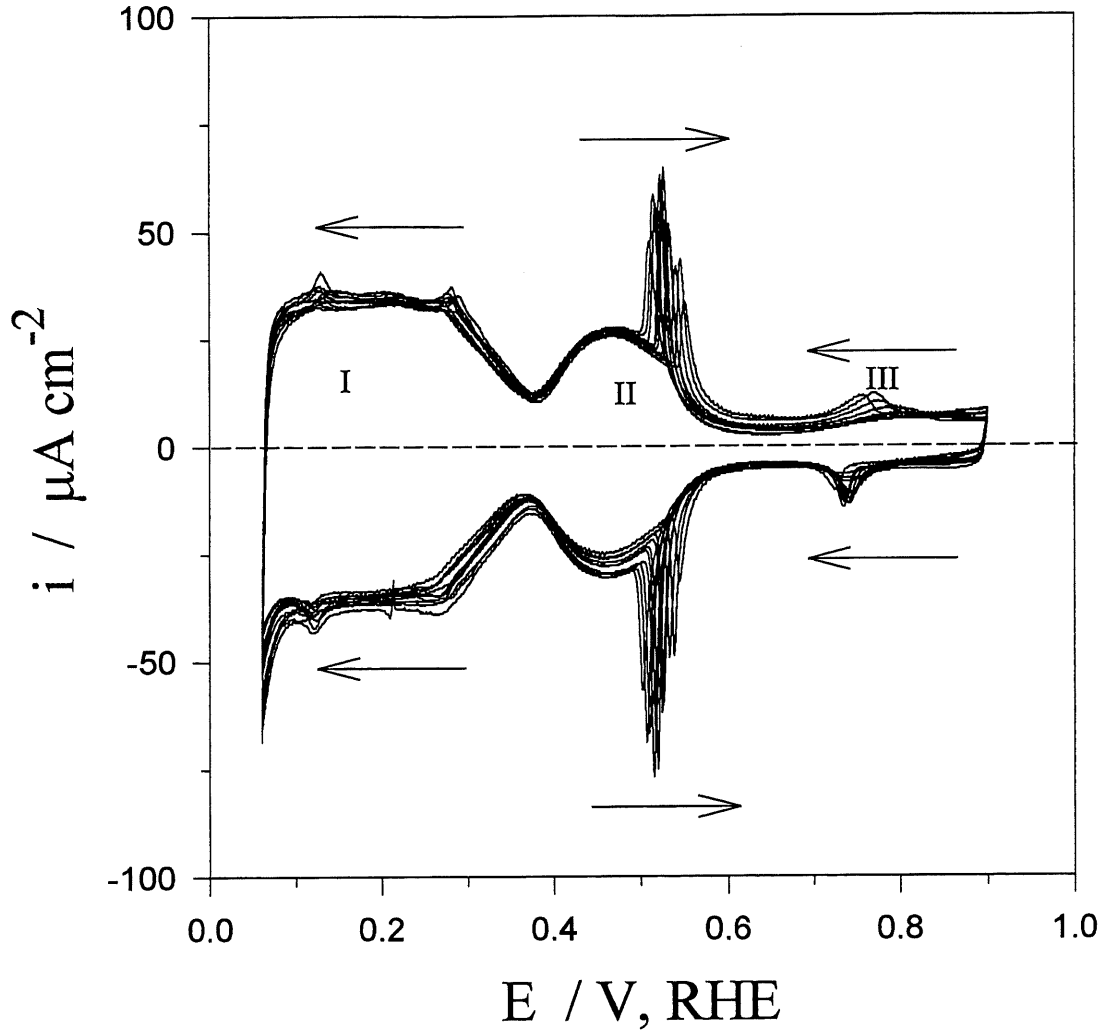

Figure 7. CV profiles for Pt(111), cooled in $H_2 + Ar$, in 0.05 M aq. H_2SO_4 solution at $273 \leq T \leq 323$ K with an interval equal to 5 K; $A = 0.058\ cm^2$ and $s = 50\ mV\ s^{-1}$. The potentials are quoted with respect to the RHE.

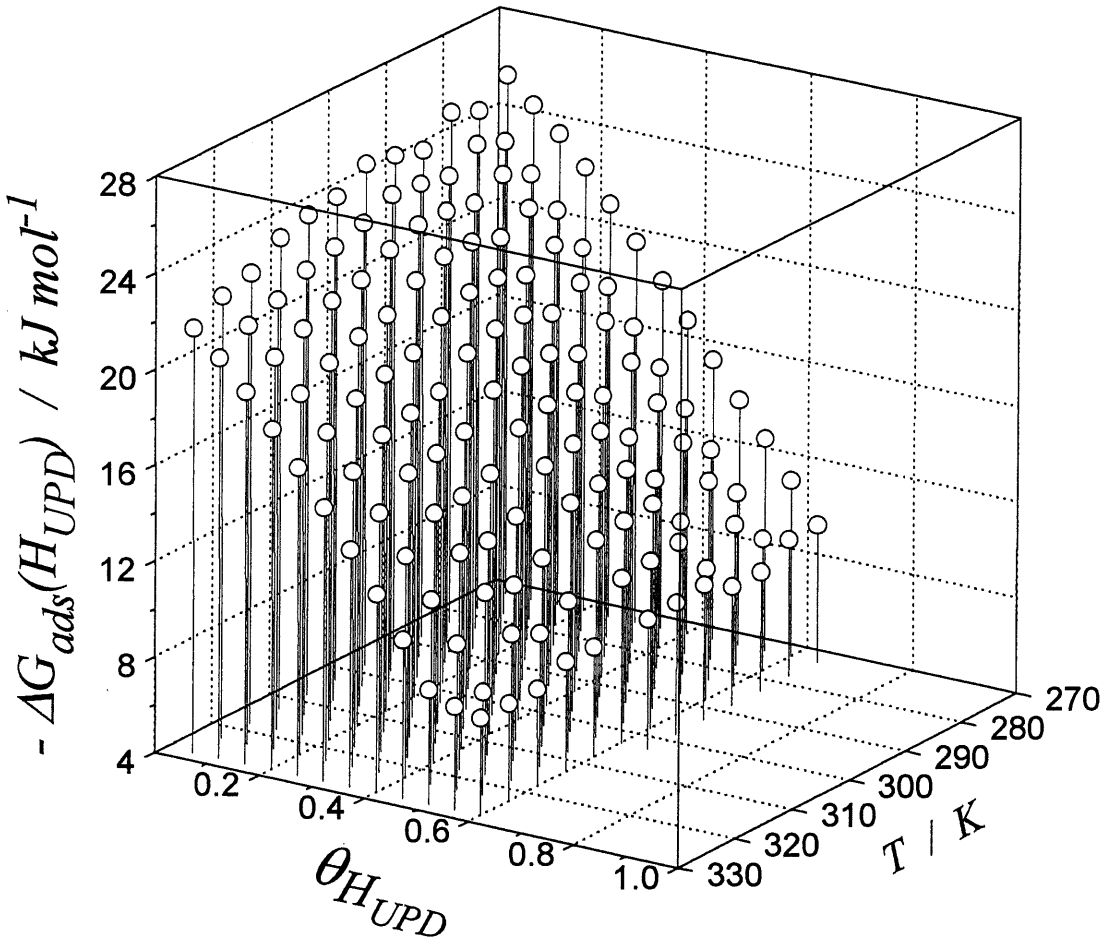

Figure 8. 3D plot showing the Gibbs free energy of adsorption, $\Delta G_{ads}(H_{UPD})$, as a function of $\theta_{H_{UPD}}$ and T, $\Delta G_{ads}(H_{UPD}) = f(\theta_{H_{UPD}}, T)$, for the UPD H on Pt(111) in 0.05 M aq. H_2SO_4 $\Delta G_{ads}(H_{UPD})$ has values from – 26 to –8 kJ mol^{-1} depending on $\theta_{H_{UPD}}$ and T; $\Delta G_{ads}(H_{UPD})$ reaches the most negative values at the lowest temperature and the smallest surface coverage, $\theta_{H_{UPD}}$. Augmentation of $\Delta G_{ads}(H_{UPD})$ with increasing $\theta_{H_{UPD}}$ for T = const points to the repulsive nature of lateral interactions between H_{UPD} adatoms.

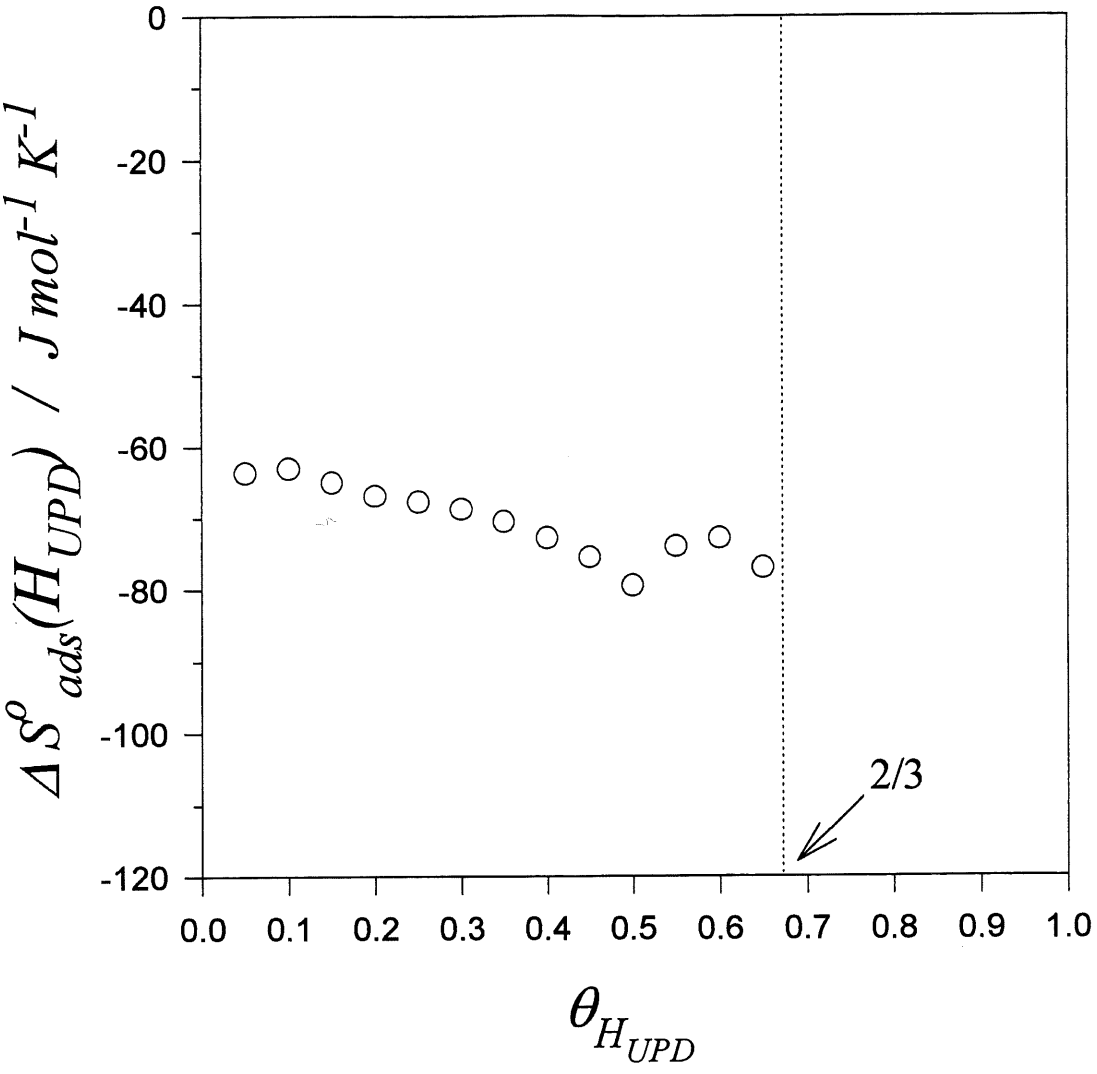

Figure 9. Dependence of $\Delta S^{\circ}_{ads}(H_{UPD})$ on $\theta_{H_{UPD}}$ for the UPD H on Pt(111) in 0.05 M aq H_2SO_4. $\Delta S^{\circ}_{ads}(H_{UPD})$ has values from -63 to -79 J mol^{-1} K^{-1} and it decreases almost linearly with increasing $\theta_{H_{UPD}}$.

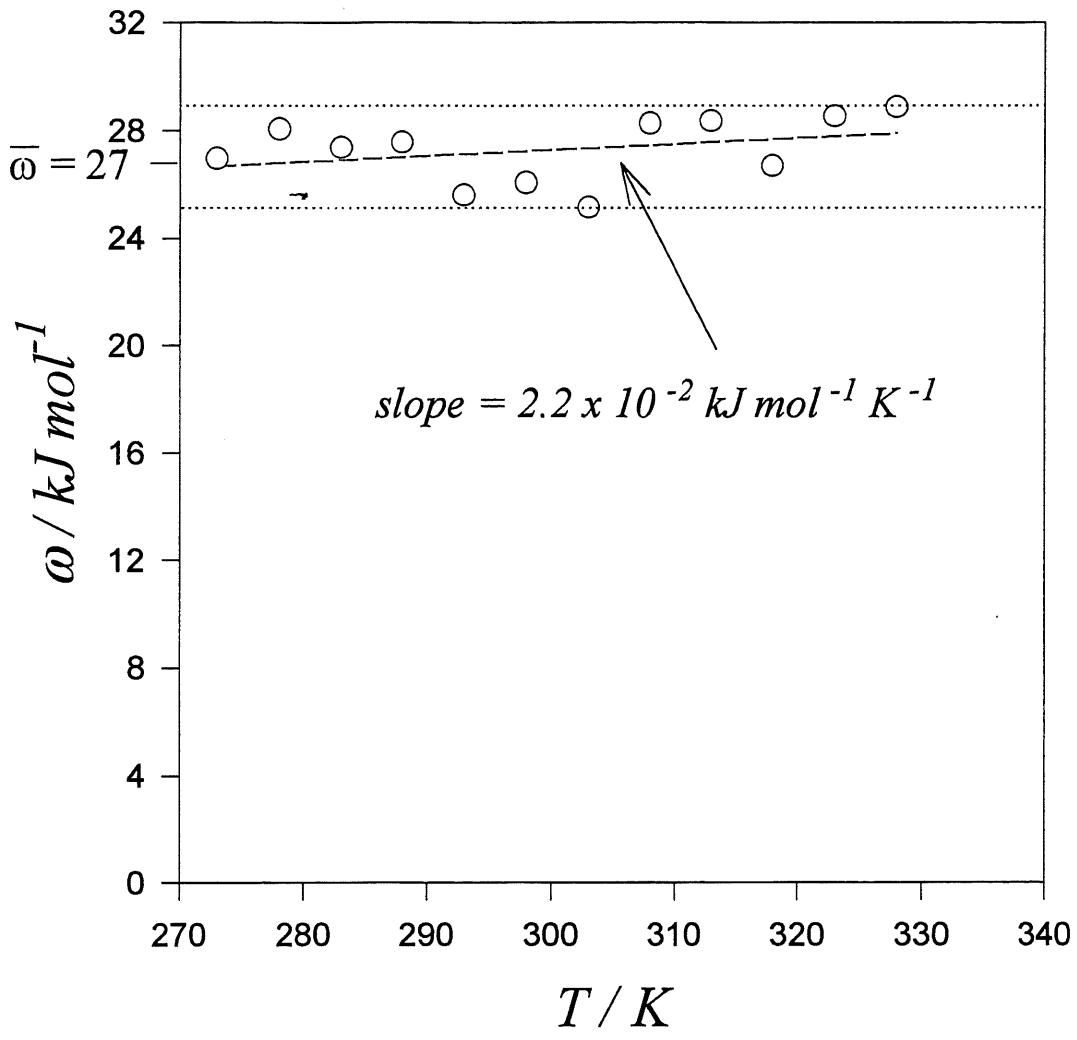

Figure 10. Dependence of $\omega(H_{UPD})$ on T for the UPD H on Pt(111) in 0.05 M aq H_2SO_4. $\omega(H_{UPD})$ has values scattered over a narrow range, namely between 25 and 29 kJ mol^{-1}; its average value, $\bar{\omega}(H_{UPD})$, is 27 kJ mol^{-1}.

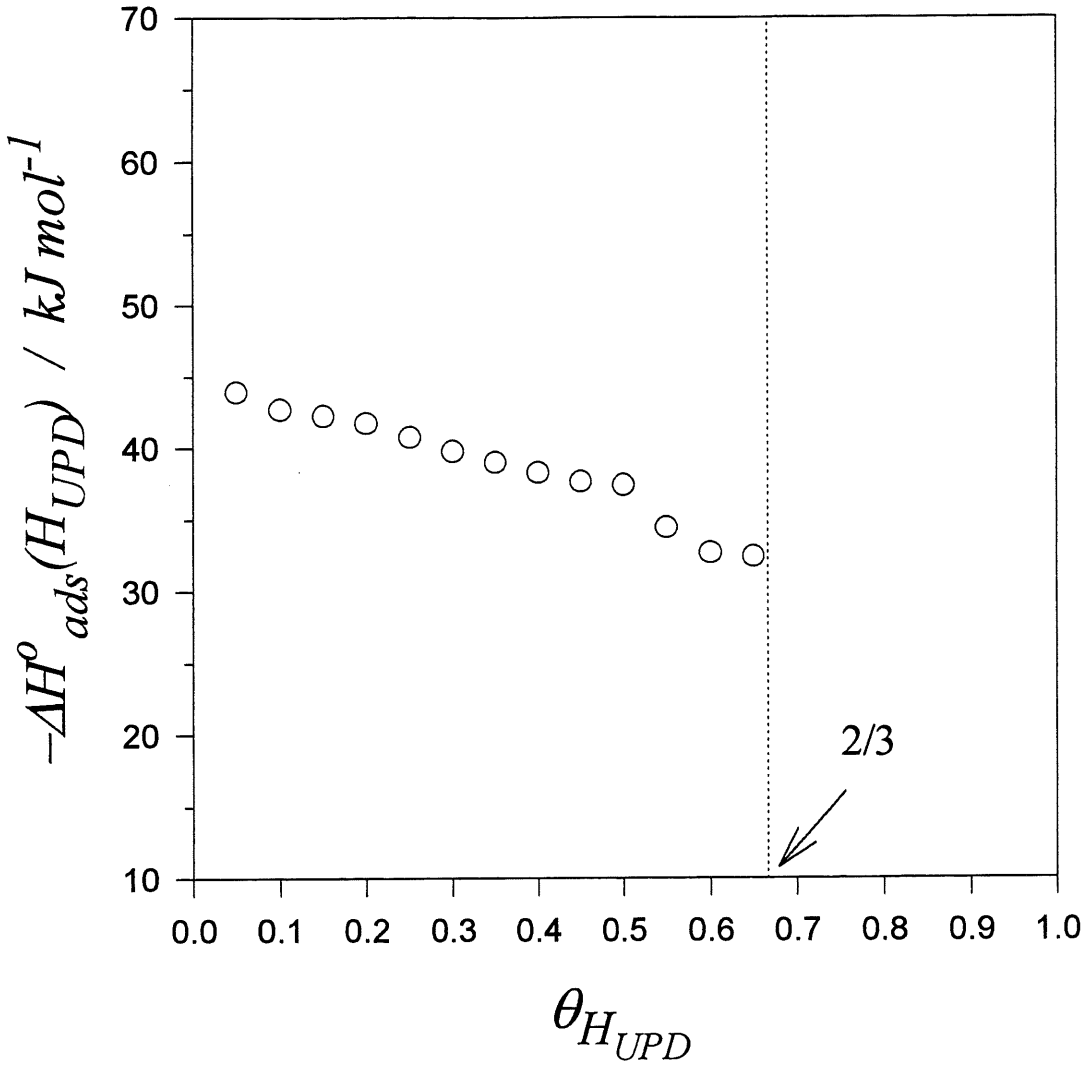

Figure 11. Dependence of $\Delta H^{\circ}_{ads}(H_{UPD})$ on $\theta_{H_{UPD}}$ for the UPD H on Pt(111) in 0.05 M aq H_2SO_4. $\Delta H^{\circ}_{ads}(H_{UPD})$ has values from -44 to -32 kJ mol^{-1}.

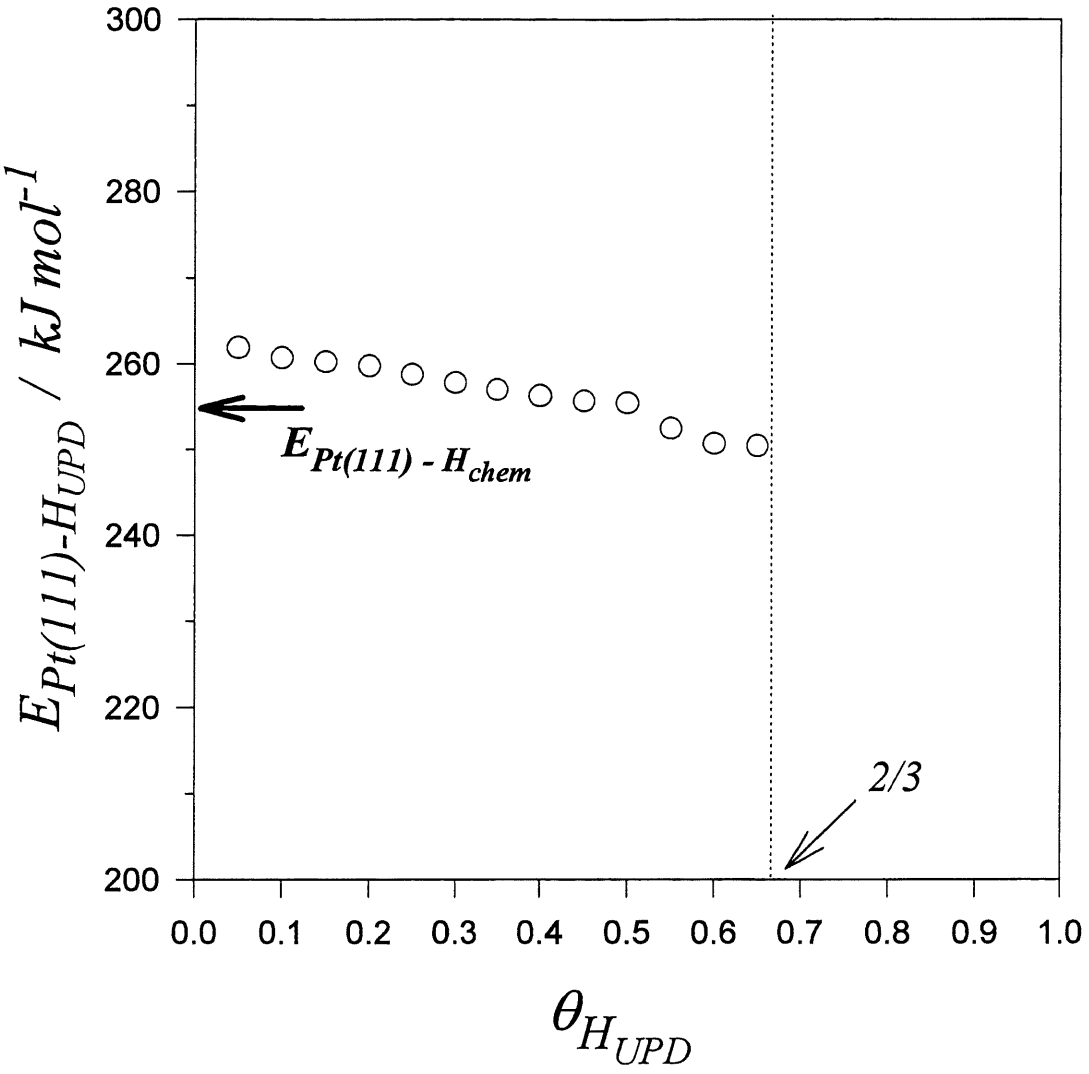

Figure 12. Dependence of $E_{Pt(111)-H_{UPD}}$ on $\theta_{H_{UPD}}$ for the UPD H on Pt(111) in 0.05 M aq H_2SO_4. $E_{Pt(111)-H_{UPD}}$ has values from 262 to 250 kJ mol^{-1}. The values of $E_{Pt(111)-H_{UPD}}$ fall close to that for the bond energy between Pt(111) and H_{chem}, $E_{Pt(111)-H_{chem}}$, the latter being 255 kJ mol^{-1}.

3.4 COVERAGE EVOLUTION OF SULFUR ON Pt(111) ELECTRODES: FROM COMPRESSED OVERLAYERS TO WELL-DEFINED ISLANDS

Y.-E. Sung *, W. Chrzanowski * and A. Wieckowski *
A. Zolfaghari, S. Blais and G. Jerkiewicz
Electrochim. Acta, Submitted (1997)

* Department of Chemistry, University of Illinois at Urbana-Champaign, Urbana-Champaign IL 61801 USA

ABSTRACT

The paper examines formation of a monolayer and submonolayers of S_{chem} on the Pt(111) electrode accomplished through its immersion in aqueous Na_2S solution. The S_{chem} monolayer, having the (1×1) structure at $\theta_{S_{chem}}=1$, can be gradually removed by oxidative desorption at $E\geq0.95$ V, RHE, and the S_{chem} coverage can be controlled with great precision. The S_{chem} layer completely suppresses the UPD H and anion adsorption as well as it affects the oxide growth behavior on Pt(111). LEED data reveal that S_{chem} forms well-defined structures on Pt(111) for $0.50\geq\theta_{S_{chem}}\geq0.25$: $c(2\times2)$ at $\theta_{S_{chem}}=1/2$, $\left(\sqrt{3}\times\sqrt{3}\right)R30°$ at $\theta_{S_{chem}}=1/3$ and $p(2\times2)$ at $\theta_{S_{chem}}=1/4$; when $\theta_{S_{chem}}\leq0.20$, structured islands of S_{chem} are observed. AES and CEELS data indicate that the adsorbed S is not present in an oxidized state; it is almost of atomic character with an incomplete negative charge due to partial charge transfer between S_{chem} the Pt(111) substrate. Presence of S_{chem} influences thermodynamics of the UPD H on Pt(111) resulting in less-negative values of $\Delta G_{ads(S)}(H_{UPD})$. In absence of S_{chem}, the UPD H is enthalpy-driven whereas in presence of S_{chem} it becomes entropy driven. The $Pt(111)-H_{UPD}$ bond energy is weaker in presence of S_{chem} than in its absence, and this bond energy diminution may be assigned to local electronic effects arising from presence of S_{chem}.

INTRODUCTION

Chemisorption of S and of S-containing compounds is important in modification of physico-chemical properties of catalysts and electrodes. The chemisorbed S, S_{chem}, blocks surface adsorption sites that otherwise would be available to adsorption of other species or would act as active reaction sites. Organic chains anchored to Au substrates through a S atom play a key role in preparation of self-assembled monolayers, SAM, and their arrangement into well-defined surface structures [21-24]. In electrochemical surface science of H, S_{chem} or S-containing species chemisorbed on electrode surfaces can influence kinetics of the hydrogen evolution reaction, HER, or the H interfacial transfer from the adsorbed, H_{ads}, to the absorbed state, H_{abs} [25-33]. It is recognized that S_{chem} is an excellent example, almost a model one, of a *site blocking species*, SBS, because of its strong chemisorption. Moreover, its coadsorption with the under-potential deposited H, H_{UPD}, is not competitive, thus adsorption of H_{UPD} does not lead to desorption of S_{chem} [14,19]. Chemisorbed S similarly to other SBS's reveal a *dual action* and behave either as *surface poisons* or as *surface promoters* of the HER or H absorption depending on their physico-chemical nature [14]. If a SBS acts as a promoter of H

absorption, then it concurrently behave as a poison of the HER and vice versa. This interfacial action is related to the local surface-electronic effects which give rise to e-transfer between H_{UPD} and S_{chem} through the underlying metal substrate [4,19]. The latter is not only a medium which brings about the lateral electronic interactions because it actively participates in the surface bond formation. It is observed that some SBS's enhance the rate of H interfacial transfer from the adsorbed to the absorbed state, thus they behave as surface promoters of the process (simultaneously, they act as surface poisons of the HER). This selective promoting action is of relevance to metal-hydride (MH) batteries because by suppressing the HER and enhancing H absorption, they increase the efficiency of H absorption, thus the current efficiency of recharge [26-31,34].

Comprehension of the interfacial action of SBS's is also very important in H-induced corrosion (H embrittlement) of metal structures [3,10-14]. While in the MH battery technology it is desirable to suppress the HER and enhance the H interfacial transfer by adsorbing a smart SBS, one would like to be able to contain H absorption and enhance the HER on metal structures which might undergo H embrittlement. This clearly requires a SBS that acts in an opposite way than a surface promoter - it acts as a surface poison. At present, the criteria of selecting a species with respect to its promoting/poisoning action are not known. Their action of SBS's was a subject of thorough theoretical research and numerical simulations based on lateral interactions between the electroadsorbed H and the coadsorbed SBS [14]. In general, SBS's affect catalytic properties of the electrified solid/liquid interface through the following action: (i) physical blockage of surface adsorption sites; (ii) alteration of energetics of the reaction within the double-layer; (iii) change of the work function of the substrate; (iv) variation of the charge transfer at the electrode/solution interface; and (v) change of the adsorption behavior of the reaction products and intermediates.

Chemisorption of S on Pt(111) electrodes was a subject of research by the present authors [19] using electrochemical and surface-science techniques, namely cyclic-voltammetry (CV), low-energy electron diffraction (LEED), Auger electron spectroscopy (AES) and core-level electron energy loss spectroscopy (CEELS). The investigation lead to: (i) examination of S_{chem} surface structure formed on the Pt(111) electrode; (ii) the mechanism of its oxidative desorption; (iii) study the nature of the $Pt(111)-S_{chem}$ surface bond; and (iv) the mutual relation between the H_{UPD} and S_{chem} surface coverages, $\theta_{H_{UPD}}$ and $\theta_{S_{chem}}$. Zolfaghari et al. [20] examined the impact of a S_{chem} submonolayer having $\theta_{S_{chem}} = 0.10$ on energetics of the UPD H on polycrystalline Pt and will report on similar research on Pt(111) electrodes.

In this paper, the authors reveal new and hitherto unpublished data on the structures of S_{chem} on the Pt(111) electrode surface in relation to its coverage and to cycling to positive potentials corresponding to its oxidative desorption. They compare the structural data on electrochemical desorption of S_{chem} with those for temperature-stimulated desorption. They demonstrate how $\theta_{S_{chem}}$ can be controlled by selecting the potential limit and the number of anodic desorption cycles. The authors show how temperature variation affects the anodic desorption behavior of S_{chem} and how it affects the control of $\theta_{S_{chem}}$.

EXPERIMENTAL

Electrode Preparation for Electrochemical, LEED, AES and CEELS Measurements.

The Pt(111) single crystals used in the T-dependence research were grown and oriented according to the procedure developed by Clavilier [35,36] and further advanced by Hamelin [37,38]. The details of the electrode preparation may be found in refs. 39 and 40. The electrodes were polished with Alumina (0.05 μm) to a mirror-like finish and its surface quality was verified by recording a CV in 0.05 and 0.5 M aqueous H_2SO_4 solution (Fig. 1). Agreement between literature data [41] and the CV profiles indicate that they were of good quality and that their surface was well ordered. For the ultra-high vacuum (UHV) LEED, AES and CEELS studies [42-45], a disk-shaped Pt(111) crystal of 6.0 mm in diameter and 3 mm in thickness (Aremco) was used. One base of the disk was polished to a mirror-like finish and it served as the electrode surface ($0.283 \pm 0.005\ cm^2$). In the case of UHV studies, the electrode was cleaned by Ar ion bombardment and oxygen annealing cycles in the UHV chamber. The electrode, free of any detectable surface contaminants as revealed from AES studies (see Results and Discussion for details), was transferred to the electrochemistry antechamber where S chemisorption and electrochemical measurements were carried out [19].

Solutions and Electrochemical Cell.

High-purity solutions were prepared from BDH "Aristar" grade H_2SO_4 and "Nanopure" water, and their cleanliness was verified by recording H_{UPD} and anion adsorption-desorption profiles and comparing them with those in the literature (Fig. 1). The electrochemical experiments were conducted in two different types of cells; one was a standard all-Pyrex, two-compartment electrochemical cell [39,40] and one was a cell coupled with a UHV chamber and its design is described in refs. 19,42-45. The glassware was pre-cleaned according to the well established procedure [46]. In the case of CV experiments conducted

outside a UHV system, the potential of the Pt(111) electrode was given with respect to a Pt/Pt-black reversible hydrogen electrode, RHE, immersed in the same electrolyte. In the case of CV experiments carried out in an electrochemistry antechamber coupled with a UHV surface analysis one, the potential of the Pt(111) electrode was given with respect to a Ag/AgCl reference electrode of $\left[Cl^-\right] = 1.0\,M$; its value was subsequently converted to the RHE scale. During the experiments high purity N_2 gas (99.99%) pre-cleaned and pre-saturated with water vapor, was bubbled through the electrochemical cell. The formation of a monolayer of chemisorbed S, S_{chem}, on Pt(111) for CV, AES and CEELS measurements was accomplished by the electrode immersion in 10 mM or 1 mM aqueous Na_2S (Aldrich) solution for 300 s followed by rinsing with "Nanopure" water. Appraisal of influence of S_{chem} on the H_{UPD} adsorption behavior was accomplished by recording CV profiles in the UPD H potential region.

In order to conduct meaningful AES and CEELS measurements on the S_{chem} monolayer and to provide sound interpretation of the spectra, the authors prepared a thin layer of Na_2S by immersion of Pt(111) in 30 mM aq. Na_2S followed by water evaporation. The Na_2S layer wase sufficiently thin to avoid surface charging but thick enough to screen AES transitions of platinum. The thin Na_2S film on Pt(111) served as templates that was used as standards for qualitative and quantitative work on the S_{chem} layers.

LEED, AES and CEELS Measurements.

The LEED, AES and CEELS experiments were conducted in a UHV apparatus on the Pt(111) electrode transferred from the electrochemistry antechamber to the UHV one without exposure to the ambient. The vacuum in the UHV analysis chamber was of the order of 10^{-10} Torr. The LEED diffractograms were obtained with a Perkin-Elmer model 15-120 LEED electron optics. The AES measurements were conducted with a primary electron beam of 3 kV energy whilst the CEELS ones with a beam of 0.5 kV energy using a PHI 10-155 cylindrical mirror analyzer in the differentiated mode. Both the AES and CEELS spectra are presented in the differentiated mode. The procedure used in interpretation of the AES results involved comparison of the peak-to-peak (p/p) ratio of sulfur at 153.0 eV relative to the Pt p/p one at 64.0 eV and application of a set of AES quantitative equations reported in refs. 43-45.

Temperature Measurements.

The two-compartment cell was immersed in a water bath (Haake W13) and the temperature was controlled to within ± 0.5 K by means of a thermostat (Haake D1); the water level in the bath was maintained above the electrolyte in the cell. The temperature in the water bath and the electrochemical cell were controlled by means of thermometers (± 0.5 K) and a K-type thermocouple (80 TK Fluke), and were found to agree to within ± 0.5 K. In order to ensure uniform temperature distribution in the cell, N_2 gas pre-heated to the temperature of the water bath was passed through the electrolyte. The CV measurements were carried out at a temperature range between 273 and 343 K with an interval of 5K.

Electrochemical Measurements.

The experimental procedure applied in this project involved standard CV measurements on Pt(111) electrodes in 0.05 and 0.50 M aqueous H_2SO_4 solutions within a temperature range between 273 and 323 K. The electrochemical instrumentation included: (a) EG&G Model 263A or EG&G Model 362 potentiostat-galvanostat; (b) IBM-compatible 80486, 66 MHz computer; and (c) EG&G M270 Electrochemical Software. All potentials are quoted with respect to the reversible hydrogen electrode, RHE, immersed in the same electrolyte.

RESULTS AND DISCUSSION

Sulfur Chemisorption on Pt(111) Electrodes and Its Oxidative Desorption.

The main objective of this research project was examination of the surface structures formed by S_{chem} on the Pt(111) substrate under electrochemical conditions by controlling the S_{chem} coverage through cycling Pt(111) to potential regions where S_{chem} undergoes oxidative desorption. The authors also focused their effort on examination of the chemical nature of S_{chem} on Pt(111) as well as on local surface electronic effects associated with electron transfer between S_{chem} and the Pt(111) substrate. This research was a part of a greater attempt which aimed at examination of thermodynamic state functions of the UPD H in absence and presence of a submonolayer of S_{chem} on Pt(111), namely $\Delta G_{ads}(H_{UPD})$ vs. $(\theta_{H_{UPD}}, T)$, $\Delta S^{\circ}_{ads}(H_{UPD})$ and $\Delta H^{\circ}_{ads}(H_{UPD})$ vs. $\theta_{H_{UPD}}$, as well as on the $Pt(111)-H_{UPD}$ surface bond energy, $E_{Pt(111)-H_{UPD}}$, vs. $\theta_{H_{UPD}}$.

Immersion of a Pt(111) electrodes in aqueous Na_2S solution leads to formation of a monolayer of S_{chem} which suppresses completely the UPD H and anion adsorption as may be

concluded from Fig. 2. FTIR, surface-science and electrochemical studies [17-20] indicate that the oxidative removal of S_{chem} results in formation of sulfate:

$$S_{chem} + 4H_2O \xrightarrow{E \geq 0.95\ V} SO_4^{-2} + 8H^+ + 6e \qquad (1)$$

The oxidative desorption of S_{chem} is represented by a sharp peak at ca. 1.0 V, RHE, which becomes less pronounced in subsequent desorption cycles [19]. The process commences at around 0.95 V. RHE, and its efficiency increases at the upper potential limit is raised [20]. Upon the scan reversal, there is a small oxidation wave at between 0.50 and 0.38 V which decreases as S_{chem} becomes desorbed. This wave does not correspond to reduction of a surface oxide since the latter takes place at more-positive potentials. Examination of its nature and meaning requires further research (it might represent reduction of a partially oxidized yet still chemisorbed S species; refs. 17, 18). The oxidative desorption of S_{chem} requires several scans to 1.20 V in order to completely desorb S_{chem}. Upon desorption of S_{chem} surface adsorption sites become available to H_{UPD} and anions (Fig. 2).

AES and CEELS Experiments.

The chemical state of adsorbed S on the Pt(111) substrate was evaluated by Auger electron spectroscopy (AES) and core electron energy loss spectroscopy (CEELS). Fig. 3 shows three AES spectra for Pt(111) in the 50 - 550 eV kinetic energy range for: (i) the clean Pt(111) surface; (ii) the Pt(111) electrode covered with sulfur; and (iii) the Pt(111) electrode covered with a thin layer of Na_2S. Characteristic absence of the AES oxygen signals (spectrum ii) indicates that sulfur oxides are not formed on the surface irrespective of the S-coverage. The high-resolution AES S(LMM) spectra in the 120 - 165 eV kinetic energy range are shown in Fig. 4A. When corrected for the 5 eV shift due to the extramolecular relaxation energy effect [19,45,47], the AES lineshape and the peak position for the Na_2S thin layer (Fig. 4A, spectrum *ii*) closely agree with those for sulfur monolayers. On the basis of the AES data, the authors conclude that S adatoms on the Pt(111) substrate are predominantly neutral. However, as shown below and discussed in ref. 19, a noticeable charge transfer between Pt(111) and S is giving rise to a partial negative charge on S, thus to ionicity of the Pt(111)-S surface bond (CEELS measurements document the electron redistribution at the Pt(111) surface, see ref. 48).

The CEELS data in the 140 - 210 eV loss energy range (Fig. 5B) for: (i) the clean Pt(111) electrode; (ii) the Pt(111) electrode covered with a S layer; and (iii) the Pt(111) electrode covered with a thin layer of Na_2S. The main core-level loss feature for the S_{chem} layer at 165 eV is attributed to electron transition from the S*2p* energy level to an empty bound state above the Fermi level but before the unoccupied continuum, such as S*3d* [19]. The S*2p* - S*3d* energy gap obtained on the basis of the theoretical studies [49] is very close to the experimentally observed 165 eV value. (The origin of the additional core-level loss feature at higher energy is not clear yet [19].) The core-level energy loss peaks for S_{chem} and the Na_2S thin film are at 165.5 eV and 164 eV, respectively, demonstrating that the main loss energy of the S-adsorbate is 1.5 eV higher than that for Na_2S. However, based on X-ray photoelectron spectroscopy (XPS) measurements [50], the S*2p* binding energy difference between elemental sulfur and Na_2S is higher, namely 2.2 eV. This highlights the difference between the surface and elemental sulfur strongly indicates that the S adatoms carry a partial negative charge due to electron density shift from Pt(111) to S.

LEED Data and Surface Structures of S_{chem}.

The authors examined the surface structures formed by S_{chem} by LEED in relation to the S_{chem} coverage, $\theta_{S_{chem}}$. The S_{chem} coverage was controlled by oxidative desorption of S_{chem} through repetitive scanning of the S_{chem}-covered Pt(111) electrode to 1.20 V, RHE. A LEED diffractogram was obtained for the clean Pt(111) surface (Fig. 5a), for the Pt(111) surface covered with a monolayer of S_{chem} (Fig. 5b) and a separate LEED pattern was recorded after each subsequent CV scan (Fig. 5c-e). The LEED data disclose that S_{chem} forms well-defined structures as $\theta_{S_{chem}}$ decreases. It is of interest to compare these structures with those formed under UHV condition during thermal desorption of S_{chem}. The UHV experiments show that upon thermal desorption of S_{chem} from the Pt(111) substrate, two well-defined structures are formed: (i) $\left(\sqrt{3}\times\sqrt{3}\right)$R30° at $\theta_{S_{chem}} = 1/3$; and (ii) $p(2\times2)$ at $\theta_{S_{chem}} = 1/4$. Thus, electrochemical oxidative desorption of S_{chem} allows improved and more precise control of the S_{chem} coverage and formation of a new structure, namely $c(2\times2)$ at $\theta_{S_{chem}} = 1/2$, which has not been achieved under UHV condition. A visual representation of the surface structures formed by S_{chem} on Pt(111) during electrochemically-stimulated and thermally stimulated desorption is shown in Fig. 6. LEED patterns were also observed for $\theta_{S_{chem}}$ below 0.2 ML, thus indicating

that the surface was covered by structured S_{chem} islands of the size higher than the coherence length of the electron beam at the kinetic energy applied, therefore some more than 50Å.

Impact of Temperature Variation on Oxidative Desorption of S_{chem}.

The authors examined the impact of temperature variation of the oxidative desorption of S_{chem} from the Pt(111) substrate. Temperature-dependence studies were carried out according to the previously described procedure [20,39,40,51-53]. In each series of measurements, *the same* S_{chem} monolayer was pre-formed according to the procedure described in Experimental and in ref. 19; the S_{chem} overlayer was subsequently desorbed by multiple scanning the Pt(111) electrode to 1.20 V, RHE until a S_{chem}-free CV profile was obtained. The first ever results on T-dependence of the oxidative desorption of S_{chem} from a well-defined Pt(111) substrate are shown in Fig. 7 and they reveal that the sharp desorption peak shifts towards less-positive values when T is raised from 273 to 323 K. An analysis of the data shows that peak potential, E_P, versus T relation is linear. This displacement of the peak potential may be ascribed to a lower value of the activation energy of desorption accomplished through T increase. The results shown in Fig. 7 form a basis of a more detail analysis of thermodynamics of the oxidative desorption of S_{chem} which will be reported in a subsequent paper.

The CV data shown in Figs. 2 and 7 combined with equation 1 create the basis for quantitative treatment of sulfur adsorption data, namely the relation between the S_{chem} coverage, T and the number of respective desorption scans to 1.20 V, RHE. In the CV profiles, the charge density generated on the positive-going scan at $E \geq 0.90$ V is due to Pt(111) surface oxidation and sulfur oxidative desorption, $q_{AN(i)} = q_{OX(i)} + q_{S(i)}$, where q is the charge density and *i* denotes the scan number. On the negative-going scan, the charge density, $q_{CATH(i)}$, corresponds to reduction of the surface oxide film. (There is no oxide film formed in the first scan but the subsequent cycles result in a disordered surface which oxidizes at lower potentials that the ordered Pt(111) surface.). The difference for every CV profile allows one to evaluate the charge density of the sulfur oxidative desorption per cycle, $q_{S(i)}$. Summation of the densities for all the CV profiles leads to the determination of the overall charge density of sulfur oxidative desorption, $q_S = \sum_i q_{S(i)}$, and, on the basis of equation 2, the amount of sulfur adatoms present on the Pt(111) substrate prior to commencement of the oxidative desorption.

$$N_S = \frac{q_S}{6\,e} \qquad (2)$$

where e is the electron charge in q_S charge units and N_S is the number of sulfur adatoms per 1 cm^2. In Fig. 8, the authors show a 3D graph which shows the relation between $\theta_{S_{chem}}$, T and the number of respective desorption scans to 1.20 V, RHE. As expected, T increase increases the effectiveness of S_{chem} desorption. An analysis of the data and the results shown in ref. 20 presents a unique methodology of control of $\theta_{S_{chem}}$ as well as the surface structure of S_{chem} through variation of the number of desorption scans, temperature and the anodic potential limit.

Energetics of the UPD H in Presence of a Submonolayer of S_{chem}.

Elsewhere [54], the authors presented the first-ever thermodynamic data on the UPD H on a well-defined Pt(111). On the basis of the data presented above, the authors were able to examine thermodynamic state functions of the UPD H on Pt(111) in presence of a submonolayer of S_{chem} having $\theta_{S_{chem}} = 0.10$. Because thermodynamics of the process will be treated in detail in a separate paper, the authors only summarize their foremost findings and the methodology applied. The Gibbs free energy of adsorption in presence of the submonolayer of S_{chem}, $\Delta G_{ads(S)}(H_{UPD})$, was evaluated on the basis equation 3 and the experimental results shown above [12-14,20,39,40]:

$$\frac{\theta_{H_{UPD}}}{1-\theta_{H_{UPD}}-\theta_S} = P_{H_2}^{1/2} \exp\left(-\frac{E\,F}{R\,T}\right) \exp\left(-\frac{\Delta G_{ads(S)}(H_{UPD})}{R\,T}\right) \qquad (3)$$

where $P_{H_2}^{1/2}$ is the partial pressure of H_2 in the reference electrode compartment, E is the potential difference between the working electrode and the reference electrode immersed in the same solution, thus E measured versus the RHE, T is the temperature, R and F are physico-chemical constants, and $\Delta G_{ads(S)}(H_{UPD})$ includes a coverage-dependent parameter, $\omega(\theta_{H_{UPD}})$, which describes their lateral interactions between the H_{UPD} adatoms, thus $\Delta G_{ads(S)}(H_{UPD})_{\theta_{H_{UPD}}\neq 0} = \Delta G_{ads(S)}(H_{UPD})_{\theta_{H_{UPD}}=0} + \omega(\theta_{H_{UPD}})$. Values of whole $\Delta G_{ads(S)}(H_{UPD})$ for the whole range of $\theta_{H_{UPD}}$ are given in Table I.

Table I. Summary of thermodynamic data for the studied systems.

State Function versus System	$\Delta G_{ads}(H_{UPD})$ kJ mol^{-1}	$\Delta S^{\circ}_{ads}(H_{UPD})$ J mol^{-1} K^{-1}	$\Delta H^{\circ}_{ads}(H_{UPD})$ kJ mol^{-1}	$E_{M-H_{UPD}}$ kJ mol^{-1}
H_{UPD} on Pt(111)	from −26 to −8	from −80 to −62	from −44 to −33	from 262 to 250
H_{UPD} on Pt(111) in presence of S_{chem} ($\theta_S = 0.1$)	from −15 to −2	from 64 to 135	from 4 to 32	from 214 to 186

$\Delta S^{\circ}_{ads(S)}(H_{UPD})$ may be determined from the dependence of $\Delta G_{ads(S)}(H_{UPD})$ on T for every $\theta_{H_{UPD}} = \text{const}$ (equation 4) and $\Delta H^{\circ}_{ads(S)}(H_{UPD})$ on the basis of the experimental values of $\Delta G^{\circ}_{ads(S)}(H_{UPD})$ and $\Delta S^{\circ}_{ads(S)}(H_{UPD})$, and the well-known formula $\Delta G^{\circ} = \Delta H^{\circ} - T\,\Delta S^{\circ}$.

$$\Delta S^{\circ}_{ads(S)}(H_{UPD}) = -\left[\frac{\partial\, {}_{ads(S)}\Delta G(H_{UPD})}{\partial T}\right]_{\theta_{H_{UPD}} = \text{const}} \qquad (4)$$

The values of $\Delta S^{\circ}_{ads(S)}(H_{UPD})$ and $\Delta H^{\circ}_{ads(S)}(H_{UPD})$ which are summarized in Table I reveal that the UPD H on Pt(111) is enthalpy-driven in absence of S_{chem} but becomes entropy-driven in presence of S_{chem}. Finally, knowledge of $\Delta H^{\circ}_{ads(S)}(H_{UPD})$ allowed the authors to determine for the first time the $Pt(111)-H_{UPD}$ surface bond energy in presence of a submonolayer of S_{chem}, $E_{Pt(111)-H_{UPD}(S)}$ (see equation 5).

$$E_{M-H_{UPD}(S)} = \frac{1}{2}D_{H_2} - \Delta H^{\circ}_{ads(S)}(H_{UPD}) \qquad (5)$$

where D_{H_2} is the dissociation energy of the hydrogen molecule and $D_{H_2} = 436$ kJ mol^{-1}. The data indicate that presence of S_{chem} decreases the surface bond energy between H_{UPD} and the Pt(111) substrate through local electron withdrawing effects which decrease the electron density at the $Pt(111)-H_{UPD}$ bond.

CONCLUSIONS

1. Immersion of Pt(111) in aqueous Na_2S solution results in formation of a layer of chemisorbed S, S_{chem}. This layer can be gradually removed by oxidative desorption at $E \geq 0.95$ V, RHE, and the S_{chem} coverage can be controlled with an accuracy of 2% of a monolayer.

2. The S_{chem} layer completely suppresses the UPD H and anion adsorption as well as it affects the oxide growth behavior on Pt(111). S_{chem} forms well-defined structures on Pt(111) for $0.50 \geq \theta_{S_{chem}} \geq 0.25$. When $\theta_{S_{chem}} \leq 0.20$ structured islands of S_{chem} observed.

3. AES and CEELS experiments indicate that the adsorbed S is not present in an oxidized or reduced state; it is almost of atomic character with an incomplete negative charge due to partial charge transfer between the Pt(111) substrate and the S adsorbate.

4. Presence of S_{chem} significantly influences thermodynamics of the UPD H resulting in less-negative values of $\Delta G_{ads(S)}(H_{UPD})$. In absence of S_{chem} the process is enthalpy-driven whereas in presence of S_{chem} it becomes entropy driven.

5. The $Pt(111)-H_{UPD}$ surface bond energy is significantly weaker in presence of S_{chem} than in its absence. This is ascribed to local electron withdrawing effects arising from the presence of coadsorbed S_{chem} which withdraws electron density from the $Pt(111)-H_{UPD}$ bond acting through the Pt(111) substrate. This may be associated with a small degree of ionicity of the $Pt(111)-S_{chem}$ bond.

ACKNOWLEDGMENTS

The research was supported by the NSERC of Canada and le FCAR du Québec. A. Zolfaghari gratefully acknowledges a graduate fellowship from the MCHE of Iran, the Departament of Energy Summer Fellowship, administered by The Electrochemical Society, Inc., and la Bourse de la famille Roger-Beaudoin of l'Université de Sherbrooke. The research performed at The University of Illinois at Urbana-Champaign was supported by the national Science Foundation, under Grant CHE 94-11184, and the Department of Energy, under Grant DE-AC02-76ER01198, administrated by the Frederick Seitz Research Laboratory at the University of Illinois at Urbana-Champaign.

REFERENCES

1. T. Louka, *J. Electroanal. Chem.*, **31**, 319 (1971).

2. A. Q. Contractor and H. Lal, *J. Electroanal. Chem.*, **96**, 175 (1979).

3. J. Oudar, *Cat. Rev. - Sci. Eng.*, **22**, 171 (1980).

4. N. D. Lang, S. Holloway and J. K. Nørskov, *Surface Sci.*, **150**, 24 (1985).

5. R. A. Oriani, J. P. Hirth and M. Smialowski, Editors, *Hydrogen Degradation of Ferrous Metals*, Noyes Publications, Park Ridge, NJ (1985).

6. D. Zurawski, K. Chan and A. Wieckowski, *J. Electroanal. Chem.*, **210**, 315 (1986).

7. E. Protopopoff and P. Marcus, *J. Electrochem. Soc.*, **135**, 3073 (1988).

8. N. Batina, J. W. McCargar, L. Laguren-Davidson, C.-H. Lin and A. T. Hubbard, *Langmuir*, **5**, 123 (1989).

9. D. Zurawski and A. Wieckowski, *Langmuir*, **8**, 2317 (1992).

10. P.K. Subramanyan, in *Comprehensive Treatise of Electrochemistry*, Vol. 4, Ch.8, J.O'M. Bockris, B.E. Conway, E. Yeager and R.E. White, Editors, Plenum Press, New York (1981).

11. B. E. Conway and G. Jerkiewicz, Editors, *Electrochemistry and Materials Science of Cathodic Hydrogen Absorption and Adsorption*, The Electrochemical Society, PV 94-21, Pennington, NJ (1995).

12. B. E. Conway and G. Jerkiewicz, *J. Electroanal. Chem.*, **357**, 47 (1993).

13. B. E. Conway and G. Jerkiewicz, *Z. Phys. Chem., Bd.*, **183**, 281 (1994).

14. G. Jerkiewicz, J. J. Borodzinski, W. Chrzanowski and B. E. Conway, *J. Electrochem. Soc.*, **142**, 3705 (1995).

15. J. Rodriguez and M. Khun, *J. Phys. Chem.*, **99**, 9567 (1995).

16. M. Khun and J. Rodriguez, *J. Vac. sci. Technol. A*, **13(3)**, 1569 (1995).

17. C. Quijada, A. Rodes, J. L. Vázquez, J. M. Pérez and A. Aldaz, *J. Electroanal. Chem.*, **394**, 217 (1995).

18. C. Quijada, A. Rodes, J. L. Vázquez, J. M. Pérez and A. Aldaz, *J. Electroanal. Chem.*, **398**, 105 (1995).

19. Y.-E. Sung, W. Chrzanowski, A. Zolfaghari, G. Jerkiewicz and A. Wieckowski, *J. Am. Chem. Soc.*, **119**, 194 (1997).

20. A. Zolfaghari, F. Villiard, M. Chayer and G. Jerkiewicz, *J. Alloys Comp.*, **253-254**, 481 (1997).

21. G. M. Whitesides, *Sci. Am.*, **273**, 146 (1995).

22. A. Ulman, *Chem. Rev.*, **96**, 1533 (1996).

23. N. Bowden, A. Terfort, J. Carbeck and G. M. Whitesides, *Science*, **276**, 233 (1997).

24. X. Feng, G. E. Fryxell, L.-Q. Wang, A. Y. Kim, J. Liu and K. M. Kemner, *Science*, **276**, 923 (1997).

25. K. M. Mackay, *Hydrogen Compounds of the Metallic Elements*, E.&F.N. Spon, London (1966).

26. G. Alefeld and J. Volkl, Editors, *Hydrogen in Metals*, Parts I and II, Springer-Verlag, New York (1978).

27. L. Schlapbach, Editor, *Hydrogen in Intermetalic Compounds*, Part I, Springer-Verlag, New York (1988); Part II, Springer-Verlag, New York (1992).

28. J. J. G. Willems, *Ph.D. Thesis*, Eindhoven, The Netherland (1984).

29. A. F. Andersen and A. J. Maeland, Editors, *Hydrides for Energy Storage*, Pergamon Press, Oxford (1978).

30. S. R. Ovshinsky, M. A. Fetcenko and J. Ross, *Science*, **260**, 176 (1993).

31. S. R. Ovshinsky, K. Sapru, B. Reichman and A. Reger, US Patents No. 4,623,597 (1986); see also S. R. Ovshinsky and M. A. Fetcenko, US Patent No. 5,096,667 (1992); No. 5,104,617 (1992); No. 5,135,589 (1992); No. 5,238,756 (1993); No. 5,277,999 (1994).

32. M. Ciureanu, D. Moroz, R. Ducharme, D. H. Ryan, J. Ström-Olsen and M. Trudeau, *Zeit. Phys. Chem. Bd.*, **183**, 365 (1994); Q. M. Yang, M. Ciureanu, D. H. Ryan and J. Ström-Olsen, *J. Electrochem. Soc.*, **141**, 2108; 2113 (1994); **141**, 2430 (1994).

33. O. Savadogo, P. R. Roberge and T. N. Veziroglu, Editors, *New Materials for Fuel Cell Systems 1*, Proceedings of the First International Symposium on New Materials for Fuel Cell Systems, Édition de l'École Polytechnique de Montréal, Montréal (1995).

34. G. D. Adzic, J. R. Johnson, S. Mukerjee, J. McBreen and J. J. Reilly, *J. Alloys Comp.*, **253-254**, 579 (1997).

35. J. Clavilier, R. Faure, G. Guinet and R. Durand, *J. Electroanal. Chem.*, **107**, 205 (1980).

36. J. Clavilier, *J. Electroanal. Chem.*, **107**, 211 (1980).

37. A. Hamelin, in J. O'M. Bockris, B. E. Conway and R. E. White (Eds.), Modern Aspects of Electrochemistry, Vol. 16, Plenum Press, New York, 1985; Ch. 1.

38. A. Hamelin, S. Morin, J. Richer and J. Lipkowski, *J. Electroanal. Chem.*, **285**, 249 (1990).

39. A. Zolfaghari and G. Jerkiewicz, *J. Electroanal. Chem.*, **420**, 11 (1997).

40. A. Zolfaghari and G. Jerkiewicz, *J. Electroanal. Chem.*, **422**, 1 (1997).

41. J. Clavilier, K. El Achi, M. Petit, A. Rodes and M. A. Zamakhchari, *J. Electroanal. Chem.*, **295**, 333 (1990).

42. M. Wasberg, L. Palaikis, S. Wallen, M. Kamrath and A. Wieckowski, *J. Electroanal. Chem.*, **256**, 51 (1988).

43. P. Mrozek, H. Han, Y.-E. Sung and A. Wieckowski, *Surf. Sci.*, **319**, 21 (1994).

44. Y.-E. Sung, S. Thomas and A. Wieckowski, *J. Phys. Chem.*, **99**, 13513 (1995).

45. S. Thomas, Y.-E. Sung, H. S. Kim and A. Wieckowski, *J. Phys. Chem.*, **100**, 11726 (1996).

46. H. Angerstein-Kozlowska, in *Comprehensive Treatise of Electrochemistry*, Eds. E. Yeager, J. O'M. Bockris, B. E. Conway and S. Sarangapani, Vol. 9, p. 15, Plenum Press, New York (1984).

47. D. Briggs and J. C. Rivière, in *Practical Surface Analysis*, Vol. 1, *Auger and X-Ray Photoelectron Spectroscopy*, D. Briggs and M. P. Seah, Editors, pp. 85, 201, John Wiley & Sons, New York (1990).

48. J. C. Rivière, *Surface Analytical Techniques*, Oxford University Press, New York (1990).

49. A. P. Hitchcock and C. E. Brion, *Chem. Phys.*, **33**, 55 (1978).

50. Moulder, J. F., Editor, *Hanboook of X-Ray Photoelectron Spectroscopy*, Perkin Elmer, Eden Prairie, MN, USA (1992).

51. G. Jerkiewicz and A. Zolfaghari, *J. Electrochem. Soc.*, **143**, 1240 (1996).

52. G. Jerkiewicz and A. Zolfaghari, *J. Phys. Chem.*, **100**, 8454 (1996).

53. A. Zolfaghari, M. Chayer and G. Jerkiewicz, *J. Electrochem. Soc.*, **144**, 3034 (1997).

54. A. Zolfaghari and G. Jerkiewicz, *Electrochim. Acta*, submitted for publication in the same issue.

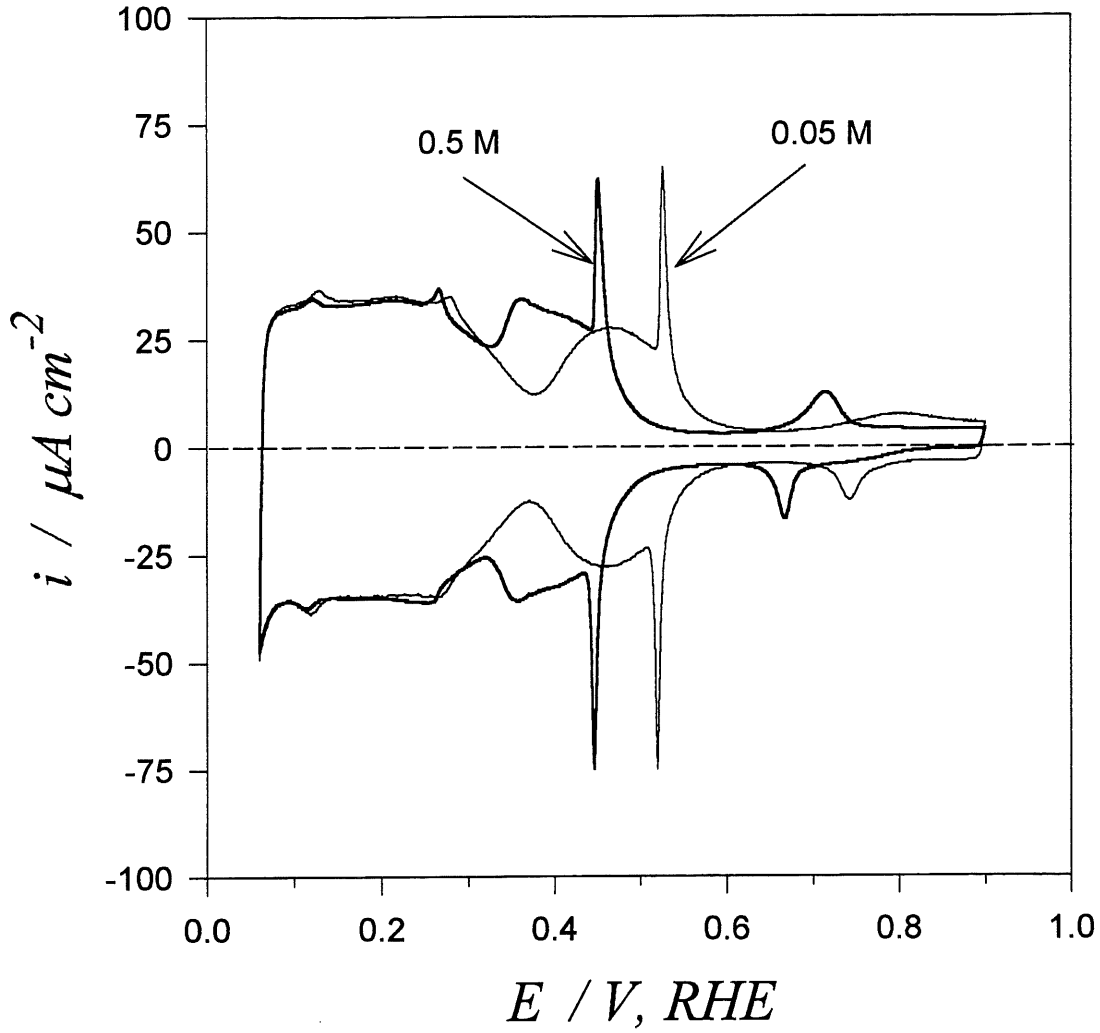

Figure 1. CV profiles for a Pt(111) electrode cooled in H_2 + Ar in 0.05 and 0.5 M aqueous H_2SO_4 solutions; A = 0.058 ± 0.001 cm^2, T = 298 K and s = 50 mV s^{-1}. The CV component corresponding to anion adsorption shifts towards less-positive values when the concentration is raised.

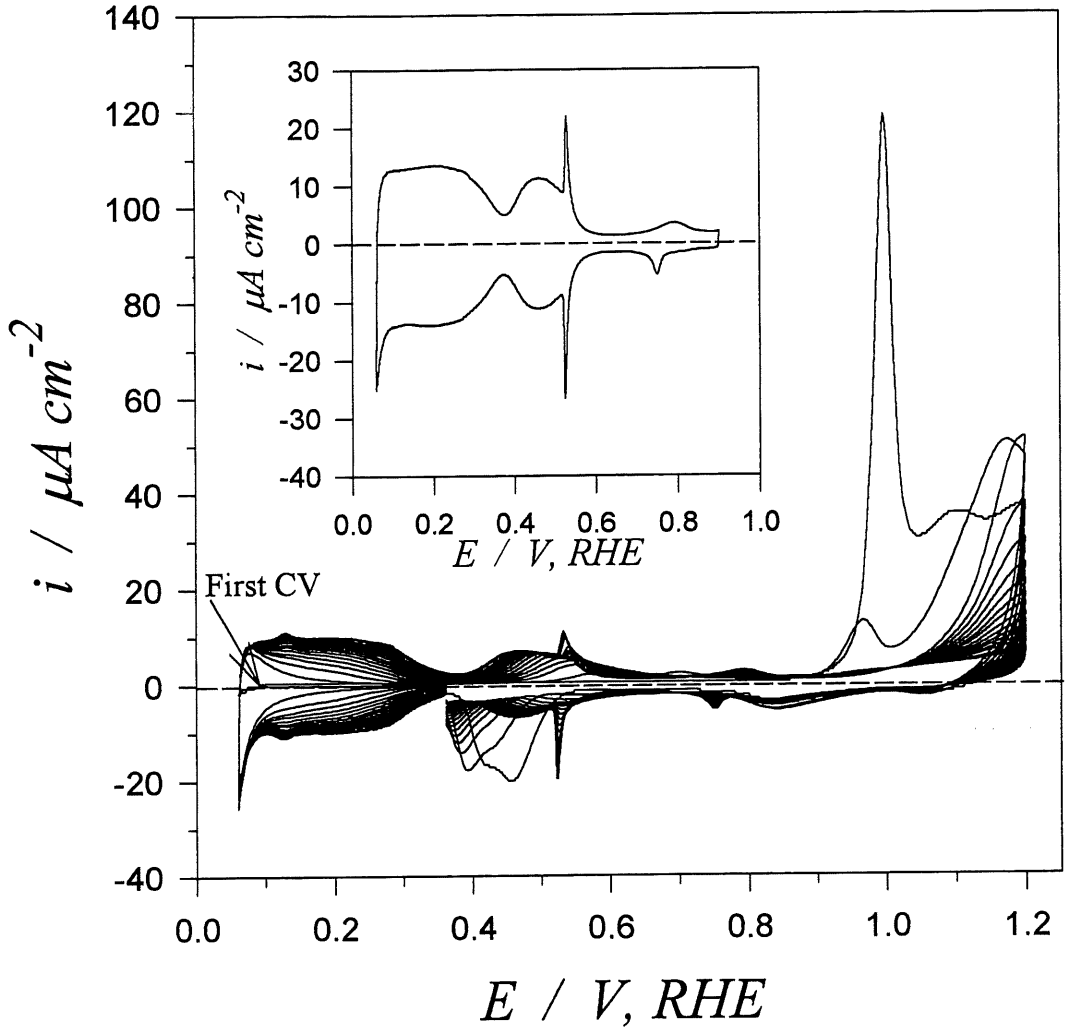

Figure 2. Series of CV profiles for a Pt(111) electrode in 0.05 M aqueous H_2SO_4 solution initially covered with a monolayer of S_{chem} and revealing the impact of the oxidative desorption of S_{chem}, by cycling to 1.20 V, on the CV behavior; $A_r = 0.720 \pm 0.005\ cm^2$, $T = 298\ K$ and $s = 20\ mV\ s^{-1}$. The inset refers to a clean Pt(111) electrode.

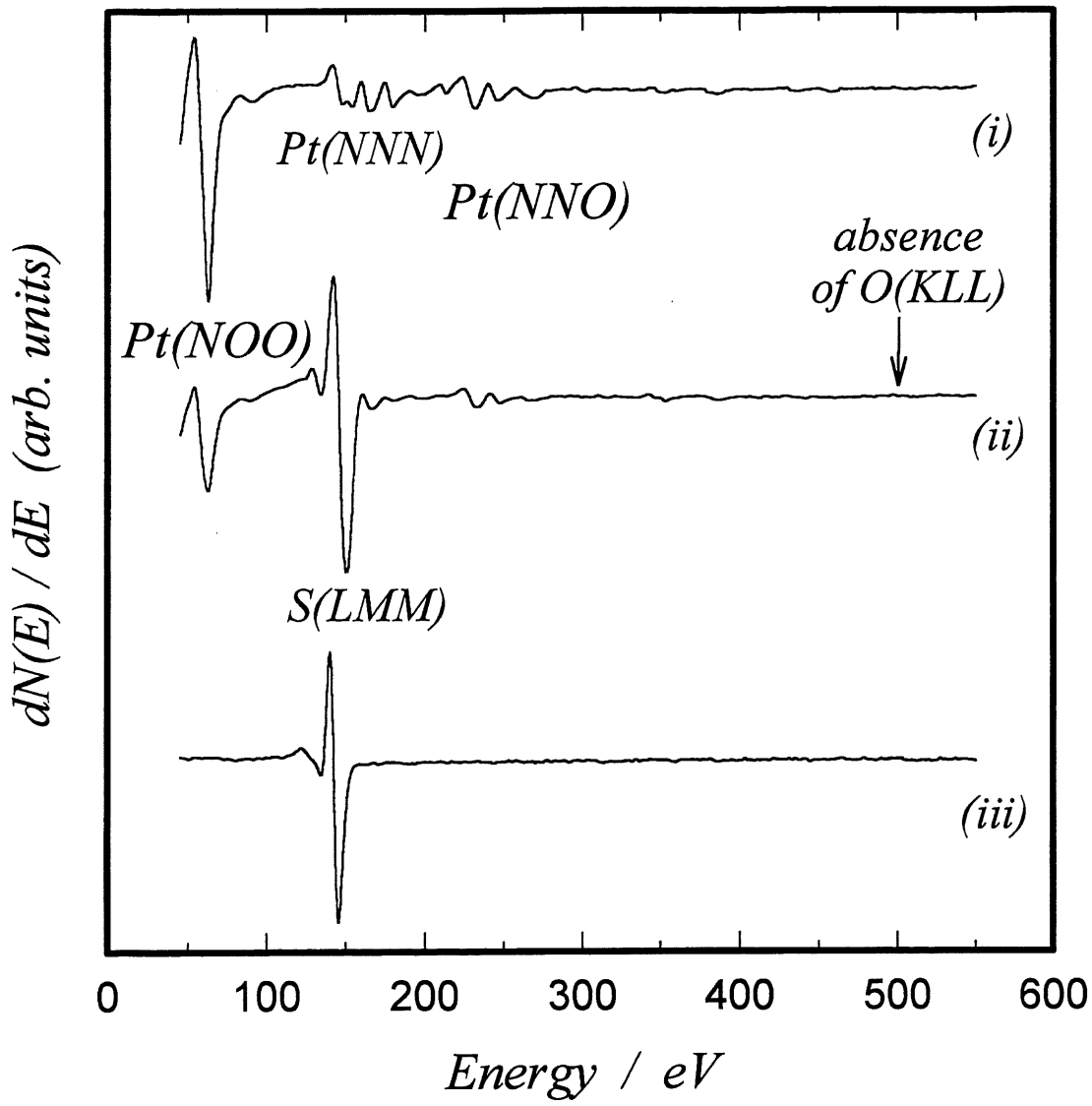

Figure 3. Auger electron spectra (AES) spectra taken at 3 keV primary beam energy in the 50 - 550 eV range. From top to bottom, data for: *(i)* the clean Pt(111) electrode; *(ii)* the Pt(111) electrode covered with a layer of chemisorbed S; *(iii)* the Pt(111) electrode covered with a thin film of Na_2S.

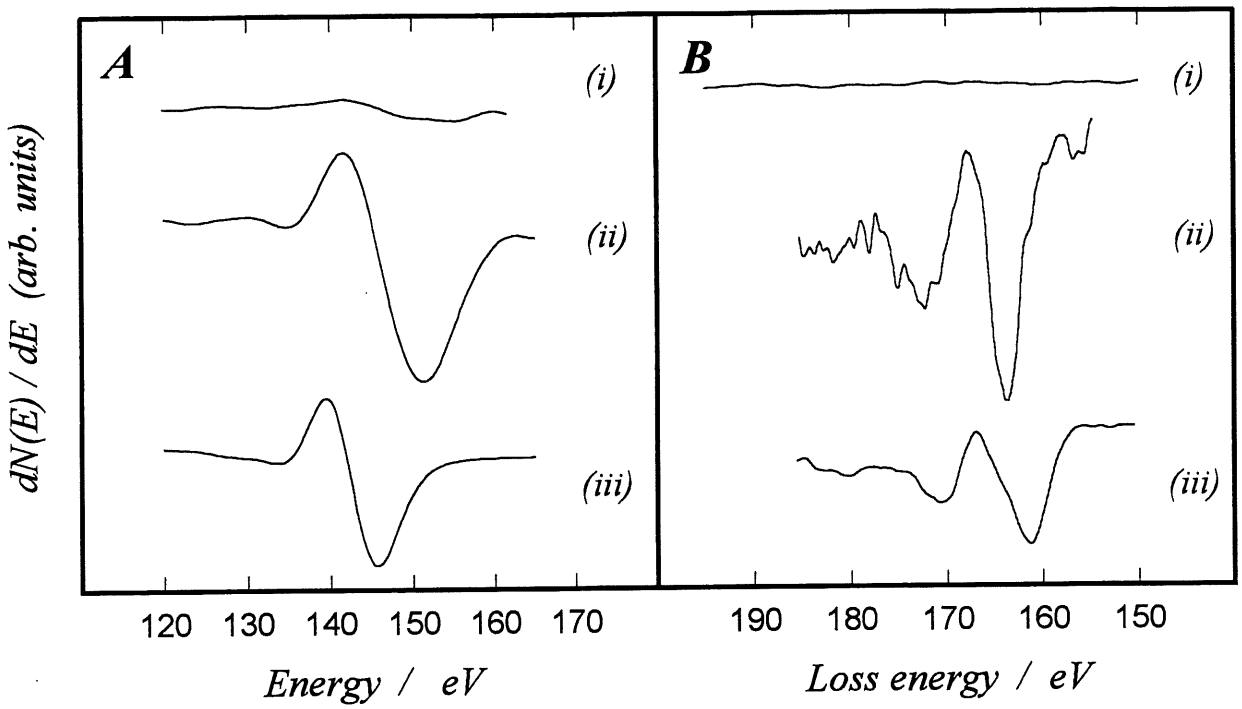

Figure 4. *(A)* High-resolution Auger electron spectra, AES, spectra taken at 3 keV primary beam energy in the 120 - 165 eV range for the S(LMM) and Pt(NNN) regions. From top to bottom, data for: *(i)* the clean Pt(111) electrode; *(ii)* the Pt(111) electrode covered with a layer of chemisorbed S; *(iii)* the Pt(111) electrode covered with a thin film of Na_2S. *(B)* Core level electron energy loss spectra (CEELS) taken at 500 eV primary beam energy in the 150 - 190 eV loss energy range for the S2p transition. From top to bottom, data for: *(i)* the clean Pt(111) electrode; *(ii)* the Pt(111) electrode covered with a layer of chemisorbed S; *(iii)* the Pt(111) electrode covered with a thin film of Na_2S.

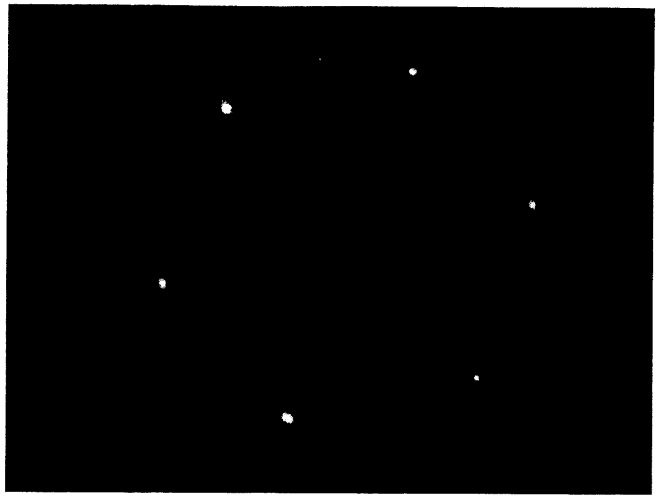

(a)

(b)

Figure 5. Low energy electron diffraction (LEED) patters for: *(a)* the clean Pt(111) electrode having the (1×1) structure; *(b)* the Pt(111) electrode covered with a monolayer of S_{chem} and having the (1×1); *(c)* the Pt(111) electrode the covered with a submonolayer of S_{chem} ($\theta_{S_{chem}} = 1/2$) and having the $c(2\times2)$ structure; *(d)* the Pt(111) electrode covered with a submonolayer of S_{chem} ($\theta_{S_{chem}} = 1/3$) and having $\left(\sqrt{3}\times\sqrt{3}\right)R30°$ structure; and *(e)* the Pt(111) electrode covered with a submonolayer of S_{chem} ($\theta_{S_{chem}} = 1/4$) and having the $p(2\times2)$ structure.

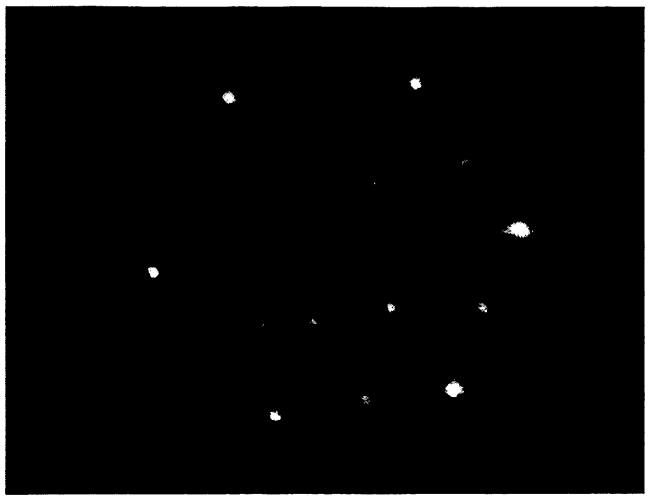

(c)

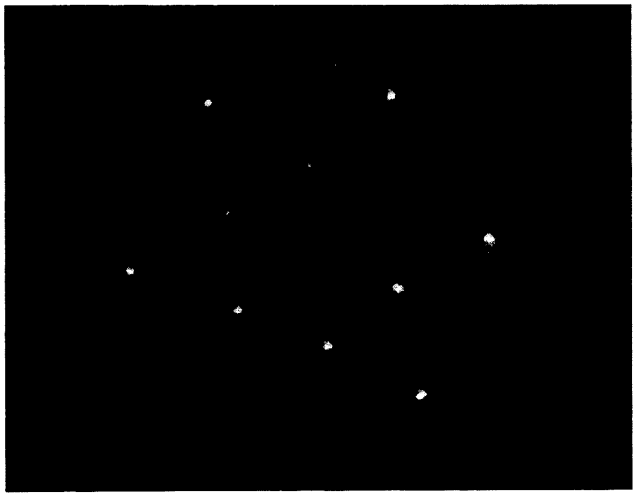

(d)

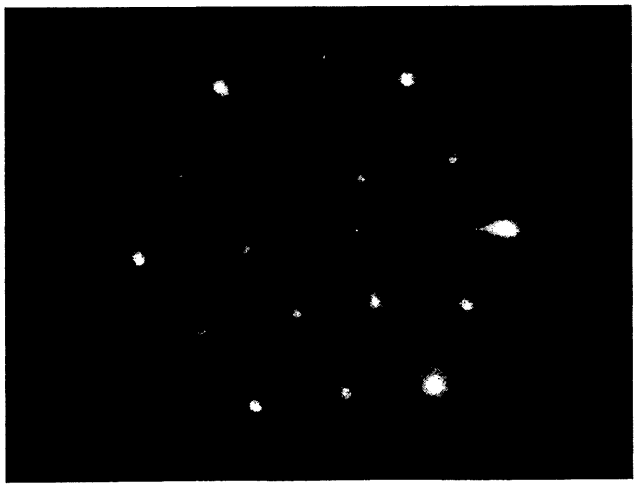

(e)

Figure 5. (continued)

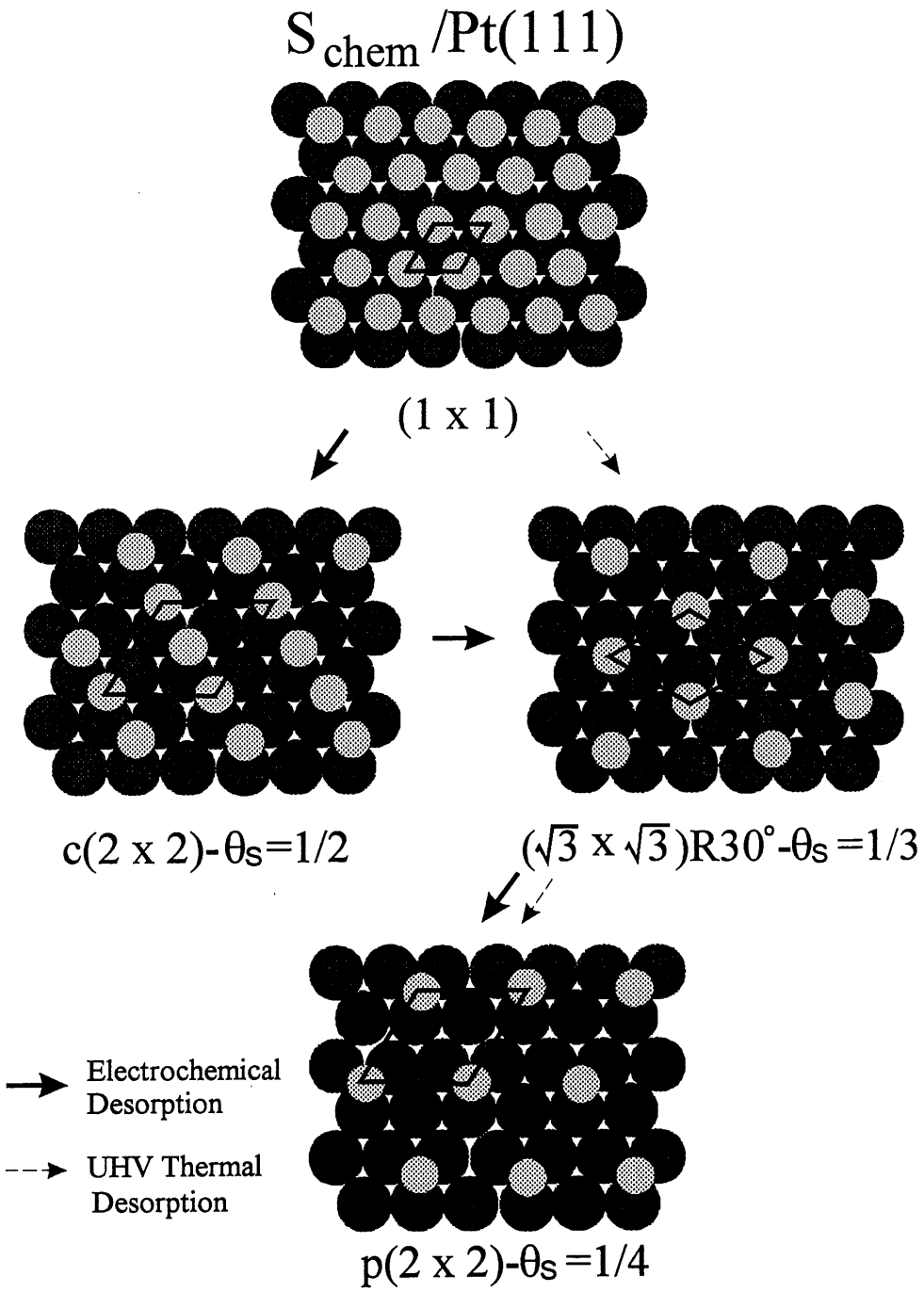

Figure 6. Visual representation of the surface structures formed by S_{chem} on Pt(111) during electrochemically and thermally stimulated desorption on the basis of the LEED results shown in Fig. 5.

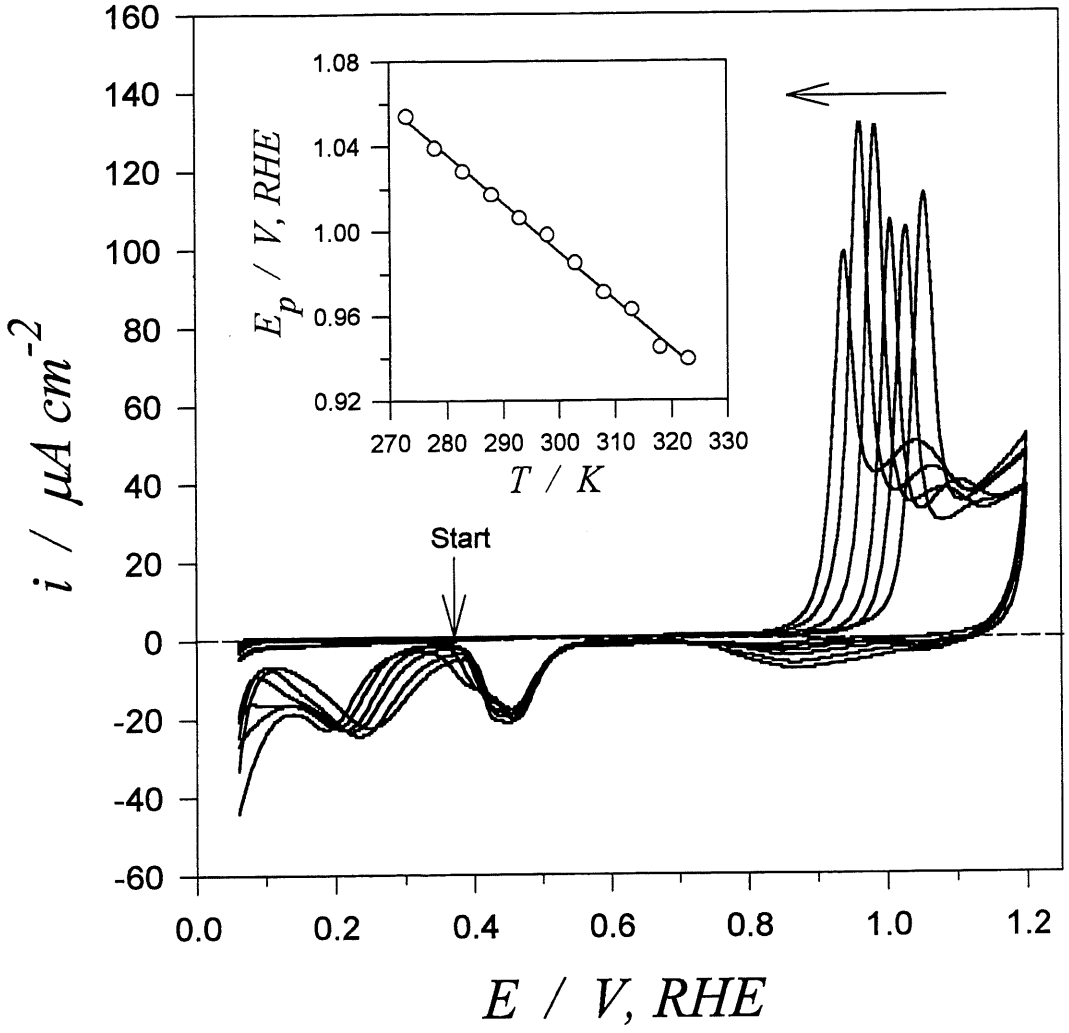

Figure 7. Series of CV profiles for a Pt(111) electrode in 0.05 M aqueous H_2SO_4 solution covered with a monolayer of S_{chem} ($\theta_{S_{chem}} = 1$) having the (1×1) structure. The CV profiles demonstrate the impact of T increase from 273 to 323 K (with an interval of 10 K) on the sharp peak of the S_{chem} oxidative desorption; $A_r = 0.720 \pm 0.005\ cm^2$, and $s = 20\ mV\ s^{-1}$. The inset show the peak potential, E_P, versus T relation.

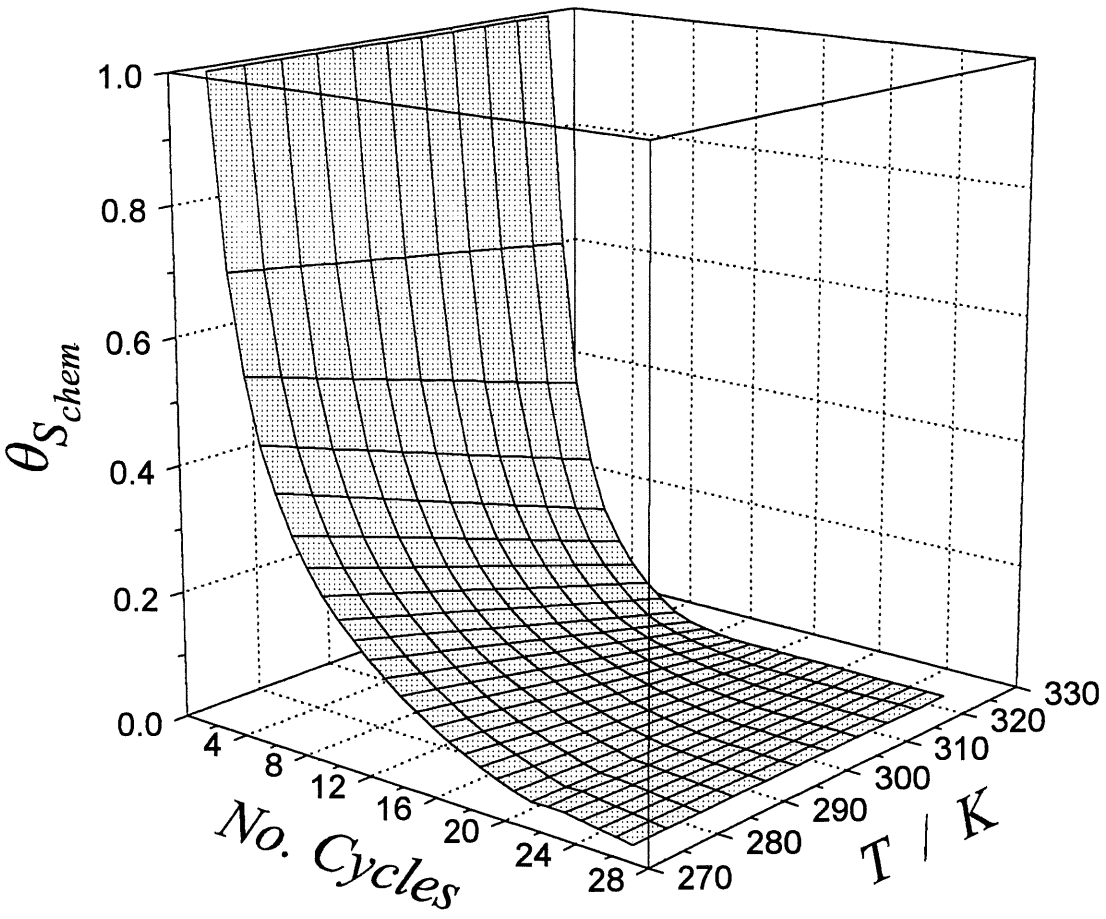

Figure 8. 3D graph showing the relation between the S_{chem} surface coverage, $\theta_{S_{chem}}$, the number of CV scans up to 1.20 V, RHE, for S_{chem} oxidative desorption and T determined on the basis of results presented in Figs. 2 and 7.

CHAPTER 4
GENERAL DISCUSSION

4.1 Temperature-Dependence of the UPD H on Rh(poly) and Pt(poly) Electrodes.

Cyclic-voltammetry, CV, and chronocoulometry (137) are experimental techniques that can be applied to evaluate temperature-dependence of the H_{UPD} surface coverage and to determine $\Delta G_{ads}(H_{UPD})$. CV is in many respects the electrochemical equivalent of temperature programmed desorption, TPD, although CV results in determination of different thermodynamic parameters than TPD. CV allows one to study the surface coverage of the adsorbed species during potential-stimulated adsorption and desorption at various temperatures. Theoretical treatment of CV experimental results leads to elucidation of important thermodynamic state functions such as ΔG_{ads}, ΔH°_{ads} and ΔS°_{ads}. Thus it is sensible to refer to it as *potential-stimulated adsorption-desorption*, PSAD.

A series of CV adsorption-desorption for the UPD H from 0.50 M aqueous solution of H_2SO_4 for various temperature between 273 and 343 K on Rh(poly) electrode demonstrate that the adsorption and desorption peaks shift towards less-positive potentials upon the temperature increase and that they are symmetric with respect to the potential axis indicating that the surface process is reversible (Fig. 1. in chapter 1.1). An increase of the cathodic current at the lower potential limit of the CV profiles, thus prior to the sweep reversal, is due to the onset of the over-potential deposition of H. Similar experiments were conducted in 0.05 and 0.10 M aqueous H_2SO_4 solutions in order to evaluate changes in the CV profiles brought about by the temperature variation (Fig. 2. in chapter 1.2). A series of UPD H cyclic-voltammetry adsorption-desorption profiles for the three concentrations of H_2SO_4 at different temperatures indicate the same behavior of the UPD H adsorption-desorption profiles which may be summarized as follows: (i) the temperature increase shifts the UPD H adsorption-desorption profiles towards less-positive values; (ii) no new features are observed in the CV profiles that could result from the temperature augmentation for a given concentration of H_2SO_4; (iii) upon diminution of the concentration of H_2SO_4, the UPD H adsorption-desorption cyclic-voltammetry peaks become less sharp (less pronounced) but the total H_{UPD} adsorption-desorption charge density remain unaffected (138-142).

Similar experiments were conducted on Pt(poly) electrode in 0.50, 0.05 and 0.10 M aqueous H_2SO_4 solutions in order to evaluate changes in the CV adsorption-desorption for the UPD H profiles brought about by the temperature (between 273 and 343 K) and concentration variation (Fig. 2. in chapter 2.1). The features may be summarized as follows: (i) upon the temperature increase, the UPD H adsorption-desorption profiles shift towards less-positive values; they are symmetric with respect to the potential axis indicating that the surface electrochemical process is reversible; (ii) the third anodic peak which appears between the two main ones decreases when the temperatures rises and gradually disappears; (iii) redistribution of the UPD H adsorption-desorption charges is observed with the temperature increase; (iv) apart from the redistribution of the adsorption-desorption charges, no new features are observed in the CV profiles that could result from the temperature increase for a given concentration of H_2SO_4; (v) upon decrease of the concentration of H_2SO_4, the UPD H adsorption-desorption peaks become less sharp (less pronounced); and (vi) an increase of the cathodic current at the lower potential limit of the CV profiles, thus prior to the sweep reversal, is due to the onset of the OPD H (24,51).

It is of interest to briefly discuss the increase of the cathodic current at the lower potential limit of the CV profiles, an aspect not scrutinized in previous literature. At first, it might be surprising to observe a cathodic current at positive potentials due to onset of adsorption of H_{OPD}, the latter being an intermediate of the HER. Indeed, the thermodynamic reversible potential of the HER, E°_{HER}, equals zero but it refers to a thermodynamic equilibrium involving the hydrogen gas evolved at the standard pressure of 1 atm. Because the hydrogen pressure in the working-electrode compartment is very small, the equilibrium potential of the HER is displaced towards positive values as expected on the basis of the Nernst equation.

4.2 Temperature-Dependence of the UPD H on Pt(100) and Pt(111) Electrodes.

The CV profile for Pt(100) in 0.5 M aq. H_2SO_4 at 298 K at potentials between 0.06 and 0.80 V, RHE, reveals that the UPD H and anion adsorption processes occur within two potential regions which overlap (Fig. 1. in chapter 3.1). A series of CV profiles for Pt(100) in 0.5 M aq. H_2SO_4 for $293 \leq T \leq 328$ K, demonstrates that the profiles are symmetric with respect to E axis, thus testifying that the surface electrochemical processes taking place in this potential range are kinetically reversible (Fig. 2. in chapter 3.1). Upon T increase, the CV

characteristics, on the SHE potential scale, corresponding to the UPD H and anion adsorption shift towards less-positive potentials (143-145); the current density of the sharp peak which corresponds to the anion adsorption significantly decreases (143-145). Integration of the CV's shows that the total adsorption charge density, q_T, decreases from 220 to 150 $\mu C\,cm^{-2}$, thus by 70 $\mu C\,cm^{-2}$, when T is raised by only 35 K, namely from 293 to 328 K (Fig. 5. in chapter 3.1). The remarkable decrease of q_T (by 32% of the total charge density at 298 K) for such a narrow T range is indicative of very strong T-dependence of the surface electrode processes. However, at present one may not conclude how much of the diminished charge density is associated with the UPD H and how much with the anion adsorption. The experimentally determined values for E_P of the sharp peak (representing the anion adsorption) as a function of T reveals alinear relationship (Fig. 3. in chapter 3.1). The E_P versus T relation has a slope, $\partial E_P / \partial T$, equal to $-0.50 \times 10^{-3}\ V\,K^{-1}$ on the RHE scale and $-1.34 \times 10^{-3}\ V\,K^{-1}$ on the SHE one (Fig. 6. in chapter 3.3).

In a CV profile for Pt(111) in 0.5 M aq. H_2SO_4 at 298 K at potentials between 0.06 and 0.90 V, RHE, the potential region of the UPD H and the anion adsorption characterized by a sharp spike distinguishable (Fig. 1. in chapter 3.2). Apart from the small peak/wave in the double-layer region, the profile is symmetric with respect to the potential axis indicating that the surface electrochemical processes are kinetically reversible. Upon T increase (from 275 to 328 K), the CV characteristics corresponding to the UPD H and anion adsorption on the standard hydrogen electrode, SHE, potential scale shift towards less-positive potentials but the displacement of the UPD H profiles is more pronounced than that of the anion one (Fig. 3. in chapter 3.3). Integration of the CV profiles leads to determination of the total adsorption charge density, q_T, as a function of T ($q_T = q_{H_{UPD}} + q_{AN}$ where $q_{H_{UPD}}$ is the charge density for the UPD H and q_{AN} is the charge density for the anion adsorption). At 298 K, the values of q_T is 252 ± 5 $\mu C\,cm^{-2}$ (Fig. 3. in chapter 3.2). It must be emphasized that does not have to give the theoretical value of one monolayer (ML) H_{UPD} (240.3 $\mu C\,cm^{-2}$) because the profile corresponds to both the surface-electrochemical processes, namely the UPD H and anion adsorption (143-145). Since the charge density does not have to equal to that of 1 ML of H_{UPD}, the overall charge density depends on the surface coverage by H_{UPD} and the adsorbed anion, $\theta_{H_{UPD}}$ and θ_{AN}, respectively, and it may vary its value accordingly. Furthermore, since the charge density of the adsorbed species is affected by their chemical identity and the degree of discharge upon adsorption of the ionic species, at the present state of knowledge, it is

difficult to predict any "theoretical charge density" of adsorption that the integration of the CV profile should provide. The experimentally determined variation of the peak potential, E_P, of the sharp peak (the "spike") in the potential region corresponding to anions adsorption as a function of T reveals two linear plots, one corresponding to the RHE potential scale and the other to the SHE one (Fig. 4. in chapter 3.3). The results testify that the E_P versus T relation is linear in both cases and that the slope, $\partial E_P / \partial T$, equals 0.57×10^{-3} V K^{-1} for the RHE scale and -0.27×10^{-3} V K^{-1} for the SHE one. The anodic and cathodic component of the wave/peak in the double-layer region is asymmetric with respect to the E axis but the difference between the peak potentials decreases upon T increase (Fig. 5. in chapter 3.2).

4.3 Thermodynamic Approach to the UPD H on Noble-Metal Electrocatalysts.

On the basis of CV profiles for the entire range of T studied and equation 4.1, one can examine energetics of the UPD H (99,146-148).

$$\frac{\theta_{H_{UPD}}}{1-\theta_{H_{UPD}}} = f_{H_2}^{1/2} \exp\left(-\frac{E_{RHE}F}{RT}\right)\exp\left(-\frac{\Delta G_{ads}(H_{UPD})}{RT}\right) \qquad [4.1]$$

Here E_{RHE} is the potential measured versus the RHE in the same electrolyte and at the same T, f_{H_2} is the fugacity of molecular hydrogen in the RHE compartment (under normal conditions $f_{H_2} \cong P_{H_2}$; P_{H_2} is corrected for the vapor pressure of the electrolyte at T), and $\Delta G_{ads}(H_{UPD})$ is the Gibbs free energy of adsorption at T and at the potential, E_{RHE}, at which the H_{UPD} coverage reaches the value of $\theta_{H_{UPD}}$. Equation 4.1 is a different form of equation 4.2 which describes the H_{UPD} surface coverage vs. potential and temperature (for derivation, see ref. 99).

$$\frac{\theta_{H_{UPD}}}{1-\theta_{H_{UPD}}} = a_{H^+} \exp\left(-\frac{E_{SHE}F}{RT}\right)\exp\left(-\frac{\Delta G^{\circ}_{ads}(H_{UPD})}{RT}\right) \qquad [4.2]$$

Here E_{SHE} is the potential measured versus the SHE, $\Delta G^{\circ}_{ads}(H_{UPD})$ is the standard Gibbs energy of adsorption, a_{H^+} is the activity of proton in electrolyte, and F and R are standard physico-chemical constants.

Equations 4.1 and 4.2 represent a general electrochemical adsorption isotherm for the UPD H, not the Langmuir or the Frumkin one, and no hypothesis is made with regard to presence/absence of lateral interactions between the H_{UPD} adatoms. Thus $\Delta G_{ads}(H_{UPD})$, as determined on the basis of equation 4.1 or 4.2, already contains the H_{UPD} coverage dependent and temperature dependent energy of lateral interactions, $\omega(\theta_{H_{UPD}}, T)$. An analysis of the experimentally examined 3D plots of $\Delta G_{ads}(H_{UPD})$ vs. $(\theta_{H_{UPD}}, T)$ allows one to assess the applicability of any of the adsorption isotherms to the system under study. If the $\Delta G_{ads}(H_{UPD})$ vs. $\theta_{H_{UPD}}$ relation is linear (equation 4.3), then one may say that the Frumkin isotherm is applicable. On the other hand, if $\Delta G_{ads}(H_{UPD})$ is constant and does not vary with $\theta_{H_{UPD}}$, then the Langmuir isotherm applies (equation 4.4).

$$\Delta G^{\circ}_{ads}(H_{UPD})_{\theta_{H_{UPD}}\neq 0} = \Delta G^{\circ}_{ads}(H_{UPD})_{\theta_{H_{UPD}}=0} + \theta_{H_{UPD}}\,\omega \qquad [4.3]$$

$$\Delta G^{\circ}_{ads}(H_{UPD})_{\theta_{H_{UPD}}\neq 0} = \Delta G^{\circ}_{ads}(H_{UPD})_{\theta_{H_{UPD}}=0} \qquad [4.4]$$

The standard entropy of adsorption, $\Delta S^{\circ}_{ads}(H_{UPD})$, is obtained by analysis of the experimental $\Delta G_{ads}(H_{UPD})$ versus T relations for every $\theta_{H_{UPD}} = \text{const}$ (equation 4.5). Because the $\Delta G_{ads}(H_{UPD})$ versus T plots are linear for every $\theta_{H_{UPD}}$ studied, one may easily determine $\Delta S^{\circ}_{ads}(H_{UPD})$ as a function of $\theta_{H_{UPD}}$.

$$\Delta S^{\circ}_{ads}(H_{UPD}) = -\left(\frac{\partial\,\Delta G_{ads}(H_{UPD})}{\partial T}\right)_{\theta_{H_{UPD}}=\text{const}} \qquad [4.5]$$

Examination of $\Delta G_{ads}(H_{UPD})$ versus $\theta_{H_{UPD}}$ (for $T = \text{const}$) leads to appraisal of the nature and strength of the energy of lateral interactions, $\omega(H_{UPD})$, acting between the H_{UPD} adatoms (equation 4.6), and to estimation of the adsorption isotherm which governs the process.

$$\omega(H_{UPD}) = -\left(\frac{\partial\,\Delta G_{ads}(H_{UPD})}{\partial\,\theta_{H_{UPD}}}\right)_{T=\text{const}} \qquad [4.6]$$

Knowledge of the average value of $\omega(H_{UPD})$ allows one to determine values of the dimensionless interaction parameter *g* which appears in the Frumkin isotherm (see refs. 10,31 and equation 4.7) and which is defined by equation 4.8. In order to avoid confusion, the authors wish to add that the parameter *g* appears on the left-hand side of equation 4.7*.

$$\frac{\theta_{H_{UPD}}}{1-\theta_{H_{UPD}}} \exp\left(g\,\theta_{H_{UPD}}\right) = a_{H^+} \exp\left(-\frac{E_{SHE}F}{RT}\right) \exp\left(-\frac{\Delta G^{\circ}_{ads}(H_{UPD})_{\theta_{H_{UPD}}=0}}{RT}\right) \qquad [4.7]$$

$$g = \frac{\omega(H_{UPD})}{RT} \qquad [4.8]$$

The enthalpy of adsorption for the UPD H , $\Delta H^{\circ}_{ads}(H_{UPD})$, is evaluated based on the above determined values of $\Delta G_{ads}(H_{UPD})$ at 298 K, thus $\Delta G^{\circ}_{ads}(H_{UPD})$, and $\Delta S^{\circ}_{ads}(H_{UPD})$, and the following well-known formula:

$$\Delta G^{\circ}_{ads}(H_{UPD}) = \Delta H^{\circ}_{ads}(H_{UPD}) - T\,\Delta S^{\circ}_{ads}(H_{UPD}) \qquad [4.9]$$

The energy of the $M-H_{UPD}$ bond, $E_{M-H_{UPD}}$, has never been evaluated for the electroadsorbed H on Rh, Pt, Ir or any other metal on which the UPD H takes place, thus it is one of the most significant contributions presented in the thesis. Moreover, evaluation of the $E_{M-H_{UPD}}$ vs. $\theta_{H_{UPD}}$ relation is of importance in determination of the influence of the electrified solid-liquid interface on the strength and nature of the metal-hydrogen bond.

The energy of the $M-H_{UPD}$ bond, $E_{M-H_{UPD}}$, can readily be calculated once the $\Delta H^{\circ}_{ads}(H_{UPD})$ values for various H_{UPD} surface coverages have been found. Appraisal of the $M-H_{UPD}$ bond energy, $E_{M-H_{UPD}}$, is based upon the following theoretical treatment.

The two single-electrode processes of the system studied are as follows:

working electrode: $H^+ + e + M \rightarrow M-H_{UPD}$ [4.10]

reference electrode: $1/2\,H_2 \rightarrow H^+ + e$ [4.11]

---

* See Appendix for discussion on limitation of this equation.

and their respective Born-Haber thermodynamic cycles are as follows:

$$\begin{array}{ccccccc} H^+_{(gas)} & + & e_{(gas)} & + & M & \xleftarrow{I_H} & H_{(gas)} + M \\ \downarrow \Delta H^\circ_{solv} & & \uparrow \Phi + EF & & & & \uparrow E_{M-H_{UPD}} \end{array} \qquad [4.12]$$

$$H^+_{(aq)} + e_{M(E\neq 0)} + M \xrightarrow{\Delta H^\circ_{WE}} M - H_{UPD}$$

and

$$\begin{array}{ccccc} H_{(gas)} & \xrightarrow{I_H} & H^+_{(gas)} & + & e_{(gas)} \\ \uparrow \frac{1}{2} D_{H_2} & & \downarrow \Delta H^\circ_{solv} & & \uparrow \Phi \end{array} \qquad [4.13]$$

$$1/2\, H_{2\,(gas)} \xrightarrow{\Delta H^\circ_{RE}} H^+_{(aq)} + e_{M(E=0)}$$

where ΔH°_{solv} is the standard enthalpy of solvation of H^+, I_H is the ionization potential of H, Φ is the metal work function and it varies linearly with the applied potential, thus $\Phi_{(E\neq 0)} = \Phi_{(E=0)} + FE$, D_{H_2} is the dissociation energy of the hydrogen molecule, ΔH°_{WE} is the enthalpy of the single-electrode process at the working electrode and ΔH°_{RE} is the enthalpy of the single-electrode process at the reference electrode (149,150). Summation of the two single-electrode processes leads to the following total reaction:

$$1/2\, H_2 + M \xrightarrow{\Delta H^\circ_{ads}(H_{UPD})} M - H_{UPD} \qquad [4.14]$$

Subsequently, upon adding the respective Born-Haber cycles and bearing in mind that there is a Volta potential difference between the metal and the solution so that the H^+ and e extracted from the two solid electrodes are at different electrostatic potentials, this difference compensates exactly the work function variation shown in scheme [4.12] at the working electrode, thus EF, one obtains the following relation for the $M - H_{UPD}$ bond energy:

$$E_{M-H_{UPD}} = \frac{1}{2} D_{H_2} + \Delta H^{\circ}_{ads}(H_{UPD}) \qquad [4.15]$$

4.4 Thermodynamics of the UPD H on Rh(poly) electrode.

The same thermodynamic approach applied to the data for the Rh(poly) electrode for various values of $\theta_{H_{UPD}}$ between 0.05 and 0.95 with an interval of 0.05 and allows determination of $\Delta G^{\circ}_{ads}(H_{UPD})$ as a function of both $\theta_{H_{UPD}}$ and T, $\Delta G^{\circ}_{ads}(H_{UPD}) = f(\theta_{H_{UPD}}, T)$. Three-dimentional plots of $\Delta G^{\circ}_{ads}(H_{UPD})$ versus $\theta_{H_{UPD}}$ and T for the three concentrations of H_2SO_4 in which the experiments have been carried out demonstrate that $\Delta G^{\circ}_{ads}(H_{UPD})$ varies between −18 and −8 kJ mol^{-1} depending on $\theta_{H_{UPD}}$ and T (Fig. 3. in chapter 1.2). The Gibbs free energy of adsorption has the most negative values at the lowest temperature and at the smallest H_{UPD} surface coverage. Augmentation of $\Delta G^{\circ}_{ads}(H_{UPD})$ with increasing $\theta_{H_{UPD}}$ for $T = const$ indicates that the lateral interactions between the H_{UPD} species are predominantly of the repulsive nature (6,8-10,44,45,60-62).

An examination of the $\Delta G^{\circ}_{ads}(H_{UPD})$ vs. $(\theta_{H_{UPD}}, T)$ plots for 0.05 and 0.10 M H_2SO_4 solutions indicates that the changes of $\Delta G^{\circ}_{ads}(H_{UPD})$ are pronounced the most in the $0 - 0.20$ range of $\theta_{H_{UPD}}$ and at low temperatures (Fig. 3. in chapter 1.2). When the temperature approaches high values, $\Delta G^{\circ}_{ads}(H_{UPD})$ does not vary more than some 4 kJ mol^{-1} and the $\Delta G^{\circ}_{ads}(H_{UPD})$ vs. $\theta_{H_{UPD}}$ relations become almost linear. In the 0.50 M H_2SO_4 solution, the $\Delta G^{\circ}_{ads}(H_{UPD})$ vs. $\theta_{H_{UPD}}$ dependence is slightly more complex. At low temperatures, $\Delta G^{\circ}_{ads}(H_{UPD})$ varies significantly with $\theta_{H_{UPD}}$ especially in the $0 - 0.40$ range of the surface coverage by H_{UPD}. However at high temperatures, the changes become less pronounced and $\Delta G^{\circ}_{ads}(H_{UPD})$ does not vary more than some 4 kJ mol^{-1} over the whole range of $\theta_{H_{UPD}}$. An analysis of the $\Delta G^{\circ}_{ads}(H_{UPD})$ vs. $\theta_{H_{UPD}}$ plots reveals that they may not be simply fitted into the Frumkin isotherm in order to evaluate the energy of lateral interactions because the dependences are non-linear, thus appraisal of the energy of lateral repulsions is not straightforward. Nevertheless, in the case of H adsorption from 0.05 and 0.10 M H_2SO_4 solutions and in the $0.20 - 0.80$ range of the H_{UPD} surface coverage, the $\Delta G^{\circ}_{ads}(H_{UPD})$ vs. $\theta_{H_{UPD}}$ relations are linear indicating applicability of the Frumkin isotherm. The $\Delta G^{\circ}_{ads}(H_{UPD})$ vs. $\theta_{H_{UPD}}$ relations (for $T = const$) for $0.20 \le \theta_{H_{UPD}} \le 0.80$ were fitted into the Frumkin isotherm and evaluated the Gibbs free energy of lateral repulsions, ω, in relation to the temperature. The data indicate that ω assumes values between 2 and

5 kJ mol^{-1} thus increasing $\Delta G^{\circ}_{ads}(H_{UPD})$ from more negative towards less negative values. The experimental results also indicate that ω varies with temperature, $\omega = f(T)$, and that it assumes the lowest values at the highest temperatures (Fig. 4. in chapter 1.2).

The entropy of the UPD H on Rh electrode was calculated based on equation 4.5. The data demonstrate that $\Delta S^{\circ}_{ads}(H_{UPD})$ varies significantly with $\theta_{H_{UPD}}$ between −125 and −15 J mol^{-1} K^{-1}; it assumes the more negative values at the lowest H_{UPD} surface coverage and it assumes less-negative values with increasing $\theta_{H_{UPD}}$ (Fig. 5. in chapter 1.2). The $\Delta S^{\circ}_{ads}(H_{UPD})$ vs. $\theta_{H_{UPD}}$ relations almost follow each other for $\theta_{H_{UPD}} \geq 0.55$ and there are significant differences for $\theta_{H_{UPD}} < 0.55$. The differences between the $\Delta S^{\circ}_{ads}(H_{UPD})$ vs. $\theta_{H_{UPD}}$ relations for the 0.05 and 0.10 M H_2SO_4 solutions are small and they almost overlap each other. The $\Delta S^{\circ}_{ads}(H_{UPD})$ vs. $\theta_{H_{UPD}}$ relation for the 0.5 M H_2SO_4 solution differs from the others and $\Delta S^{\circ}_{ads}(H_{UPD})$ has more-negative values especially in the 0 – 0.55 range of $\theta_{H_{UPD}}$. At this preliminary level, the $\Delta S^{\circ}_{ads}(H_{UPD})$ vs. $\theta_{H_{UPD}}$ behavior may be assigned to the specific anion adsorption being more pronounced in the more concentrated electrolyte. The $\Delta S^{\circ}_{ads}(H_{UPD})$ vs. $\theta_{H_{UPD}}$ dependences presented here indicate that the entropy of the under-potential deposition of H depends on the concentration of the electrolyte, thus is associated with the anion concentration at the solid/liquid interface. In order to evaluate the entropy of the very first H_{UPD} adatom deposited on the Rh electrode, the $\Delta S^{\circ}_{ads}(H_{UPD})$ vs. $\theta_{H_{UPD}}$ plots were fitted into a third order polynomial and $\Delta S^{\circ}_{ads}(H_{UPD})_{\theta_{H_{UPD}} \to 0}$ was elucidated from the Y-intercept. In the case of H adsorption from the 0.05 and 0.10 M H_2SO_4 solutions, the values of $\Delta S^{\circ}_{ads}(H_{UPD})_{\theta_{H_{UPD}} \to 0}$ are the same and equal to −99 J mol^{-1} K^{-1} whereas in the case of the 0.5 M H_2SO_4 solution it is equal to −138 J mol^{-1} K^{-1}.

The enthalpy of the under-potential deposition of H on Rh electrodes, $\Delta H^{\circ}_{ads}(H_{UPD})$, from aqueous H_2SO_4 solutions is determined based on the above determined values of $\Delta G^{\circ}_{ads}(H_{UPD})$ and $\Delta S^{\circ}_{ads}(H_{UPD})$ for the three concentrations of H_2SO_4, namely 0.05, 0.10 and 0.5 M H_2SO_4 and equation 4.9. The $\Delta H^{\circ}_{ads}(H_{UPD})$ vs. $\theta_{H_{UPD}}$ dependences demonstrate that $\Delta H^{\circ}_{ads}(H_{UPD})$ accepts negative values between −45 and −15 kJ mol^{-1} (Fig. 6. in chapter 1.2). For the three concentrations of H_2SO_4, $\Delta H^{\circ}_{ads}(H_{UPD})$ increases towards less-negative values with increasing $\theta_{H_{UPD}}$. In order to evaluate the enthalpy change associated with deposition of the very first H_{UPD} adatom on the Rh electrode, the $\Delta H^{\circ}_{ads}(H_{UPD})$ vs. $\theta_{H_{UPD}}$ plots were fitted

into a third order polynomial and $\Delta H^{\circ}_{ads}(H_{UPD})_{\theta_{H_{UPD}}\to 0}$ was elucidated from the Y-intercept. In the case of H adsorption from the 0.05 and 0.10 M H_2SO_4 solutions, the values of $\Delta H^{\circ}_{ads}(H_{UPD})_{\theta_{H_{UPD}}\to 0}$ are the same and equal to -45 kJ mol^{-1} whereas in the case of the 0.5 M H_2SO_4 solution it is equal to -56 kJ mol^{-1}. Decrease of $\Delta H^{\circ}_{ads}(H_{UPD})$ with increasing $\theta_{H_{UPD}}$ points to the repulsive nature of the lateral interactions between the H_{UPD} adatoms.

It is essential to assess whether the under-potential deposition of H on Rh electrodes is an enthalpy-driven or entropy-driven process. Comparison of the experimentally determined values of $\Delta H^{\circ}_{ads}(H_{UPD})$ with the product $T\,\Delta S^{\circ}_{ads}(H_{UPD})$ for various H_{UPD} surface coverages reveals that $\left|\Delta H^{\circ}_{ads}(H_{UPD})\right| > \left|T\,\Delta S^{\circ}_{ads}(H_{UPD})\right|$, thus indicating the process in enthalpy-driven.

The values of the $Rh-H_{UPD}$ bond energy, $E_{Rh-H_{UPD}}$, for H_{UPD} electroadsorbed from the 0.05, 0.10 and 0.5 M H_2SO_4 solutions fall in the $230-270$ kJ mol^{-1} range and that the variation of $E_{Rh-H_{UPD}}$ versus $\theta_{H_{UPD}}$ follows the changes of $\Delta H^{\circ}_{ads}(H_{UPD})$ as a function of $\theta_{H_{UPD}}$ through equation 4.15 (Fig. 7. in chapter 1.2). The $Rh-H_{UPD}$ bond energy varies the most in the case of the 0.5 M H_2SO_4 electrolyte whereas in the case of the 0.05 and 0.1 M H_2SO_4 solutions the plots follow each other. The variation of $E_{Rh-H_{UPD}}$ with the concentration of H_2SO_4 is assigned to the specific anion adsorption at the electrodes surface which is pronounced the most for the most concentrated electrolyte (134,151-153).

It is essential to compare the above determined values of $E_{Rh-H_{UPD}}$ to those for H chemisorbed dissociatively from the gas phase on Rh (H_{chem}). The value of the $Rh-H_{chem}$ bond energy, $E_{Rh-H_{chem}}$, for H chemisorbed on Rh(111) and Rh(110) single-crystal faces (6) is 255 kJ mol^{-1} on both surfaces. These data and the experimental results for $E_{Rh-H_{UPD}}$ indicate that the bond energies for the electroadsorbed H and the chemisorbed H are close to each other, say within some 25 kJ mol^{-1}. Prior to any further discussion of the relation between $E_{Rh-H_{UPD}}$ and $E_{Rh-H_{chem}}$, it is essential to elaborate on the $M-H_{chem}$ bond energy for various transition metals.

In the review article by Christmann (6), it is recognized that the values of the $M-H_{chem}$ bond energies, $E_{M-H_{chem}}$, for various transition metals fall into the $250-270$ kJ mol^{-1} range and that they are almost the same for various single-crystal faces of the transition metals. Proximity of

the values of $E_{M-H_{chem}}$ and their independent of the surface geometry points to a similar surface binding mechanism on various transition metal surfaces. Thus, one may conclude (6) that the H_{chem} adatom is strongly embedded in the metal surface lattice being coplanar with the metal topmost surface atoms or that it penetrates into the metal surface lattice occupying sites between the first and the second metal surface layer (Fig. 2. in chapter 1.1).

It has been shown above that $Rh-H_{UPD}$ bond energy, $E_{Rh-H_{UPD}}$, falls close to that for $Rh-H_{chem}$, say within the proximity of some 25 kJ mol^{-1}. Based on these data and on the discussion of the nature of the $M-H_{chem}$ surface bond (6), it is apparent that the binding mechanism between Rh and H_{UPD} involving the electrified double-layer is similar to that under gas-phase conditions. In other words, the under-potential deposited H, H_{UPD}, is also embedded in the surface metal lattice in a manner similar to that for the chemisorbed H. This conclusion coincides with the observation (56-59) that the H_{UPD} species is unavailable to form a bond with H_2O molecules in the double-layer region.

4.5 Thermodynamics of the UPD H on Pt(poly) Electrode.

Examination of the $\Delta G_{ads}(H_{UPD})$ versus $(\theta_{H_{UPD}}, T)$ relations for the three concentrations of the aqueous H_2SO_4 solution leads to the following general observations (Fig. 3. in chapter 2.1): (i) $\Delta G_{ads}(H_{UPD})$ varies from −11 to −25 kJ mol^{-1}; (ii) $\Delta G_{ads}(H_{UPD})$ has the most negative values at the lowest temperature and at the smallest H_{UPD} surface coverage; (iii) changes of $\Delta G_{ads}(H_{UPD})$ are pronounced the most in the $0.20-0.80$ range of $\theta_{H_{UPD}}$; (iv) increase of $\Delta G_{ads}(H_{UPD})$ towards less-negative values with increasing $\theta_{H_{UPD}}$ (for $T = const$) indicates that the lateral interactions between H_{UPD} adatoms are predominantly of the repulsive nature (6,8-10,44,45,60-62); the lateral repulsions are the most noticeable, thus the strongest, in the $0.20-0.80$ range of $\theta_{H_{UPD}}$; (v) for a given, constant H_{UPD} surface coverage, $\Delta G_{ads}(H_{UPD})$ assumes less-negative values when the temperature increases; (vi) for a given, constant temperature, T, $\Delta G_{ads}(H_{UPD})$ has less-negative values when the H_{UPD} surface coverage increases.

An important aspect that should be discussed is the anion adsorption on Pt, here sulfate of bisulfate, attained by discharge which is represented by the following equation:

$$Pt + A^- \rightarrow Pt-A_{ads} + e \qquad [4.16]$$

Recent data (134,151-153) demonstrate that the anion adsorption can overlap the potential region corresponding to the UPD H. At present, the charge associated with the anion adsorption on Pt from the 0.05, 0.10 and 0.50 M aqueous solutions of H_2SO_4 is not well established, thus one is unable to account for it at peresent research. The anion surface coverage depends on its bulk concentration and already at low concentrations of the order of 0.001 or 0.01 M it reaches a maximal (saturation) value. In the case of the results presented in the paper, the sulfate surface coverage is not affected significantly by the change of the bulk concentration of H_2SO_4. Thus the experimentally evaluated value of $\Delta G_{ads}(H_{UPD})$ may contain an anion contribution, $\Delta G_{ads}(A_{ads})$, but it seems reasonable to consider it constant for the three concentrations of H_2SO_4. Hence, even if the $\Delta G_{ads}(H_{UPD})$ values are obscured by a certain anion contribution, it is sensible to assume that it is almost constant and that the $\Delta G_{ads}(H_{UPD})$ versus $(\theta_{H_{UPD}}, T)$ variations are meaningful. The recent interest in anion adsorption has led to new and interesting data on the anion surface concentration. Future advancement of experimental approaches into temperature dependence measurements followed by theoretical treatment will result in precise determination of $\Delta G_{ads}(A_{ads})$, $\Delta S^{\circ}_{ads}(A_{ads})$ and $\Delta H^{\circ}_{ads}(A_{ads})$.

The standard entropy of the UPD H on Pt(poly), $\Delta S^{\circ}_{ads}(H_{UPD})$, was determined based on the temperature dependence of $\Delta G_{ads}(H_{UPD})$. An analysis of the $\Delta G_{ads}(H_{UPD})$ versus $(\theta_{H_{UPD}}, T)$ plots shows that for $\theta_{H_{UPD}} = \text{const}$ the relation between $\Delta G_{ads}(H_{UPD})$ and T is linear and it allows evaluation of the entropy of adsorption on the basis of equation 4.5. The main observations of the examination of relations of $\Delta S^{\circ}_{ads}(H_{UPD})$ versus $\theta_{H_{UPD}}$ for the three concentrations of H_2SO_4 may be summarized as follows (Fig. 4. in chapter 2.1): (i) $\Delta S^{\circ}_{ads}(H_{UPD})$ varies significantly with $\theta_{H_{UPD}}$ and it has values from –40 to –90 J mol^{-1} K^{-1}; (ii) the $\Delta S^{\circ}_{ads}(H_{UPD})$ versus $\theta_{H_{UPD}}$ relations reveal two waves which are associated with two adsorption-desorption peaks in the CV profiles; (iii) the $\Delta S^{\circ}_{ads}(H_{UPD})$ versus $\theta_{H_{UPD}}$ relations have a local minimum at $\theta_{H_{UPD}} = 0.45$ and the minimal value of $\Delta S^{\circ}_{ads}(H_{UPD})$ varies from –75 to –90 J mol^{-1} K^{-1}, depending on the H_2SO_4 concentration; this local minimum of $\Delta S^{\circ}_{ads}(H_{UPD})$ corresponds to the potential between the two CV adsorption-desorption peaks;

(iv) $\Delta S^{\circ}_{ads}(H_{UPD})$ has the least-negative values for the UPD H from 0.50 M aq. H_2SO_4; (v) the $\Delta S^{\circ}_{ads}(H_{UPD})$ versus $\theta_{H_{UPD}}$ relations for H adsorption from 0.05 and 0.10 M aq. H_2SO_4 solutions almost follow each other throughout the whole $\theta_{H_{UPD}}$ range; (vi) the $\Delta S^{\circ}_{ads}(H_{UPD})$ versus $\theta_{H_{UPD}}$ relations are complex and fitting them into an n-th order polynomial does not provide any new insight. At this preliminary level, changes of the $\Delta S^{\circ}_{ads}(H_{UPD})$ versus $\theta_{H_{UPD}}$ behavior brought about by varying the H_2SO_4 concentration may be assigned to the anion adsorption. The $\Delta S^{\circ}_{ads}(H_{UPD})$ versus $\theta_{H_{UPD}}$ plots show that the entropy of the UPD H depends on the concentration of the electrolyte, thus it is associated with the anion concentration at the solid/liquid electrified interface (134,151-153).

The enthalpy of the under-potential deposition of H on Pt(poly) electrodes, $\Delta H^{\circ}_{ads}(H_{UPD})$, versus $\theta_{H_{UPD}}$ relations for the three concentrations of H_2SO_4 demonstrate that $\Delta H^{\circ}_{ads}(H_{UPD})$ varies from –27 to –46 kJ mol^{-1} (Fig. 5. in chapter 2.1). The $\Delta H^{\circ}_{ads}(H_{UPD})$ versus $\theta_{H_{UPD}}$ plots show two waves, the first one in the $0-0.45$ range of $\theta_{H_{UPD}}$ and the second one for $\theta_{H_{UPD}} \rangle 0.45$; the enthalpy of adsorption reaches a local minimum of some –40 or –45 kJ mol^{-1} (depending on the electrolyte concentration) at $\theta_{H_{UPD}} \cong 0.45$.

Comparison of the experimentally determined values of $\Delta H^{\circ}_{ads}(H_{UPD})$ with the product $T\,\Delta S^{\circ}_{ads}(H_{UPD})$ for various H_{UPD} surface coverages for Pt(poly) electrodes reveals that $\left|\Delta H^{\circ}_{ads}(H_{UPD})\right| \rangle \left|T\,\Delta S^{\circ}_{ads}(H_{UPD})\right|$, thus indicating the process in enthalpy-driven.

The values of $\Delta H^{\circ}_{ads}(H_{UPD})$ for Pt(poly) applied to equation 4.15 allows determination $E_{Pt-H_{UPD}}$ whose values fall in the $245-265$ kJ mol^{-1} range (Fig. 6. in chapter 2.1). The $Pt-H_{UPD}$ bond energy varies the most in the case of the 0.50 M H_2SO_4 electrolyte whereas in the case of the 0.05 and 0.10 M H_2SO_4 solutions the $E_{Pt-H_{UPD}}$ vs. $\theta_{H_{UPD}}$ plots follow each other, however these differences are small and of the order of some 10 kJ mol^{-1}, thus some 4% of the value of $E_{Pt-H_{UPD}}$. The dependence of $E_{Pt-H_{UPD}}$ on the concentration of H_2SO_4 is assigned to the anion interaction with the electrode surface and the water molecules at the solid/liquid interface (134,151-153).

It is essential to elaborate on the two waves of the $\Delta H^{\circ}_{ads}(H_{UPD})$ versus $\theta_{H_{UPD}}$ and $E_{Pt-H_{UPD}}$ versus $\theta_{H_{UPD}}$ relations. The spectroscopic data from the laboratory of Bewick (56-59) lead to

distinction of two kinds of adsorbed H: the weakly bonded H and the strongly bonded H; these two surface species interact with the substrate in a distinct manner giving rise to different physico-chemical properties as revealed by electroreflectance studies. These two electroadsorbed H species are associated with the two waves of the $\Delta H^{\circ}_{ads}(H_{UPD})$ versus $\theta_{H_{UPD}}$ and $E_{Pt-H_{UPD}}$ versus $\theta_{H_{UPD}}$ relations; the wave in the $0-0.45$ range of $\theta_{H_{UPD}}$ represents the strongly bonded H whereas that for $\theta_{H_{UPD}} \rangle 0.45$ refers to the weakly bonded H.

It is fundamental to compare the values of $E_{Pt-H_{UPD}}$ to those for H_{chem} on well-defined Pt surfaces. The values of the $Pt-H_{chem}$ bond energy, $E_{Pt-H_{chem}}$, for H chemisorbed on three low-index surfaces, namely (111), (110) and (100) single-crystal faces (6) are 255, 243 and 247 kJ mol^{-1}, respectively. These data and the experimental results for $E_{Pt-H_{UPD}}$ indicate that the bond energies for the electroadsorbed H and the chemisorbed H are very close to each other, say within some 10 kJ mol^{-1}. Proximity of the values of $E_{M-H_{chem}}$ and their relative independence of the surface geometry may point to a similar surface binding mechanism on various transition metals. Thus one may conclude that the H_{chem} adatom is strongly embedded in the surface lattice of the metal substrate being coplanar with the topmost surface atoms of the metal substrate or that it penetrates into the metal surface lattice occupying sites between the first and the second surface layer. In the light of these observations and the experimentally determined values of $E_{Pt-H_{UPD}}$ it can be concluded that the binding mechanism between Pt and H_{UPD} involving the electrified double-layer is similar to that under the gas-phase conditions. In other words, the under-potential deposited H, H_{UPD}, might also be embedded in the surface lattice of Pt in a manner similar to that for the chemisorbed H. The H_{UPD} adsorbed on Pt(poly) electrodes is unavailable to form a bond with H_2O molecules in the double layer region. At this point, the specific interaction of H_{UPD} adatoms with co-adsorbed anions is not taken into account although the anion effect is observed through the concentration dependence of $\Delta G_{ads}(H_{UPD})$, $\Delta S^{\circ}_{ads}(H_{UPD})$, $\Delta H^{\circ}_{ads}(H_{UPD})$ and $E_{Pt-H_{UPD}}$. This aspect is investigated for Pt(111).

From comparison of $\Delta G_{ads}(H_{UPD})$ for Pt(poly) and Rh(poly) it may be concluded that the driving force of the UPD H on Pt(poly) is larger than in the case of Rh(poly) and the lateral repulsions between the H_{UPD} adatoms are stronger on Pt(poly) than on Rh(poly).

4.6 Thermodynamics of the UPD H on Pt(poly) Electrode in the Presence of Chemisorbed Sulfur.

The idea which was the guided light throughout the project was elucidation of the influence of S_{chem} on thermodynamics of the UPD H and on the bond $Pt-H_{UPD}$ energy. Coupled AES, CEELS and electrochemical measurements on the S chemisorbtion on Pt(poly) indicate that S_{chem} is in its atomic form, thus it is not bonded to the surface in the form of S oxides or sulfides. It was presumed that S_{chem} adatoms, forming a submonolayer and coadsorbed with H_{UPD} can withdraw electron gas from the Pt atoms with which they form a surface bond. This electron withdrawal gives rise to a localized electron deficit which is compensated by withdrawing electron gas from the neighboring Pt atoms as well as from those involved in the $Pt-H_{UPD}$ bond (27,154). The Pt substrate acts as a mediator bringing about lateral $S_{chem}-H_{UPD}$ interactions. It was assumed that the electron density of the $Pt-H_{UPD}$ bond should be decreased by the coadsorbed S_{chem} adatoms, thus the $Pt-H_{UPD}$ bond should be weaker in presence of a submonolayer of S_{chem} that in its absence. This concept was tested experimentally and theoretically and the results are presented below.

The Gibbs free energy of adsorption in presence of S_{chem}, $\Delta G_{ads(S)}(H_{UPD})$, is evaluated on the basis equation 4.17 (27):

$$\frac{\theta_{H_{UPD}}}{1-\theta_{H_{UPD}}-\theta_S} = f_{H_2}^{1/2} \exp\left(-\frac{E\,F}{R\,T}\right) \exp\left(-\frac{\Delta G_{ads\,(S)}(H_{UPD})}{R\,T}\right) \qquad [4.17]$$

In presence of the S_{chem} submonolayer having $\theta_{Schem} = 0.10$, $\Delta G_{ads(S)}(H_{UPD})$ has values between –22 and –9 kJ mol^{-1}, thus values less negative than those in absence of S_{chem}; it assumes the most negative values at the lowest T and the lowest $\theta_{H_{UPD}}$; $\Delta G_{ads}(H_{UPD})$ increases towards less negative values with increase of $\theta_{H_{UPD}}$ (Fig. 9. in chapter 2.2). This change of $\Delta G_{ads}(H_{UPD})$ with $\theta_{H_{UPD}}$ indicates that the lateral interactions between the H_{UPD} adatoms are repulsive and the slope of the $\Delta G^{\circ}_{ads}(H_{UPD})$ versus $\theta_{H_{UPD}}$ plots is a measure of their strength (6,155-157). In the case of the UPD H in presence of S_{chem}, the variations of $\Delta G_{ads(S)}(H_{UPD})$ with $\theta_{H_{UPD}}$ are more pronounced at low T than at high T whereas in absence of S_{chem} they are roughly of the same magnitude. Thus one may conclude that in presence of

the S_{chem} submonolayer the lateral repulsions between the H_{UPD} adatoms are stronger at low T than at high T.

The entropy of adsorption in presence of the S_{chem} submonolayer, $\Delta S^{\circ}_{ads(S)}(H_{UPD})$, was evaluated based on the $\Delta G_{ads(S)}(H_{UPD})$ versus T relations for $\theta_{H_{UPD}} = const$; it has values between −46 and 41 J mol^{-1} K^{-1} (Fig. 3. in chapter 2.2). The results show that the slope of the $\Delta G_{ads(S)}(H_{UPD})$ versus T relations varies from negative values at low $\theta_{H_{UPD}}$ to positive ones at high $\theta_{H_{UPD}}$ thus indicating that $\Delta S^{\circ}_{ads(S)}(H_{UPD})$ increases with $\theta_{H_{UPD}}$. Comparison of $\Delta S^{\circ}_{ads}(H_{UPD})$ with $\Delta S^{\circ}_{ads(S)}(H_{UPD})$ reveals that presence of the S_{chem} submonolayer significantly increases the entropy of the UPD.

The enthalpy of adsorption in presence of S_{chem}, $\Delta H^{\circ}_{ads(S)}(H_{UPD})$, has values between −34 and 3 kJ mol^{-1} (Fig. 4. in chapter 2.2). An analysis of the data indicates that the presence of the submonolayer of S_{chem} significantly increases the enthalpy of the UPD H with respect to its values in absence of S_{chem}.

Determination of $\Delta H^{\circ}_{ads(S)}(H_{UPD})$ allowed evaluation of the influence of presence of the S_{chem} submonolayer having $\theta_{Schem} = 0.10$ on the $Pt-H_{UPD}$ bond energy, $E_{Pt-H_{UPD}(S)}$. The values of $E_{Pt-H_{UPD}(S)}$ for various $\theta_{H_{UPD}}$ are between 214 and 252 kJ mol^{-1} (Fig. 5. in chapter 2.2). The results demonstrate that the presence of the S_{chem} submonolayer decreases the $Pt-H_{UPD}$ bond energy by some 12 – 31 kJ mol^{-1}, depending on $\theta_{H_{UPD}}$. The decrease of the $Pt-H_{UPD}$ bond energy in presence of S_{chem} indicates that the S_{chem} adatoms create an electron deficit at the $Pt-H_{UPD}$ bond giving rise to a weaker $Pt-H_{UPD}$ bond.

4.7 Thermodynamics of the UPD H on Pt(111) Electrode.

Some work was performed on energetics of the UPD H on Pt electrodes claimed to be of single-crystal nature (92-94) but an analysis of the CV profiles discloses that the electrodes were disordered, thus that they were of polycrystalline nature (92).

Research on thermodynamics of the UPD H on Pt(111) by application of CV as an experimental tool followed by theoretical treatment of the experimental data, as described

above, is feasible only in a diluted aq. H_2SO_4 solution because the two components of the CV profile corresponding to the UPD H and anion adsorption are separated. A scrutiny of the CV's discloses that the H_{UPD} and anion adsorption slightly overlap, therefore the deconvolution of the profiles into two components representing the two processes carries some uncertainty (less than 2%; it is resolved on the basis of the charge under the overlapping components) because the form of their adsorption isotherms for H_{UPD} and anion is not well defined yet. Nevertheless, even with an uncertainty of some 2%, the current interpretation is of importance and it represents an substantial contribution.

The numerically assessed values of $\Delta G_{ads}(H_{UPD})$ fall in the -26 to -8 kJ mol^{-1} range and $\Delta G_{ads}(H_{UPD})$ has the most negative values at the smallest $\theta_{H_{UPD}}$ and the lowest T (Fig. 8. in chapter 3.3).

The standard entropy of adsorption, $\Delta S^{\circ}_{ads}(H_{UPD})$, determined on the ground of equation 4.5 has values from -63 to -79 J mol^{-1} K^{-1} (Fig. 9. in chapter 3.3).

The values of $\omega(H_{UPD})$ for various T reveal that $\omega(H_{UPD})$ is scattered over a narrow range, namely between 25 and 29 kJ mol^{-1}, the average value of lateral interactions, $\bar{\omega}(H_{UPD})$, being 27 kJ mol^{-1} (Fig. 10. in chapter 3.3). In order to examine if $\omega(H_{UPD})$ as a function of T, the data were fitted into a linear relation and the slope of the $\omega(H_{UPD})$ versus T plot was found to be 2.2×10^{-2} kJ mol^{-1} K^{-1}, thus there was practically no T-dependence of $\omega(H_{UPD})$ because an increase of T by 100 K would result in a very small (2.2 kJ mol^{-1}) variation of $\omega(H_{UPD})$. Positive values of $\omega(H_{UPD})$ indicate that *the lateral interactions are repulsive*. It is essential to emphasize, for the first time, that the UPD H on Pt(111) in 0.05 M aq. H_2SO_4 follows *the Frumkin electrochemical isotherm*. This conclusion is of importance in comprehension of the nature of H_{UPD} and in analysis of its adsorption site by combining spectroscopic (56-59,158,159) and thermodynamic results. Knowledge of the average value of $\omega(H_{UPD})$ allows one to determine the value of the dimensionless interaction parameter *g* which appears in the Frumkin isotherm (equation 4.8). The average value of the interaction parameter equals to 11 and it indicates that the lateral interaction between the H_{UPD} adatoms on Pt(111) are strongly repulsive.

The enthalpy of adsorption for the UPD H on Pt(111) in 0.05 M aq. H_2SO_4, $\Delta H^{\circ}_{ads}(H_{UPD})$, is evaluated based on the above determined values of $\Delta G_{ads}(H_{UPD})$ at 298 K, thus $\Delta G^{\circ}_{ads}(H_{UPD})$, and $\Delta S^{\circ}_{ads}(H_{UPD})$. $\Delta H^{\circ}_{ads}(H_{UPD})$ vs. $\theta_{H_{UPD}}$ relation demonstrates that $\Delta H^{\circ}_{ads}(H_{UPD})$ accepts negative values between -44 and -32 kJ mol^{-1} (Fig. 11. in chapter 3.3).

The $Pt(111)-H_{UPD}$ surface bond energy, $E_{Pt(111)-H_{UPD}}$, had never been evaluated for H_{UPD} on a well-defined single-crystal electrode and became a key objective of the project. Also, evaluation of the $E_{Pt(111)-H_{UPD}}$ versus $\theta_{H_{UPD}}$ relation is of importance in determination of the influence of the electrified solid-liquid interface on the strength and nature of the $Pt(111)-H_{UPD}$ surface bond. The values of $E_{Pt(111)-H_{UPD}}$ for various H_{UPD} coverages, $\theta_{H_{UPD}}$, for the UPD H in 0.05M aq. H_2SO_4 reveal that the $Pt(111)-H_{UPD}$ bond energy falls in the $250-262$ kJ mol^{-1} range and that its variation with $\theta_{H_{UPD}}$ is rather negligible (Fig. 12. in chapter 3.3).

The values of the $Pt(111)-H_{chem}$ bond energy is 255 kJ mol^{-1} (6); the datum for $E_{Pt(111)-H_{chem}}$ and the data for $E_{Pt(111)-H_{UPD}}$ indicate that the respective bond energies for H_{UPD} and H_{chem} are close to each other, say within some less than 10 kJ mol^{-1}. Proximity of the values of $E_{M-H_{chem}}$ and their independence of the surface geometry points to a similar surface binding mechanism on various transition metals (6). It is tempting to state that H_{UPD} should occupy the same surface adsorption site as H_{chem} based on the consistency of the respective bond energies (99,146-148). However, the SFG IR experimental results of Tadjeddine and Peremans (158,159) do not support the viewpoint and the authors conclude that H_{UPD} occupies the on-top surface adsorption site. Thus, the issue of the adsorption site of H_{UPD} still remains open albeit the surface bond energy is known at the present time. Confirmation of the SFG IR data by another technique would lead to conclusion that the electrochemical interface selects a different adsorption site for H_{UPD} on Pt(111), yet results in a bond being energetically equivalent to H_{chem}. Should this be correct, one would have to consider the surface electronic structure of the top-most layer by taking into account local electronic effects associated with the metal surface geometry and respective density of surface states.

4.8 Thermodynamics of the UPD H on Pt(111) Electrode in the Presence of Chemisorbed Sulfur

Immersion of a Pt(111) electrodes in aqueous Na_2S solution leads to formation of a monolayer of S_{chem} which suppresses completely the UPD H and anion adsorption. The chemical state of adsorbed S on the Pt(111) substrate was evaluated by Auger Electron Spectroscopy (AES) and Core Level Electron Energy Loss Spectroscopy (CEELS). Characteristic absence of the AES oxygen signals indicates that sulfur oxides are not formed on the surface irrespective of the S-coverage. On the basis of the AES data, the authors conclude that S adatoms on the Pt(111) substrate are predominantly neutral. However, as shown below and discussed in ref. 160, a noticeable charge transfer between Pt(111) and S is giving rise to a partial negative charge on S, thus to ionicity of the Pt(111)-S surface bond (CEELS measurements document the electron redistribution at the Pt(111) surface; see ref. 161).

The main core-level loss feature for the S_{chem} layer at 165 eV is attributed to electron transition from the S*2p* energy level to an empty bound state above the Fermi level but before the unoccupied continuum, such as S*3d* (160). The S*2p* - S*3d* energy gap obtained on the basis of the theoretical studies (162) is very close to the experimentally observed 165 eV value (Fig. 4. in chapter 3.4). The origin of the additional core-level loss feature at higher energy is not clear yet (160). The CEELS peaks for S_{chem} and the Na_2S thin film are at 165.5 eV and 164 eV, respectively, demonstrate that the main loss energy of the S-adsorbate is 1.5 eV higher than that for Na_2S. However, based on X-ray Photoelectron Spectroscopy (XPS) measurements (163), the S*2p* binding energy difference between elemental sulfur and Na_2S is higher, namely 2.2 eV. This highlights the difference between the surface and elemental sulfur strongly indicating that the S adatoms carry a partial negative charge due to electron density shift from Pt(111) to S.

The surface structures formed by S_{chem} were examined by LEED in relation to the S_{chem} coverage, $\theta_{S_{chem}}$ (Fig. 5. in chapter 3.4). The S_{chem} coverage was controlled by oxidative desorption of S_{chem} through repetitive scanning of the S_{chem}-covered Pt(111) electrode to 1.20 V, RHE (Fig. 2. in chapter 3.4). The LEED data disclose that S_{chem} forms well-defined structures as $\theta_{S_{chem}}$ decreases. It is of interest to compare these structures with those formed

under UHV condition during thermal desorption (Fig. 6. in chapter 3.4). The UHV experiments show that upon thermal desorption of S_{chem} from the Pt(111) substrate two well-defined structures are formed: (i) $\left(\sqrt{3}\times\sqrt{3}\right)R30°$ at $\theta_{S_{chem}} = 1/3$; and (ii) $p(2\times2)$ at $\theta_{S_{chem}} = 1/4$. Thus, electrochemical oxidative desorption of S_{chem} allows improved and more precise control of the S_{chem} coverage and formation of a new structure, namely $c(2\times2)$ at $\theta_{S_{chem}} = 1/2$, which has not been achieved under UHV condition. LEED patterns were also observed for $\theta_{S_{chem}}$ below 0.2 ML, thus indicating that the surface was covered by structured S_{chem} islands of the size higher than the coherence length of the electron beam at the kinetic energy applied, therefore some more than 50Å.

On the basis of the thermodynamic approach presented above, thermodynamic state functions of the UPD H on Pt(111) in presence of a submonolayer of S_{chem} having $\theta_{S_{chem}} = 0.10$ were examined. The Gibbs free energy of adsorption in presence of the submonolayer of S_{chem}, $\Delta G_{ads(S)}(H_{UPD})$, was evaluated on the basis equation 4.17.

In presence of the S_{chem} submonolayer having $\theta_S = 0.1$, $\Delta G_{ads(S)}(H_{UPD})$ has values between -15 and -2 kJ mol^{-1}, thus values less negative than those in absence of S_{chem}; it assumes the most negative values at the lowest T and the lowest $\theta_{H_{UPD}}$. It has been mentioned above that for T = const $\Delta G_{ads}(H_{UPD})$ increases towards less negative values with increase of $\theta_{H_{UPD}}$. This change of $\Delta G_{ads}(H_{UPD})$ with $\theta_{H_{UPD}}$ indicates that the lateral interactions between the H_{UPD} adatoms are repulsive and the slope of the $\Delta G_{ads}(H_{UPD})$ versus $\theta_{H_{UPD}}$ plots is a measure of their strength (6,155-157). In the case of the UPD H in presence of S_{chem}, the variations of $\Delta G_{ads(S)}(H_{UPD})$ with $\theta_{H_{UPD}}$ are more pronounced at low T than at high T whereas in absence of S_{chem} they are roughly of the same magnitude. Thus one may conclude that in presence of the S_{chem} submonolayer the lateral repulsions between the H_{UPD} adatoms are stronger at low T than at high T.

The entropy of adsorption in presence of the S_{chem} submonolayer, $\Delta S°_{ads(S)}(H_{UPD})$ has values between 64 and 135 J mol^{-1} K^{-1}. Comparison of $\Delta S°_{ads}(H_{UPD})$ with $\Delta S°_{ads(S)}(H_{UPD})$ reveals that presence of the S_{chem} submonolayer significantly increases the entropy of the UPD.

The enthalpy of adsorption in presence of S_{chem}, $\Delta H^{\circ}_{ads(S)}(H_{UPD})$ has values between 4 and 32 kJ mol^{-1}. An analysis of the data indicates that presence of the submonolayer of S_{chem} significantly increases the enthalpy of adsorption with respect to its values in absence of S_{chem}.

The values of $\Delta S^{\circ}_{ads(S)}(H_{UPD})$ and $\Delta H^{\circ}_{ads(S)}(H_{UPD})$ reveal that the UPD H on Pt(111) is enthalpy-driven in absence of S_{chem} but becomes entropy-driven in presence of S_{chem}. The data indicate that presence of S_{chem} decreases the surface bond energy between H_{UPD} and the Pt(111) substrate through local electron withdrawing effects which decrease the electron density at the $Pt(111)-H_{UPD}$ bond.

The values of $E_{Pt-H_{UPD}(S)}$ for various $\theta_{H_{UPD}}$ are between 214 and 186 kJ mol^{-1}. The results demonstrate that presence of the S_{chem} submonolayer decreases the $Pt-H_{UPD}$ bond energy. The decrease of the $Pt-H_{UPD}$ bond energy indicates that the S_{chem} adatoms create an electron deficit at the $Pt-H_{UPD}$ bond giving rise to a weaker $Pt-H_{UPD}$ bond.

The results represent an important contribution to comprehension of the atomic-level mechanism of the action of SBE's and their impact on coadsorbed H_{UPD} adatoms and that they will serve in subsequent development of criteria for selection and design of surface species which could act selectively either as surface poisons or surface poisons of H adsorption and absorption.

CONCLUSIONS

The importance of thermodynamic studies of the under potential deposition of hydrogen (UPD H) on noble-metal electrocatalysts such as Rh and Pt has been and the validity of the theoretical methodology has been examined. The theoretical treatment which leads to determination of important thermodynamic state functions requires knowledge of the relation between the H_{UPD} surface coverage, potential and temperature as achieved on the basis of cyclic-voltammetry studies. Theoretical treatment of the experimental data results in determination of the Gibbs free energy, entropy and enthalpy of adsorption, ΔG_{ads}, ΔS°_{ads} and ΔH°_{ads}, respectively. It has been established that the UPD H can occur when the following thermodynamic condition is fulfilled: $1/2\, D_{H_2} - \Delta H^{\circ}_{ads}(H_{UPD}) \rangle 0$. The new theoretical approach presented in the thesis leads to determination of the bond energy between the noble-metal substrate, S, and the under-potential deposited H, H_{UPD}, $E_{S-H_{UPD}}$. This theoretical methodology has been advanced to metallic and semiconductor species and a formula for the bond energy, $E_{S-M_{UPD}}$, between the noble-metal substrate, S, and the adsorbate, M, has been proposed. It has been emphasized that knowledge of $E_{S-H_{UPD}}$ or $E_{S-M_{UPD}}$ is essential in evaluation of the binding forces acting between the substrate and the deposit, thus the forces that are responsible for adhesion of the deposit to the substrate.

Temperature-dependence of the UPD H on Rh electrodes from 0.05, 0.1 and 0.5 M aqueous H_2SO_4 solutions by cyclic-voltammetry followed by theoretical treatment of the data has allowed determination of $\Delta G_{ads}(H_{UPD})$, $\Delta S^{\circ}_{ads}(H_{UPD})$ and $\Delta H^{\circ}_{ads}(H_{UPD})$ of the process. $\Delta G_{ads}(H_{UPD})$ accepts values from −8 to −18 kJ mol^{-1}, $\Delta S^{\circ}_{ads}(H_{UPD})$ from −15 to −125 J mol^{-1} K^{-1}, and $\Delta H^{\circ}_{ads}(H_{UPD})$ from −15 to −52 kJ mol^{-1}. In the case of the UPD H on Pt electrodes from 0.05, 0.10 and 0.50 M aqueous H_2SO_4 solutions, $\Delta G_{ads}(H_{UPD})$ varies from −11 to −25 kJ mol^{-1}, $\Delta S^{\circ}_{ads}(H_{UPD})$ from −40 to −90 J mol^{-1} K^{-1}, and $\Delta H^{\circ}_{ads}(H_{UPD})$ from −27 to −46 kJ mol^{-1}. Increase of $\Delta G_{ads}(H_{UPD})$ towards less-negative values with the increasing H_{UPD} surface coverage, $\theta_{H_{UPD}}$, in the case of both Rh and Pt indicates that the lateral interactions between H_{UPD} adatoms are of the repulsive nature. Knowledge of $\Delta H^{\circ}_{ads}(H_{UPD})$ has allowed elucidation of the surface bond energy between the noble-metal substrate and H_{UPD}. The value of $E_{Rh-H_{UPD}}$ is between 235 and 265 kJ mol^{-1}, depending on the H_{UPD} surface coverage ($\theta_{H_{UPD}}$). The value of $E_{Rh-H_{UPD}}$ is close to that of the bond energy between Rh and the chemisorbed H (H_{chem}), $E_{Rh-H_{chem}}$, the latter being 255 kJ mol^{-1}. The value of

$E_{Pt-H_{UPD}}$ falls in the 245 to 265 kJ mol^{-1} range, depending on the H_{UPD} surface coverage, $\theta_{H_{UPD}}$. The value of $E_{Pt-H_{UPD}}$ is within 10 kJ mol^{-1} of the bond energy between Pt and the chemisorbed H, H_{chem}, $E_{Pt-H_{chem}}$, the latter being in the $243-255$ kJ mol^{-1} range for the low-index single-crystal faces. Proximity of these values points to a similar binding mechanism under the conditions involving presence of an electric field and the electrolyte and under gas-phase conditions. It is concluded that H_{UPD} and H_{chem} might occupy the same surface adsorption site since thermodynamically they are equivalent species. Thus, H_{UPD} alike H_{chem} might be embedded in the surface lattice of the noble-metal substrate.

Immersion of Pt in aqueous Na_2S solution leads to formation of a monolayer of S_{chem} which completely suppressed the UPD H; a submonolayer of S_{chem} having its surface coverage of less than 0.33 blocks the UPD H but only partially. The S_{chem} monolayer can be gradually desorbed by scanning the potential to $E \geq 1.2$ V, thus by oxidative desorption. By application of this methodology, the S_{chem} coverage can be controlled with an precision of 2% of a ML. In presence of a submonolayer of S_{chem} ($\theta_S = 0.1$), $\Delta G_{ads}(H_{UPD})$ as well as $\Delta S^{\circ}_{ads}(H_{UPD})$, $\Delta H^{\circ}_{ads}(H_{UPD})$ and $E_{Pt-H_{UPD}}$ assume different values than in its absence. $\Delta G_{ads}(H_{UPD})$ varies from -22 to -9 kJ mol^{-1}, $\Delta S^{\circ}_{ads}(H_{UPD})$ from -46 to 41 J mol^{-1} K^{-1}, and $\Delta H^{\circ}_{ads}(H_{UPD})$ from -34 to 3 kJ mol^{-1}. The $Pt-H_{UPD}$ bond energy has values from 214 to 252 kJ mol^{-1}. The decrease of the $Pt-H_{UPD}$ bond energy brought about by a submonolayer of S_{chem} is explained as follows: The S_{chem} adatoms chemisorbed on Pt create an electron-density deficit at the Pt surface atoms to which they are bonded. This deficit propagates through the Pt substrate and gives rise to local electron withdrawal from the $Pt-H_{UPD}$ bond, thus to a lower electron density, and consequently to a weaker $Pt-H_{UPD}$ bond. The repulsive interactions between the H_{UPD} adatoms are stronger in presence of the S_{chem} submonolayer than in its absence.

Studies of temperature dependence of the UPD H and anion adsorption on Pt(100) in 0.5 M aqueous H_2SO_4 solution by cyclic-voltammetry indicate that the overall adsorption/desorption charge density decreases by about 1/3 with respect to the charge density at the lowest T. The sharp peak at 0.375 V vs. RHE assigned to the anion adsorption decreases its potential, current density and charge density. The CV feature assigned to the UPD H, a wide shoulder overlapping the sharp peak, also decreases with T augmentation but the decline of its charge density is less pronounced. The results indicate that the H_{UPD} and anion surface coverages ($\theta_{H_{UPD}}$ and θ_{AN}), are strongly temperature-dependent. This behavior may be assigned to

lateral repulsive interactions between the respective species. Similar cyclic-voltammetry experiments on Pt(111) in 0.5 M aqueous H_2SO_4 solution indicate that the adsorption-desorption charge density decreases only slightly (by 25 $\mu C\,cm^{-2}$) when T is raised 63 K. The CV component corresponding to the UPD H shifts towards less-positive values when T is increased whereas that of the anion adsorption towards more-positive ones. The surface coverage by the H_{UPD} adatoms and the adsorbed anions decreases slightly upon T extension indicating that the lateral interactions between alike species are repulsive. The asymmetric wave in the double-layer region reveals a complex comportment upon T augmentation. The behavior of the anodic wave is distinct from that for the cathodic one.

An analysis of the CV profiles for Pt(111) and Pt(100) shows that the UPD H and the anion adsorption regions shift towards less-positive potentials when T is raised. Integration of the CV's for Pt(111) discloses that the overall adsorption-desorption charge density decreases from 255 to 230 $\mu C\,cm^{-2}$ when T is raised from 275 to 328 K. In the case of Pt(100), the overall adsorption-desorption charge density decreases from 220 to 150 $\mu C\,cm^{-2}$, thus by 70 $\mu C\,cm^{-2}$ when T is raised from 293 to 328 K. Because the H_{UPD} and anion adsorption regions on Pt(111) in 0.05 M aq. H_2SO_4 are separated, one may determine $\Delta G_{ads}(H_{UPD})$, $\Delta S^{\circ}_{ads}(H_{UPD})$, $\Delta H^{\circ}_{ads}(H_{UPD})$ and the $Pt(111)-H_{UPD}$ surface bond energy, $E_{Pt(111)-H_{UPD}}$. The data show that $\Delta G_{ads}(H_{UPD})$ varies from -26 to -8 $kJ\,mol^{-1}$, $\Delta S^{\circ}_{ads}(H_{UPD})$ from -80 to -62 $J\,mol^{-1}\,K^{-1}$, $\Delta H^{\circ}_{ads}(H_{UPD})$ from -44 to -33 $kJ\,mol^{-1}$, and $E_{Pt(111)-H_{UPD}}$ from 262 to 250 $kJ\,mol^{-1}$. An analysis of the $\Delta G_{ads}(H_{UPD})$ versus $\theta_{H_{UPD}}$ plots reveal that the UPD H follows the Frumkin isotherm and the energy of lateral interactions (here repulsive), ω, is 27 ± 2 $kJ\,mol^{-1}$, and the corresponding dimensionless parameter g is close to 11. The value of $E_{Pt(111)-H_{UPD}}$ is close to the surface bond energy between the chemisorbed H, H_{chem}, and Pt(111), $E_{Pt(111)-H_{chem}}$, the later being 255 $kJ\,mol^{-1}$. Proximity of $E_{Pt(111)-H_{UPD}}$ to $E_{Pt(111)-H_{chem}}$ points to a similar binding mechanism of H under gas-phase and electrochemical conditions. Moreover, similar binding energies indicate that the two species might occupy the same surface adsorption site.

Immersion of Pt(111) in aqueous Na_2S solution results in formation of a compact monolayer of chemisorbed S, S_{chem}, having the (1×1). This layer can be gradually removed, but still with formation of well-defined structures, by oxidative desorption of S_{chem} through scanning the electrode to $E \geq 0.95$ V, RHE; the S_{chem} coverage can be controlled with a precision of 2% of

a monolayer. The compact S_{chem} monolayer completely suppresses the UPD H and anion adsorption as well as it affects the oxide growth behavior on Pt(111). S_{chem} forms well-defined structures on Pt(111) for $0.50 \geq \theta_{S_{chem}} \geq 0.25$. When $\theta_{S_{chem}} \leq 0.20$, the S_{chem} adatoms form structured islands. AES and CEELS experiments indicate that the chemisorbed S is not present in an oxidized or a reduced state; it is almost of atomic character with an incomplete negative charge due to partial charge transfer between the Pt(111) substrate and the S adsorbate. Presence of submonolayers of S_{chem} having a well-defined coverage significantly influences thermodynamics of the UPD H. In the case of a S_{chem} submonolayer having $\theta_{S_{chem}} = 0.10$ $\Delta G_{ads(S)}(H_{UPD})$ has values from -15 to -2 kJ mol^{-1}, thus values less-negative than in absence of S_{chem}. In presence of this S_{chem} submonolayer $\Delta S^{\circ}_{ads}(H_{UPD})$ has values from 64 to 135 J mol^{-1} K^{-1} whereas $\Delta H^{\circ}_{ads}(H_{UPD})$ values from 4 to 32 kJ mol^{-1}. Comparison of $\Delta S^{\circ}_{ads}(H_{UPD})$ with $\Delta S^{\circ}_{ads(S)}(H_{UPD})$ reveals that the presence of the S_{chem} submonolayer significantly increases the entropy of the UPD. Increase of $\Delta H^{\circ}_{ads}(H_{UPD})$ from negative values to positive ones in presence of S_{chem} affects both the $Pt(111) - H_{UPD}$ surface bond energy as well as the nature of the driving force of the UPD H. While in absence of S_{chem} the UPD H on Pt(111) is enthalpy-driven, the process becomes entropy-driven in presence of S_{chem}. Finally, the data indicate that presence of S_{chem} decreases the $Pt(111) - H_{UPD}$ surface bond energy and the values of $E_{Pt-H_{UPD}(S)}$ fall in the 214-186 kJ mol^{-1} range. The diminution of the $Pt(111) - H_{UPD}$ bond energy caused by the S_{chem} submonolayer may be explained as follows: The S_{chem} adatom is an electron-withdrawing species and occupies the three-fold hollow site on Pt(111). Because its orbitals overlap those of the three top-most Pt surface atoms as well as one in the second layer, S_{chem} increases its ionicity and creates a partial positive charge on the Pt surface atoms to which it is bonded. These Pt surface atoms compensate this electron-density deficit by withdrawing electron density from neighboring surface atoms as well as those involved in forming a bond with the H_{UPD}, consequently resulting in a lower electron density at the $Pt(111) - H_{UPD}$ bond. This reduction of the electron density translates into a weaker surface bond.

APPENDIX

Reference states in the electrochemical adsorption isotherm*

i) Definition of Standard State for Gibbs Free Energy H UPD

It is necessary to explain the meaning of standard Gibbs free energy, $\Delta G^{\circ}_{ads}(H_{UPD})$, introduced in general electrochemical isotherm in the Appendix in chapter 2.2. First, one can consider the two single-electrode processes taking place at the working electrode (WE), metal M_1, and the reference electrode (RE), metal M_2:

$$H^+ + e + M_1 \leftrightarrow M_1 - H_{UPD} \qquad \text{(WE)} \qquad [1]$$

$$H^+ + e \leftrightarrow 1/2\, H_2 \qquad \text{(RE)} \qquad [2]$$

Based upon these two reactions one can write the following balance of the electrochemical potentials for reaction [1]:

$$\mu^{\circ}_{M_1}(T_1) + \bar{\mu}_{H^+}(T_1, a_{H^+,1}) + \bar{\mu}^{M_1}_{e}(T_1) = \mu_{M_1-H_{UPD}}(T_1, \theta_{H_{UPD}}) \qquad [3]$$

and for reaction [2]:

$$\bar{\mu}_{H^+}(T_2, a_{H^+,2}) + \bar{\mu}^{M_2}_{e}(T_2) = \tfrac{1}{2}\mu_{H_2}(T_2, f_{H_2}) \qquad [4]$$

where the temperature in each compartment is T_1 and T_2, respectively. Subtraction of the two single-electrode processes, [2] from [1], leads to the following total reaction:

$$1/2H_2 + M_1 \rightarrow M_1 - H_{UPD} \qquad [5]$$

Subtraction of the equation [4] from equation [3] gives the corresponding isotherm for reaction [5]:

*Equations in this appendix are developed by Prof. A. Lasia.

$$\frac{\theta_{H_{UPD}}}{1-\theta_{H_{UPD}}} = \frac{f_{H_2}^{1/2}\, a_{H^+,1}}{a_{H^+,2}} \exp\left(-\frac{F(E_1 - E_2)}{RT}\right) \exp\left(-\frac{\Delta G^{\circ}_{ads,\,H_{UPD}}\left(T_1, T_2, \theta_{H_{UPD}}\right)}{RT}\right) \qquad [6]$$

where:

$$\Delta G^{\circ}_{ads,\,H_{UPD}}\left(T_1, T_2, \theta_{H_{UPD}}\right) = \left[\mu^{0}_{M_1-H_{UPD}}(T_1,\theta) - \mu^{\circ}_{M}(T_1) - \mu^{\circ}_{H^+,1}(T_1)\right] - \left[\tfrac{1}{2}\mu^{\circ}_{H_2}(T_2) - \mu^{\circ}_{H^+,2}(T_2)\right] \qquad [7]$$

When two compartments contain the same activity of H^+ at the same temperature, $T_1 = T_2 = T$, activities in equation [6] cancel and equation [7] is simplified to:

$$\Delta G^{\circ}_{ads,\,H_{UPD}}\left(T, \theta_{H_{UPD}}\right) = \mu^{0}_{M_1-H_{UPD}}(T, \theta_{H_{UPD}}) - \mu^{\circ}_{M}(T) - \tfrac{1}{2}\mu^{\circ}_{H_2}(T) \qquad [8]$$

which is exactly $\Delta G^{\circ}_{ads,\,H_{UPD}}\left(T, \theta_{H_{UPD}}\right)$ for reaction [5]. However, when the temperatures is in both compartments are not identical the significance of this term is more complex.
Moreover, when the two temperatures are different and that for reaction [2] is constant, the derivative $\partial \Delta G^{\circ}_{ads,\,H_{UPD}}\left(T, \theta_{H_{UPD}}\right)/\partial T$ gives the standard entropy of reaction [1] instead of the reaction [5] while the corresponding derivative for two reactions at the same temperature gives the thermodynamic parameters of reaction [5]. Therefore, in Appendix in chapter 1.2, equation [17] is equivalent to equation [20] only at the standard temperature.

For the Langmuir isotherm one can write:

$$\mu_{M_1-A}(T, \theta_A) = \mu^{\circ}_{M_1-A}(\theta_{r,A} = 0.5) + RT \ln \frac{\theta_A}{1-\theta_A} \qquad [9]$$

where A is adsorbed species and the standard chemical potential, $\mu^{\circ}_{M_1-A}(\theta_{r,A} = 0.5)$, correspond to the surface coverage equal 0.5. However, this isotherm can not be used for electroadsorption of hydrogen because this process has not Langmurian behavior. The general form of isotherm can be expressed as:

$$\mu_{M_1-H_{UPD}}\left(T,\theta_{H_{UPD}}\right)=\mu^{\circ}_{M_1-H_{UPD}}(T,\theta_{H_{UPD}})+RT\ln\frac{\theta_{H_{UPD}}}{1-\theta_{H_{UPD}}} \qquad [10]$$

$$\mu_{M_1-H_{UPD}}\left(T,\theta_{H_{UPD}}\right)=\mu^{\circ,\circ}_{M_1-H_{UPD}}(T,\theta_{r,H_{UPD}})+f(T,\theta_{H_{UPD}})+RT\ln\frac{\theta_{H_{UPD}}}{1-\theta_{H_{UPD}}} \qquad [11]$$

where $\mu^{\circ,\circ}_{M_1-H_{UPD}}(T,\theta_{r,H_{UPD}})$ is *surface coverage independent standard chemical potential of hydrogen adsorption at the surface coverage* $\theta_{r,H_{UPD}}$. However, its reference state is determined by the equation [12] (46, 154, 155):

$$f(\theta_{r,H_{UPD}},T)+RT\ln\frac{\theta_{r,H_{UPD}}}{1-\theta_{r,H_{UPD}}}=0 \qquad [12]$$

for example, assuming the Frumkin isotherm $f(T,\theta_{H_{UPD}})=\omega\theta_{H_{UPD}}$ and for $\omega = 27$ kJ mol^{-1} for UPD H on Pt(111) $\theta_{r,H_{UPD}}=0.155$ (for T=298 K). This means that $\Delta G^{\circ}_{ads}(H_{UPD})$ from the thesis, extrapolated for $\theta_{H_{UPD}}=0$ is, in fact, $\Delta G^{\circ}_{ads,H_{UPD}}\left(T,\theta_{r,H_{UPD}}\right)$ at $\theta_{r,H_{UPD}}$. Therefore, for comparison all the values should be recalculated for the same value of $\theta_{r,H_{UPD}}$. It should be added that the reference state of $\theta_{r,H_{UPD}}=0.5$ is suggested also for Frumkin isotherm, however, some additional recalculations are necessary (155).

It should be kept in mind that, in general, $\Delta G_{ads,H_{UPD}}\left(T,\theta_{H_{UPD}}\right)$ is described as:

$$\Delta G_{ads,H_{UPD}}\left(T,\theta_{H_{UPD}}\right)=\mu_{M_1-H_{UPD}}\left(T,\theta_{H_{UPD}}\right)-\mu^{\circ}_{M_1}(T)-\tfrac{1}{2}\mu_{H_2}(T,f_{H_2}) \qquad [13]$$

$$=\left[\mu^{\circ}_{M_1-H_{UPD}}\left(T,\theta_{H_{UPD}}\right)-\mu^{\circ}_{M_1}(T)-\tfrac{1}{2}\mu^{\circ}_{H_2}(T)+RT\ln\frac{\theta_{H_{UPD}}}{1-\theta_{H_{UPD}}}\right]-RT\ln f^{1/2}_{H_2} \qquad [14]$$

$$=\Delta G^{c}_{ads}\left(T,\theta_{H_{UPD}}\right)-RT\ln f^{1/2}_{H_2} \qquad [15]$$

$$=\left[\mu^{\circ,\circ}_{M_1-H_{UPD}}(T,\theta_{r,H_{UPD}})-\mu^{\circ}_{M_1}(T)-\tfrac{1}{2}\mu^{\circ}_{H_2}(T)\right]+f(T,\theta_{H_{UPD}})+RT\ln\frac{\theta_{H_{UPD}}}{1-\theta_{H_{UPD}}}-RT\ln f^{1/2}_{H_2} \qquad [16]$$

$$= \Delta G^{o,o}_{ads}(T,\theta_{r,H_{UPD}}) + f(T,\theta_{H_{UPD}}) + RT\ln\frac{\theta_{H_{UPD}}}{1-\theta_{H_{UPD}}} - RT\ln f_{H_2}^{1/2} \quad [17]$$

$$\Delta G_{ads,\,H_{UPD}}\left(T,\theta_{H_{UPD}}\right) = -FE \quad [18]$$

where $\Delta G^{o,o}_{ads,H_{UPD}}(T,\theta_{r,H_{UPD}})$ is *the surface coverage independent standard Gibbs free energy of hydrogen adsorption at the surface coverage* $\theta_{r,H_{UPD}}$. Using the formula [18], free energy of adsorption may be calculated at any surface coverage. Figure 1b shows 3D plot of the Gibbs free energy of adsorption, $\Delta G_{ads,\,H_{UPD}}\left(T,\theta_{H_{UPD}}\right)$, as a function of $\theta_{H_{UPD}}$ and T, is calculated based on equation 18, for the UPD H on Pt(111) in 0.05 M aq. H_2SO_4. $\Delta G_{ads,\,H_{UPD}}\left(T,\theta_{H_{UPD}}\right)$ has values from -32 to -7 kJ mol^{-1} depending on $\theta_{H_{UPD}}$ and T. After correction for $-RT\ln f_{H_2}^{1/2}$, $\Delta G^{c}_{ads,H_{UPD}}\left(T,\theta_{H_{UPD}}\right)$ can be calculated based on equation [15]. $\Delta G^{c}_{ads,H_{UPD}}\left(T,\theta_{H_{UPD}}\right)$ has not effect of fugacity change due to temperature change. One may compare $\Delta G^{c}_{ads,H_{UPD}}\left(T,\theta_{H_{UPD}}\right)$ values with $\Delta G^{o}_{ads,H_{UPD}}(T,\theta_{H_{UPD}})$ based on the electrochemical isotherm equation [6] which is presented as a 3D plot (Figure 1a). $\Delta G^{c}_{ads,H_{UPD}}\left(T,\theta_{H_{UPD}}\right)$ has the configurational Gibbs free energy of adsorption, $RT\ln\frac{\theta_{H_{UPD}}}{1-\theta_{H_{UPD}}}$.

ii) Definition of Standard State for Entropy and Enthalpy of H UPD

Thermodynamic parameters of adsorption process are determined by differentiation of $\Delta G^{o}_{ads,\,H_{UPD}}\left(T,\theta_{H_{UPD}}\right)$:

$$\left(\frac{\partial \Delta G^{o}_{ads,\,H_{UPD}}\left(T,\theta_{H_{UPD}}\right)}{\partial T}\right)_{\theta} = -\Delta S^{o}_{ads,\,H_{UPD}}\left(T,\theta_{H_{UPD}}\right) \quad [19]$$

and

$$\left(\frac{\partial \Delta G^{o}_{ads,\,H_{UPD}}\left(T,\theta_{H_{UPD}}\right)/T}{\partial (1/T)}\right)_{\theta} = \Delta H^{o}_{ads,\,H_{UPD}}\left(T,\theta_{H_{UPD}}\right) \quad [20]$$

However, taking into account equation [12], the following expression is obtained:

$$\left(\frac{\partial\Delta G^{\circ}_{ads,\,H_{UPD}}\left(T,\theta_{H_{UPD}}\right)}{\partial T}\right)_{\theta}=\left(\frac{\partial\Delta G^{\circ,o}_{ads,\,H_{UPD}}\left(T,\theta_{r,H_{UPD}}\right)}{\partial T}\right)_{\theta}+\left(\frac{\partial f\left(T,\theta_{H_{UPD}}\right)}{\partial T}\right)_{\theta} \qquad [21]$$

Subsequently, from equations [19] and [21], one gets the following equation:

$$\left(\frac{\partial\Delta G^{\circ}_{ads,\,H_{UPD}}\left(T,\theta_{H_{UPD}}\right)}{\partial T}\right)_{\theta}=-\Delta S^{\circ,o}_{ads,H_{UPD}}(\theta_{r,H_{UPD}})-\left(\frac{\partial f\left(T,\theta_{H_{UPD}}\right)}{\partial T}\right)_{\theta} \qquad [22]$$

$$\left(\frac{\partial\Delta G^{\circ}_{ads,\,H_{UPD}}\left(T,\theta_{H_{UPD}}\right)/T}{\partial(1/T)}\right)_{\theta}=\Delta H^{\circ,o}_{ads,\,H_{UPD}}\left(\theta_{r,H_{UPD}}\right)+\left(\frac{\partial(f(T,\theta_{H_{UPD}})/T)}{\partial(1/T)}\right)_{\theta} \qquad [23]$$

where $\Delta S^{\circ,o}_{ads,H_{UPD}}(\theta_{r,H_{UPD}})$ is *the surface coverage independent standard entropy of H UPD at the surface coverage* $\theta_{r,H_{UPD}}$. One can calculate *the surface coverage coverage independent standard enthalpy of H UPD at the surface coverage* $\theta_{r,H_{UPD}}$, $\Delta H^{\circ,o}_{ads,H_{UPD}}(\theta_{r,H_{UPD}})$. Knowing the dependence of $f(\theta_{H_{UPD}})$ on $\theta_{H_{UPD}}$ the corrections may be made and the thermodynamic parameters may be compared for the same value of $\theta_{H_{UPD}}$.
Also, $\Delta H^{\circ,o}_{ads,H_{UPD}}(\theta_{r,H_{UPD}})$ can be determined by equation [24]:

$$\Delta H^{\circ,o}_{ads,H_{UPD}}(\theta_{r,H_{UPD}})=\Delta G^{\circ,o}_{H_{UPD}}(T,\theta_{r,H_{UPD}})+T\Delta S^{\circ,o}_{H_{UPD}}(\theta_{r,H_{UPD}}) \qquad [24]$$

$\Delta S^{c}_{ads,H_{UPD}}(\theta_{H_{UPD}})$ can be determined by the following equation:

$$\left(\frac{\partial\Delta G^{c}_{ads,\,H_{UPD}}\left(T,\theta_{H_{UPD}}\right)}{\partial T}\right)_{\theta}=-\Delta S^{\circ,o}_{ads,H_{UPD}}(\theta_{r,H_{UPD}})+\left(\frac{\partial f\left(T,\theta_{H_{UPD}}\right)}{\partial T}\right)_{\theta}+\left(\frac{\partial\left(RT\ln\frac{\theta_{H_{UPD}}}{1-\theta_{H_{UPD}}}\right)}{\partial T}\right) \qquad [25]$$

$$\left(\frac{\partial\Delta G^{c}_{ads,\,H_{UPD}}\left(T,\theta_{H_{UPD}}\right)}{\partial T}\right)_{\theta}=-\Delta S^{c}_{ads,H_{UPD}}(\theta_{H_{UPD}}) \qquad [26]$$

$\Delta H^{c}_{ads,H_{UPD}}(\theta_{H_{UPD}})$ can be determined by the following equation:

$$\Delta H^{c}_{H_{UPD}}(\theta_{H_{UPD}}) = \Delta G^{c}_{H_{UPD}}(T,\theta_{H_{UPD}}) + T\Delta S^{c}_{H_{UPD}}(\theta_{H_{UPD}}) \qquad [27]$$

One may determine $\Delta S^{c}_{ads,H_{UPD}}(\theta_{H_{UPD}})$ as a function of $\theta_{H_{UPD}}$ based on the equation [26] (Fig. 2) and determine $\Delta H^{c}_{ads,H_{UPD}}(\theta_{H_{UPD}})$ as a function of $\theta_{H_{UPD}}$ based on the equation [27] and can be presented as Fig. 3. The energy of the $Pt(111)-H_{UPD}$ bond can be determined based on the values of $\Delta H^{c}_{ads,H_{UPD}}(\theta_{H_{UPD}})$ for various H_{UPD} surface coverages (Fig. 3) and equation 9 in chapter 3.4.

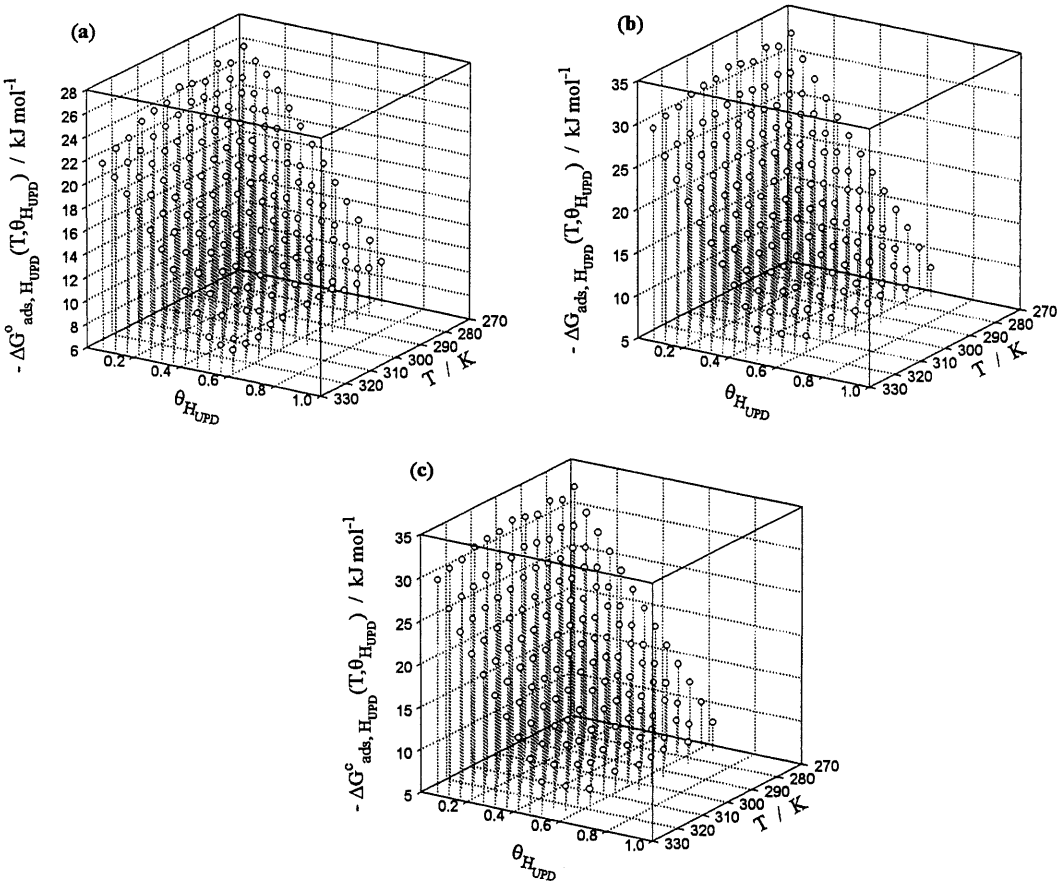

Figure 1. 3D plots showing the Gibbs free energy of adsorption as a function of $\theta_{H_{UPD}}$ and T, $\Delta G_{ads,H_{UPD}}(T,\theta_{H_{UPD}})$, for the UPD H on Pt(111) in 0.05 M aq. H_2SO_4, (a) $\Delta G^{o}_{ads,H_{UPD}}(T,\theta_{H_{UPD}})$ is calculated based on electrochemical isotherm equation [6] has values from -25 to -8 kJ mol^{-1}; (b) $\Delta G_{ads,H_{UPD}}(T,\theta_{H_{UPD}})$ is calculated based on equation [18], $\Delta G_{ads,H_{UPD}}(T,\theta_{H_{UPD}}) = -FE$, has values from -32 to -6 kJ mol^{-1} (c) $\Delta G^{c}_{ads,H_{UPD}}(T,\theta_{H_{UPD}})$ is calculated based on equation [15] has values from -32 to -6 kJ mol^{-1}

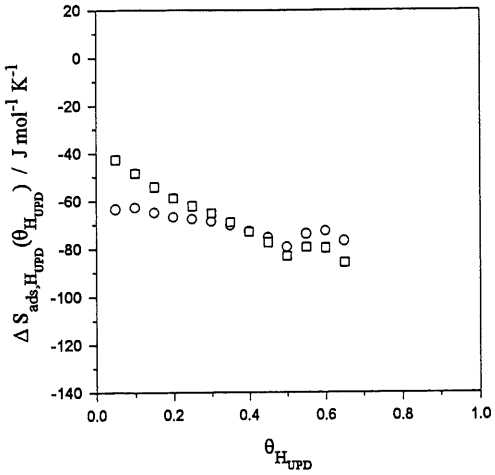

Figure 2. Dependence of $\Delta S_{ads,H_{UPD}}(\theta_{H_{UPD}})$ on $\theta_{H_{UPD}}$ for the UPD H on Pt(111) in 0.05 M aq H_2SO_4. O presents $\Delta S^{\circ}_{ads,H_{UPD}}(\theta_{H_{UPD}})$ based on equation [19] has values from -63 to -79 J mol^{-1} K^{-1}; □ presents $\Delta S^{c}_{ads,H_{UPD}}(\theta_{H_{UPD}})$ based on equation [26] has values from -39 to -86 J mol^{-1} K^{-1}

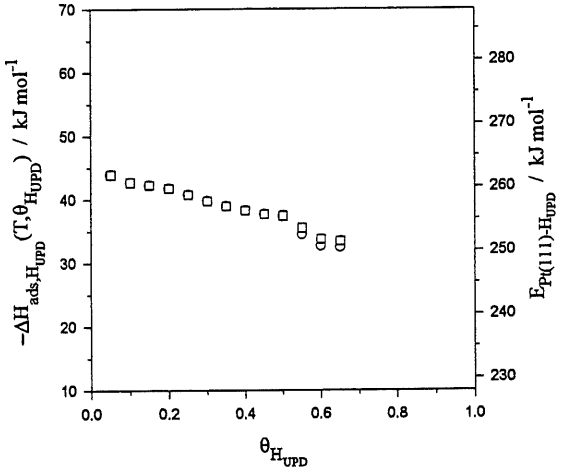

Figure 3. Dependence of $\Delta H_{ads,H_{UPD}}(T,\theta_{H_{UPD}})$ and $E_{Pt(111)-H_{UPD}}$ on $\theta_{H_{UPD}}$ for the UPD H on Pt(111) in 0.05 M aq H_2SO_4. O presents $\Delta H^{\circ}_{ads,H_{UPD}}(T,\theta_{H_{UPD}})$ based on equation [20] has values from -44 to -32 kJ mol^{-1}. □ shows $\Delta H^{\circ}_{ads,H_{UPD}}(T,\theta_{H_{UPD}})$ based on equation [27] has values from -44 to -33 kJ mol^{-1}. Dependence of $E_{Pt(111)-H_{UPD}}$ on $\theta_{H_{UPD}}$ for the UPD H on $E_{Pt(111)-H_{UPD}}$ can be determined based on $\Delta H^{\circ}_{ads,H_{UPD}}(T,\theta_{H_{UPD}})$ (presented by O) and $\Delta H^{\circ}_{ads,H_{UPD}}(T,\theta_{H_{UPD}})$ (presented by □) and equation 9 in chapter 3.4 both have values from 262 to 251 kJ mol^{-1}.

REFERENCES

1. G. ALEFELD and J. VOLKL, Hydrogen in Metals, Parts I and II, Springer-Verlag, New York, 1978.
2. L. SCHLAPBACH, Hydrogen in Intermetalic Compounds, Part I, Springer-Verlag, New York, 1988; Part II, Springer-Verlag, New York, 1992.
3. K.M. MACKAY, Hydrogen Compounds of the Metallic Elements, E.&F.N. Spon, London, 1966.
4. F.G. WILL and C.A. KNORR, Z. Electrochem., 64, 258; 270 (1960).
5. P.K. SUBRAMANYAN in Comprehensive Treatise of Electrochemistry, Edited by J.O'M. BOCKRIS, B.E. CONWAY, E. YEAGER, and R.E. WHITE, Plenum Press, New York, Vol. 4, 1981, Chapter 8.
6. K. CHRISTMAN, Surface Sci. Rep., 9, 1 (1988).
7. B.E. CONWAY, Sci. Prog. Oxf., 71, 479 (1987); see also M. ELAM and B. E. CONWAY, J. Appl. Electrochem., 17, 1002 (1987); J. Electrochem. Soc., 135 1678 (1988).
8. W. BÖLD and M. W. BREITER, Z. Elektrochem., 64, 897 (1960).
9. M. W. BREITER and B. KENNEL, Z. Elektrochem., 64, 1180 (1960).
10. A. N. FRUMKIN in Advances of Electrochemistry and Electrochemical Engineering, Edited by P. DELAHEY, Interscience Publishers, New York, 3, 287, 1963.
11. M. ENYO in Modern Aspects of Electrochemistry, Edited by B. E. CONWAY and J. O'M. BOCKRIS, Vol. 11, Plenum Press, New York 1975.
12. M. ENYO in Comprehensive Treatise of Electrochemistry, Edited by B. E. CONWAY and J. O'M. BOCKRIS, Vol. 7, Plenum Press, New York, 1983.
13. E. FROMM, Z. Phys. Chem. Neue Folge, Bd., 147, 61 (1986).
14. F.D. MANCHESTER and D. KHATAMIAN, Materials Science Forum, 31, 261 (1988).
15. J. J. G. WILLEMS, Ph.D. Thesis, Eindhoven (1984).
16. S. R. OVSHINSKY, M. A. FETCENKO, and J. ROSS, Science, 260, 176 (1993).
17. S. R. OVSHINSKY, K. SAPRU, B. REICHMAN, and A. REGER, US Patents No. 4,623,597; see also S. R. OVSHINSKY and M. A. FETCENKO, US Patent No. 5,096,667; No. 5,104,617; No. 5,135,589; No. 5,238,756; No. 5,277,999.

18. M. CIUREANU, D. MOROZ, R. DUCHARME, D. H. RYAN, J. STRÖM-OLSEN, and M. TRUDEAU, Zeit. Phys. Chem. Bd., 183, 365 (1994); Q. M. YANG, M. CIUREANU, D. H. RYAN, and J. STRÖM-OLSEN, J. Electrochem. Soc., 141, 2108 (1994); 141, 2113 (1994); 141, 2430 (1994).
19. S. R. OVSHINSKY, M. A. FETCENKO, S. VENKATESAN, and B. CHAO in Electrochemistry and Materials Science of Cathodic Hydrogen Absorption and Adsorption, Edited by B. E. CONWAY and G. JERKIEWICZ, The Electrochemical Society, 1995.
20. W. BOELD and M. W. BREITER, Electrochim. Acta, 5, 145 (1961).
21. M. W. BREITER, Electrochim. Acta, 7, 25 (1962).
22. M. W. BREITER, Ann. N.Y. Acad. Sci., 101, 709 (1963).
23. B. E. CONWAY, H. ANGERSTEIN-KOZLOWSKA, and W. B. A. SHARP, Trans. Faraday Soc.,19, 1373 (1977).
24. B. E. CONWAY, H. ANGERSTEIN-KOZLOWSKA, and F. C. HO, J. Vac. Sci. Technol., 14 351 (1977).
25. H. ANGERSTEIN-KOZLOWSKA, B. MACDOUGALL, and B. E. CONWAY, Electrochem. Soc., 120, 756 (1977).
26. R. R. ADZIC, D. N. SIMIC, D. M. DRAZIC, and A.R. DESPIC, Electrochem. Soc., 80, 81 (1977).
27. B. E. CONWAY and G. J. JERKIEWICZ, Electroanal. Chem., 357, 47 (1993); see also JERKIEWICZ, G., J. J. BORODZINSKI, W. CHRZANOWSKI, and B. E. CONWAY, J. Electrochem. Soc., 142, 3755 (1995).
28. E. YEAGER, W. O`GRADY, M. WOO, and P. HAGANS, J. Electrochem. Soc., 125, 348 (1978).
29. J. CLAVILIER, R. PARSONS, R. DURAND, C. LAMY, and J.W. LEGER, J. Electroanal. Chem., 124, 321 (1981).
30. P. N. ROSS, Surf. Sci., 102, 463 (1981).
31. B. E. CONWAY, Theory and Principle of Electrode Processes, The Roland, New York, 1965.
32. D. M. MOHILNER, Electroanal. Chem., 1, 241(1966).
33. R. PARSONS, Trans. Faraday Soc., 55, 999 (1959).
34. R. PARSONS, J. Electroanal. Chem., 7, 136 (1964).
35. P. DELAHAY, Double Layer and Electrode Kinetics, Wiley-Interscience, 1965.

36. A. N. FRUMKIN and B. B. DAMASKIN in Modern Aspects of Electrochemistry, Vol 3, Edited by J. O'M. BOCKRIS, Butterworths, London, 1964.

37. R. PARSONS in Advances in Electrochemistry and Electrochemical Engineering, Edited by P. DELAHAY, Interscience, New York, 1, 1, 1961.

38. I. LANGMUIR, Trans. Faraday Soc., 17, 621 (1921).

39. I. LANGMUIR, J. Am. Chem. Soc., 38, 2221 (1916); 40, 1361 (1918).

40. I. LANGMUIR, J. Am. Chem. Soc., 38, 1145 (1916).

41. K. J. LAIDLER, Chemical Kinetics, Harper and Row, New York, 1987.

42. M. TEMKIN and V. PYZHEV, Acta Physicochim., USSR 2, 473 (1935).

43. A. N. FRUMKIN, Z. Physik., 35, 792 (1926).

44. M. W. BREITER in Transactions of the Symposium on Electrode Processes, Edited by E. YEAGER, John Wiley and Sons, New York, 1961.

45. R. WOODS in Electroanalytical Chemistry, Edited by A.Bard, Marcel Dekker, New York, 9, 27, 1977.

46. B. E. CONWAY, H. ANGERSTEIN-KOZLOWSKA, and H. P. DHAR, Electrochim. Acta, 19, 460 (1974).

47. B. E. CONWAY and H. ANGERSTEIN-KOZLOWSKA, Acc. Chem. Res., 14, 49 (1981).

48. M. BALDAUF and D. M. KOLB, Electrochim. Acta, 38, 2145 (1993).

49. M. J. HAISSINSKY, Chim. Phys., 43, 21 (1946).

50. D. M. KOLB, M. PRZASNYSKI, and H. GERISCHER, J. Electroanal. Chem., 54, 25 (1974).

51. B. E. CONWAY, H. ANGERSTEIN-KOZLOWSKA, and W. B. A. SHARP, J. Chem. Soc., Faraday Trans. I, 74, 1373 (1978).

52. B. E. CONWAY, and G. JERKIEWICZ, Electroanal. Chem., 357, 47 (1993)

53. G. JERKIEWICZ, J. J. BORODZINSKI, W. CHRZANOWSKI, and B. E. CONWAY, J. Electrochem. Soc., 142, 3755 (1995).

54. B. E. CONWAY and G. JERKIEWICZ, Z. Phys. Chem. Bd., 183, 281 (1994).

55. J. MCBREEN, J. Electroanal. Chem., 287, 279 (1990).

56. A. BEWICK and A. M. TAXFORD, J. Electroanal. Chem., 47, 255 (1973).

57. A. BEWICK and J. W. RUSSELL, J. Electroanal. Chem., 132, 329 (1982).

58. A. BEWICK and J. W. RUSSELL, J. Electroanal. Chem., 142, 337 (1982).

59. R. J. NICHOLS and A. BEWICK, J. Electroanal. Chem., 243, 445 (1988).

60. E. PROTOPOPOFF and P. MARCUS, J. Vac. Sci. Technol. A, 5, 944 (1987).
61. E. PROTOPOPOFF and P. MARCUS, C. R. Acad. Sci. Paris, t 308, Serie II, 1127 (1989).
62. E. PROTOPOPOFF and P. MARCUS, J. Chim. Phys., 88, 1423 (1991).
63. D. PLETCHER, J. Appl. Electrochem., 14, 403 (1984).
64. A. T. HUBBARD, Acc. Chem. Res., 13, 177 (1980).
65. A. T. HUBBARD, J. Vac. Sci. Technol., 17 (1), 49 (1980).
66. B.E. CONWAY, Sci. Prog. Oxf., 16, 1 (1984).
67. F.G. WILL, J Electrochem. Soc., 112, 451 (1965).
68. H. ANGERSTEIN-KOZLOWSKA, W. B. A. SHARP, and B. E. CONWAY in Proc. of the Symposium on Catalysis, Edited by M.W. BREITER, The Electrochemical Society, Inc., Princeton, N. J., 97, 1974.
69. R. M. ISHIKAWA, A. T. HUBBARD, J. Electroanal. Chem., 69, 317 (1976).
70. A. T. HUBBARD, R. M. ISHIKAWA, J. KATEKARU, J. Electroanal. Chem., 86, 271 (1978).
71. P. N. ROSS, J. Electroanal. Chem., 76, 139 (1977).
72. W. E. O'GRADY, M .Y. C. WOO, P. L. HAGANS, and E. YEAGER, J. Vac. Sci. Technol., 14, 365 (1977).
73. E. YEAGER, W. E. O'GRADY, M .Y. C. WOO, and P. L. HAGANS, J. Electrochem. Soc., 125, 396 (1978).
74. K. YAMAMOTO, D. M. KOLB, R. KÖTZ, and G. LEHMPFUHL, J. Electroanal. Chem., 96, 233 (1979).
75. P. N. ROSS, J. Electrochem. Soc., 126, 67 (1979).
76. A. T. HUBBARD, Acc. Chem. Res., 13, 177 (1980).
77. E. YEAGER, J. Electrochem. Soc., 160C, 128 (1981).
78. J. CLAVILIER, J. Electroanal. Chem., 107, 211 (1980).
79. J. CLAVILIER, R. FAURE, G. GUINET, and R. DURAND, J. Electroanal. Chem., 107, 205 (1980).
80. J. CLAVILIER, D. ARMAND, and B. L. WU, J. Electroanal. Chem., 135, 159 (1982).
81. C. L. SCORTICHINI, F. E. WOODDARD, and C. N. REILLY, J. Electroanal. Chem., 139, 265 (1982).
82. F. E. WOODDARD, C. L. SCORTICHINI, and C. N. REILLY, J. Electroanal. Chem., 151, 109 (1983).

83. C. L. SCORTICHINI, C. N. REILLY, J. Electroanal. Chem., 152, 255 (1983).
84. S. MOTOO and N. FURUYA, J. Electroanal. Chem., 172, 339 (1984).
85. D. A. SCHERSON and D. M. KOLB, J. Electroanal. Chem., 176, 353 (1984).
86. F. El OMAR and R. DURAND, J. Electroanal. Chem., 178, 343 (1984).
87. K. Al. JAAF-GOZE, D. M. KOLB, and D. SCHERSON, J. Electroanal. Chem., 200, 353 (1986).
88. F. T. WAGNER and P. N. ROSS, J. Electroanal. Chem., 150, 141 (1983).
89. R. FAURE, Thése de Doctorat, Institut National de Grenoble, Grenoble (1982).
90. D. ABERDAM, R. DURAND, R. FAURE, and El OMAR, Surface Sci., 171, 303 (1986).
91. R. A. ORIANI, J. P. HIRTH, and M. SMIALOWSKI, Hydrogen Degradation of Ferrous Metals, Noyes Publications, Park Ridge, NJ, 1985.
92. P. MARCUS and E. PROTOPOPOFF, Surface Sci., 161, 533 (1985).
93. P. MARCUS and E. PROTOPOPOFF, Surface Sci. Letters, 169, L237 (1986).
94. P. MARCUS and E. PROTOPOPOFF, J. Vac. Sci. Technol., A5, 944 (1986).
95. J. MCBREEN, J. Electroanal. Chem., 287, 279 (1990).
96. S. MORIN and B. E. CONWAY, J. Electroanal. Chem., 376, 135 (1994).
97. D. ZURAWSKI, K. CHAN, and A. WIECKOWSKI, J. Electroanal. Chem., 210, 315 (1986).
98. D. ZURAWSKI and A. WIECKOWSKI, Langmuir, 8, 2317 (1992).
99. G. JERKIEWICZ and A. ZOLFAGHARI, J. Phys. Chem., 100, 8454 (1996).
100. A. LASIA and D. GRÉGOIRE, J. Electrochem. Soc., 142, 3393 (1995).
101. C. QUIJADA, A. RODES, J. L. VÁZQUEZ, J. M. PÉREZ, and A. ALDAZ, J. Electroanal. Chem., 394, 217 (1995).
102. C. QUIJADA, A. RODES, J. L. VÁZQUEZ, J. M. PÉREZ, and A. ALDAZ, J. Electroanal. Chem., 398, 105 (1995).
103. A. SEVCIK, Coll. Czech. Chem. Comm., 13, 349 (1948).
104. Southampton Electrochemistry Group, Instrumental Methods in Electrochemistry, John Wiley and Sons, New York, 1985.
105. E. HEITZ and G. KREYSA, Principles of Electrochemical Engineering, VCH Publishers, W. Germany, New York, 1986.
106. J. E. B. RANDLES, Trans. Faraday Soc., 44, 327 (1948).
107. P. DELAHAY and G. PERKINS, J. Phys. Coll. Chem. 55, 586 (1951).

108. R. S. NICHOLSON and I. SHAIN, Anal. Chem., 36, 706 (1964).
109. R. S. NICHOLSON and I. SHAIN, Anal. Chem., 37, 178 (1965).
110. R. S. NICHOLSON, Anal. Chem., 37, 1351 (1965).
111. S. SRINIVASAN and E. GILEADI, Electrochim. Acta, 11, 321 (1966).
112. B. D. CULLITY, Elements of X-ray Diffraction, Addison-Wesley, USA, 1958.
113. B. E. WARREN, X-ray Diffraction, Addison-Wesley, USA, 1969.
114. C. S. BARNET and T. B. MASALSKI, Structure of Metals; Crystallographic Methods, Principles and Data, McGraw-Hill, London, 1966.
115. A. HAMELIN in Modern Aspects of Electrochemistry, Edited by B. E. CONWAY, R. E. WHITE and J. O'M. BOCKRIS, Plenum Press, New York, Vol. 16, 1985, Chapter 1.
116. A. B. GRENINGER, Zeit, für Krist. A 91, 424 (1935).
117. J. B. PENDRY, Low Energy Electron Diffraction, Academic Press, New York, 1974.
118. L. E. DAVIS, N. C. MACDONALD, P. W. PALMBERG, G. E. RIACH, and R. E. WEBER, Handbook Of Auger Electron Spectroscopy, 2nd edition, Physical Electronics Inc., Eden Prairie, Minn., 1976.
119. T. A. CARLSON, Photoelectron and Auger Spectroscopy, Plenum, New York, 1975.
120. A.P. HITCHCOCK, Jpn. J. Appl. Phys. 32, suppl. 32-2, 176 (1992).
121. CH. KLEINT and S. MAHMOUD Abd El HALIM, Surface Sci. 247, 375 (1991).
122. J. CAZAUX, O. IBARA, and K. H. KIM, Surface Sci., 247, 360 (1991).
123. G. STRASSER, G. ROSINA, J. A. D. MATTHEW, and F. P. NETZER, J. Phys. F 15, 739 (1985). M. OKU, S. SUZUKI, K. ABIKO, H. KIMURA, and K. HIROKAWA, J. Electron. Spectrsc. Rel. Phenom. 34, 55 (1985).
124. A. SULYOK and G. GREGELY, Surface Sci., 213, 327 (1989).
125. B. GRUZZA and C. PARISET, Surface Sci., 247, 408 (1991).
126. T. LOUCKA, J. Electroanal. Chem., 36, 355 (1972).
127. N. RAMASUBRAMANIAN, J. Electroanal. Chem., 64, 21 (1975).
128. A. Q CONTRACTOR, H. LAL, J. Electroanal. Chem., 96, 175 (1979).
129. J. OUDAR, Catalysis Rev.-Sci. Eng., 22, 171 (1980).
130. M. SZKLARCZYK, A. CZERWINSKI, J. SOBKOWSKI, J. Electroanal. Chem., 132, 263 (1982).
131. P. MARCUS, J. OUDAR in Hydrogen Degradation of Ferrous Alloys, Edited by R. A. ORIANI, J. P. HIRTH, M. SMIALOWSKI, Noyes Publications: Park Ridge, NJ, 36, 1985, Chapter 3.

132. N. BATINA, J. W. MCCARGAR, G. N. SALAITA, F. LU, L. LAGUREN-DAVIDSON, C.-H. LIN, and A. T. HUBBARD, Langmuir, 5, 123 (1989).

133. T. MEBRAHTU, M. E. BOTHWELL, J. E. HARRIS, G. J. CALI, M. P. SORIAGA, J. Electroanal. Chem., 300, 487 (1991).

134. E. K. KRAUSKOPF, A. WIECKOWSKI in Adsorption of Molecules at Metal Electrodes, Edited by J. LIPKOWSKI, P. N. ROSS,VCH, New York, 119 (1992).

135. V. SVETLICIC, J. CLAVILIER, V. ZUTIC, J. CHEVALET, K. ELACHI, J. Electroanal. Chem., 344, 145 (1993).

136. J. SZYNKARCZUK, P. G. KOMOROWSKI, J. C. DONINI, Electrochim. Acta, 40, 487 (1995).

137. J. LIPKOWSKI, L. STOLBERG in Adsorption of Molecules at Metal Electrodes, Edited by J. LIPKOWSKI, P. N ROSS, VCH: New York, 171, 1992.

138. M. WASBERG, M. HOURANI, and A. WIECKOWSKI, J. Electroanal. Chem., 278, 425 (1990).

139. M. HOURANI, M. WASBERG, C. RHEE, and A. WIECKOWSKI, Croatica Chim. Acta., 63, 373 (1990).

140. P. ZELENAY, G. M. HORÁNYI, C. K. RHEE, and A. J. WIECKOWSKI, Electroanal. Chem., 300, 499 (1991).

141. J. CLAVILIER, M. WASBERG, M. PETIT, and L. H. KLEIN, J. Electroanal. Chem., 374, 123 (1994).

142. L.-J. WAN, S.-L. YAN, G. M. SWAIN, and K. ITAYA, J. Electroanal. Chem., 381, 105 (1995).

143. J. CLAVILIER, R. ALBALAT, R. GÓMEZ, J. M. ORTS, and J. M. FELIU, J. Electroanal. Chem., 360, 325 (1992).

144. R. GÓMEZ and J. CLAVILIER, J. Electroanal. Chem., 354, 189 (1993).

145. J. CLAVILIER, J. M. ORTS, R. GÓMEZ, J. M. FELIU, and A. ALDAZ in Electrochemistry and Materials Science of Cathodic Hydrogen Absorption and Adsorption, Edited by B. E. CONWAY and G. JERKIEWICZ, The Electrochemical Society, Pennington, NJ, PV 94-21, 1995.

146. G. JERKIEWICZ and A. ZOLFAGHARI, J. Electrochem. Soc., 143, 1240 (1996).

147. A. ZOLFAGHARI, F. VILLIARD, M. CHAYER, and G. JERKIEWICZ, J. Alloy Comp., 253-254, 481 (1997).

148. A. ZOLFAGHARI, M. CHAYER, and G. JERKIEWICZ, J. Electrochem. Soc., 144, 3034 (1997).

149. D. R. LIDE, CRC Handbook of Chemistry and Physics, 72nd Edition, CRC Press, Boston, 1991.

150. A. J. BARD, R. PARSONS, and J. JORDAN, Standard Potentials in Aqueous Solutions, Marcel Dekker, Inc., New York, 1985.

151. A. WIECKOWSKI, Electrochemical Interfaces, Abruña, H. (Ed.), VCH, New York, p. 65; and refs. therein, 1991.

152. Z. SHI,, S. WU., and LIPKOWSKI, J. Electrochim. Acta, 40, 9 (1995).

153. Z. SHI,, S. WU., and J. LIPKOWSKI, J. Electroanal. Chem., 384, 171 (1995).

154. A. ZOLFAGHARI, G. JERKIEWICZ, Y.-E. SUNG, and A. WIECKOWSKI in Electrode Processes VI, Edited by K. ITAYA, and A. WIECKOWSKI, The Electrochemical Society, Pennington, NJ, PV 96-8, 1996.

155. R. H. FOWLER and F. A. GUGGENHEIM, Statistical Thermodynamics, Cambridge University Press, London, 1939.

156. A. W. ADAMSON, Physical Chemistry of Surfaces, John Wiley and Sons, New York, 1990.

157. G. A. SOMORJAI, Introduction to Surface Chemistry and Catalysis, John Wiley and Sons, New York, 1994.

158. A. PEREMANS and A. TADJEDDINE, Phys. Rev. Lett., 73, 3010 (1994).

159. A. TADJEDDINE and A. PEREMANS, J. Chim. Phys., 93, 662 (1996).

160. Y.-E. SUNG, W. CHRZANOWSKI, A. ZOLFAGHARI, G. JERKIEWICZ, and A. WIECKOWSKI, J. Am. Chem. Soc., 119, 194 (1997).

161. J. C. RIVIÈRE, Surface Analytical Techniques, Oxford University Press, New York, 1990.

162. A. P. HITCHCOCK and C. E. BRION, Chem. Phys., 33, 55 (1978).

163. J. F. MOULDER, Editor, Handbook of X-Ray Photoelectron Spectroscopy, Perkin Elmer, Eden Prairie, MN, USA, 1992.

164. J. O'M. BOCKRIS and S. U. M. KHAN, Surface Electrochemistry, Plenum, p. 147, 1993.

165. A. J. APPLEBY, M. CHEMLA, H. KITA, and G. BRONÖEL, in Encyclopedia of Electrochemistry of the Elements, A. J. BARD, Editor, Marcel Dekker, vol IX A, p. 501, 1982.